INFORMATION TO USERS

This material was produced from a microfilm copy of the original document. While the most advanced technological means to photograph and reproduce this document have been used, the quality is heavily dependent upon the quality of the original submitted.

The following explanation of techniques is provided to help you understand markings or patterns which may appear on this reproduction.

1. The sign or "target" for pages apparently lacking from the document photographed is "Missing Page(s)". If it was possible to obtain the missing page(s) or section, they are spliced into the film along with adjacent pages. This may have necessitated cutting thru an image and duplicating adjacent pages to insure you complete continuity.

2. When an image on the film is obliterated with a large round black mark, it is an indication that the photographer suspected that the copy may have moved during exposure and thus cause a blurred image. You will find a good image of the page in the adjacent frame.

3. When a map, drawing or chart, etc., was part of the material being photographed the photographer followed a definite method in "sectioning" the material. It is customary to begin photoing at the upper left hand corner of a large sheet and to continue photoing from left to right in equal sections with a small overlap. If necessary, sectioning is continued again — beginning below the first row and continuing on until complete.

4. The majority of users indicate that the textual content is of greatest value, however, a somewhat higher quality reproduction could be made from "photographs" if essential to the understanding of the dissertation. Silver prints of "photographs" may be ordered at additional charge by writing the Order Department, giving the catalog number, title, author and specific pages you wish reproduced.

5. PLEASE NOTE: Some pages may have indistinct print. Filmed as received.

Xerox University Microfilms
300 North Zeeb Road
Ann Arbor, Michigan 48106

THE UNIVERSITY OF OKLAHOMA

GRADUATE COLLEGE

THE PYROLYSIS ENERGY OF WILDLAND FUELS

A DISSERTATION

SUBMITTED TO THE GRADUATE FACULTY

in partial fulfillment of the requirements for the

degree of

DOCTOR OF PHILOSOPHY

BY

MURTHY SURYANARAYANA DUVVURI

Norman, Oklahoma

1974

THE PYROLYSIS ENERGY OF WILDLAND FUELS

APPROVED BY

C. M. Sliepcevich

J. Fred Weller

F. M. Townsend

Arthur Wm. Aldag, Jr.

William N. Huff

DISSERTATION COMMITTEE

ABSTRACT

The amount of energy required to bring the fuel to the ignition point is one of the important aspects to be considered in modeling the rate of fire spread in wildland fuels. Determination of the pyrolysis energy effects leads to the prediction of the heat of preignition. Both the weight loss during pyrolysis and the energy required for pyrolysis are dependent on parameters such as the fuel composition, the moisture content of the fuel and the heating rate during the preignition phase of the flame spread process.

Experimental weight loss and rate of weight loss data were obtained using a Perkin-Elmer TGS-1, thermogravimetric balance, and a Cahn (Mark II) time derivative computer. The heating rates studied were 10°, 20°, 40°, 80° and 160°C/min, and the materials studied included cellulose, extracted and unextracted dead Ponderosa pine needles, extracted and unextracted excelsior, fourwing saltbush leaves, larch wood, and a decayed form of Douglas fir snags (punky wood) assumed to be nearly pure lignin. The pyrolysis energy data were measured using a Perkin-Elmer DSC-2 at heating rates of 40°, 80° and 160°C/min for the same materials except for larch wood.

A model was developed to predict the energy of pyrolysis of wildland fuels based on the composition of the fuel. The fuel was considered to consist of cellulose and lignin fractions. Therefore, the model contains two additive terms, chosen to be of the Arrhenius type, one for cellulose and one for lignin. When combined, the two terms provide rate of weight loss and weight loss profiles with respect to temperature at any heating rate. A set of kinetic parameters for cellulose and a second set for lignin were obtained from the experimental data by a least-squares technique. The kinetic parameters thus obtained were incorporated into the proposed model for the pyrolysis of wildland fuels. The calculated weight loss and rate of weight loss profiles and the total energy of pyrolysis predicted by the model are compared with experimentally obtained data for excelsior. Additional comparison of weight loss data for larch wood further substantiates the model.

ACKNOWLEDGMENTS

It is nearly impossible to extend here my appreciation and gratitude to each and every individual involved in making this research effort possible. To such of those not mentioned here I am sincerely grateful.

I want to thank Dr. C. M. Sliepcevich, George Lynn Cross Research Professor of Engineering, the chairman of my committee for his interest and guidance, and Dr. F. M. Townsend, Dr. A. W. Aldag, and Dr. W. H. Huff for serving on my graduate committee.

I particularly wish to extend my gratitude to Dr. J. R. Welker for his constant guidance, inspiration, and tremendous zeal in this research effort.

Sincere appreciation is also extended to Dr. L. E. Brown, Dr. W. M. Woodard and Ms. Judy Homer for their many helpful suggestions.

The efforts of Ms. Bobbie Everidge and Ms. Carlotta Wood in organizing and typing the manuscript are highly appreciated.

Last but not least, I wish to thank the Northern Forest Fire Laboratory, Missoula, Montana, for providing financial assistance.

TABLE OF CONTENTS

LIST OF TABLES

LIST OF ILLUSTRATIONS

LIST OF ILLUSTRATIONS--Continued

LIST OF ILLUSTRATIONS--Continued

LIST OF ILLUSTRATIONS--Continued

LIST OF ILLUSTRATIONS--Continued

LIST OF ILLUSTRATIONS--Continued

LIST OF ILLUSTRATIONS--Continued

LIST OF ILLUSTRATIONS--Continued

LIST OF ILLUSTRATIONS--Continued

LIST OF ILLUSTRATIONS--Continued

LIST OF ILLUSTRATIONS--Continued

LIST OF ILLUSTRATIONS--Continued

Dedicated to my parents

Narasa Raju and Narasamma

CHAPTER I

INTRODUCTION

At a time when the world is going through severe shortages of many natural resources, it is needless to say that the value of such resources can no more be estimated strictly in terms of money. Wood, or more generally, wildland fuels definitely fall into the category of such invaluable natural resources. The preservation and proper utilization of wildland resources is therefore a matter of extreme importance. In addition, wood does play an important role in the day-to-day life of man to the extent that home and abroad man is constantly exposed to the safety hazards involved in the use of wood. For the reasons explained above there is a growing need for a basic knowledge of the behavior of wildland fuels under different conditions to which they could be exposed. The non-isotropicity and non-homogeniety of wood makes the study of its basic thermal and physical properties and their interactions under fire conditions very complex.

The Flame Dynamics Laboratory at the University of Oklahoma has initiated intense systematic studies on fire

research since 1966. Considerable progress has been made in terms of understanding some physical characteristics such as thermal conductivity (14). However, considerable work still remains to be done. Naturally, one of the important aspects that needs close attention is the energy involved in the process of combustion. Combustion occurs when the products of pyrolysis (i.e., the gases evolved as a result of heating wood) react with oxygen. Pyrolysis occurs when sufficient energy is supplied to the fuel (wood) to raise the temperature of the fuel so that the molecules begin to decompose. Therefore a method needs to be devised by which the energy of pyrolysis for any wildland fuel can be predicted knowing certain fuel characteristics.

The objects of this study are:

1. Obtain and analyze thermogravimetric (TG) and differential thermogravimetric (DTG) data for cellulose, dead Ponderosa pine needles, excelsior, saltbush leaves, and punky wood;
2. Devise a method for extracting kinetic parameters with no assumptions at all (except the model itself) for cellulose and punky wood;
3. Obtain energy of pyrolysis data for all the species mentioned above;
4. Develop a generalized model based on the cellulose and lignin energies of pyrolysis to predict the energy of pyrolysis of any wood with known cellulose and lignin composition;

5. Check the model developed against experimental results for excelsior whose lignin content is accurately known; The cellulose content can be assumed by difference; and
6. Study the effect of moisture on the process of pyrolysis.

It is necessary to explain some of the terminology used in this thesis to avoid confusion or ambiguity. The terms are listed below:

TGA: thermogravimetric analysis; this pertains to the data obtained from the thermogravimetric balance. TG in particular refers to the weight loss curves, while DTG refers to the differential weight loss curves with respect to time.

DSC: differential scanning calorimetry. This term refers to either the differential scanning calorimeter, or the differential energy curves with respect to temperature, according to the context.

DCA: differential calorimetric analysis, the same as DSC curves.

Energy of pyrolysis: refers to the total energy involved in the process of pyrolysis. By total energy it is meant the sum of the sensible energy and that part of the energy involved in pyrolysis other than the sensible energy. For convenience ΔH_p is defined as the difference between the total energy and the sensible energy. In moist wood, the total energy naturally would include the energy effects due to evaporation of water, in addition to the sensible energy and ΔH_p.

Extracted Wood: refers to wood extracted with ether for 176 hours.

Some of the sample species tested in this thesis have been referred to at times slightly differently. Dead Ponderosa pine needles are in places referred to as Ponderosa pine; fourwing saltbush leaves are referred to as saltbush leaves; lignin which was obtained from Douglas fir snags is referred to as punky wood.

CHAPTER II

REVIEW OF PREVIOUS WORK

Several investigators have attempted to explain the mechanism of wood pyrolysis. Due to the inherently complex structure, composition and behavior of wood and the influences of different experimental conditions on studies of pyrolysis, the results and conclusions have been significantly different among these investigators. Several investigators assumed certain characteristics (e.g., wood char thermal conductivity) without experimental evidence and built up theories based on these assumptions. Such theories proved to be baseless when these assumptions were experimentally shown to be wrong.

A significant contribution in this respect was made by Brown (14). He developed an experimental procedure which consisted of pyrolyzing wood cylinders to varying degrees and then measuring the thermal conductivity of the char phase. The cylindrical wood pieces were 4.45 cm in diameter and 15 cm in length. The wood specimens were subjected to pyrolysis in a plastic bell cover purged continuously with nitrogen.

At steady state the radial temperature profile for a cylindrical sample exposed to a flux is given by

$$\frac{d}{dr}\left(r \frac{dT}{dr}\right) = 0 \qquad \text{(II-1)}$$

where r = radial position (cm)

T = temperature (°C)

upon integration

$$T_r = A \ln r + B \qquad \text{(II-2)}$$

where T_r = temperature ar radius r (°C)

A,B = constants of integration

Equation II-2 shows that if radial heat transfer data are consistent, a plot of ln r versus T should yield a straight line.

If the temperatures are measured at radial positions r_1 and r_2, the integration constants A and B in Equation II-2 can be determined, resulting in Equation II-3.

$$T_r = \frac{(T_1-T_2) \ln (r/r_2)}{\ln (r_1/r_2)} + T_2 \qquad \text{(II-3)}$$

where T_1,T_2 = temperature at radial positions and r_1 and r_2 respectively (°C)

Using Fourier's law of heat conduction for the radial dependence of temperature yields

$$q = -K \frac{d}{dr}\left[\frac{(T_1-T_2) \ln (r/r_2)}{\ln (r_1/r_2)} + T_2\right] \qquad \text{(II-4)}$$

where q = heat flux in the radial direction (cal/cm^2-sec)

K = thermal conductivity of the test wood sample (cal/cm^2-sec-°C/cm)

Since the lateral area of a cylinder of length ℓ is $2 \pi r\ell$, the flux can be written as

$$q = P/2\ \pi\ r\ell \qquad \text{(II-5)}$$

where P = the heat leaving the heating element (cal/sec)

Substituting Equation II-5 into II-4 and solving for K yields

$$K = \frac{P \ln (r_2/r_1)}{2\ \pi\ \ell\ (T_1-T_2)} \qquad \text{(II-6)}$$

A total of five conductivity runs were made using a nickel chromium heating element. The first two runs were used to develop the technique. The last three runs were used to compute K.

The values of thermal conductivity obtained by the above procedure were approximately three times as great as those predicted by the density correlation of Havens (37). While Havens used assumed values of thermal conductivity of wood char, Brown used the measured values of thermal conductivity in the model developed by Havens.

Brown concluded that the overall chemistry of wood pyrolysis was independent of the heating rate over the range of heating rates studied, i.e., from 10°C/min to 160°C/min. He deduced the independence of energy of pyrolysis from the heating rate even above the range of heating rates he studied (by the TG experiments) from the excellent agreement between experimental and computed temperature profile and weight loss data for oak and white pine.

Studies on isothermal kinetics of wood pyrolysis were conducted by Stamm (64), Akita (1) and Tang (66). Results of the isothermal method of investigation are questionable because the sample may undergo considerable reaction in being raised to the temperature of interest. Hence, the above mentioned studies are not discussed in this thesis.

The dynamic temperature technique was used by several investigators. Roberts and Clough (54) studied the pyrolysis of 2 cm by 15 cm beech cylinders at 10°C/min. The experimental data from five runs are summarized in Table II-1. The data were fitted to the first order kinetic expression

$$-\frac{dw}{dt} = (w-w')\ A \exp\ (-E/RT) \qquad \text{(II-7)}$$

where w = weight of specimen at time t (gm)

t = time (sec)

w' = final weight of specimen (gm)

T = absolute temperature (°K)

R = Universal gas constant (1.987 cal/gm-mole-°K)

A = pre-exponential factor (min^{-1})

The results are listed in Table II-1.

Separating the variables in Equation II-7 and integrating yielded

$$\ln \frac{w - w'}{w_o - w'} = A \int_0^t \exp\ (-E/RT)\, dt \qquad \text{(II-8)}$$

where w_o = initial weight of specimen (gm)

TABLE II-1

THERMAL DECOMPOSITION DATA, ROBERTS AND CLOUGH (54)

	Run No. 1	2	3	4	5
Maximum temperature achieved by specimen (°C)	445.0	353.0	505.0	394.0	282.0
$\frac{\text{Final weight}}{\text{Initial weight}}$ (%)	30.9	52.5	28.0	39.7	78.6
Maximum rate of weight loss (mg/sec)	92.0	26.0	193.0	40.0	8.0
Surface area of specimen (cm^2)	97.0	88.0	88.0	88.0	85.0

Since in the experiments the temperature of the specimen was not uniform, Equation II-8 was applied to each of five hypothetical sections into which the specimen was divided. Temperature variations across these sections were negligible. Denoting w, w', w_o and T corresponding to the i^{th} section by w_i, w_i', $w_{i,o}$ and T_i, and assuming $w_i' = w'/5$, $w_{i,o} = w_o/5$, Equation II-8 can be written

$$\ln \frac{w_i - w_i'}{w_{o,i} - w_i} = -A \int_0^t \exp\,(-E/RT_i)\, dt \qquad \text{(II-9)}$$

also

$$w = \Sigma\, w_i \qquad \text{(II-10)}$$

Equations II-9 and II-10 were applied to the data by

1. Assuming a value for E;
2. Evaluating the integral in II-9 for each annulus at t = 23 minutes (the time by which half the total weight loss had occurred);

3. Choosing a value for k so that the calculated value of w agreed with the experimental value;
4. Calculating values of w_i, and hence w, for different times throughout the period of significant weight loss.

The values used by Roberts and Clough for evaluating the data are listed below.

	Activation Energy (kcal/g-mole)	Pre-exponential factor (min^{-1})
First four runs	15	9.1×10^4
Fifth run	25	2.6×10^9

It could be observed that two distinct sets of results were obtained for the first four runs as compared to the last run. An experiment (fifth run) in which the wood temperature did not exceed 280°C gave values for activation energy and heat of reaction which were different from the one set of values obtained from the four experiments carried out at higher temperatures. It was concluded by Roberts and Clough that in lower temperature experiments an initial reaction of activation energy 25 kcal/mole predominated, whereas in higher temperature experiments this reaction was rapidly completed, and a further reaction of activation energy 15 kcal/mole became important.

The work of Blackshear and Kanury (8) concerning pyrolysis of cellulose cylinders is felt to be of little value in developing a generalized model for pyrolysis of wood because the kinetic parameters included heat transfer effects and thus depended upon test sample size and shape.

In a report of the Forest Products Laboratory (25) it was pointed out that different investigators found different minimum temperatures required to produce charring or ignition of wood. The causes for the differences mentioned were

1. The specific conditions under which the tests were carried out by the investigators; and
2. Definition of "ignition" temperature.

Most of the investigators exposed their samples to relatively high temperatures; this approach did not simulate the actual use conditions. The report stressed the importance of prolonged exposure of wood to relatively low elevated temperatures. Maple wood samples (oven-dry) of size 1-1/4 inch x 1-1/4 inch x 4 inches were exposed to temperatures ranging from 107° to 150°C over a period of 16 to 1235 days and the observations were listed. Samples exposed to 140° to 150°C were like charcoal in appearance but none of the samples ignited during this exposure. Shrinkage in the transverse dimensions of the specimen was noticed. The explanation offered for lack of ignition was that at low temperatures decomposition proceeded so slowly that the concentration of combustible gases evolved never reached the level required for ignition.

In other work the Forest Products Laboratory (26) studied normal combustion preceeded by pyrolysis. If wood were heated in the absence of air four zones were formed progressively: zones A, B, C and D over the temperature ranges of 0-200°, 200°-280°C, 280°-500°C, and above 500°C, respectively.

First, Zone A formed and with continued heating, this zone moved inward (away from the heating source) giving place to Zone B and so on. The details of chemical species in each zone were described. At the start (Zone A), the surface became dehydrated and evolved water vapor, with perhaps traces of CO_2, HCOOH, CH_3COOH and glyoxal. Then Zone B set in with the evolution of the above products and some CO. Thus far the pyrolysis remained slow and endothermic. In Zone C active pyrolysis set in and the reaction became exothermic. The flammable tars and other combustible gases diluted with water and CO_2 appeared as smoke. The char of Zone B now turned to charcoal. Secondary pyrolysis, i.e., further pyrolyzing of products of initial pyrolysis, occurred. The process at this stage again became endothermic. In Zone D more highly combustible products were produced.

The course of combustion when wood was heated in air was similarly classified into zones but was modified by oxidation reactions, and, after ignition, by combustion of pyrolysis and oxidation products. According to this article, when wood ignited spontaneously it was the charcoal that caught fire first when the first dense emission of gases cleared giving way for air to come in contact with the surface. This view seemed to be in agreement with the measured temperature of spontaneous ignition of wood by investigators such as Lawson and Simms (47), 350°-450°C; Fire Research Board (23),

380°C; Fons (24), 343°C; Hawley (38), above 300°C; and Jones and Scott (40), 270-290°C. The spread in the temperature of spontaneous ignition reported by the different investigators could be due to different experimental conditions such as heating rate, etc.

There was also a discussion of several pyrolysis products that supported combustion and on how to prevent or reduce such effects. In discussing the possibilities of ignition, charcoal was stated as having only one third to one half the thermal conductivity of wood and that this was the chief reason that charcoal retarded penetration of heat and delayed the attainment of the exothermic state. According to Brown's findings, the thermal conductivity of char was much higher than that of wood which suggests the incorrectness of the above theory.

Beall (8) used DSC (differential scanning calorimetry) to determine heats of reaction. The various advantages involved in using DCA for this purpose were outlined. DSC measurements were reported as being sensitive to changes in sample mass porosity or thermal conductivity which altered the baseline or reference. The effects of particle size on the baseline drift were not definite.

Sergeeva and Vaivads (63) degraded birch cellulose in air and obtained DTA thermograms. According to them the various zones were classified as: endothermic peak 95°-100°C exothermic peak from 259°-389°C, endothermic peak 500°-524°C.

The study of Sergeeva and Vaivads covered DTA analyses of lignin, hemicellulose and wood. DTA studies on wood reviewed by their paper are as shown in Table II-2.

DTA curves for cellulose, lignin, hemicelluloses, and hard and soft woods were drawn at a heating rate of 10°C/min in nitrogen. Filter paper and powdered cellulose produced almost identical thermograms, but the powder had a slightly lower heat of reaction during the main endotherm. The lignins showed considerable difference in thermograms probably due to different carbohydrate content, molecular weight, or variations in lignin structure. The softwood hemicelluloses which were referred to as softwood xylans differed considerably from those of hardwood xylans. Thermogram of hardwood xylan showed an endothermic peak between 200° and 250°C while that of softwood xylan exhibited an exothermic peak between 250° and 300°C. An oscillatory pattern in the region 25° to 400°C with cellulose endotherm at 380°C was present in the hardwood thermogram. In the softwood thermogram the curve was smooth but for the cellulose endotherm at 380°C. It is claimed that this feature could be used to classify hardwoods from softwood. However, the individual species could not be identified using this feature.

Kung and Kalelkar (46) developed a model which included mechanisms for transient conduction, internal convection, thermal properties, Arrhenius decomposition and heat of reaction. They assumed cylindrical samples of 1 cm radius

TABLE II-2

REVIEW OF DTA STUDIES BY SERGEEVA AND VAIVADS (63)

Investigators	Types of Wood	Observations
Sergeeva, Vaivads (1954) (63)	Air-dry birch	Peaks exhibited by different components were distinguishable in the thermograms.
Keylwerth, Christoph (1960) (42)	Birch, beech, teak, oak, spruce, pine, larch, poplar and black locust	No difference in the nine species.
Arsenau (1961) (4)	Powdered balsam fir in air	Wood thermogram was a composite of individual component thermograms.
Domansky, Rendos (1962) (19)	Spruce, beech, alder, poplar, oak, white birch (all oven-dry)	Same as above.
Sandermann and Augustin (1963) (61)	Powdered beech and spruce. Also synthetic wood.	Only lignin exotherm appeared consistently in all samples.
Domburgs and Sergeeva (1964) (20)	--	Optimum heating rate 6°C/min for undiluted 1 gm sample. Most convenient particle size: 100-200 m.
Domburgs, et al. (1966) (21)	Birch, xylan, lignin, cellolignin, cellulose, holocellulose	Normal wood thermogram was explained by interactions among wood components.

in their theoretical model. They contended that Roberts and Clough (54) and Tang and Neill (70) used a greatly simplified model using transient heat conduction and a single Arrhenius decomposition rate. However, pyrolysis seemed to consist of several competing reactions rather than just one and hence more than one Arrhenius decomposition rate steps needed to be used in order to have a more comprehensive model. However, in their study Kung and Kalelkar also used only a single Arrhenius decomposition rate.

The assumptions made by Kung and Kalelkar need to be commented upon:

1. The fuel volatiles were regarded to be in close thermal contact with the solid as they flowed out through the solid following their generation. This is a reasonable assumption, as they explained later.
2. Secondary char cracking reactions were neglected--there was no experimental evidence as to how influential the secondary pyrolysis was. This neglect of secondary reactions was one limitation of their model.
3. The energy accumulation of the gaseous species within the solid was ignored. This assumption is also reasonable.
4. The moisture migration toward the center of the solid was ignored--this assumption was fairly reasonable so long as the samples were fairly dry.

The main aim of their study seemed to be the development of a model consisting of all dimensionless groups. The thermal conductivity of char was obtained under the assumption that it was less than the virgin wood value by a factor proportional to the density reduction between virgin and charred wood. This certainly weakens their work involving thermal conductivity since the measured data of Brown clearly showed that the thermal conductivity of char actually increased over that of virgin wood.

Kung and Kalelkar used their theoretical model to generate some typical temperature and density profiles as a function of time using an endothermic energy of pyrolysis. They observed that the rate of pyrolysis was sensitive to the specific heat of char, to the thermal conductivity, and also to the heat of reaction.

They also observed that most investigators mistook endothermic pyrolysis for exothermicity since the temperature at the center of a cylindrical piece of wood rose higher than at the surface at the end of a pyrolysis process. This was explained by considering the equation

$$L(T) = (-Q_p) + hg - \left(\frac{\rho_w}{\rho_w-\rho_f}\right) c_{p_w} T + \left(\frac{\rho_f}{\rho_w-\rho_f}\right) c_{p_f} T \qquad \text{(II-11)}$$

where $\rho_w/(\rho_w-\rho_f)$ = the mass of active material consumed per unit mass of volatiles generated (dimensionless)

$\rho_f/(\rho_w-\rho_f)$ = the fraction of char produced (dimensionless)

$$hg = \int_{T_\infty}^{T} c_{p_g}\, dT \quad \text{(cal/gm)}$$

$L(T)$ = effective local heat of vaporization at temperature T (cal/gm)

Q_p = heat of reaction (cal/gm)

c_{p_g} = specific heat of volatiles (cal/gm-°C)

ρ_w = virgin wood density (gm/cm^3)

ρ_f = char density (gm/cm^3)

c_{p_w} = specific heat of virgin wood at ambient temperature (cal/gm-°C)

c_{p_f} = specific heat of char (cal/gm-°C)

Since they assumed that the specific heat of virgin wood was higher than that of char, it would be seen that as T increased, $(\rho_w/[\rho_w-\rho_f])c_{p_w}T$ increased more than $(\rho_f/[\rho_w-\rho_f]) \times c_{p_f}T$ so that the value of L(T) decreased. They argued that for high T the entire expression would be negative, and in addition, Q_p had the effect of making the expression more negative. This phenomenon led to what they called thermal explosion, which caused the temperature at the central portion to rise above that of the surface. The definition of the heat of reaction as used by Kung and Kalelkar is ambiguous. Because of this the relationship between L(T) and Q_p does not make sense. L(T) has been referred to as local heat of vaporization. Q_p has been used as heat of pyrolysis. The main purpose of their work seemed to be to develop a model using dimensionless groups even if they had to make some invalid assumptions.

A study of the initial stage in pyrolysis of veneer wood and Ponderosa pine sapwood was conducted by Browne and Tang (68). Tests also were run on some samples impregnated with inorganic salts. The pyrolysis of cellulose not only started at a higher temperature than that of wood or lignin but was also more rapid. This result was explained by the nature of the macromolecules. Cellulose was considered to be a single monomer forming a polymer while lignin was considered as more intricate due to its varied constituents. They studied the effects on pyrolysis caused by treating wood with salts of sodium, potassium, ammonium, etc., by comparison with data obtained from untreated wood specimens. They observed that salts tended to lower the temperature of onset of pyrolysis. However, the extent to which a salt might lower the temperature at which pyrolysis began depended more on the nature of the salt than on the quantity of salt in the wood. They further noticed an increase in the amount of char with treated woods. They stated that in trying to record the weight loss data, the initial 35 percent of the weight loss had to be ignored as it occurred during the heating period before the sample attained the constant furnace temperature. They plotted percent weight loss versus sample temperature from which they found k (velocity constant) values for different temperatures. Then by using these k values in the Arrhenius equation

$$k = Ae^{-E/RT}$$

or

$$\ln k = C - E/RT$$

and plotting ln k versus 1/T they found E, the activation energy (-E/R is the slope of the above line).

After measuring DTA, TGA and DSC data for wood specimens treated with different salts and using untreated wood thermograms as reference, Browne and Tang arrived at certain conclusions. Noteworthy among them were: The inorganic salts they tested fell into four categories as far as their effects on pyrolysis were concerned, namely, ineffective flame retardants, very effective flame retardants, moderately effective flame retardants and those which lowered the temperature of active pyrolysis and changed the pattern of volatilization.

Two weak points of their work seemed to be the assumption of first-order kinetics, and isothermal pyrolysis study where the sample underwent considerable reaction in being raised to the temperature of interest.

Beall (7) contended that though the structural components of wood consisted of cellulose, hemicelluloses and lignin, more attention was given to cellulose and not so much to hemicelluloses and lignin. In his work five forms of lignin and nine preparations of hardwood and softwood hemicelluloses were studied by means of TG. The structures of lignin and hemicelluloses were discussed in some detail.

The kinetics were evaluated by differential difference method using

$$-\frac{dW}{dt} = kW^n \qquad \text{(II-12)}$$

where w is the weight at time t. The Arrhenius-type relation between k and T is taken as

$$k = Ae^{-E/RT}$$

Substituting in II-12 yields

$$-\frac{dW}{dt} = Ae^{-E/RT}\ W^n$$

$$\ln\ (-\frac{dW}{dt}/W^n) = \ln A - E/RT$$

or

$$\ln\ (-\frac{dW}{dt}) - n \ln W = \ln A - E/RT \qquad \text{(II-13)}$$

where E = activation energy (cal/gm-mole)

n = order of reaction

A = pre-exponential factor (min^{-1})

W = weight loss fraction

k = velocity constant (min^{-1})

t = time (min)

By plotting ln (-dW/dt) - n ln W versus 1/T, the activation energy was found from the slope of the line (which yields E/R). An attempt was made to determine the order of reaction from the pyrolysis data. Hard and soft wood hemicelluloses were treated the same way. Degradation of hard and soft wood hemicelluloses was compared with the behavior of cellulose and lignin. It was observed that all hemicelluloses decomposed similarly in the final stages. Beall

suggested that further research should be carried out in studying the behavior of compressed wood (wood boards obtained by compressing sheets of wood) under fire conditions.

The effect of low concentrations of flame retardants on the kinetics of pyrolysis was studied by Tang and Neill (70). The flame retardants investigated were $Na_2B_4O_7 \cdot 10H_2O$ $AlCl_3 \cdot 6H_2O$, $KHCO_3$ and $NH_4H_2PO_4$. They were found to lower the active pyrolysis temperatures and to increase the yield of char.

In the above investigation the kinetics of pyrolysis were examined by the difference method of Freeman and Carroll (30) and Anderson and Freeman (3) who derived the equation

$$\frac{\frac{-E}{2.3R}\,\Delta\left(\frac{1}{T}\right)}{\Delta \log w_r} = -n + \frac{\Delta \log (dw/dt)}{\Delta \log w_r} \qquad \text{(II-14)}$$

where E = activation energy of reaction (cal/mole)

n = kinetic order of reaction

T = absolute temperature (°K)

R = gas constant (1.987 cal/°K-mole)

$w_r = w_c - w$ (mg)

w_c = weight loss at the completion of reaction (mg)

w = weight loss at the completion of reaction up to time t (mg)

They plotted $[\Delta \log(dw/dt)/\Delta \log w_r]$ versus $[\Delta(1/T)/\Delta \log w_r]$ so that the slope yielded $-E/2.3R$ and the intercept yielded $-n$.

The data Tang and Neill obtained agreed with the above plot for $n = 1$ for most of the pyrolysis. However, the data

obtained in the initial stages of pyrolysis showed a lot of scatter. The authors then proposed a pseudo-zero order reaction (n = 0) and found the initial stage data fit the model well. They suggested that this difference in the behavior of data could be due to different mechanisms for the initial stage of pyrolysis and the later stages of pyrolysis, and magnification of errors by the difference method in the initial pyrolysis data where weight loss was small.

They observed that for α-cellulose treated with $Na_2B_4O_7 \cdot 10H_2O$ the intensity of flaming was reduced because less tar was made available. However, glowing combustion continued and contributed an increased amount of heat because of the greater yield of char.

Heat of pyrolysis was estimated by obtaining DTA thermograms of samples and measuring the area under the curve (graphical integration). Then the heat of reaction was obtained by using

$$(\Delta H_s) = \frac{A_s w_r}{A_r w_s} (\Delta H_r) \qquad \text{(II-15)}$$

where ΔH_s = heat of reaction of the sample (cal/gm)

ΔH_r = known heat of reaction of reference substance (cal/gm)

w_s, w_r = weight of sample and reference substances, respectively (gm)

A_s, A_r = integrated area under DTA curve for sample and reference, respectively (cm^2)

They concluded that since the end products of complete combustion of both treated and untreated α-cellulose were the same, the total heat of combustion must be practically the same but for the heat effects due to the chemical used in the flame retardant treatment.

The heat of combustion was calculated from the integrated area of the thermogram. The heat of combustion obtained by oxygen bomb calorimeter was 12 percent higher than that obtained from DTA. Tang and Neill suggested that the lower value in the case of DTA could be due to a loss of unburned volatiles in the gas stream.

Brenden (9) found that at 350°C the pyrolysis products, if quickly withdrawn from the pyrolysis zone, could be separated by vacuum distillation into four fractions: char residue, low vapor pressure tar, water, and "non-condensable" gases. Most salts tended to increase the char and water fractions and decrease the proportion of the tar fraction. The reduction in the tar fraction was characteristic of fire-retardants since tars constitute the flammable part of the pyrolysis products.

Brenden stressed that the purity of the samples might be of prime importance and would have been a cause of the errors in the current ideas about cellulose decomposition.

Quantitatively, very small amounts of chemicals (of the order of one percent) markedly affected pyrolysis, decreasing tars and increasing char, water and gases. Also, small

concentrations of various chemicals were less effective at 250°C than at 350°C in altering the composition of the pyrolysis products.

Browne and Tang (67) reported several existing theories concerning mechanisms of flame retardance. These were coating theories, thermal theories, gas theories, and chemical theories. Coating theory held that melted or foaming chemicals trapped flammable vapors and reduced access to O_2. Thermal theories suggested that coatings insulated wood against penetration of heat. An opposite theory was that some coatings or treatments that increased the thermal conductivity of wood carried heat away fast enough to prevent the attainment of ignition temperature. Yet another explanation was that the chemical reacted endothermally causing the temperature always to be below the point of ignition.

Gas theories include the following:

1. The non-flammable gases released by the chemical diluted the flammable gases preventing the formation of a flammable gas-oxygen mixture.
2. The chemical evolved a gas that acted as a chain breaker for the free radical chain reaction on which flaming depended.

Chemical theories state that chemicals directly alter the pyrolysis of wood

1. By dehydrating the cellulose fiber to carbon;

2. Because chemicals of strong acid (base) and weak base (acid) dissociate upon heating and attack cellulose, reducing the chance of flaming; and
3. By having groups (-OH, O-etc.) which were bonded by some chemicals and held the carbon atoms of cellulose and lignin in the char preventing volatilization.

Browne and Tang also showed the calculation of the composition of the samples at the start of TGA and the percent of dry wood volatilized at various stages of pyrolysis.

Browne and Brenden (16) studied the heats of combustion of treated and untreated Ponderosa pine cylinders 1/4 in diameter and 1 in long to determine whether the volatile products released during the initial stages of pyrolysis have heats of combustion less than untreated wood. A standard oxygen bomb calorimeter was used to determine the heat of combustion of the original wood specimens and residues. The chemicals used for treatment were sodium tetraborate, diammonium phosphate and sodium chloride. The data showed that treatment of wood with any of the chemicals studied materially diminished the heat of combustion of the volatile products released during the initial stages of pyrolysis. This result means that the combustible volatile products, which are the usual source for the ignition and spread of fire, would have considerably less available heat when produced from the pyrolysis of treated wood than when produced from untreated wood.

Several factors concerning forest fuels were described by Hall (35). He suggested that "prescribed burning" meant burning that helped in causing minimum damage to the forests and general environment. For instance, he suggested the burning of easily flammable material like dry grass and small pine needles, etc., lying on the ground in a pine forest, or burning of slash in forests of the Western states, etc.

Burning forest fuels involved complex products of decomposition for which the knowledge of heats of combustion, etc., was scant. Hall described several species of trees, their physical characteristics and the chemical species involved. Further, even though many of the components in the products of combustion might be identified, quantitative measurements could have meaning only if the conditions of burning were described.

Hall gave an interesting account of air pollution stressing the fact that man's contribution to pollution was of importance only extremely locally while nature contributed to it much more on the whole. He also stated that prescribed burning of slash, etc., was only a means of minimizing forest wildfires but that slash, ground growth, etc., could be put to better use than being burned. However, the cost of converting them into usable material was more than the worth of the products with the constraints of current technology.

Rothermel (59) developed a model to predict fire-spread in wild land fuels. He used the basic model given by Frandsen (29) who applied the conservation of energy principle to a unit volume of fuel ahead of an advancing fire in a homogeneous fuel bed. From this base, by defining an effective heating number (dimensionless), propagating flux, and effect of wind and slope, Rothermel arrived at an approximate rate of spread equation. He then divided the different terms which were involved in the equation into two classes, namely those forming heat sinks and those serving as heat sources. The heat of preignition and effective bulk density were classified as heat sinks while the reaction intensity, reaction velocity, moisture damping coefficient, mineral damping coefficient and physical fuel parameters were classified as heat sources. It could be observed that Rothermel arrived at all the empirical corrections necessary to define his model by actual experimental data. Throughout his treatise this was an attractive and noteworthy feature. The assumptions he made on different occasions were reasonable and were made only because data and/or research in those areas were lacking. He measured reaction velocity experimentally (by taking the derivative of the weighing system). Reaction intensities were calculated from a derived equation using data obtained in weight loss experiments. No-wind propagation flux and the rate of spread were also calculated. He used three fuel sizes, namely excelsior beds 8 ft x 3 ft x 4-1/2 in

and 1/2 inch stick cribs. The only probable inaccuracy in measurement of reaction velocity occurred with the excelsior beds because of the difficulty in constructing a fuel bed having only a few strands of excelsior per square foot, and the lack of sensitivity of the weighing system at extremely light fuel loadings. Wind coefficient and slope coefficients were also determined experimentally.

Then Rothermel discussed the various modifications necessary for using the model to predict rate of spread and intensity in heterogeneous mixtures of fuel types and particle sizes. A unit fuel cell was defined, for this purpose, as the smallest volume of fuel within a stratum of mean depth that had sufficient fuel to be statistically representative of the fuel in the entire fuel complex. The modifications were based on the concept that a singular characteristic parameter could be found for each of the parameters involved by properly weighting the variations involved for the particular parameter in the heterogeneous mixture. In order to implement this concept, Rothermel considered the influence each fuel parameter exerted on the three characteristic features of a spreading fire, namely the energy source, the energy sink, and the flow of air or heat within the array.

Since the processes that controlled the combustion rate occurred through the surface of the fuel particle, Rothermel weighted the fuel parameters by surface area. This weight factor eliminated the problem of making arbitrary decisions as to which fuel sizes should be considered.

Using the weighting concept he formulated the model for fire spread. A single value of reaction velocity for the entire fuel complex was calculated.

It could be argued that a single value of each parameter and reaction velocity for the entire heterogeneous fuel complex would be of questionable validity. However, this simplification was the only practical means of developing a model close to reality with the multitudes of fuel varieties, environmental conditions and fuel parameters which exist in the wildland environment.

Results obtained from computations using the eleven fuel models as inputs showed variations in fire spread rate and intensity. Even if the particle size was held constant the variations existed. The variations could be attributed to the sensitivity of the input parameters and also partly to the fact that very little research has been done on the burning rates of living fuels.

The heat transfer rate to forest fuels ahead of a flaming fire front was highly variable over the interval of time required to preheat the fuels. Fosberg (27) derived an analytic function which permitted the inclusion of this varying transfer rate in the calculation of temperature rise for forest fuels. He started with the equation

$$\frac{\partial T}{\partial t} = \frac{k}{\rho c} \frac{\partial^2 T}{\partial r^2} + \frac{k}{\rho c r} \frac{\partial T}{\partial r} \qquad \text{(II-16)}$$

where T = temperature (°C)

k = thermal conductivity (cal/cm-sec-°C)

ρ = density of the fuel particle (gm/cm^3)

c = specific heat of the fuel particle (cal/gm-°C)

t = time (sec)

r = radial coordinate (cm)

By defining $\phi = (T - T_s)/(T_o - T_s)$ where T_o, T_s and T were temperatures at the start, at the surface and at time t, respectively, Equation II-16 was reduced to

$$\frac{\partial \phi}{\partial t} = \frac{k}{\rho c} \frac{\partial^2 \phi}{\partial r^2} + \frac{k}{\rho c r} \frac{\partial \phi}{\partial r} \qquad \text{(II-17)}$$

[$\phi(r,0) = 1$ because $T = T_o$ at $t = 0$ and $\phi(R,t) = 0$ because $T = T_s$ at $r = R$, the radius.]

An infinite series involving Bessel functions was obtained by solving the above equation. By using the temperature profile predicted by this equation as a new initial temperature a new ϕ could be defined so that the restriction of an initially homogeneous condition was removed. Similarly an equation for moisture content m was developed involving moisture diffusivity (instead of $k/\rho c$). Values of k, c, and ρ were obtained from the literature. Curves of time versus integral temperature for Ponderosa pine dowels were drawn. It was concluded that the distribution of temperature within the fuel particle had an effect on the rate of temperature rise along with other physical properties.

Differential thermal analyses on untreated wood (Ponderosa pine), cellulose and lignin and the same material treated with some inorganic salts were conducted by Tang and Eickner (69) in inert (helium) as well as oxidizing atmospheres using an American Instrument Co. "Thermograv." The combustion studies are not discussed here as only pyrolysis is of interest. Twenty to thirty mg of lignin or 40 to 50 mg of wood or cellulose packed in a capsule were used under nitrogen atmosphere. In the helium atmosphere 100 mg sample of each was used.

For a heating rate of 12°C/min the thermograms for Ponderosa pine runs in helium had initial endothermic absorption of energy between room temperature and 200°C with nadir at 125°C primarily due to evaporation of water. Above 200°C active pyrolysis took place. The results had both exothermic and endothermic heats of reaction (pyrolysis). According to Tang and Eickner the energy and temperature ranges observed were as in Table II-3. It was further observed that untreated samples produced a greater endothermic heat of pyrolysis than did treated samples; they also had less char residue than the treated samples. The endothermic and exothermic effects were not a measure of individual homogeneous reactions. Rather, they were the net values of opposing reactions.

Broido (13) studied thermal decomposition of α-cellulose and ash-free cellulose using the same equipment as Tang and Neill (70). His results, shown in Figure II-1, were in

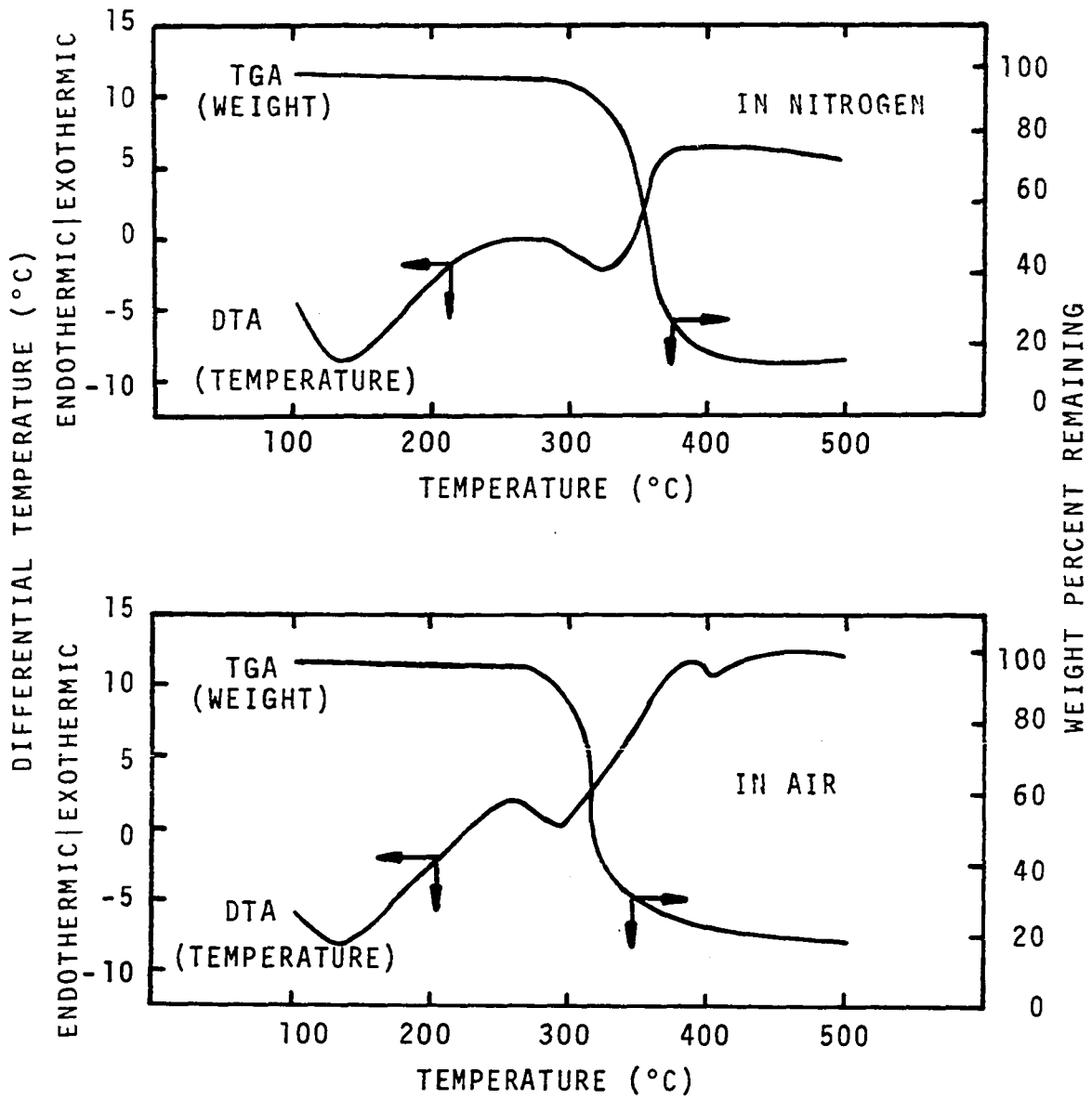

Figure II-1. DTA Results of Broido (13) for Cellulose in Nitrogen and Air.

TABLE II-3

ENERGY AND TEMPERATURE RANGES, TANG AND EICKNER (69)

Specimen	Temp Range °C	Endothermic Energy cal/gm	Temp Range °C	Exothermic Energy cal/gm
Wood (Ponderosa pine)	200-390	77	390-500	31
Cellulose	240-450	88	--	--
Lignin	190-345	19	345-500	40

obvious conflict with those of Tang and Neill. His thermograms indicated exothermic effects for cellulose above 325°C. The exothermic effect of Broido is also in conflict with the results of this study for cellulose. Broido used samples of 5 gm for each run with the samples centered in a reaction tube mounted in a vertical tube furnace. Such an arrangement could cause a lag in the sample temperature. The poor experimental set-up coupled with the sample size probably accounts for the inconsistencies in the TG and DTA curves shown in Figure II-1.

Havens (37) developed an experimental DSC procedure to measure the heat of pyrolysis for white pine and oak sawdust in a flowing nitrogen atmosphere. The same procedure was used by Brown (14) to measure the heat of pyrolysis. Thermograms obtained by Havens at a heating rate of 20°C/min are shown in Figures II-2 and II-3. Havens obtained endothermic energies of pyrolysis of 47.5 and 26.2 cal/gm, for

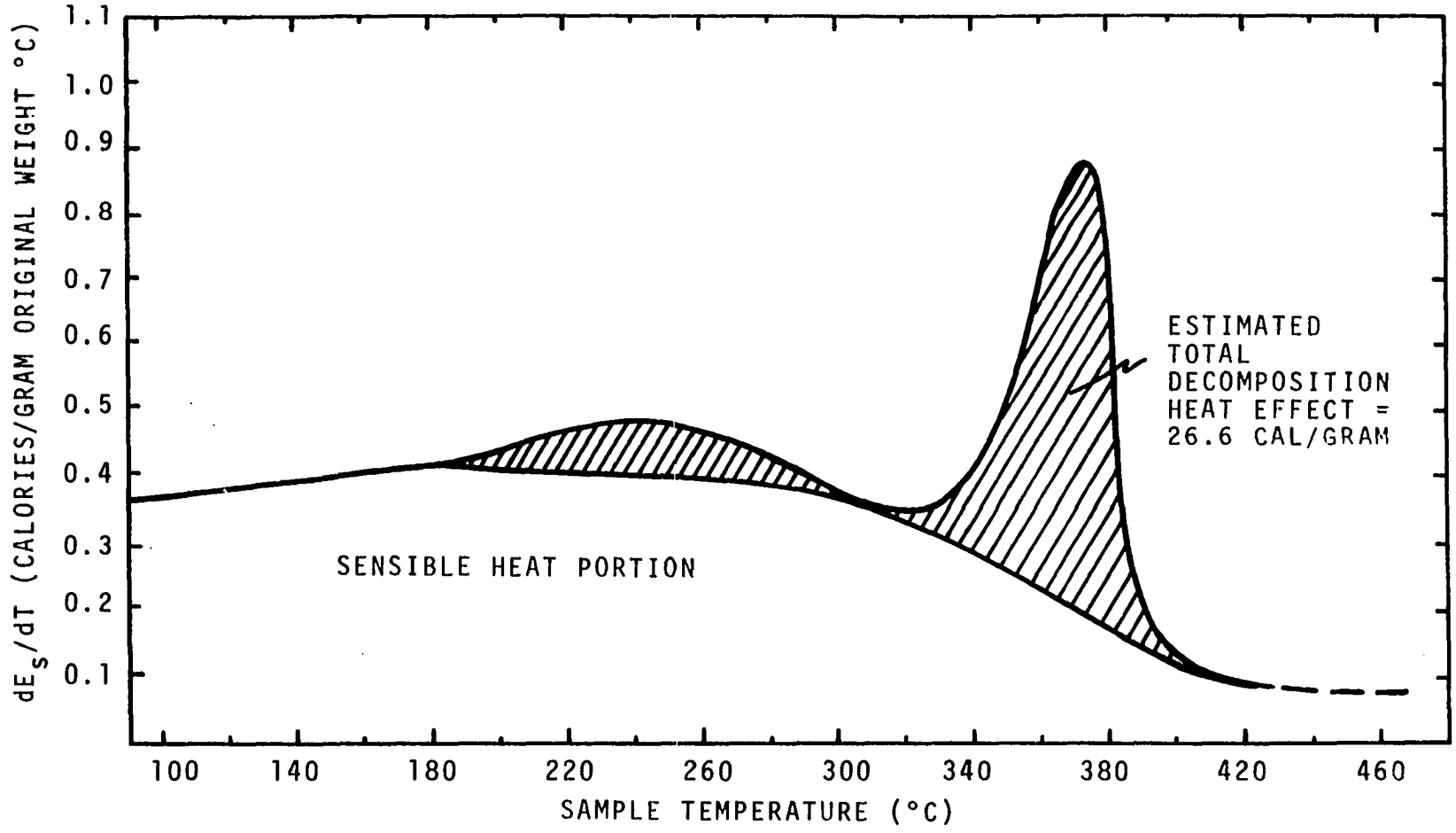

Figure II-2. "Energy Capacity" of Oak Wood as a Function of Temperature in Nitrogen Atmosphere (from Reference 37).

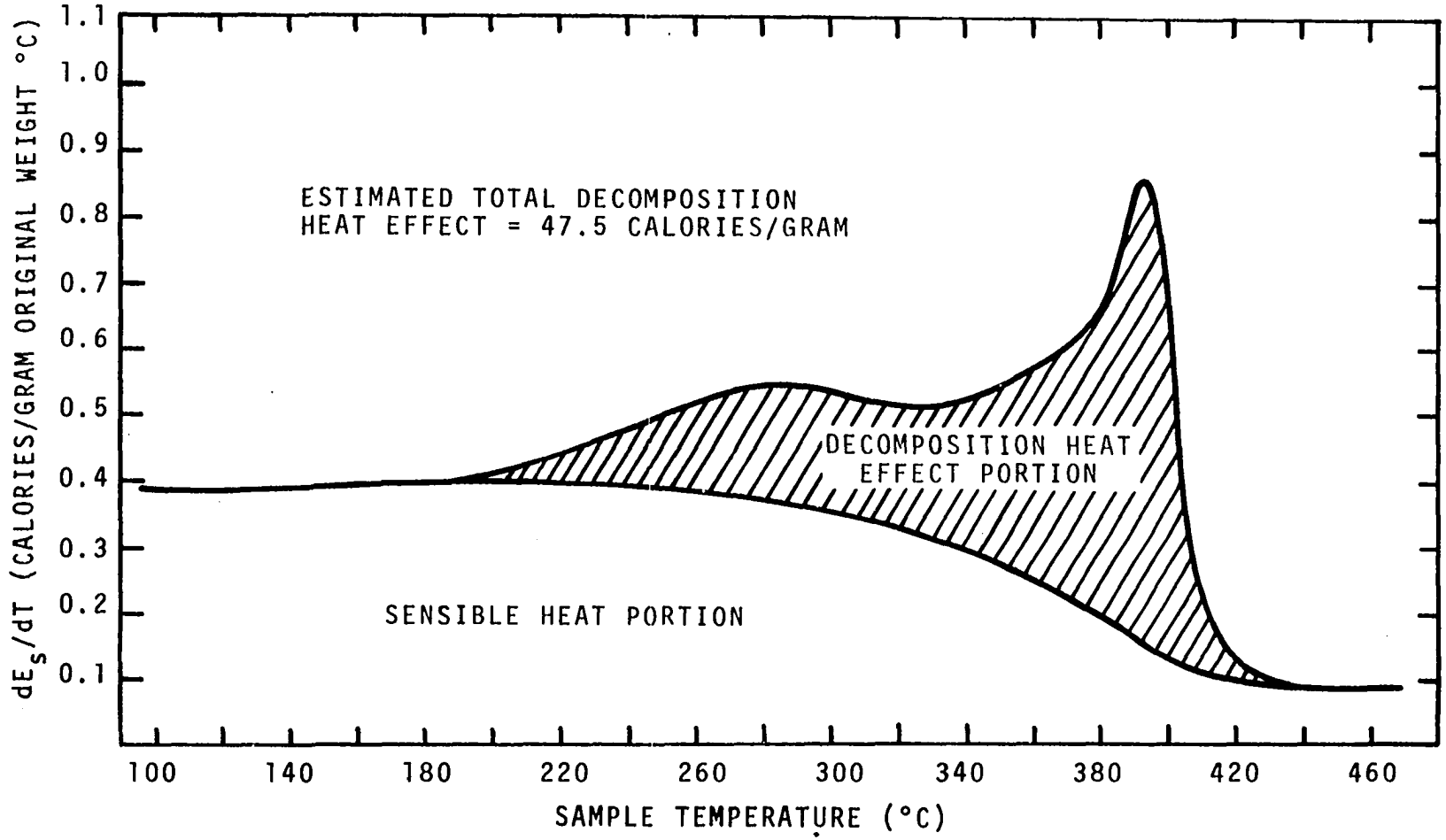

Figure II-3. "Energy Capacity" of Pine Wood as a Function of Temperature in Nitrogen Atmosphere (Based on Original Non-Decomposed Sample Weight), Showing Sensible Heat and Decomposition Effect Regions (37).

white pine and oak respectively. Brown reported 43.2 and 27.0 cal/gm (endothermic) for white pine and oak, respectively. The specific heat of 0.36 cal/gm-°C obtained by Brown for the charred residue is in good agreement with the specific heat data reported by Widell (76).

An important method of analysis relevant to this thesis is the quasi-linearization technique of Burningham and Seader (17) with regard to polymer degradation. This method utilized experimental data points directly and selected kinetic parameters by a least-square optimization procedure to best fit the data. The power law rate function considered was of the form

$$-\frac{1}{w_o}\frac{dw}{dt} = k\left[\frac{w - w_r}{w_o}\right]^n \qquad \text{(II-18)}$$

where w_o = initial weight of polymer (mg)

w_r = final weight of residue after complete degradation (mg)

w = instantaneous weight of polymer residue material during the degradation process (mg)

t = time (sec)

n = order of the reaction

$k = Ae^{-E/RT}$ (sec^{-1})

A = pre-exponential (frequency) factor (sec^{-1})

E = activation energy (cal/g-mole)

R = universal gas constant = 1.987 (cal/g-mole-°K)

T = absolute temperature (°K)

The authors assumed initial values of A, E and n and solved the equation

$$\frac{dW}{dt} = -Ae^{-E/RT} W^n \qquad \text{(II-19)}$$

where $W = (w - w_r)/w_o$, by the Runge-Kutta numerical procedure. They stated that convergence of the quasi-linearization technique was the major difficulty in its application. Good initial guesses of the values of the constants were necessary for convergence of the computer program. They actually had to use graphical methods to obtain the initial values. Besides, for the sake of positive convergence, they had to constrain one of the parameters.

The present study merits over the above method in that there was no need to assume or constrain any of the parameters as will be shown in the discussion of results.

Thermal and Physical Properties

Wood is well known to be non-isotropic and non-homogeneous. The directional grain structure, non-homogeneity and non-isotropicity result from variable growth rate as evidenced by the difference between spring wood and summer wood from the structure of the wood fibers and with their light and dark rings as stated by Havens (37).

Specific Heat

The major reference on this topic was Dunlap (22). He reported that the specific heat of 20 types of wood ranging

in density from 0.23 to 1.10 gm/cm^3 could be described by the empirical relation

$$c = 0.266 + 0.00116T \qquad \text{(II-20)}$$

where c = specific heat (cal/gm-°C)

T = temperature (°C)

Kollman (57) proposed the relation, for wet wood:

$$\bar{c}_x = X(c_w) + (1 - X)\bar{c} \qquad \text{(II-21)}$$

where $\bar{c}_x$ = mean specific heat of moist wood (cal/gm-°C)

X = moisture content as a fraction of net weight

c_w = specific heat of water (cal/gm-°C)

c = specific heat of oven dry wood (cal/gm-°C)

A comparison of the computed specific heats using Kollman's relation and those experimentally obtained for moist wood in this study is presented in Chapter IV.

Widell (76) plotted specific heat and mean specific heat of charcoal as a function of temperature. His results are shown in Figure II-4. Specific heat of oven-dry spruce pine wood and bark was studied by Koch (43). He examined wood and bark from 72 trees of spruce pine. A total of 6696 observations were made. Some of the noteworthy conclusions of Koch were:

1. For wood representative of the trees, specific heat = 0.2651 + (0.001004)T where T is the temperature in °C. Species values stratified by tree age and growth rate were established.

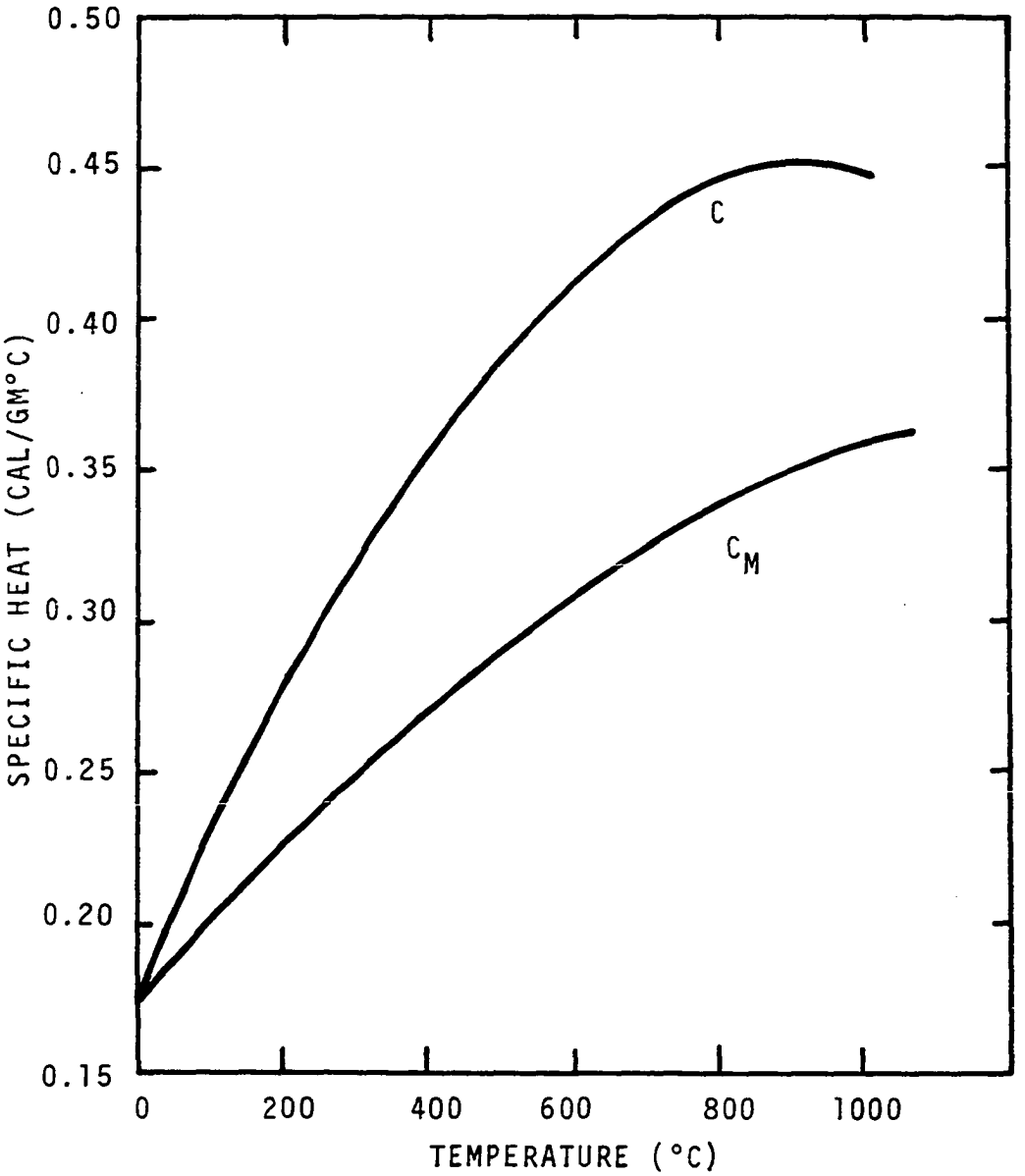

Figure II-4. Specific Heat C and Mean Specific Heat C_M for Charcoal as a Function of Temperature (76).

2. Heart wood appeared to have a higher specific heat than sap wood.
3. No sampling point was located from which specific heat for wood of the entire tree could be predicted with accuracy.

It should be noted that the conclusions of Koch are applicable only to oven dry spruce pine wood in the temperature range of 60° to 140°C. The specific heat varied from 0.3213 to 0.4086 for spruce pine of all ages and all geographic locations in the temperature range of 60° to 140°C. In his analytical study made on the specific heat of loblolly pine wood in relation to temperature, McMillin (49) reported that in the range of 60° to 140°C the specific heat of oven-dry loblolly pine wood was expressed by a linear function of temperature. Fifty loblolly pine wood trees were used in his study. Specific heats were ascertained using 144 observations on samples which were air-dried, dissected into early and late wood slivers, and ground to pass a 40-mesh screen in a Wiley mill. A Perkin-Elmer DSC-1B differential scanning calorimeter was used for the determination of specific heat. The specific heat varied over a range of 0.3215 to 0.4074 for a temperature range of 40° to 160°C. The equation developed by McMillin was

$$c_p = 0.0115321 + 0.000949T$$

where T = temperature (°K)

McMillin found no relationship of specific heat with specific gravity, growth rate, or distance from the pith, nor any difference between early and late wood in terms of specific heat.

McMillin (50) studied the specific heat of some oven-dry chemical constituents of loblolly pine wood. The constituents studied were α-cellulose, holocellulose, lignin, and alcohol-benzene extractives. Specific heats were determined using Perkin-Elmer DSC-1B differential scanning calorimeter at 60°, 100° and 160°C. The mean specific heat value for holocellulose (0.3529) was nearly identical to that for α-cellulose (0.3526). The average specific heat of lignin was somewhat lower (0.3477) and that for alcohol-benzene extractives was substantially greater (0.4770). Specific heat increased with increasing temperature for all constituents. For the range of temperatures studied, the specific heat of each constituent was found to be a positive linear function of temperature only. The higher value of specific heat for the extractives was partly attributed to the presence in the extractives of inorganic elements which have high specific heats.

Moisture Content

With the exception of Tang and Eickner's measurements (69), discussion of the transition energy involved in moisture loss when wood was heated was not found in the literature.

Even Tang and Eickner have not measured the transition energy of moist samples. Consequently, the quantitative study of the effect of moisture (on dead Ponderosa pine needles and excelsior) was carried out for the first time in this study.

Britton, et al. (12) studied the effects of relative humidity, air temperature, and wind speed on moisture content of Tobosa grass. Moisture loss was observed under ambient conditions at regular intervals for three samples maintained at 50°, 65° and 80°F at 25, 50 and 75 percent relative humidity. It was observed that even though there was rapid initial loss of moisture, after some time the loss stabilized into an exponential decay.

Density

Density versus temperature profiles were obtained by Blackshear and Kanury (8). These were discussed in detail by Brown (14) and Havens (37).

Thermal Conductivity

The thermal conductivity of wood was known to be strongly dependent on wood grain direction, local nonhomogeneities, and density variations within the specimen. Of importance in this context are the investigations of Griffith and Kaye (33), Rowley (60), Wangaard (72, 73), MacLean (48), Kanury (41), Koohyar (45), Havens (37), and Vyas (71). Kanury, Koohyar, and Havens used a transient temperature technique proposed by Chung and Jackson (18) for determining

the thermal conductivity for materials having low conductivity. Panton and Rittman (53) suggested that the thermal conductivity of pyrolyzing wood and char were linearly dependent on the conductivity of the virgin wood and the densities of the pyrolyzing wood and char.

Mita, et al. (51) measured the isothermal heat of mixing and the heat of vaporization of alcohol-benzene mixtures. They used a modified Perkin-Elmer DSC-1B in which the solute was added in small quantities to the solvent in the pan through a micro-syringe. Forty micro-liters of benzene were taken in the pan and 2 to 4 micro-liters of alcohol were injected into the cell which was maintained below the boiling point of benzene (40°C). The cell was closed so that only the micro-syringe could get through the cover on the cell and the sample pan. Endothermic thermograms were obtained for stepwise addition of ethyl alcohol. The total ethyl alcohol added was plotted against the cumulative heats of mixing at each step. The accuracy was checked by plotting points for different amounts of alcohol added at each step. The same procedure was repeated for pyridine (solute) and acetic acid (solvent) to obtain exothermic mixing. Thermograms were also obtained for vaporization of benzene. At best it could be said that the above method is simple, rapid, and useful for rough estimation of the heat of vaporization of a liquid at its boiling point.

Brennan and others (11) used DSC-1B to measure the thermal conductivity of cylindrical samples of PTFE (poly-tetrafluoro-ethylene). They used two cylinders of identical shape and size (an unknown, x, and a reference, R). With the recorded DSC output and the value of ΔT across the pair it was possible, once the steady-state conditions were achieved, to determine the thermal conductivity of the unknown by using the Fourier equation of heat flux. Thus

$$q_1 = k_R(A/L)(T - t) \qquad \text{(II-22)}$$

$$q_2 = k_x(A/L)(T - t) \qquad \text{(II-23)}$$

where q_1, q_2 = DSC output

A = cross-sectional area of the sample (cm^2)

L = length of the sample (cm)

T = DSC temperature setting (°C)

t = thermocouple readout (°C)

k_x, k_R = sample and reference thermal conductivities (cal/cm-°C-sec)

Subtracting II-23 from II-22 yields

$$q_1 - q_2 = (A/L)(T - t)(k_R - k_x) \qquad \text{(II-24)}$$

or

$$k_x = k_R - \frac{(q_1 - q_2)}{(A/L)(T - t)} \qquad \text{(II-25)}$$

In a somewhat simplified method, only the cylinder with unknown conductivity was used while the reference side was capped to suppress its heat loss. During this operation, q_1 was

approximately zero, and the DSC output became q_2. Thus k_x could be directly calculated from Equation II-25.

Rogers and Morris (56) used the DSC-1B to measure the emissivity coefficients with the DSC. The net emissivity of the sample was plotted against the correction due to changes in emissivity of the sample with temperature as the parameter. The effect of operating conditions on thermal emissions was also demonstrated by obtaining thermograms of (a) benzoic acid in open sample pan at room temperature; (b) benzoic acid in an open pan maintained at 120°C; (c) benzoic acid in open pan with reference and sample pan supports covered by polished gold pan covers. Painting the inside of the pan covers with optically black paint was suggested. This was indeed done during the course of the present study with excellent results. The disagreement of their emissivity data with published data was attributed to the profound effect that impurities, surface roughness, and extremely thin coatings have on the radiation properties of surfaces.

In another study Rogers and Morris (57) demonstrated the use of DSC measurements to calculate the rate constants and activation energies. They claimed that the method they developed was ideally suited to the study of the decomposition kinetics of organic explosives. The activation energies of $KMnO_4$, PETN, tetryl, etc. (explosives), were calcualted using the expression

$$-E = \frac{R \log (d_1/d_2)}{1/T_1 - 1/T_2} \qquad \text{(II-26)}$$

where d_1 and d_2 were any two distances from the baseline to the thermogram at any two absolute temperatures T_1 and T_2. Because a ratio of the displacement was used the proportionality constants cancelled out. Neither the sample weight nor the heat of reaction needed to be known to calculate the activation energy.

This method is not foolproof by the authors' own admission. Compounds that are quite volatile below their decomposition range cannot be studied by this method. Difficulties could be encountered in the measurement of exothermic reactions. The heat flux from the sample can exceed the rate at which energy is supplied by the instrument and heat can be lost through the thermal resistance of the instrument to its surroundings.

Guttman and Flynn (34) showed a method of drawing the baseline for the differential scanning calorimetric calculation of heats of transition. It was suggested that the correct baseline could be obtained by extrapolating the heat capacities of the initial and final temperature states to the transition temperature. Essentially an attempt was made to show that the correction required in such an extrapolation was small enough to be neglected.

Brennan, et al. (10) examined some standard baseline interpolations and pointed out the dangers of such interpolations. They proposed a method for the determination of the true baseline. It was suggested that three runs be made to establish the true baseline. These were empty pan run, sample-in-one-pan run, and recycled product run. The baseline run was then established by an iterative procedure. The three required runs are shown in Figure II-5. The iterative procedure is as follows:

1. An indicated straight line between initial point A and final point B is assumed.
2. Trial values of f, the weight fraction reacted, are calculated at various points during the event, for instance at point M, by the relationship

$$f = \frac{\text{Area I}}{\text{Area I + Area II}} \qquad \text{(II-27)}$$

3. Using these values of f the sensible heat effects due to the reactant and product at the same points are calculated.
4. The sensible heat effects of the previous step are added at different points to yield a revised baseline and a new f is calculated from this revised baseline.
5. Iterations are carried out until the baseline does not change.

Rogers (55) used a method for the direct determination of reaction rate constants of cupferron tosylate decomposition by the differential scanning calorimeter. A first order

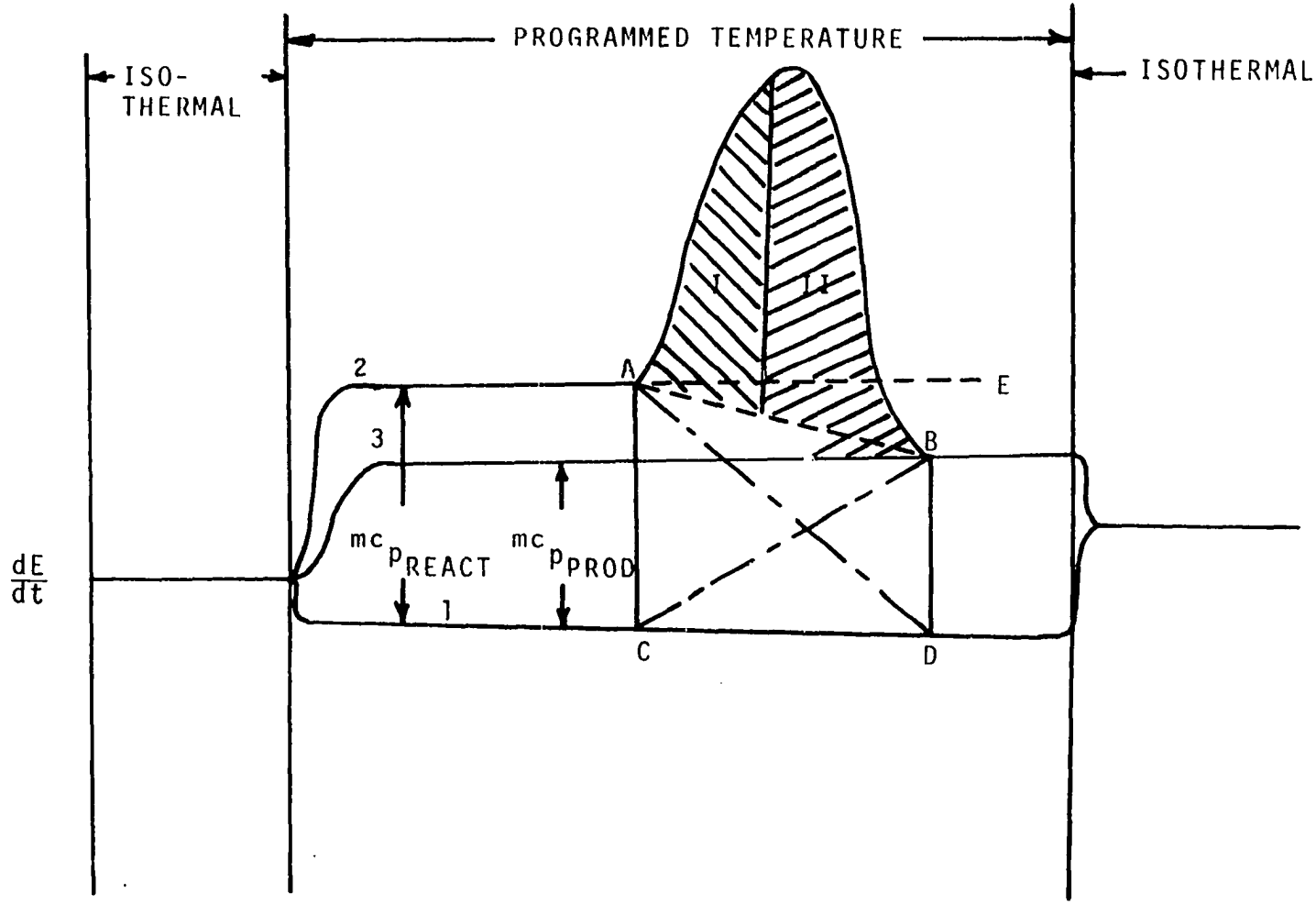

Figure II-5. Construction for the Calculation of True Baseline by Brennan, et al. (10).

reaction was assumed. If the deflection of the thermogram above the baseline was b, then

$$\alpha b = \beta \frac{dq}{dt} = k(1 - a) \qquad \text{(II-28)}$$

where q = energy absorbed or released by the sample (cal)

α, β = proportionality constants

a = weight of the reactant at time t (mg)

k = rate constant (min^{-1})

Hence,

$$\ln b = \ln (k/\alpha) + \ln (1-a)$$

For a first order reaction,

$$-\ln (1-a) = kt + c$$

where c is a constant, i.e., $\ln b = C - kt$, where C is $\ln (k/\alpha) - c$. Hence rate constants for first order reactions can be directly obtained from a plot of ln (deflection) versus time.

O'Neil (52) gave a detailed account of measurement of specific heat functions by differential scanning calorimetry and the merits of this method over adiabatic or drop calorimetric methods, both of which lack precision at transition temperatures in the sample material. Adequate resolution of sharp transitions is possible only at extremely slow scanning rates, and with a resultant loss in sensitivity and signal-to-noise ratio. The heat flow rate into the sample in the DSC is given by

$$\frac{dH}{dt} = mc_p \frac{dT}{dt} \qquad \text{(II-29)}$$

where $\frac{dH}{dt}$ = energy flow rate (cal/sec)

m = sample mass (gms)

c_p = sample specific heat (cal/gm-°C)

$\frac{dT}{dt}$ = heating rate (°C/sec)

If m', c_p' are the corresponding quantities for a material of known specific heat such as synthetic sapphire, and y and y' are the ordinate displacements due to sample and sapphire in that order,

$$Ky = mc_p \frac{dT}{dt} \qquad \text{(II-30)}$$

for the sample, and

$$Ky' = m' c_p' \frac{dT}{dt} \qquad \text{(II-31)}$$

for sapphire, where K is the calibration constant for the instrument in cal/in-sec. Dividing Equation II-30 by Equation II-31 yields

$$\frac{c_p}{c_p'} = \frac{m'y}{my'}$$

It can be seen that the calculation of specific heat by this method would be correct even if the ordinate calibration and the heating rate were temperature dependent.

O'Neill demonstrated the accuracy of specific heat measurement by DSC by measuring the specific heat of gold,

diamond, graphite, polycarbonate, and silver nitrate in the range of 27° to 277°C.

Rogers and Smith (58) proposed a simple method for the estimation of A, the pre-exponential factor, knowing E, the activation energy. It should at once be pointed out that the method is valid only for first order reactions and that the accuracy of estimation of A depends upon the accuracy of determining the activation energy. The rate law for a first order decomposition can be written as

$$b = \alpha m A e^{-E/RT} \qquad \text{(II-32)}$$

where b = deflection of the DSC curve from the baseline
$= -\alpha\, dm/dt$

α = heat of reaction per unit weight of the sample divided by the sensitivity factor of the instrument

$-\frac{dm}{dt}$ = rate of decomposition of the sample (gm/sec)

E = activation energy

R = universal gas constant

T = absolute temperature

Differentiation of Equation II-32 yields

$$\frac{db}{dt} = \alpha \frac{dm}{dt} A e^{-E/RT} + \alpha m A e^{-E/RT} \frac{E}{RT^2} \frac{dT}{dt}$$

$$= -bAe^{-E/RT} + \frac{bE}{RT^2} \frac{dT}{dt} \qquad \text{(II-33)}$$

At the maximum rate of weight loss, db/dt = 0, which yields

$$A = (BE\, e^{E/RT_{max}})/RT_{max}^2$$

where B = dT/dt

T_{max} = absolute temperature corresponding to the peak rate of weight loss

Rogers and Smith used this method to determine the pre-exponential factor for Tetryl (N-methyl-N,2,4,6-tetranitro-aniline), PETNC (pentaerythritol tetra nitrate), and RDX (hexahydro trinitrotriazine).

CHAPTER III

EXPERIMENTAL PROCEDURE

The experimental techniques and apparatus devised to obtain data seem to undergo continuous modification in order to achieve a better degree of accuracy. The present study is no exception to this observation. Experiments were undertaken to obtain data capable of kinetic analysis for five different species of wood, namely, dead Ponderosa pine needles, excelsior, cellulose, saltbush leaves and a decayed form of Douglas fir snags consisting essentially of lignin which will be referred to as "punky" wood. Dead Ponderosa pine needles and excelsior extracted with ether for 176 hours were also examined. The extracted dead Ponderosa pine needles and excelsior have been referred to as extracted Ponderosa pine and extracted excelsior in this thesis. Additionally, data on larch wood also was obtained to provide a further corroboration of the proposed model. The chemical analyses of the above samples are shown in Appendix D. The materials were provided by the Northern Forest Fires Laboratory, Missoula, Montana.

Equipment

Weight loss data required for kinetic analysis of the results from the degradation studies were obtained by means of a Perkin-Elmer TGS-1 thermobalance and UU-1 temperature control unit. A photograph of this equipment is shown in Figure III-1. The TGS-1 thermobalance has the capability of internally differentiating the weight loss signal with respect to time and giving an output signal of this derivative. However, the TGS-1 can only send one signal, either the weight loss or the rate of weight loss (the derivative), at one time. This design made it necessary to run a sample of a material separately in two runs to obtain the two outputs. Hence, the advantage of being able to obtain and relate the weight loss and the rate of weight loss data for the same run was lost. In order to facilitate this simultaneous observation of the two output signals, an additional accessory, the Cahn No. 3100 time derivative computer Mark II, was obtained. It is shown in Figure III-2. A Texas Instruments Servowriter-II was used to record the output signals from the thermobalance. The chart paper used in the recorder had a span of 25 cm.

As the name suggests, the TGS-1 electrobalance mainly consists of a sensitive balance with provision for heating a sample. The sensitive weighing mechanism, the Cahn-RG electrobalance, is capable of detecting weight changes of 10^{-6} grams. A fine "hang-down" wire (nichrome) free of kinks is suspended

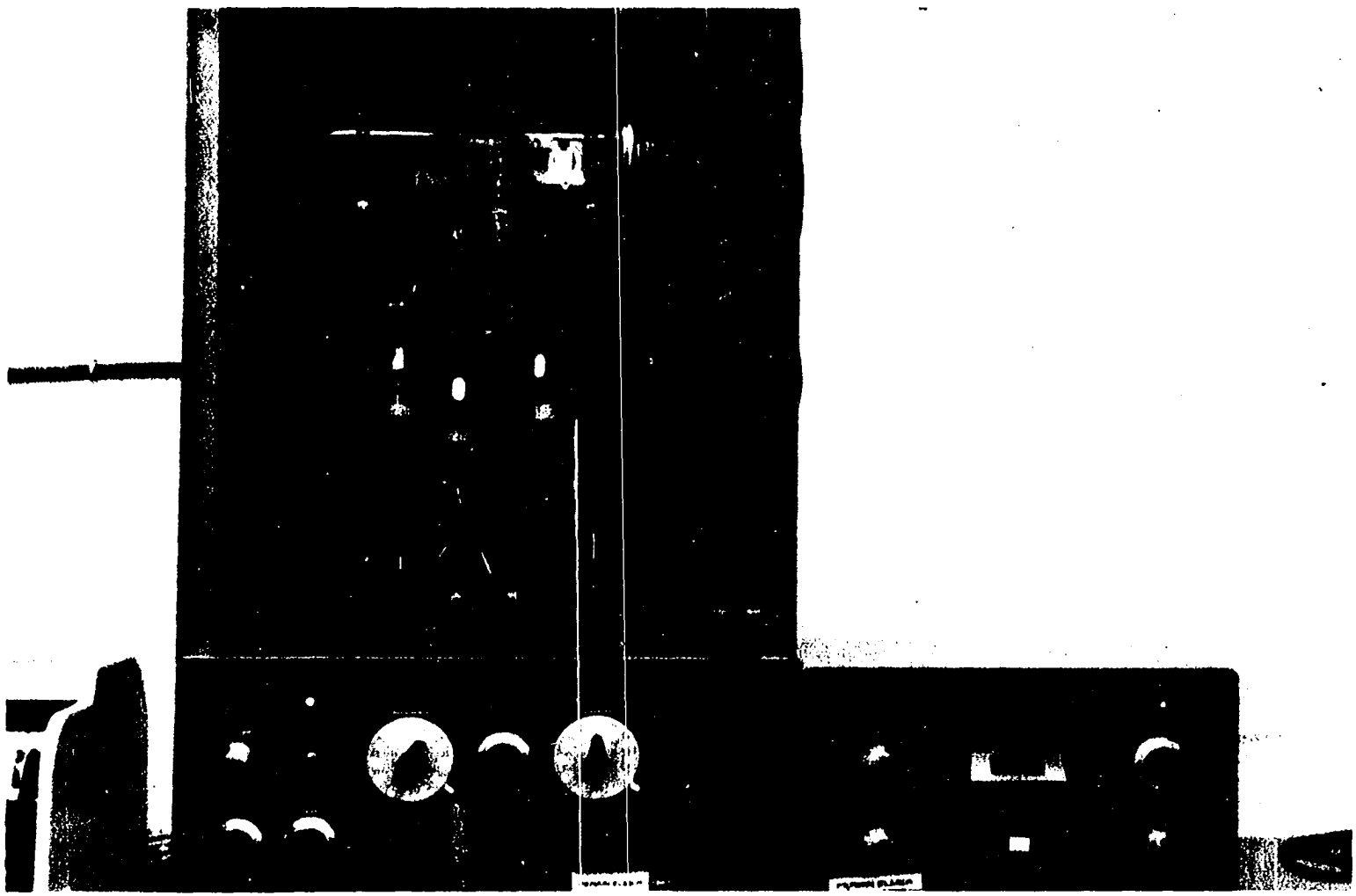

Figure III-1. Perkin-Elmer TGS-1 Thermobalance and UU-1 Temperature Controller.

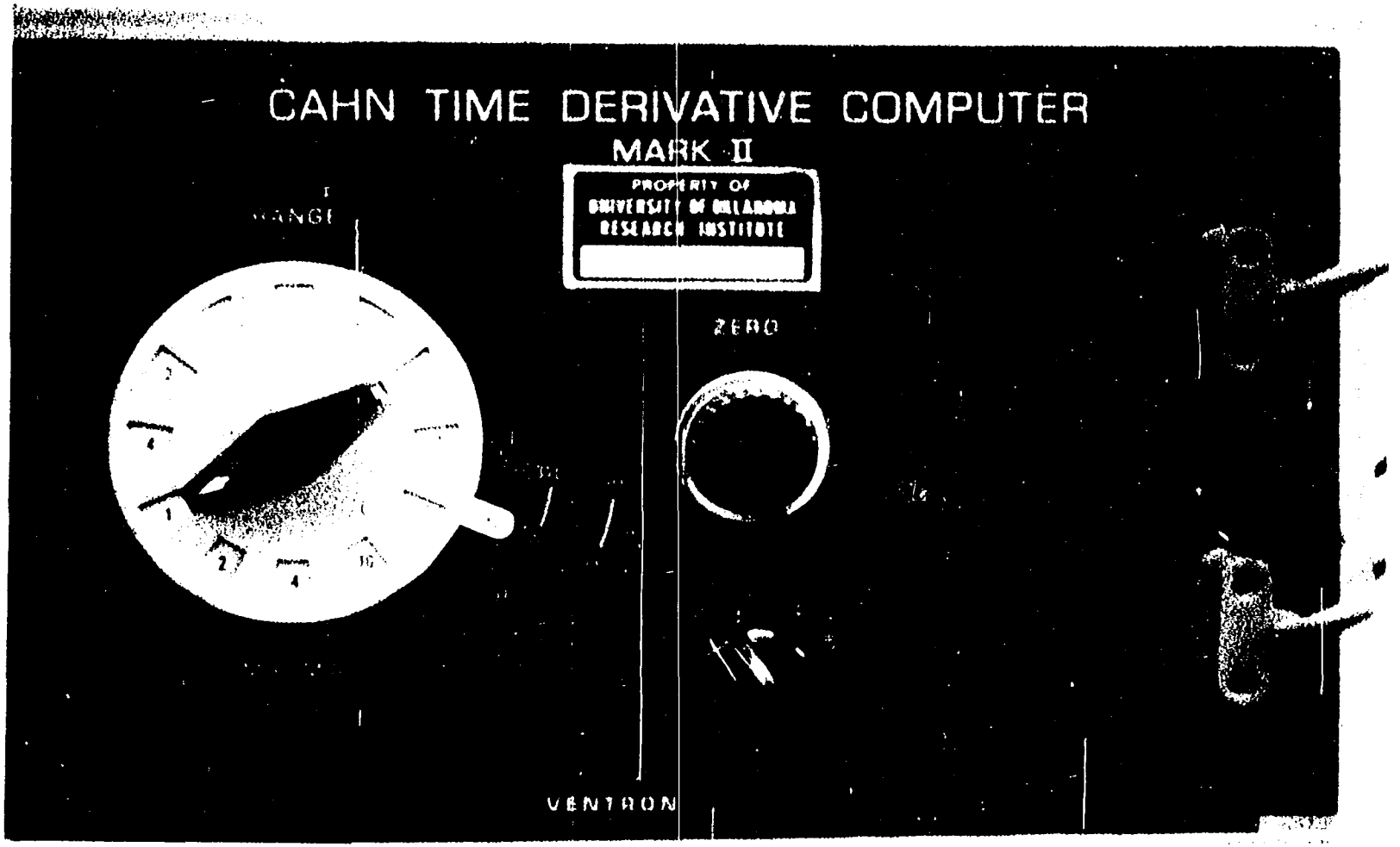

Figure III-2. Cahn Time Derivative Computer.

from one arm of the beam. The wire measures about 7 cm in length and has an end hook at the free end. A stirrup holding a pan hangs from the end hook. When assembled properly, the hang-down wire with the stirrup and pan is suspended freely through a flat baffle ring located about 1/2 in above the top of the furnace. The baffle plate assembly is shown in Figure III-3. The baffle plate helps to reduce air (or nitrogen) motion above the furnace. The furnace used to heat the sample surrounds the sample pan and extends approximately 1/2 in above the level of the pan. A 6-mil platinum wire wound cylindrically in a 3/8 in diameter ceramic cylinder and connected to the external lead wires through a 1/16-in diameter stem provides the heat to the furnace. The platinum wire is shielded by a thin coating of insulating material. The furnace acts as both heater and temperature sensor. A schematic drawing of the baffle plate, hang-down wire, furnace assembly, and the weighing mechanism is shown in Figure III-4. The hang-down wire serves two extremely important purposes in isolating the test sample from the weighing mechanism. First, the length of the hang-down wire is such that in spite of the high temperature developed in the furnace the weighing mechanism is maintained at ambient temperature. Second, enough isolation is provided so that the product vapors (due to pyrolysis or combustion) are swept away by the purge gas and do not come into contact with the delicate parts of the weighing mechanism. The base of the furnace assembly is a plug that

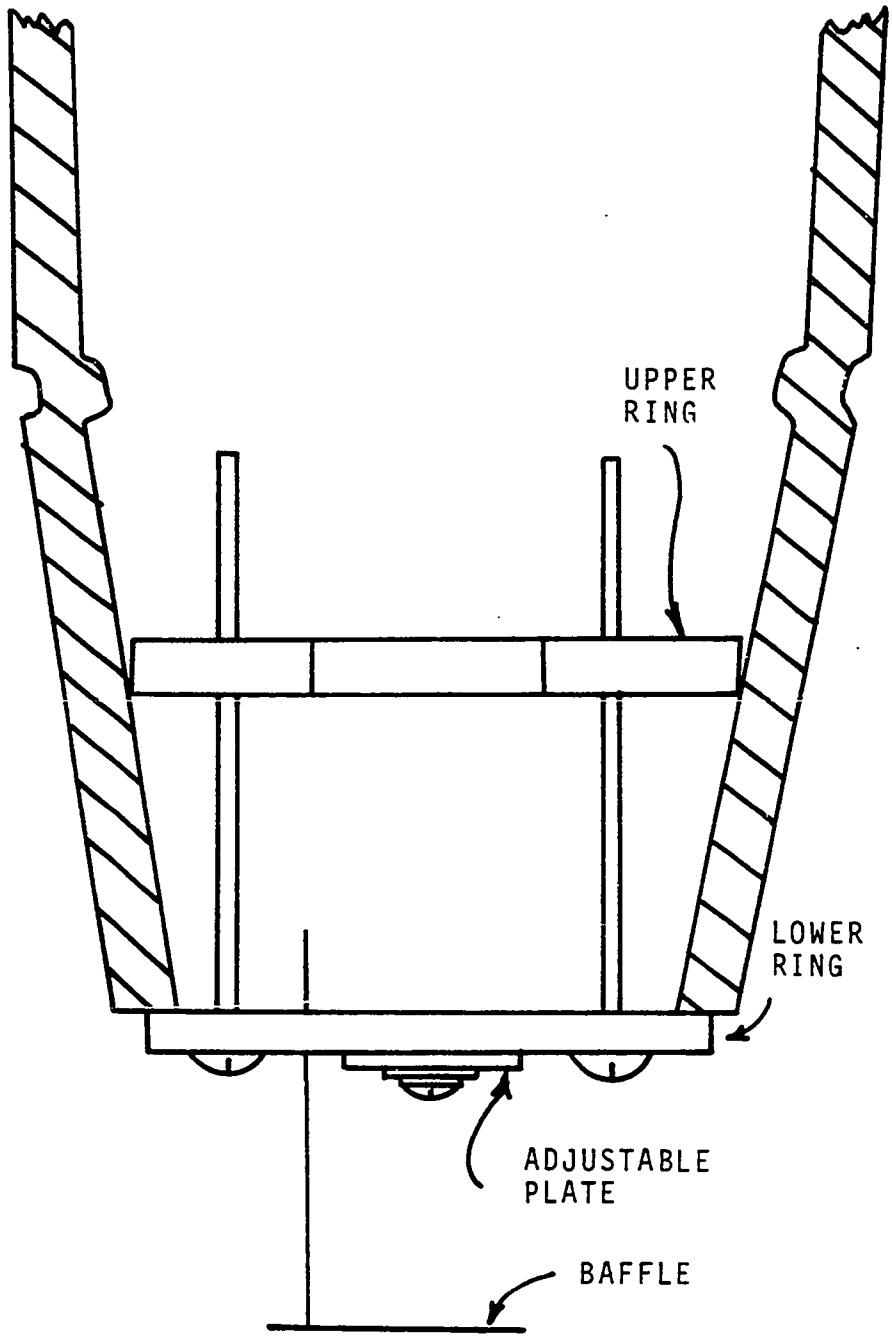

Figure III-3. Baffle Plate Assembly of TGS-1 Thermobalance.

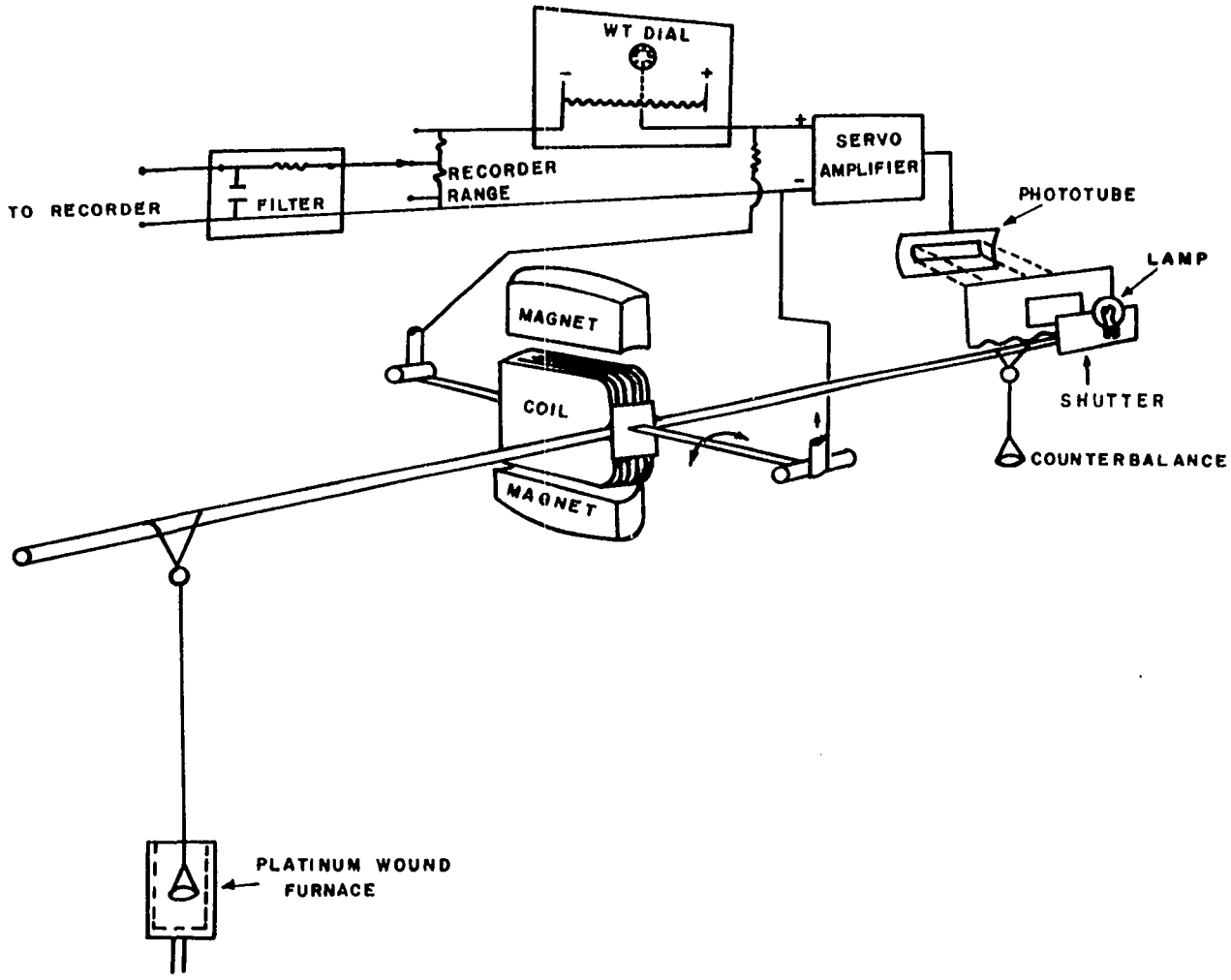

Figure III- 4. Schematic of Perkin-Elmer TGS-1 Furnace and Weigh Assembly.

screws into the bottom of the hang-down tube and also holds a gas inlet tube for atmosphere control. The hang-down tubes are provided with coil springs to make up a ring to encircle the tubes and help secure them to the hang-down ports when ready. The entire weighing mechanism is encased in a glass vacuum bottle provided with three hang-down ports. O-Rings lubricated with high vacuum grease, are placed on the hang-down ports so that when the hang-down tubes are slipped on and fastened the entire system is air-tight.

Brown (14) found that the insulating material coated on the platinum wire of the furnace failed after a few heating cycles. The condensation of the pyrolysis products on the wire where the insulation failed caused a short circuit, thus shortening the furnace life. Hence, a modified furnace with a ceramic collar extending on the bottom side of the furnace was obtained. However, this also had failed in a short time due to the flow pattern of the volatiles. Therefore, Brown placed a quartz wool plug around the base of the furnace and inside the collar and effectively blocked the flow of volatiles into the heating element. This same modification was continued in the present work with excellent results. Whereas the furnaces (prior to the above modification) used by Havens (37) and Brown were good for a maximum of about twenty heating cycles, the modified furnace used in the present study has already yielded more than 150 runs.

The furnace temperature and heating rate were controlled with a Perkin-Elmer UU-1 temperature control unit. The heating rate is adjustable in multiples of two from 0.312 to 160°C/min. The temperature may be programmed to increase or decrease and be stopped at any temperature manually or automatically in the range of ambient temperature to 1000°C. A small indicator light is mounted on the TGS-1 control panel that is lighted when the UU-1 is in control of the furnace temperature. An electronic plug-in unit is provided to actuate the "event-marker" in the recorder for marking the temperature during the heating or cooling cycle.

Two calibrations of the TGS-1 thermobalance are required, one for temperature and the other for weight. Perkin-Elmer developed a unique method for temperature calibration based on the reversible magnetic transitions in ferromagnetic alloys. Small samples (1-3 mg each) of different ferromagnetic alloys are placed in the sample pan. The pan is then filled with aluminum oxide (Al_2O_3) for providing uniform heat transfer characteristics. A magnet is then placed on the outside of the hang-down tube as shown in Figure III-5. The magnet is so placed that the pan swings freely at the center of the magnetic field without touching the furnace walls. The improper positioning of the magnet with respect to the pan is normally indicated by excessive noise or spiking of the recorder pen. The magnetic field causes the metal alloys to exert a downward force on the sample pan. As the temperature of

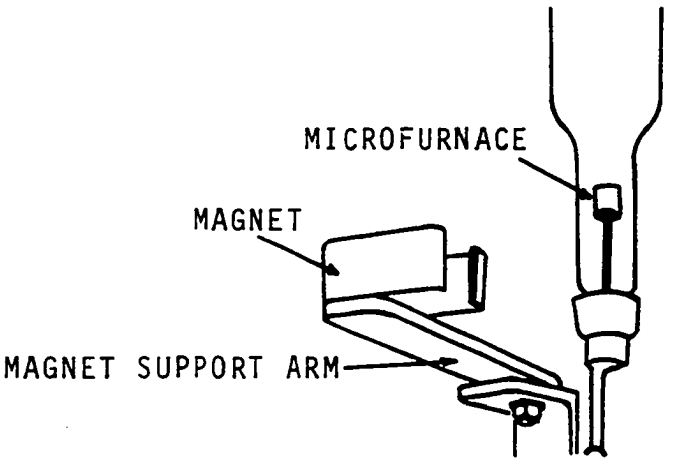

MAGNET IN NORMAL OPERATING POSITION

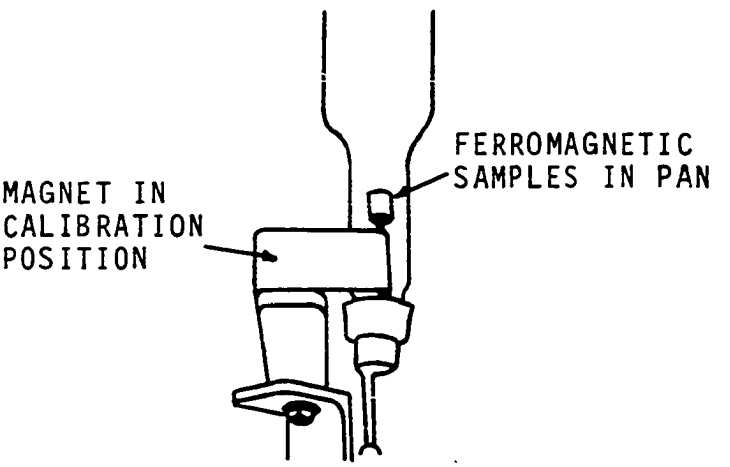

MAGNET IN TEMPERATURE CALIBRATION POSITION

Figure III-5. Schematic of TGS-1 Temperature Calibration System.

the pan is increased, each ferromagnetic alloy loses its magnetic property at a known, repeatable temperature. This temperature is known as the magnetic transition temperature. As and when each alloy reaches its magnetic transition temperature, there is a sudden reduction in the downward force exerted on the pan. This sudden apparent reduction in weight is indicated by the recorder. A list of the alloys provided for this purpose by Perkin-Elmer Corporation, along with their respective transition temperatures, is shown in Table III-1. By comparing the digital temperature readout on the UU-1 temperature control unit with the known transition temperatures, the TGS-1 may be adjusted to give a linear temperature increase and calibrated for temperature. A typical calibration curve is shown in Figure III-6. The results of four separate checks on this one calibration setting are shown to give an idea of how the curves vary with the heating rate.

It can be seen from Figure III-6 that the temperature calibration varied from 0° to 15°C in the range of interest (50° to 600°C). Woodard (77) reported that there was considerable deviation of the calibration at 438°C (Nicoseal transition). During the course of this study such behavior was not noticed.

There are two methods of making the temperature calibration runs. The first is to adjust the TGS-1 control panel settings of "zero" and "range" at each heating rate so that

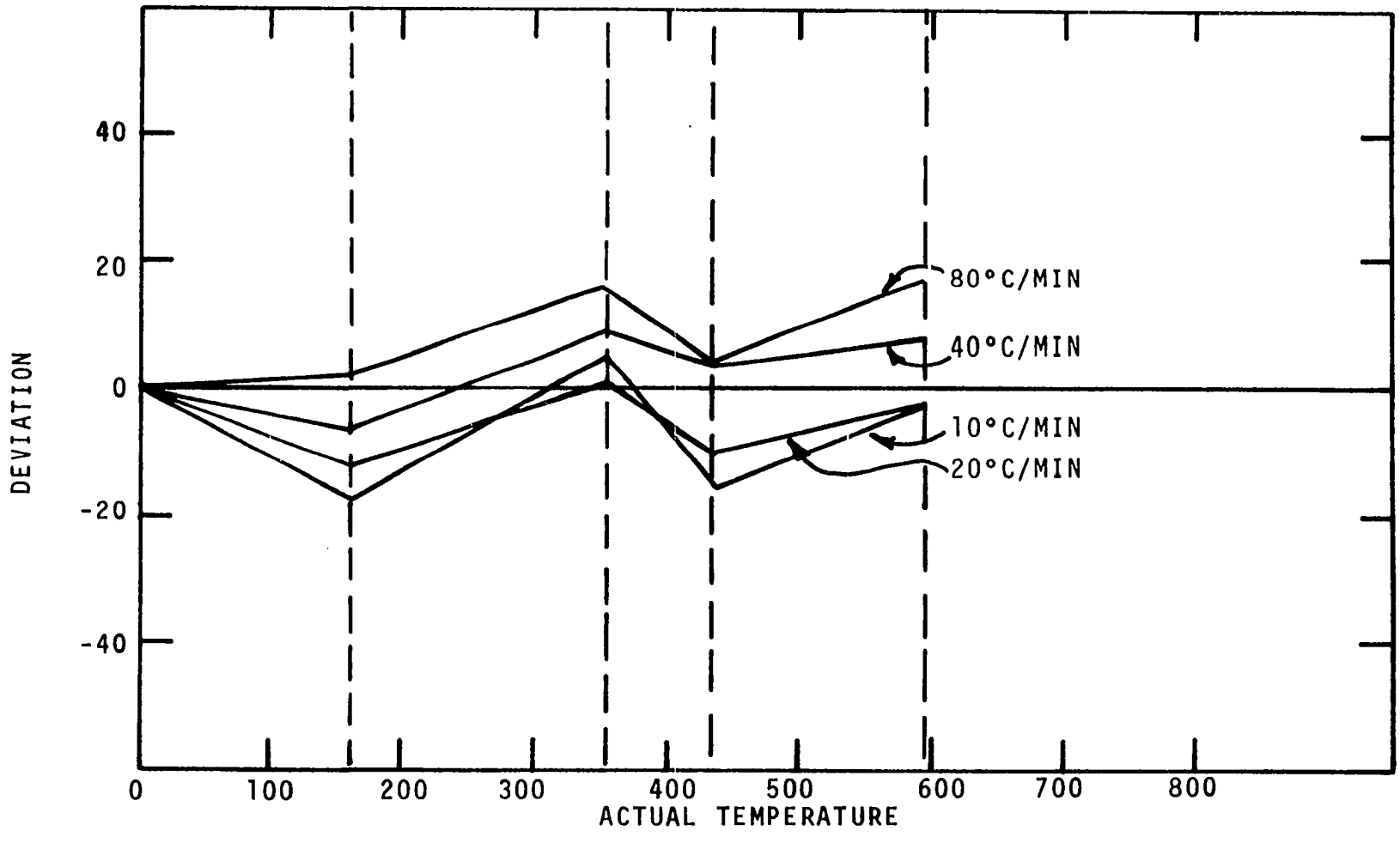

Figure III-6. Temperature Calibration Curve for TGA Studies Determined by Using Magnetic Standards (10, 20, 40 and 80°C/MIN).

TABLE III-1

MAGNETIC STANDARDS FOR TGS-1 FURNACE CALIBRATION

Metal	Magnetic Transition Temperature, °C
Monel	65
Alumel	163
Nickel	354
Mumetal	393
Nicoseal	438
Perkalloy	596
Iron	780
Hi-Sat 50	1000

when the resulting deviation is insignificant there will be no need to apply temperature correction. The second is to fix the "zero" and "range" settings on TGS-1 control panel after they are adjusted for a particular heating rate and use the temperature calibration curves to correct the indicated temperature at other heating rates. It was found during the course of this study that the second method is simpler and faster to use without any sacrifice of accuracy.

The Cahn time derivative computer was essentially calibrated for each run. The area under the dw/dt curve given by the computer represents the total weight lost by a sample during the run.

The accuracy of indicated weight loss was checked by physically weighing the residue left after each run and comparing the actual weight lost with the indicated loss.

Brown (14) made five runs on one sample at one heating rate. First and fifth runs were made to check temperature calibration, two runs were made for obtaining weight loss data and one run for obtaining the rate of weight loss curve. Because of the time derivative computer it was possible in the present study to make three sample runs and obtain simultaneous weight loss and rate of weight loss ($\bar{d}w/dt$) curves for all the three runs. This procedure provided a direct correspondence between the weight loss and rate of weight loss data for each run.

Energy changes occurring during decomposition were studied by using the Perkin-Elmer DSC-2 differential scanning calorimeter. A photograph of the calorimeter is shown in Figure III-7. A comprehensive discussion on calorimetry had been presented by Havens (37). Havens, Brown (14), and Woodard (77) all used the DSC-1B. The chief advantages of the DSC-1B over other standard methods of calorimetric measurement were discussed by Havens. Some of these are:

1. The DSC-1B was capable of being heated at programmed rates up to 80°C/min.
2. Specific heat measurements could be made by measuring the ordinate displacement at any temperature in the range of 25° to 500°C.
3. By the design of the equipment, the energy of transition could be so measured that the sensible heat energy terms could be separated from the total transition energy.

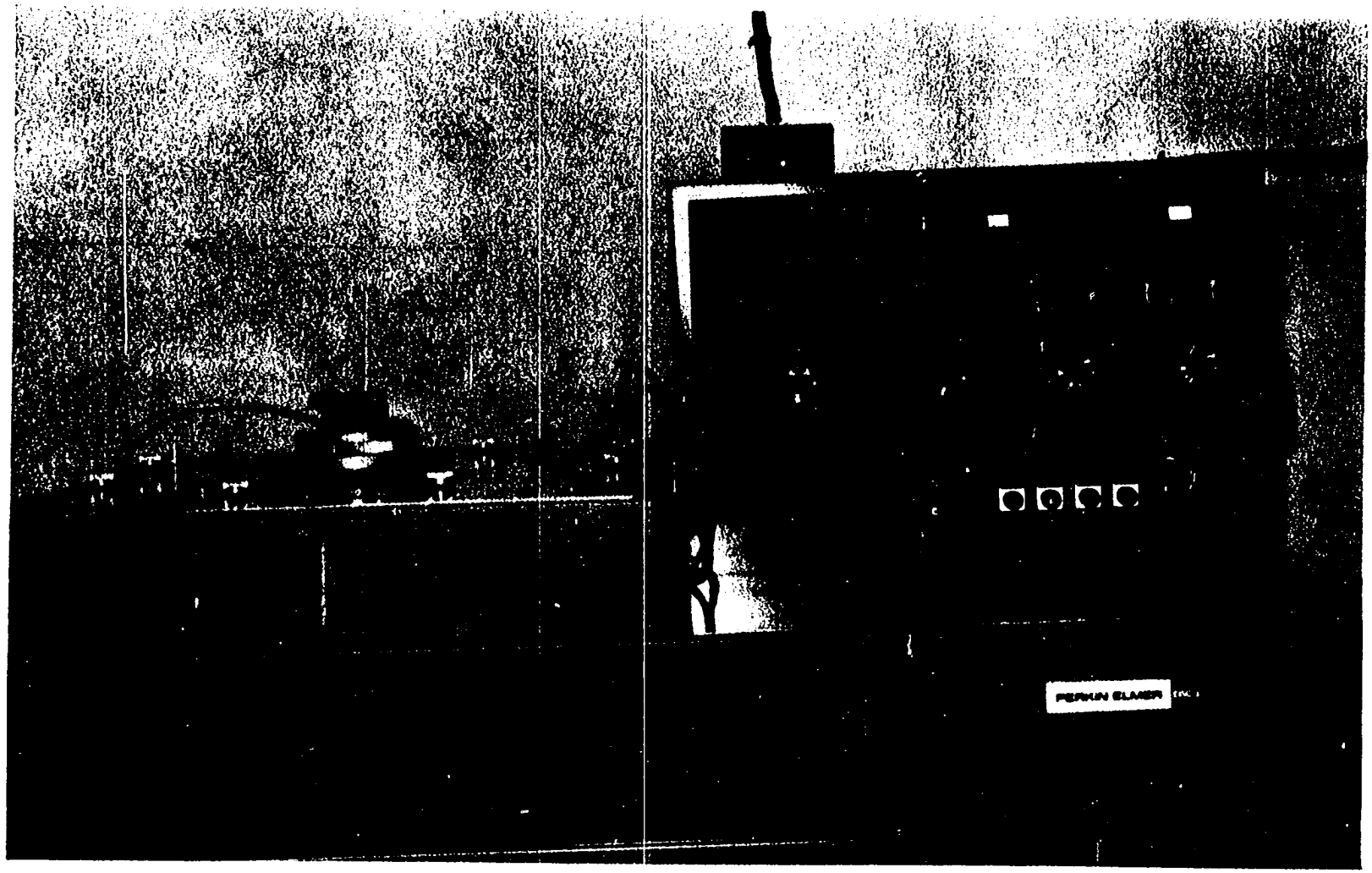

Figure III-7. Perkin-Elmer Differential Scanning Calorimeter DSC-2.

4. The distinct peaks in the thermogram generated on the recorder chart by the DSC-1B yielded not only the qualitative information (e.g., exothermic or endothermic transition along with their temperature ranges), but also quantitative information (e.g., area between the empty pan baseline run and the sample thermogram gave the total energy of transition).
5. Microsamples (sample size of the order of a few mg) could be used with excellent results.

The DSC-2 has several features which make it superior to the DSC-1B in its application. The maximum heating and cooling rate in the DSC-2 is 320°C/min as against only 80°C/min in the DSC-1B. The range of temperature of operation in the DSC-1B is -50° to +500°C where as in the DSC-2 the range is -175° to +725°C. The suggested purge gas flow rate for the DSC-1B is 40 ml to 100 ml/min. However, Havens (37) reported that at the upper limit of 100 ml/min of purge gas rate the chart readout was excessively noisy. The typical purge gas rate used in the DSC-1B was 60-80 ml/min. Purge gas flow rates of 200 ml/min can be used in the DSC-2 with negligible noise in the recorder readout. The volume of the enclosed space around a closed pan-and-heater assembly is so much greater in the DSC-1B than in the DSC-2 that thorough purging of the sealed unit takes much longer in the DSC-1B than in the DSC-2 for a given purge gas flow rate. The digital temperature readout in the DSC-2 is more distinct than the dial

readout in the DSC-1B and shows 0.1°C which the DSC-1B does not. The maximum sensitivity for the DSC-1B is 1.0 mcal/sec full scale as against 0.1 mcal/sec full scale for the DSC-2.

The DSC-2 is eqipped with a lamp located above the digital temperature display. This lamp, when lit, indicates when the sample holders are in temperature control. The rate of heating or cooling and the range of temperature are also digitally displayed on the control panel. The upper and lower temperature limits can be selected by means of digital thumb wheels.

When a transition such as melting, boiling, dehydration, or crystallization occurs in the sample material, an endothermic or exothermic transition takes place. The change in power required to maintain the sample holder at the same temperature as the reference holder (i.e., its programmed temperature) during the transition is recorded as a peak. The chart abscissa indicates the transition temperature and the peak area indicates the total energy transferred to or from the sample.

The sample holders are mounted in a massive aluminum block to provide constant temperature environment. This assembly is shown in Figure III-8. For work above ambient (from 50° to 725°C), provision is made to circulate cooling fluid (distilled water in the present study) through the block to maintain it at a constant temperature, independent of the temperature range of the experiment. The direct calorimetric

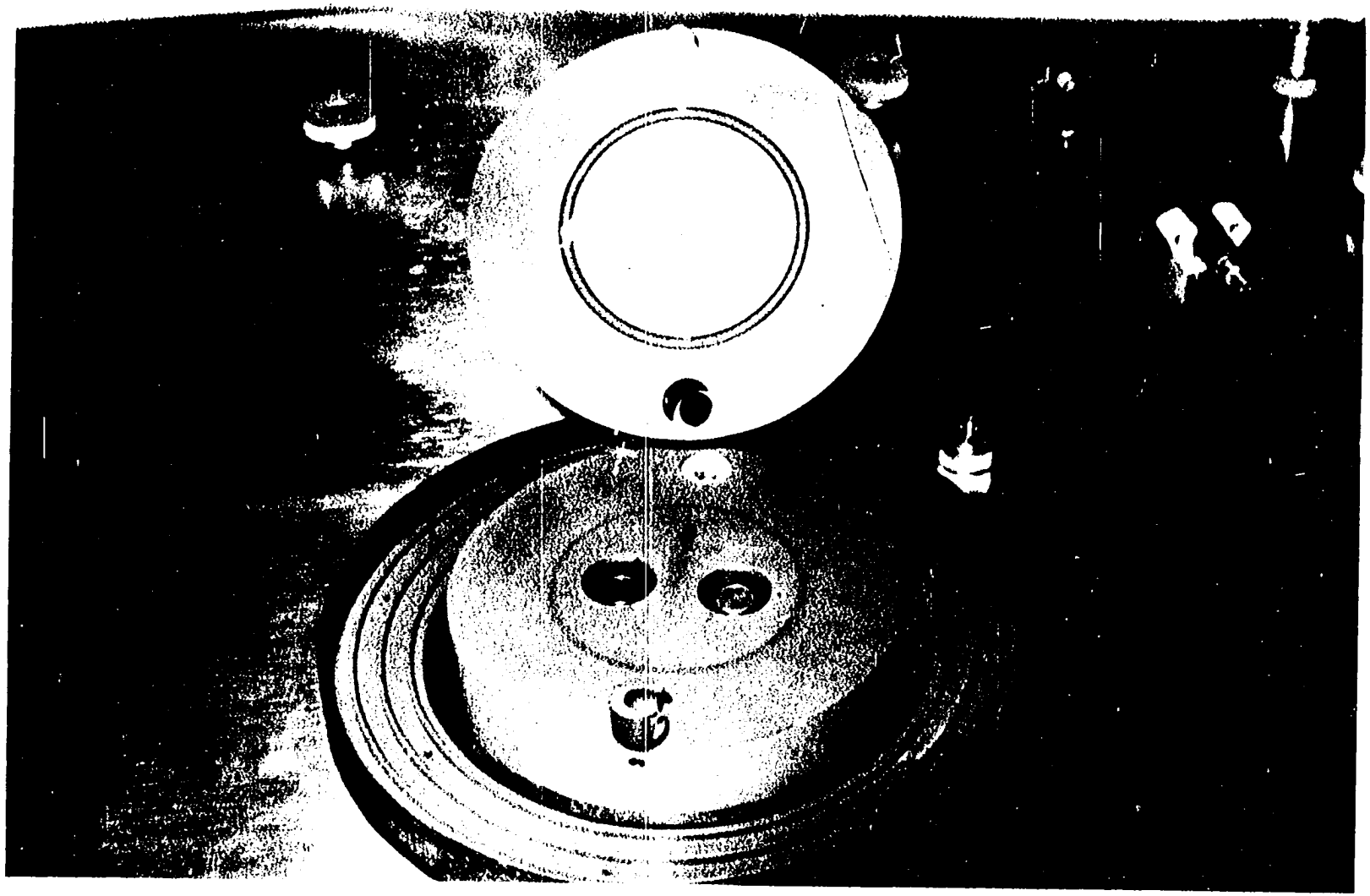

Figure III-8. DSC-2 Sample Holder Assembly.

measuring principle of the instrument requires that each sample holder have a built-in heater and a temperature sensor. The sample holders are made of platinum-iridium alloy. Below these holders are platinum resistance thermometers and platinum wire heater elements. A high-gain closed-loop electronic system that provides differential electrical power to the heaters to compensate precisely for temperature is essentially unaffected by the sample behavior. The differential power required to maintain the "balance" condition is read out directly in millicalories per second on the recorder, and is at all times equivalent to the rate of energy absorption or evolution of the sample. The calibration procedure required to establish the correction in the range is described later in this chapter.

The maximum deviation of true temperature from the perfectly linear program temperature is less than 1°C from 50°C to 725°C. In the DSC-1B the maximum deviation was 7°C from 0°C to 500°C. The free cooling rate of the DSC-2 from 725°C to 100°C is 4 minutes and to 50°C is 10 minutes without auxiliary cooling. The DSC-1B takes 10 minutes to cool from 500°C to 100°C and an additional 5 minutes to cool to 55°C.

In addition to the panel controls on the DSC-2, there are nine concealed panel controls. Of these, only three were used during the course of the present study. The other controls were factory-set and it was suggested that they not be adjusted.

The "vacuum pump" switch turns on the vacuum pump for the vacuum pickup device. The "CIRC" switch turns on the circulating pump and heat exchanger fan for the water circulating system. The other control (ΔT balance) was used for minimizing the "baseline" (i.e., the chart output pertaining to the run made with empty sample and reference pans) curvature. Increasing the "ΔT balance" reading reduced curvature in the direction of the sample endotherm. The indicator readings are in arbitrary units.

Even though the DSC-2 operates over a range of 0° to 750°C, for better baseline maneuverability it has been suggested that the operation best be carried out over smaller temperature ranges. All the species of wood studied in this thesis had decomposed completely or almost completely by the time the sample reached 500°C. For this reason, and also to minimize baseline problems arising from too wide a range, the baseline and sample runs were confined to the range of 50° to 500°C. The initial temperature was lowered from 50° to 30°C during the wet sample studies. The baseline was optimized using the "slope" control, "ΔT balance" control and "zero" control for the temperature range of interest.

The Perkin-Elmer Corporation has developed a very reliable method of temperature calibration. Temperature calibration was required whenever the temperature scale and/or "ΔT balance" control were changed. This calibration involved

the observation of the transition temperatures of standard materials like indium, tin, lead, zinc, K_2SO_4 or K_2CrO_4, whose transition points are accurately known, and comparing the observed values against the reference values. Calibrations were carried out by adjusting "temp calib zero" and "temp calib range" controls located on the hidden panel. The base-line was optimized and the indium and K_2CrO_4 melts were observed at a convenient heating rate (40°C/min) for fixing approximate temperature ranges followed by 10°C/min for accurate temperatures). The change, if at all, needed in the setting of the "temp calib range" control was determined by the equation

$$\Delta R = R^2 \left[\frac{\Delta T_{IND} - \Delta T_{ACT}}{\Delta T_{ACT}}\right] \times \frac{1}{1000} \qquad \text{(III-1)}$$

where ΔR = number of divisions change required to "temp calib range" control

R = setting of "temp calib range" control

ΔT_{IND} = difference between measured transition temperatures of K_2CrO_4 and indium

ΔT_{ACT} = difference between the actual reference transition temperatures

Table III-2 gives the transition temperatures of several standards.

As an example, a "temp calib range" setting of 850, an observed indium melt temperature of 167.4°C, and observed K_2CrO_4 transition temperature of 702.6°C are assumed. Then

the difference ΔT_{IND} = 702.6 - 167.4 = 535.2

the difference ΔT_{ACT} = 670.5 - 156.6 = 513.9

$$R = (850)^2 \left[\frac{535.2 - 513.9}{513.9}\right] \times \frac{1}{1000} = +30 \text{ divisions}$$

The "temp calib range" control is adjusted by 30 divisions and the indium and K_2CrO_4 scans are repeated. These steps are repeated until ΔT_{IND} is 513.9 ± 0.5.

Throughout the course of the present work the factory set value of 458.6 for "temp calib range" was found to yield a ΔT_{IND} value of within 0.5 of 513.9.

TABLE III-2

TRANSITION TEMPERATURES AND ENERGIES OF CERTAIN STANDARD MATERIALS

Standard	Transition Temp °C	Transition Energy (H_t) cal/gm
Indium	156.6	6.8
Tin	231.88	14.45
Lead	327.47	5.5
Zinc	419.47	25.9
K_2SO_4	585.0 ± 0.5	7.95
K_2CrO_4	670.5 ± 0.5	8.50

Energy Calibration

There are two types of calorimetric measurements made from a Model DSC-2 thermogram:

1. Peak area for the determination of the heat of transition.
2. Ordinate displacement for the determination of specific heat or transition rate.

Peak Area Measurement

It is important to note that the sensitivity of DSC-2 (i.e., the peak area) is essentially independent of heating rate, mode of operation (i.e., heating, cooling, or isothermal), and the temperature of operation. Although the Perkin-Elmer standard kit contains six calorimetric standards, only one (indium) was used for this calibration.

1. With the temperature of the sample holders set at 400°K and the "temperature" lamp lit (i.e., the sample holders were in temperature control), a weighed sample (5.62 mg in the present study) of indium encapsulated in an aluminum pan was placed in the left hand sample holder while an encapsulated gold pan was placed in the right hand sample holder. The sample holders are covered with platinum lids to minimize heat loss due to radiation.
2. The indium melt was run at 10°C/min at a chart speed of 1.0 in/min. The sensitivity of the instrument (range) used was 10 mcal/sec.
3. The baseline under the transition peak was extrapolated and the peak area was measured with a planimeter.
4. The instrument constant K was computed using the relation

$$K = \frac{\Delta H_f \times w_{st} \times S_{st}}{R \times A} \qquad \text{(III-2)}$$

where ΔH_f = the heat of transition of the standard (indium) in mcal/mg

w_{st} = the weight of indium (mg)

S_{st} = chart speed for the indium run (in/sec)

R = setting of "range" control in mcal/sec divided by chart span in inches to yield mcal/sec-in

A = area under the curve (in^2)

Then range actual equals K times range indicated. Table III-3 gives the values of A, w_{st}, S_{st}, R, ΔH_f, and K values used in this work.

TABLE III-3

CALIBRATION OF THE INSTRUMENT CONSTANT K

Material	ΔH_f mcal/mg	w_{st} mg	R mcal/sec	S_{st} in/min	A cm^2	K
Indium	6.8	5.62	10	1.0	3.95	1.023
Indium	6.8	5.62	10	1.0	4.08	0.9913
Indium	6.8	5.62	10	1.0	3.92	1.0317
Indium	6.8	5.62	10	1.0	3.98	1.0162

Ideally, the value of K should be unity. "W calib" control could be adjusted to yield a K value of 1. K values greater than 1 indicate low actual sensitivity. It should be noted that K need not be 1. In the course of this study, the "W calib" control was never adjusted. Rather, the computed K values were used to obtain the actual sensitivity of the instrument.

Transition energies (ΔH_t) were calculated as follows:

$$\Delta H_t = \frac{K \times R \times A}{w_{sam} \times S_{sam}} \qquad \text{(III-3)}$$

where ΔH_t = heat of transition of sample (mcal/mg)

w_{sam} = weight of sample (mg)

S_{sam} = chart speed for the sample run (in/sec)

Ordinate Displacement (Specific Heat) Calibration

The ordinate displacement of the DSC-2 was calibrated by means of a sample of known specific heat (synthetic sapphire) contained in the "specific heat kit." The procedure followed was:

1. After optimizing the baseline and calibrating the instrument for temperature, a weighed sapphire sample (1.33 mg) was placed in a weighed gold sample pan and covered with a gold lid. The pan was kept in the left hand holder and covered with the platinum lid.
2. A gold pan similar to that used for the sample was weighed, encapsulated and placed in the right hand holder. The holder was covered with a platinum lid.
3. The enclosure cover was swung into position and closed.
4. The upper and lower limits on temperature were adjusted to 773°K and 323°K, respectively.

   The recorder was always run for about one minute at the lower and upper temperature limits isothermally.
5. The "zero" control on the DSC-2 control panel was used to adjust the pen position on the chart paper.

   Quite frequently it was found necessary to adjust the pen position on the chart paper depending upon the sample to be run, the sample size, the purge gas rate, etc.

However, each set of two runs, namely the sample run and the baseline run (with char), were made without altering any adjustments. The empty pan baseline and sapphire scan were run at the same purge rate as the sample runs though not necessarily at the same "zero" control adjustment.

6. Proper "range" control setting and heating rates (10 mcal/sec for 40°C and 80°C/min, and 20 mcal/sec for 160°C/min) were chosen.

It was not necessary to run the sapphire scan at each heating rate because the ordinate displacement was directly proportional to the heating rate used (Figure III-9).

Ideally, the position of the upper isothermal level should be within two divisions of the lower isothermal level (Figure III-9). However, it was found in this study that the effort involved in achieving this result was much more than could be justified by the difference in the results obtained. Perkin-Elmer meant this adjustment to be achieved over much narrower temperatures ranges (e.g., 350°-500°C). According to Perkin-Elmer Corporation, the difference in the upper and lower isothermal levels could be as much as 4.5 inches in the extreme temperature range of 50°-750°C. For the range of 50°-500°C used in the present study, the difference in the isothermal levels was about 4.0 inches.

7. The sapphire run was made after the sample and char runs. The unit was cooled and a "no-sample" baseline run was made with sapphire removed from the pan.

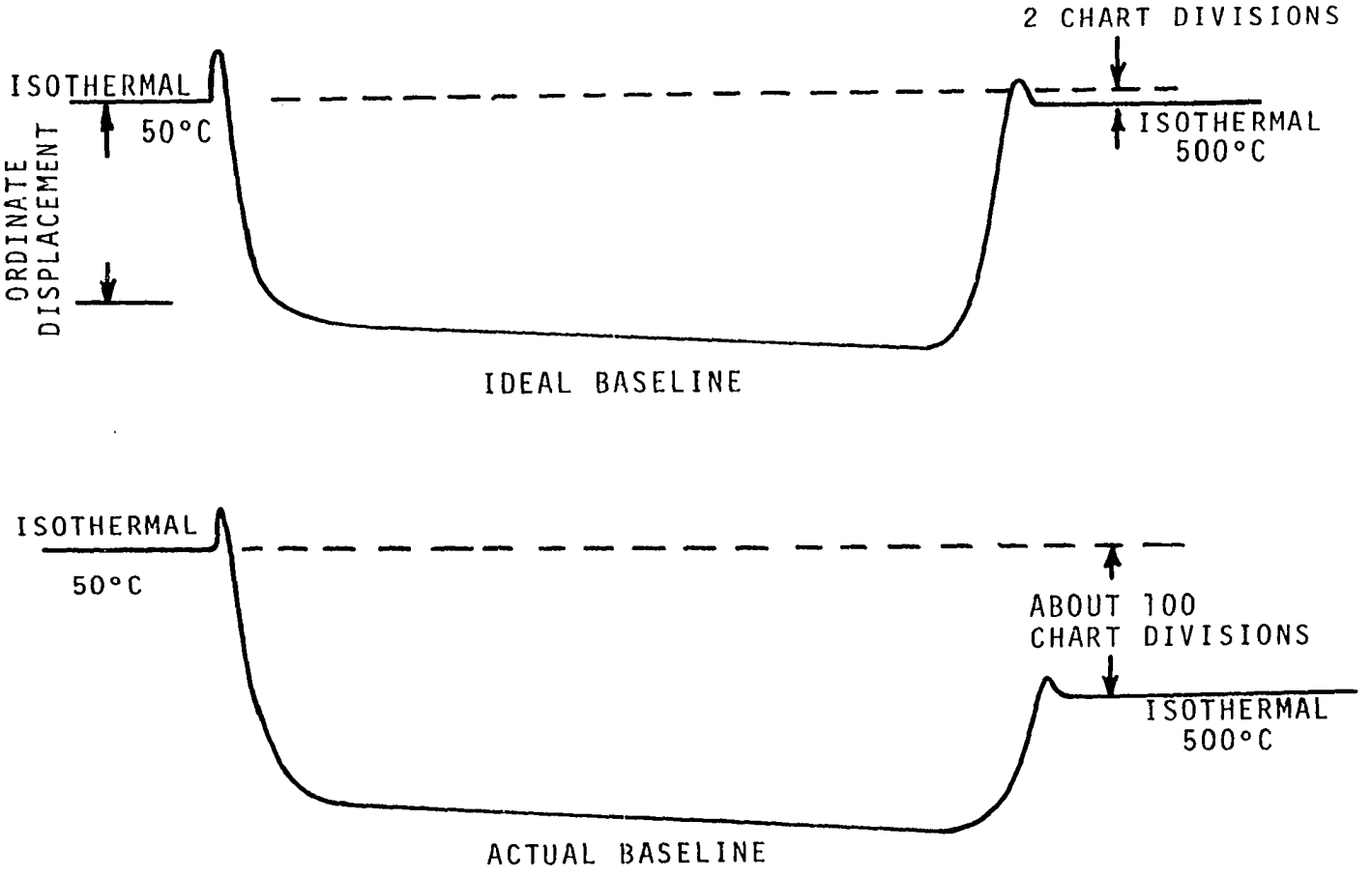

Figure III-9. Comparison of Ideal and Experimental Baseline in DSC-2.

8. The unit was cooled to the lower limit and the scan was repeated with a weighed sample of wood encapsulated in the same gold pan. The platinum holder covers were replaced as before and the sample run was made under identical conditions as the sapphire and no-sample runs (i.e., using the same sensitivity (range), heating rate, and purge gas rate).

9. The scan was repeated over the same chart recording of the sample run after cooling the DSC-2 to 50°C without disturbing any of the settings (charred sample run). Woodard (77) reported that better isothermal baseline agreement was achieved when the empty pan (no sample) run was made following the sample run rather than, as Havens (37) and Brown (14) did, preceding it. The difference in these techniques is as follows. In the no sample-sample sequence of runs, it was required that between the baseline and sample runs the cover of the sample holder assembly be removed and replaced, the left hand side platinum holder cover as well as the pan be removed and replaced after weighing the sample into the sample pan. The sample holder assembly was then purged thoroughly with nitrogen before scanning the sample run. It was important that for good isothermal baseline agreement these various parts be undisturbed. By changing the sequence of runs, i.e., run the sample first and then the baseline, there was no need to disturb the instrument.

This technique would work only in the case of materials which decompose completely, or with negligible char residue, like polymers. In the present study with woods it was found that significant amount of char was formed (except in the case of cellulose) during the course of pyrolysis so that the sequence of operation was not of any particular consequence. The "char-run" was made following the sample run to check the char specific heat, however.

10. Reference values of sapphire specific heat versus temperature are plotted in Figure III-10. The values were obtained from Reference 31. The specific heat of the sample at the temperature of interest was obtained by applying the formula

$$c_{p_{sam}} = \frac{w_{saph}}{w_{sam}} \times \frac{D_{sam}}{D_{saph}} \times c_{p_{saph}} \qquad \text{(III-4)}$$

where $c_{p_{sam}}$ = specific heat of sample (cal/gm-°C)

$c_{p_{saph}}$ = specific heat of sapphire (cal/gm-°C)

w_{saph} = weight of sapphire (mg)

w_{sam} = weight of sample (mg)

D_{saph} = pen deflection with sapphire (cm)

D_{sam} = pen deflection with sample (cm)

The power calibration using the specific heat of sapphire was made three times during this study. The indium heat of fusion was checked four times during this study. Most

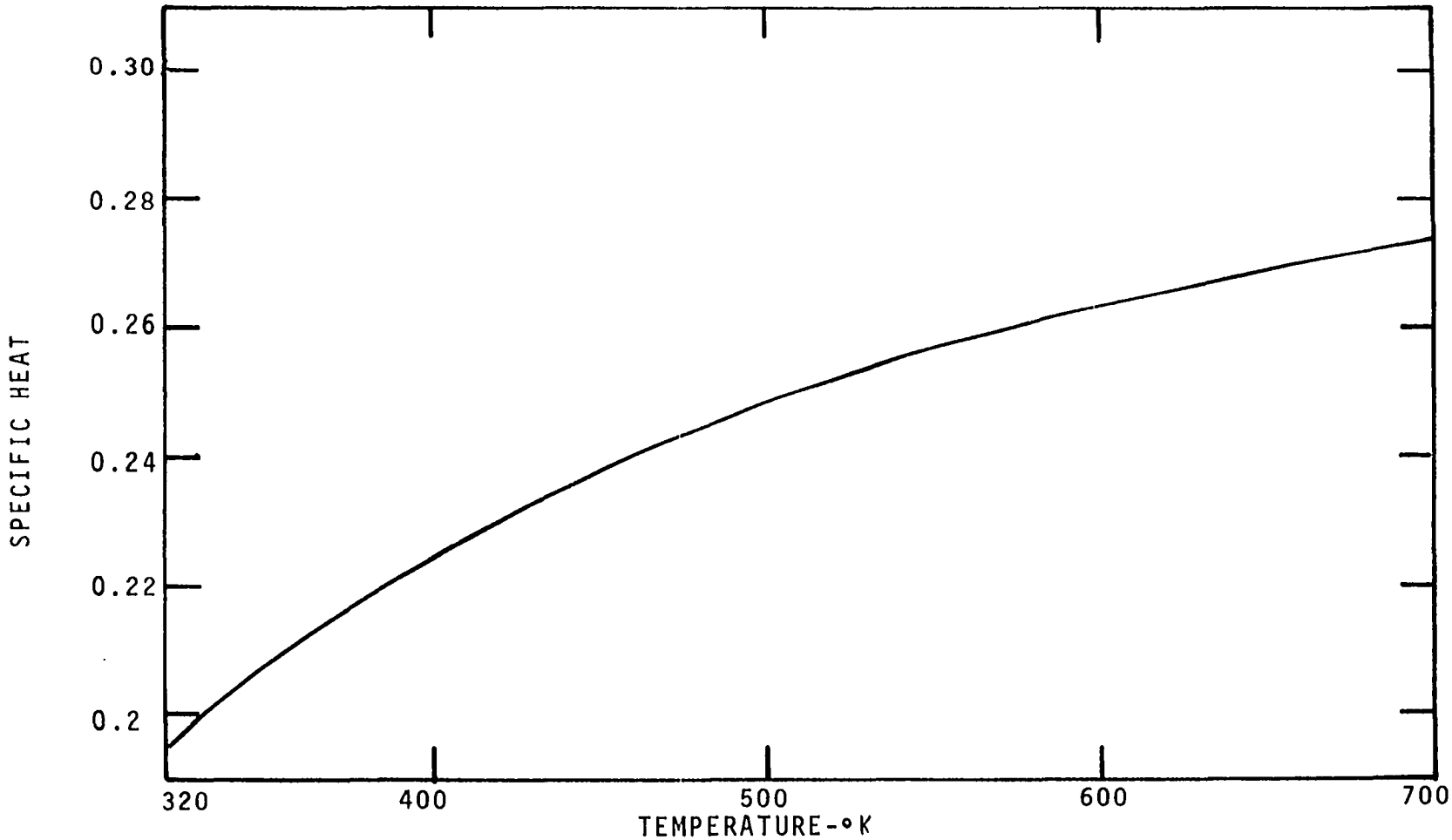

Figure III-10. Specific Heat Curve for Sapphire (31).

of the samples were run twice at a particular heating rate. The "slope" control on the front panel control and "ΔT balance" were adjusted thrice during the entire course of this study. The heating rates used were 40°, 80° and 160°C/min. Both dry and moist samples of all seven species were examined.

Havens (37), Brown (14), and Woodard (77) all reported a problem concerning the "base-line drift," the chief reason for which seemed to be the condensation of the heavy volatile pyrolysis fractions on the platinum lid and on the bottom of the sample holder which in turn altered the heat transfer characteristics of the sample holder. The sensitivity of DSC measurements due to changes in radiative heat transfer properties can be demonstrated by a hypothetical heat capacity test. Suppose that a 10 mg sample of wood is heated at 20°C/min in a DSC. Assuming the specific heat of the wood sample to be 0.35 cal/gm-°C, the differential heat that must be supplied to offset the effect of heat capacity is

$$\frac{dq}{dt} = m\, c_p\, \Delta T = 10 \times 0.35 \times \frac{20}{60} = 1.167 \text{ mcal/sec}$$

If during a run the surface emissivity should change by 0.1 at say 400°C, the differential energy to be supplied to counteract the change in surface emissivity is

$$\frac{dq}{dt} = 0.1\, \sigma A T^4$$

where σ = the Stefan-Boltzmann constant, 1.355×10^{-9} (mcal/sec-cm^2-°K)

A = surface area of the sample holder cover (cm^2)

T = temperature (°K)

The change in radiation loss is then

$$(0.1)(1.355 \times 10^{-9})(1)(673)^4 = 27.8 \text{ mcal/sec}$$

It can be seen that a small change in surface emissivity is a dominant factor during a wood heat capacity measurement. For this reason Havens (37) observed that the heat transfer characteristic of the sample holder cover of the DSC-1B changed from run to run resulting in poor baseline repeatability between two successive runs over a wide temperature range. The suggested maximum purge gas flow rate for the DSC-1B was found to be insufficient to sweep away the volatiles before they condensed on the radiation dome (sample holder cover). Havens reported that because of this problem about 60 percent of the thermograms he obtained were of little value.

The problem of changing emissivity was overcome in the DSC-2 by two changes in the operation and equipment. The major change was in the sample holder cover which was a shiny metallic surface at the start of a sample run. As the temperature rose, volatiles were emitted which condensed on the sample holder cover and changed the emissivity as explained earlier. To start with, if the holder cover surface had an emissivity equal to or greater than that resulting due to the condensation of the volatiles on it, there should be no

baseline drift (in other words, essentially that of black body). To this end the sample holder covers were sprayed with black paint and let dry in the oven for two hours. The sample holder covers were then placed in the DSC-2 and run through a heating cycle of 50°-500°C in an atmosphere of nitrogen. When they were removed the black of the spray paint was gone leaving a layer of pyrolyzed residue from the enamel on the under side of the sample holders; this residue provided a good diffuse medium. A layer of black "India ink" was applied to the residue layer and again allowed to dry. The sample holders were then run through a few heating cycles up to 500°C in nitrogen as before. The black coating adhered quite well to the platinum surface. It was found that as long as the optically black coating was not exposed to air at elevated temperatures it was not changed. The baseline drift was thus minimized to insignificance.

The second factor that helped a little in minimizing baseline drift was the increased purge gas rate which swept away a large part of the volatiles before they had a chance to condense on the cooler walls of the sample holder. This higher rate of purge gas flow rate could not have been achieved for the DSC-1B, because the required flow rate of 120 cc/min produced excessive noise. It is felt that the previous investigators using DSC-1B over-emphasized the significance of sample size in relation to the baseline drift.

CHAPTER IV

EXPERIMENTAL RESULTS AND DISCUSSION OF THE PROPOSED MODEL

The experimental procedure described in Chapter III was used to obtain the weight loss and rate of weight loss data for cellulose, dead Ponderosa pine needles, extracted Ponderosa pine needles, excelsior, extracted excelsior, four wing saltbush leaves, and punky wood (essentially lignin). A table of chemical properties of the species studied is in Appendix D. The heating rates used were 10°, 20°, 40°, 80°, and 160°C/min. Additionally, weight loss and rate of weight loss data were obtained for larch at 10°, 40° and 160°C/min. Larch data were obtained to check the model developed in this thesis. The model was also verified using excelsior data. The weight loss and rate of weight loss data of cellulose plotted against temperature are shown in Figures IV-1 through IV-5. The weight loss and rate of weight loss versus temperature plots for all other woods are shown in Appendix E. A summary of part of the weight loss and rate of weight loss data is given in Appendix A. As the heating rate was increased, the weight loss and rate of weight loss curves shifted toward

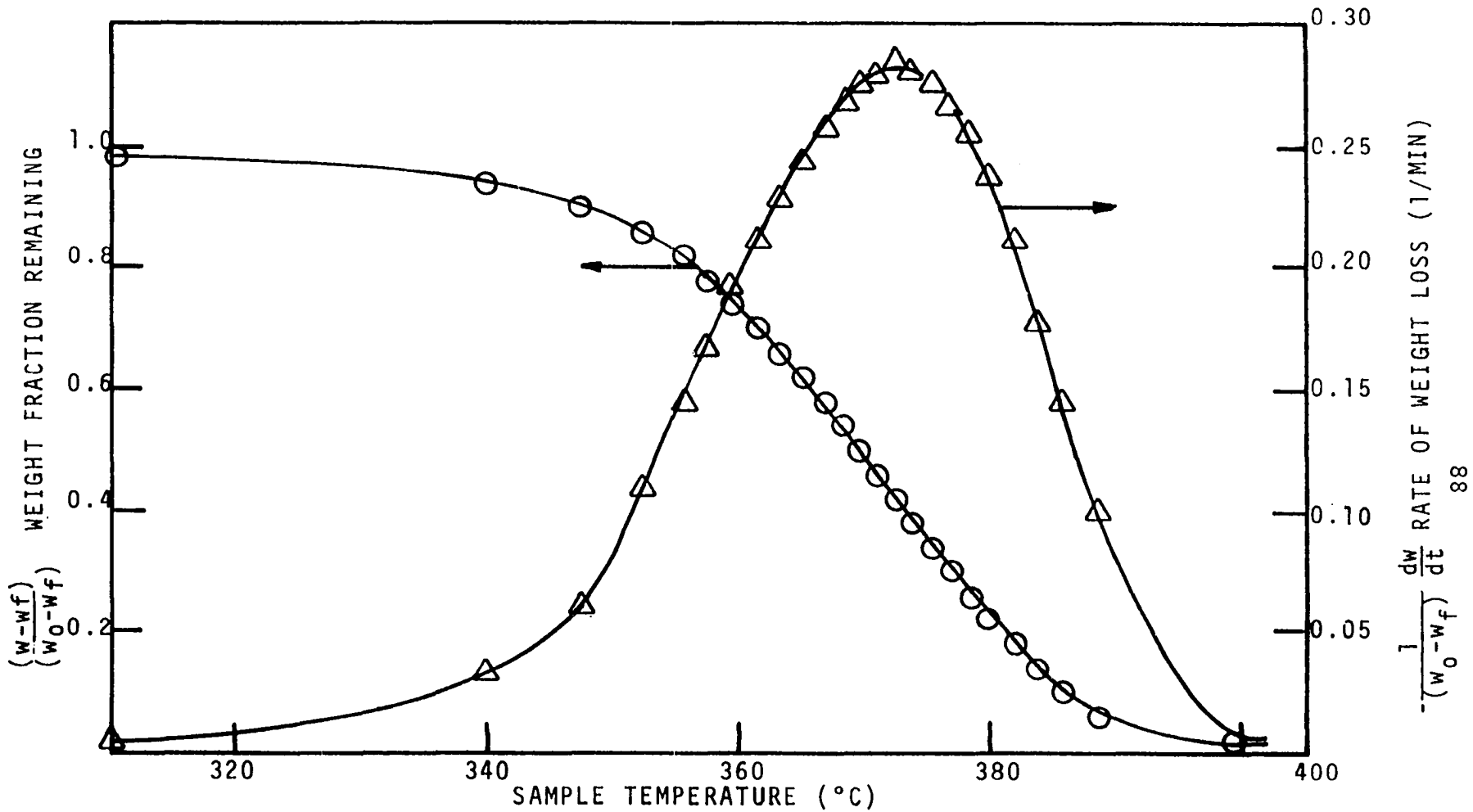

Figure IV-1. Weight Loss and Rate of Weight Loss for Munktell's Cellulose. Heating Rate - 10°C/MIN.

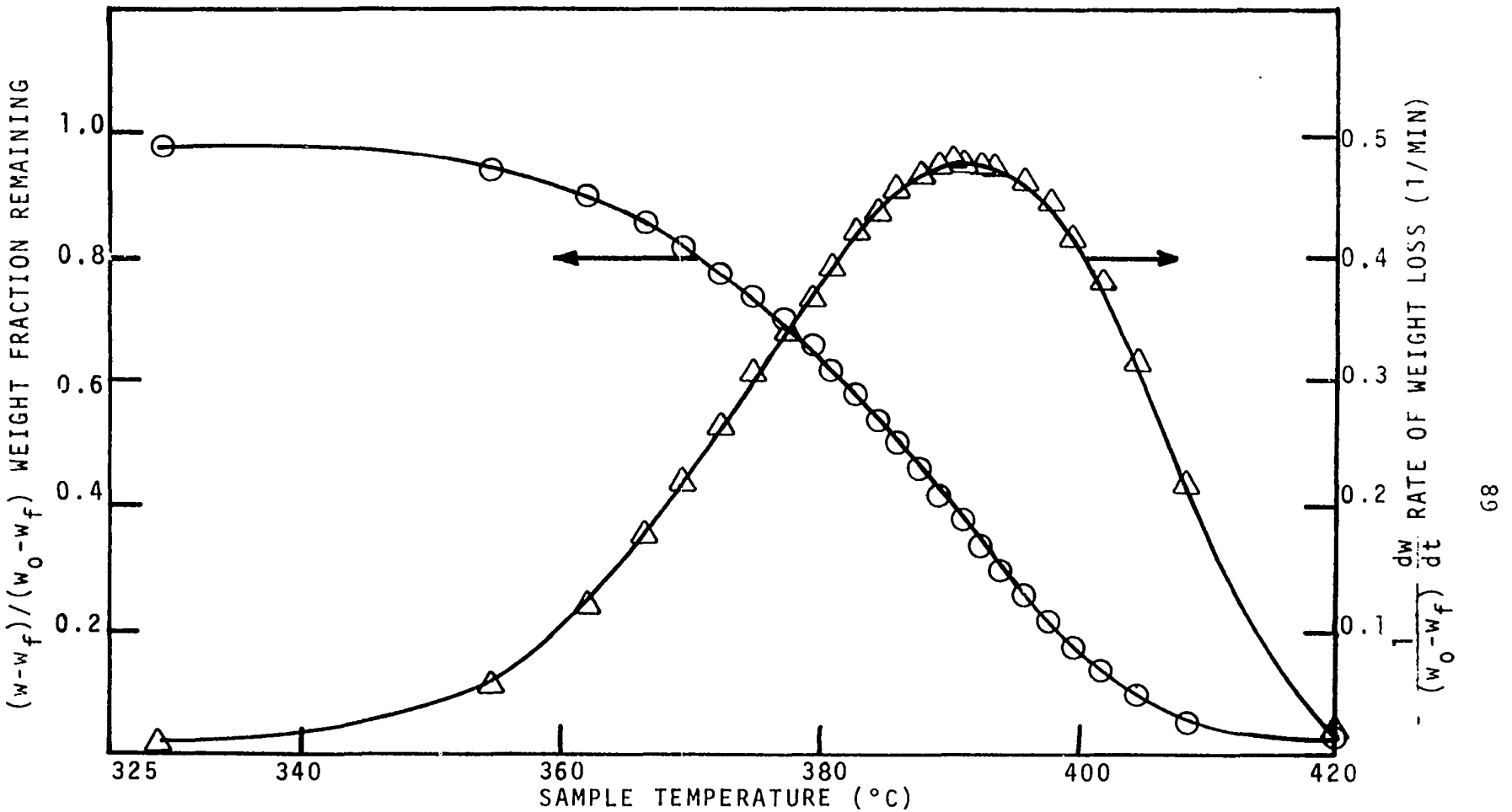

Figure IV-2. Weight Loss and Rate of Weight Loss for Munktell's Cellulose. Heating Rate - 20°C/MIN.

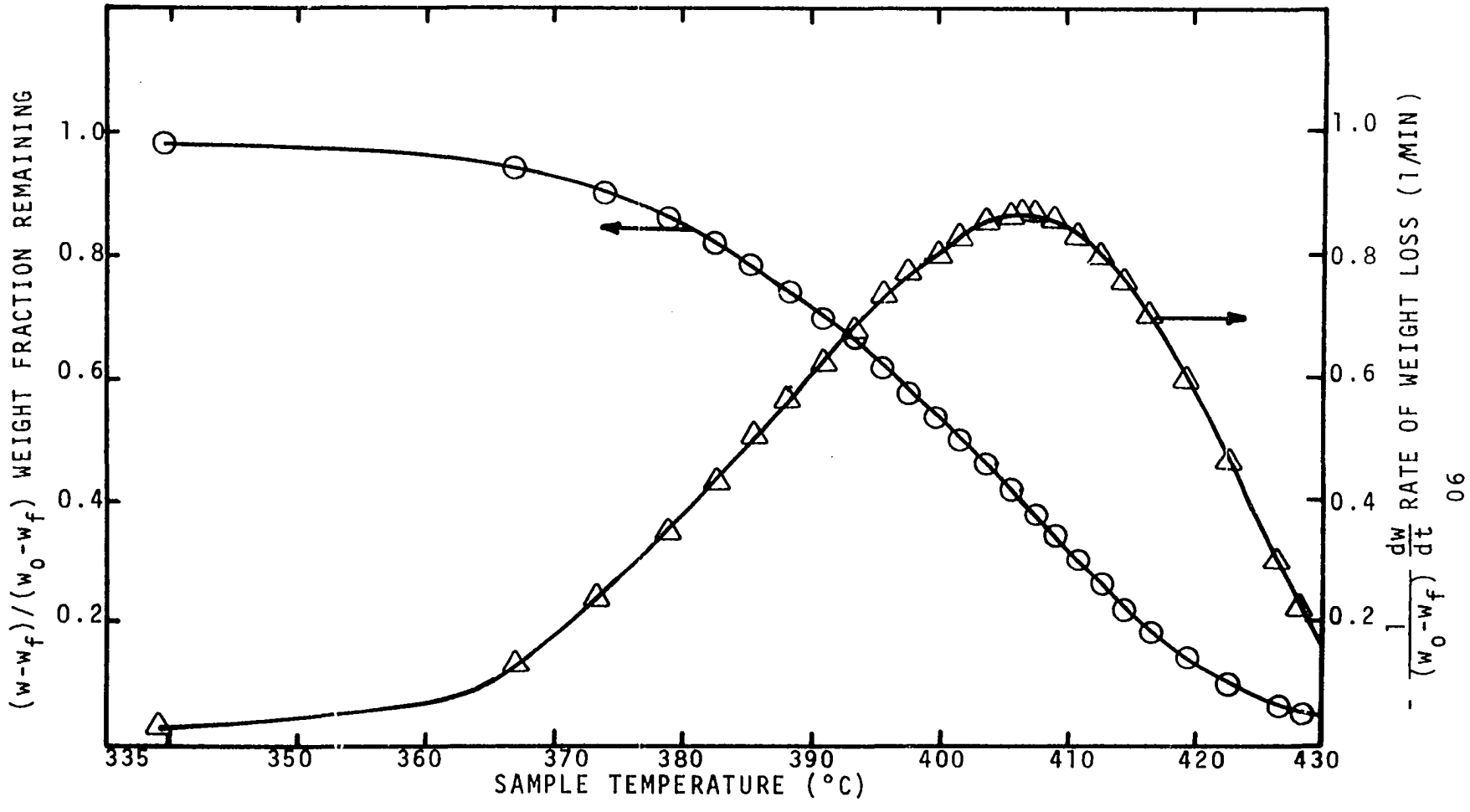

Figure IV-3. Weight Loss and Rate of Weight Loss for Munktell's Cellulose. Heating Rate - 40°C/MIN.

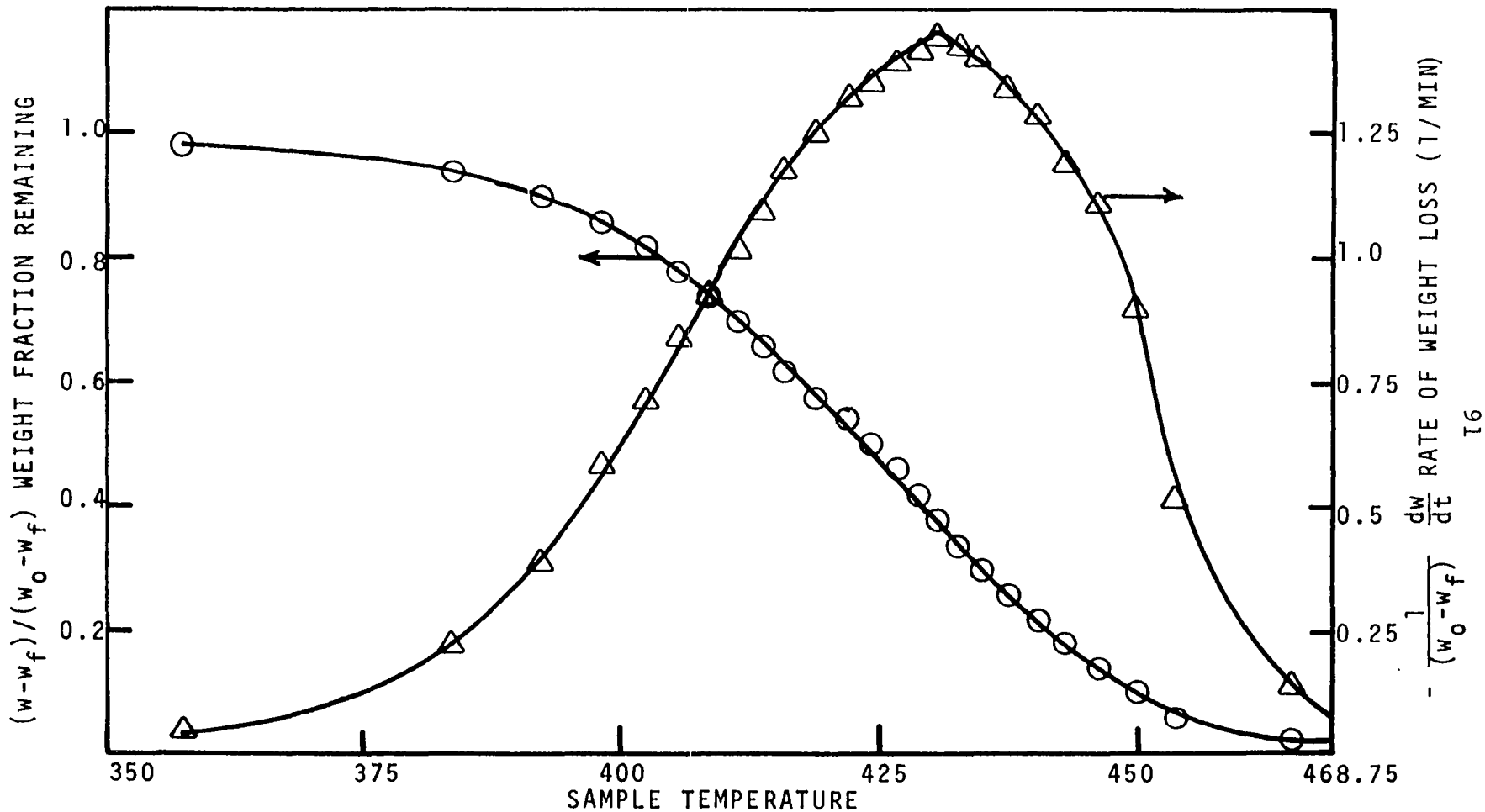

Figure IV-4. Weight Loss and Rate of Weight Loss for Munktell's Cellulose. Heating Rate - 80°C/MIN.

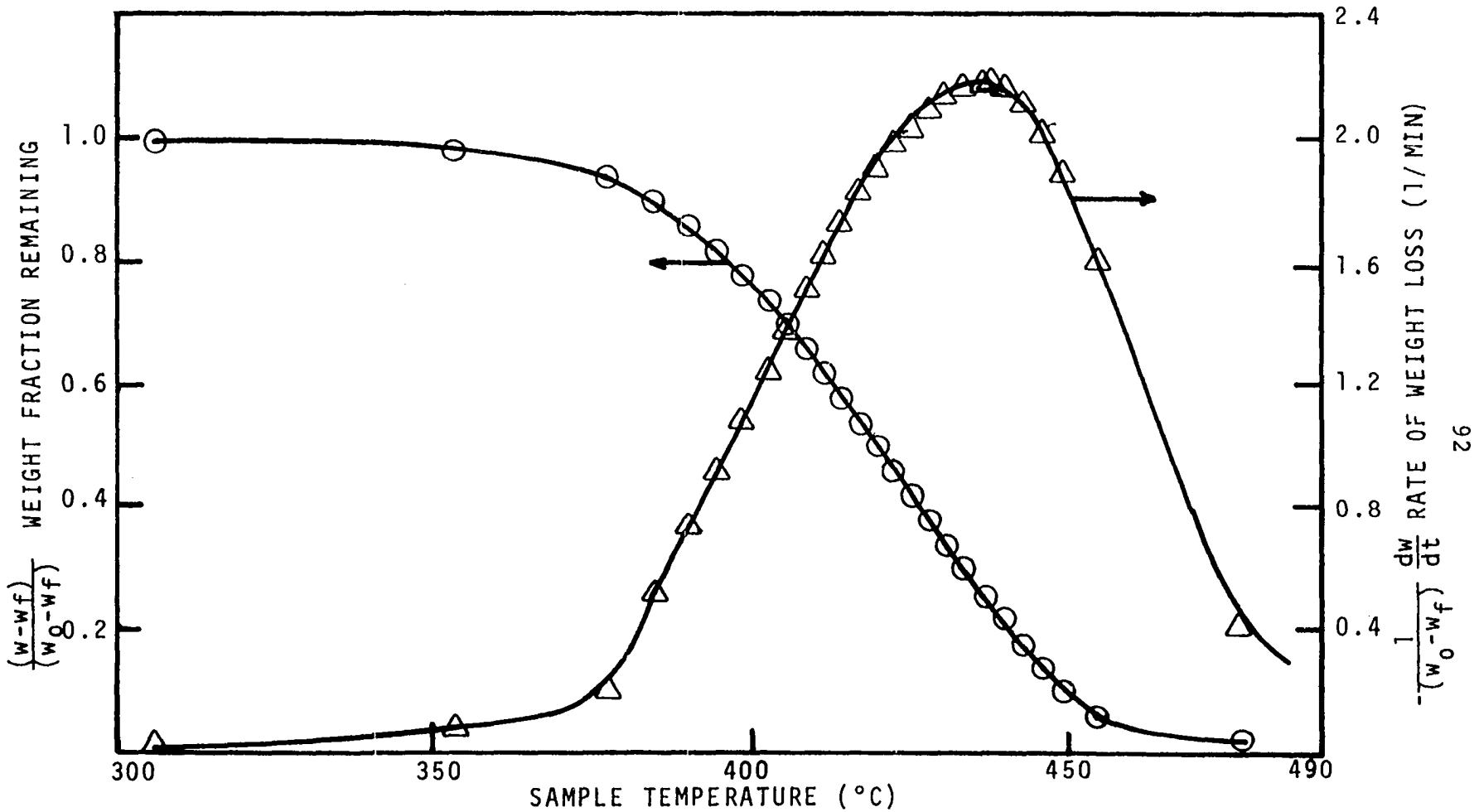

Figure IV-5. Weight Loss and Rate of Weight Loss for Munktell's Cellulose. Heating Rate - 160°C/MIN.

higher temperatures as shown in Figure IV-6 for cellulose. The heating rate shift is easily explained by considering the equation (due to Goldfarb, et al. (32))

$$-\frac{dW}{dt} = Ae^{-E/RT}(W)^n \qquad \text{(IV-1)}$$

where W = a function of the sample weight = $(w-w_f)/(w_o-w_f)$

w_o = initial sample weight (mg)

w = weight of sample remaining at time t (mg)

w_f = weight of the residue (mg)

A = frequency factor (sec^{-1})

E = activation energy (cal/g-mole)

R = gas constant (1.986 cal/mole-°K)

T = temperature (°K)

n = order of reaction (dimensionless)

t = time (sec)

If the heating rate, β, is incorporated in Equation IV-1,

$$-\frac{dW}{dT} = (A/\beta)e^{-E/RT}(W)^n \qquad \text{(IV-2)}$$

Integration of Equation IV-2 yields

$$\int_{1.0}^{W} \frac{dW}{(W)^n} = A/\beta \int_{T_o}^{T} e^{-E/RT}\, dT \qquad \text{(IV-3)}$$

As heating rate β increases the term A/β will decrease. Hence, for achieving a specified weight function, W, it can be seen that a higher temperature is required. Differentiation of Equation IV-2 with respect to temperature yields

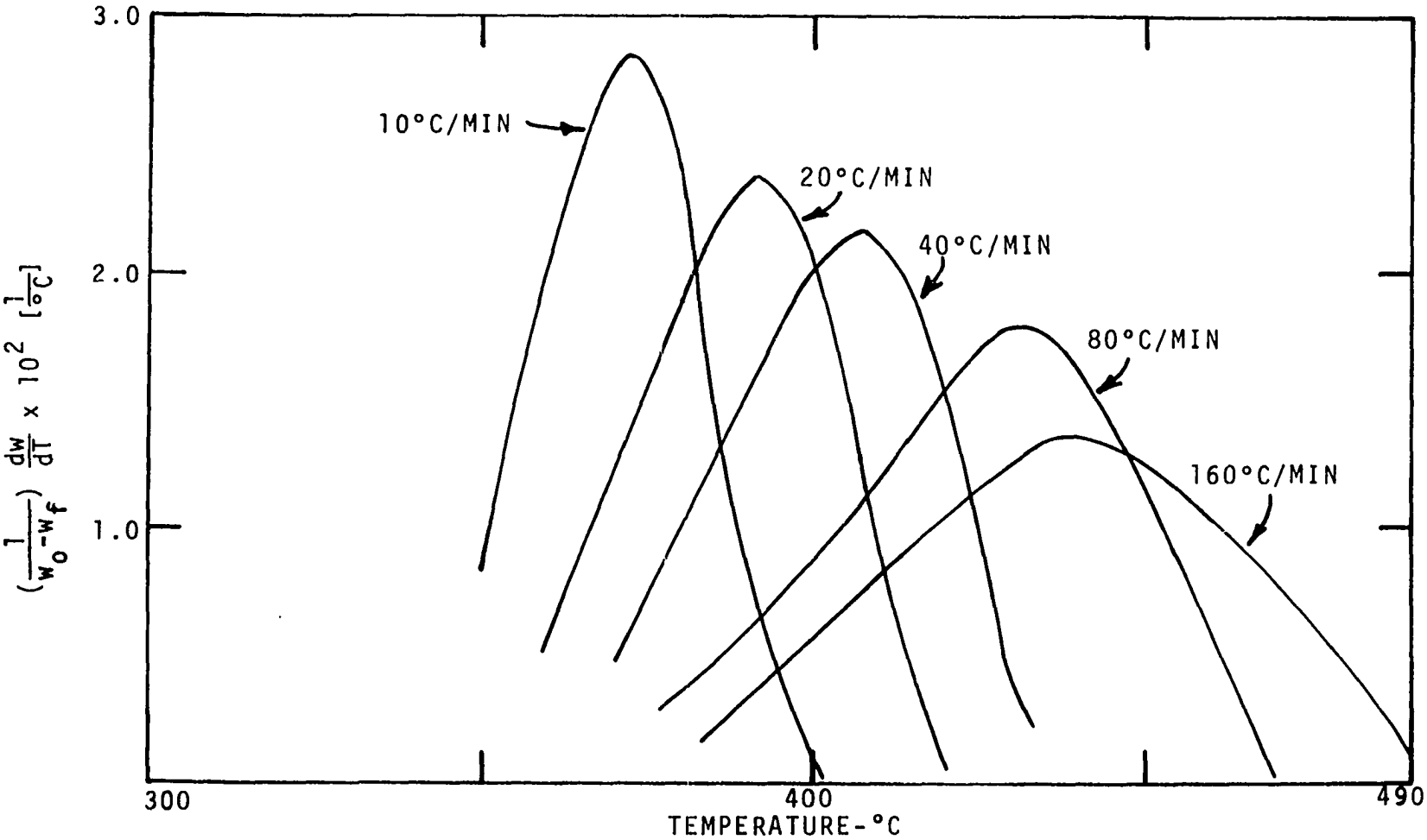

Figure IV-6. Effect of Heating Rate on the Rate of Weight Loss of Cellulose.

$$-\frac{d^2W}{dT^2} = \left(-\frac{dW}{dT}\right)\frac{E}{RT^2} + \frac{n}{W}\left(\frac{dW}{dT}\right)^2 \qquad \text{(IV-4)}$$

At the maximum rate of weight loss, $d^2W/dT^2 = 0$ or

$$\frac{E}{RT^2_{max}} = \frac{n}{W_{max}}\left(\frac{dW}{dt}\right)_{max}$$

$$\left(\frac{dW}{dt}\right)_{max} = \frac{EW_{max}}{nRT^2_{max}} \qquad \text{(IV-5)}$$

It can be seen from Equation IV-5 that $(dW/dT)_{max}$ will decrease due to an increase in T_{max} provided that the maximum rate of weight loss occurs near the same fractional decomposition for each rate. This behavior is shown in Figure IV-6 for cellulose.

Woodard (77) and Sardesai (62) used a modified method of Goldfarb, et al., called Friedman's method of analysis, to analyze their data. The basic equation is obtained by taking the logarithm of Equation IV-1.

$$\ln\left(-\frac{dW}{dt}\right)_\beta = \ln A + n \ln W - \frac{E}{RT_\beta} \qquad \text{(IV-6)}$$

where the subscript β, the heating rate, indicates that the rate and temperature at any specific value of conversion W depend upon the heating rate. It is convenient to express W as a fraction of the volatiles, $(w-w_f)/(w_o-w_f)$, where w is the weight of the sample remaining at time t, w_o is the initial sample weight and w_f is the weight of the residue (all weights in mg).

If $W = (w-w_f)/(w_o-w_f)$ is incorporated into Equation IV-6, the result is

$$\log \left[-\frac{1}{w_o-w_f} \quad \frac{dw}{dt}\right] = \log A - \frac{E}{2.3RT} + n \log W \qquad \text{(IV-7)}$$

At various values of conversion throughout the degradation range, values of $\log \{[-1/(w_o-w_f)]\ dw/dt\}_\beta$ are obtained. A plot of $\log\{[-1/(w_o-w_f)]\ dw/dt\}_\beta$ versus $1/T_\beta$ is made. The activation energy may be obtained from the slope of this line, and $\log A + n \log W$ may be obtained from the intercept for each value of conversion. The plots of $\log \{[-1/(w_o-w_f)] \times dw/dt\}_\beta$ versus $1/T_\beta$ are shown for all the sample materials in Figures IV-7 through IV-13. Average values of activation energy are then calculated over the entire degradation range. The average values are then used to calculate $\log [A\ W^n]$ values at each conversion. Then, by plotting $\log [A\ W^n]$ versus $n \log W$, log A can be obtained from the intercept and n from the slope. The weakness of this method of analysis is at once evidenced by the fact that the average activation energy, rather than the individual values of the activation energy, is used to calculate $\log [A\ W^n]$. Two graphs plotted using the average activation energy for cellulose and punky wood data obtained in this study are presented in Figures IV-14 and IV-15. To show the scatter if individual activation energies are used, cellulose data are plotted in Figure IV-16. The scatter in the data suggests a curved fit rather than a

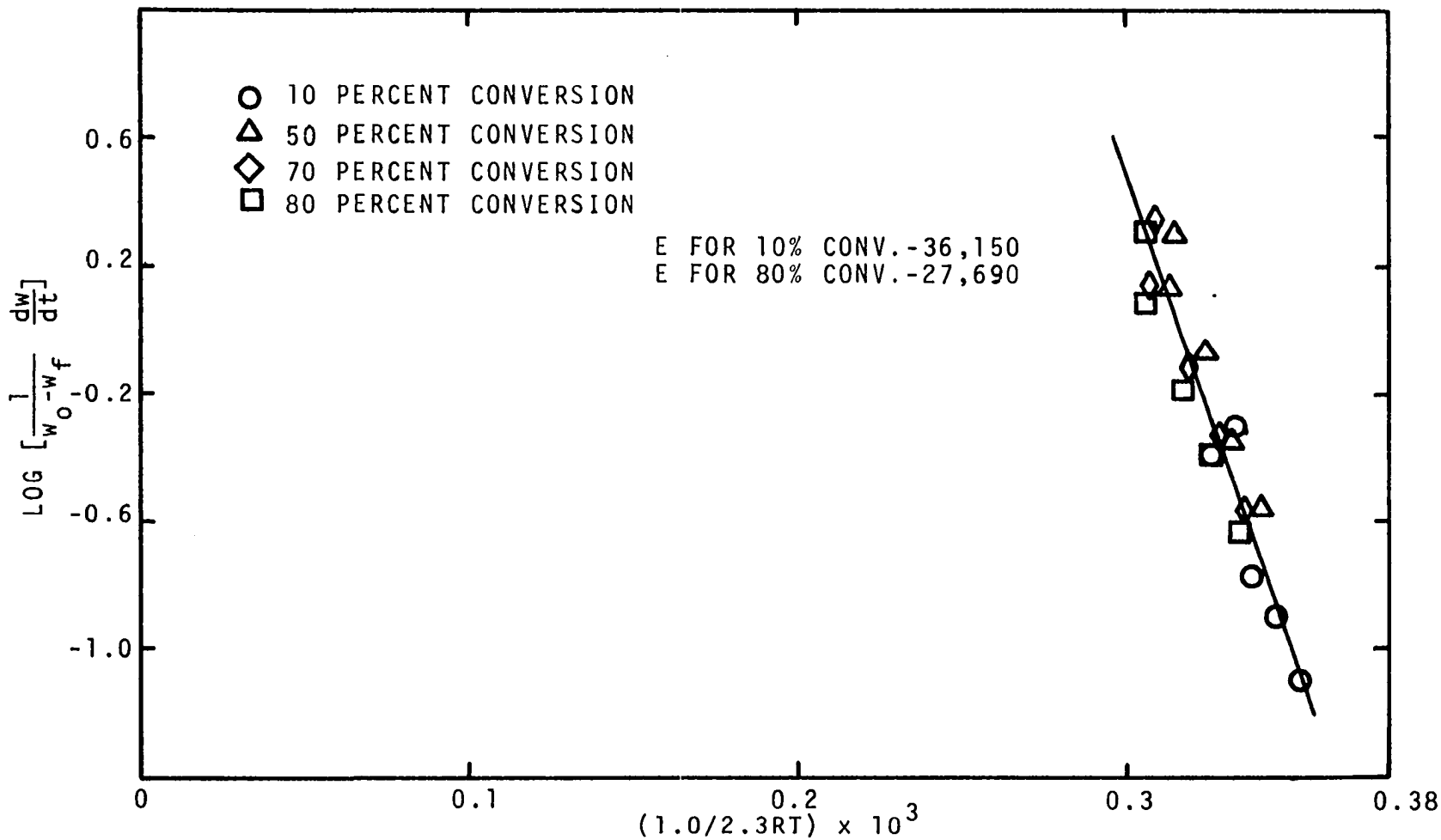

Figure IV-7. Plot for Obtaining Activation Energies Using the Method of Friedman. Munktell's Cellulose Decomposition.

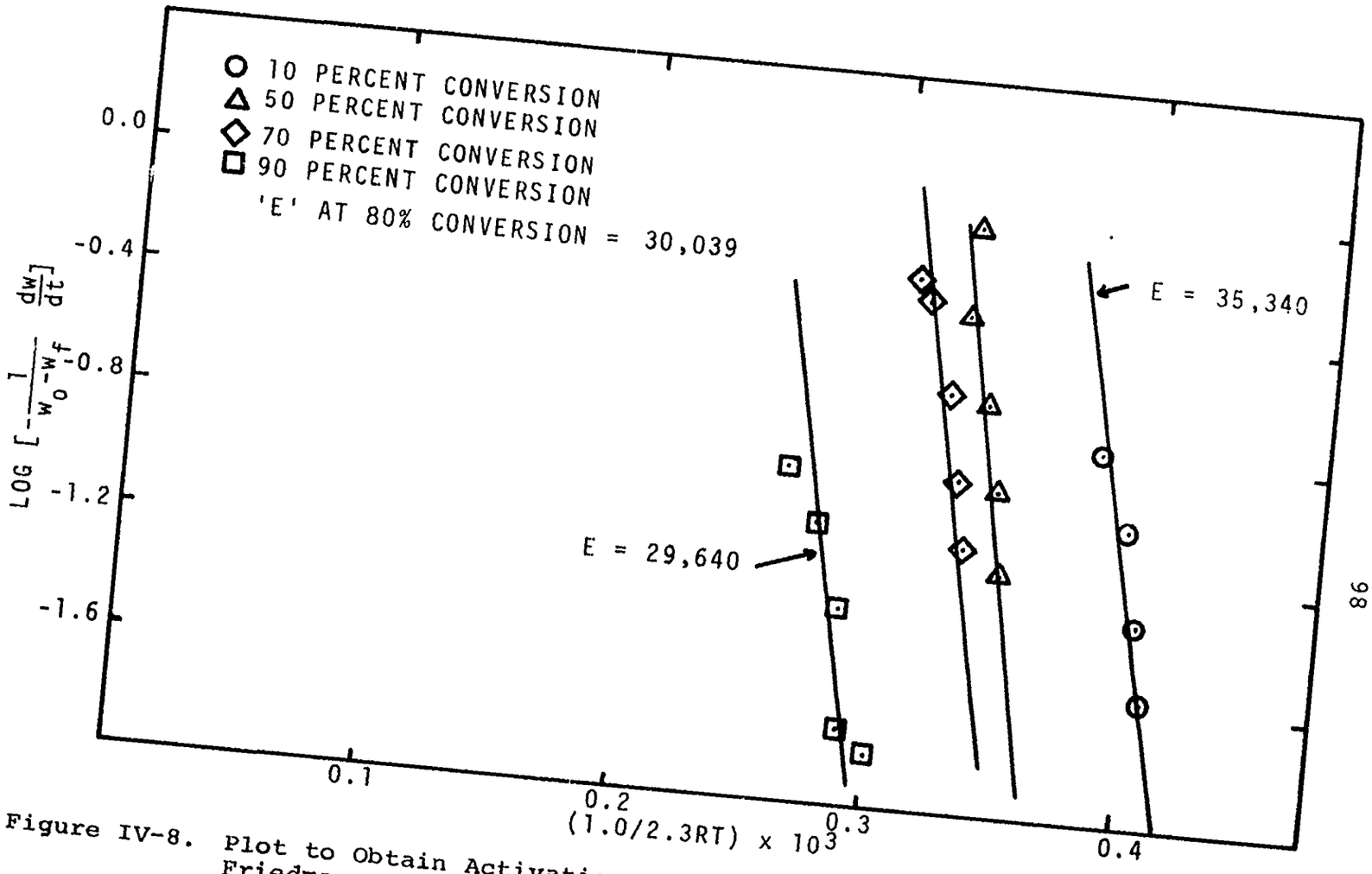

Figure IV-8. Plot to Obtain Activation Energies Using the Method of Friedman. Ponderosa Pine Decomposition.

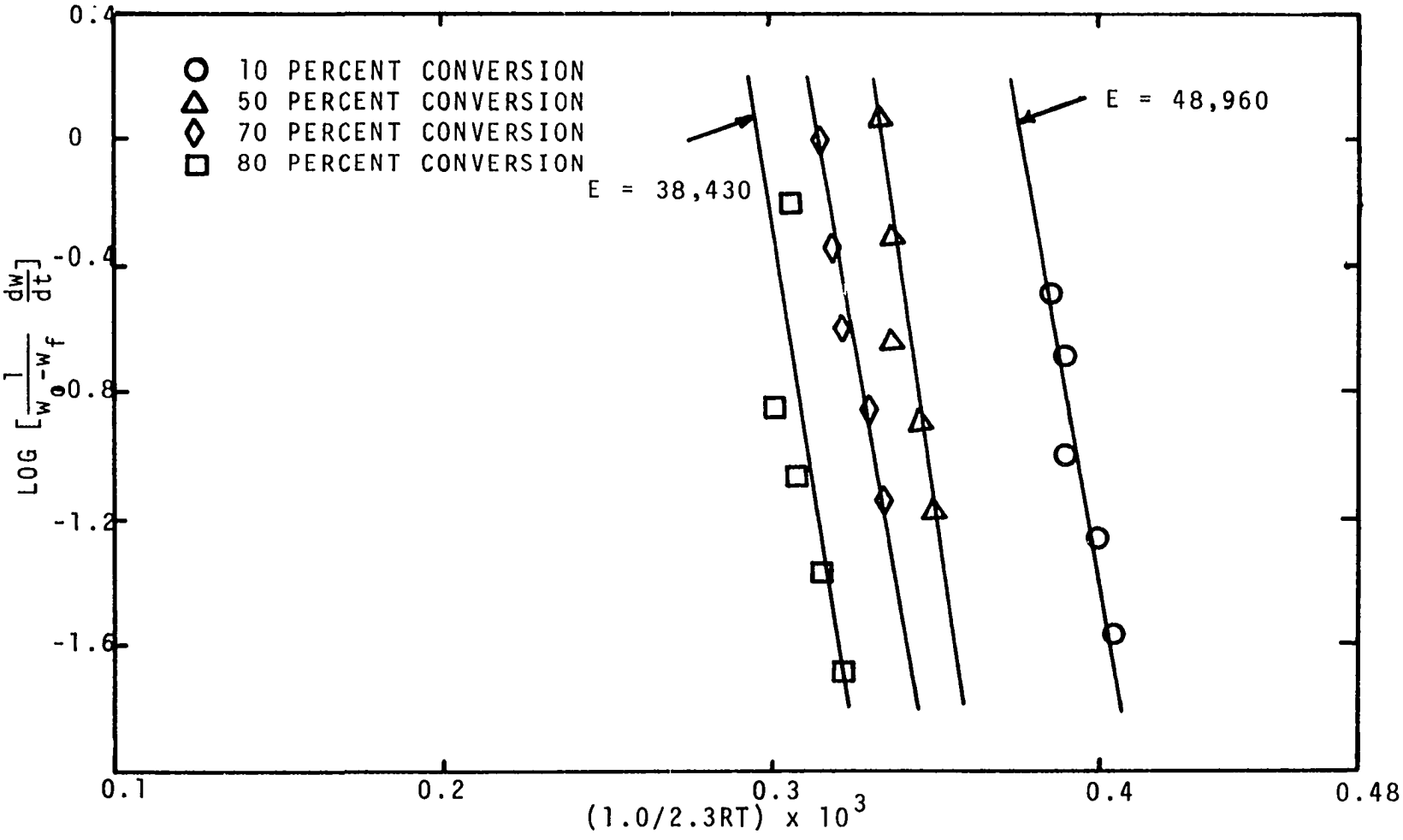

Figure IV-9. Plot to Obtain Activation Energies Using The Method of Friedman. Extracted Ponderosa Pine Decomposition.

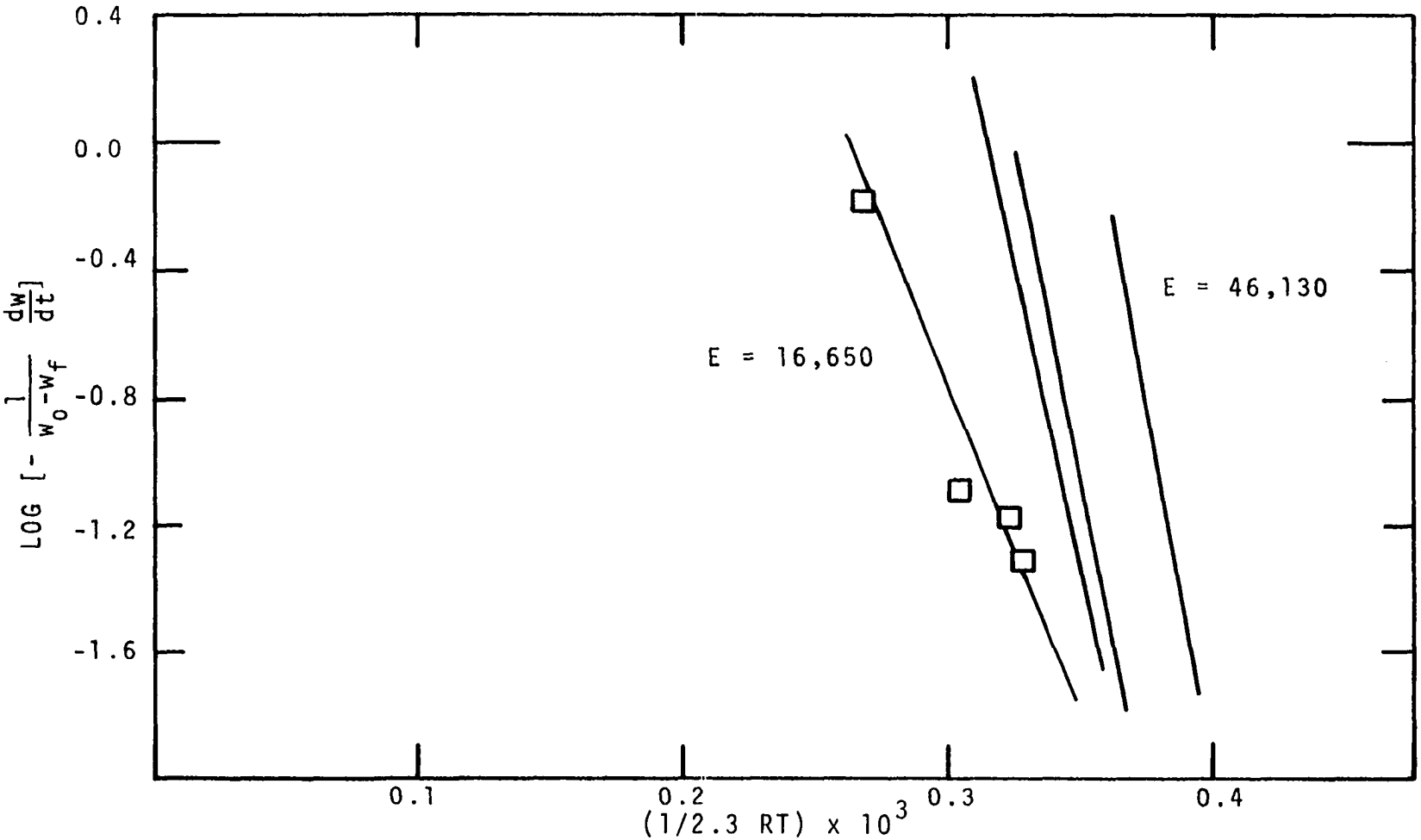

Figure IV-10. Plot to Obtain Activation Energies Using the Method of Friedman. Excelsior Decomposition.

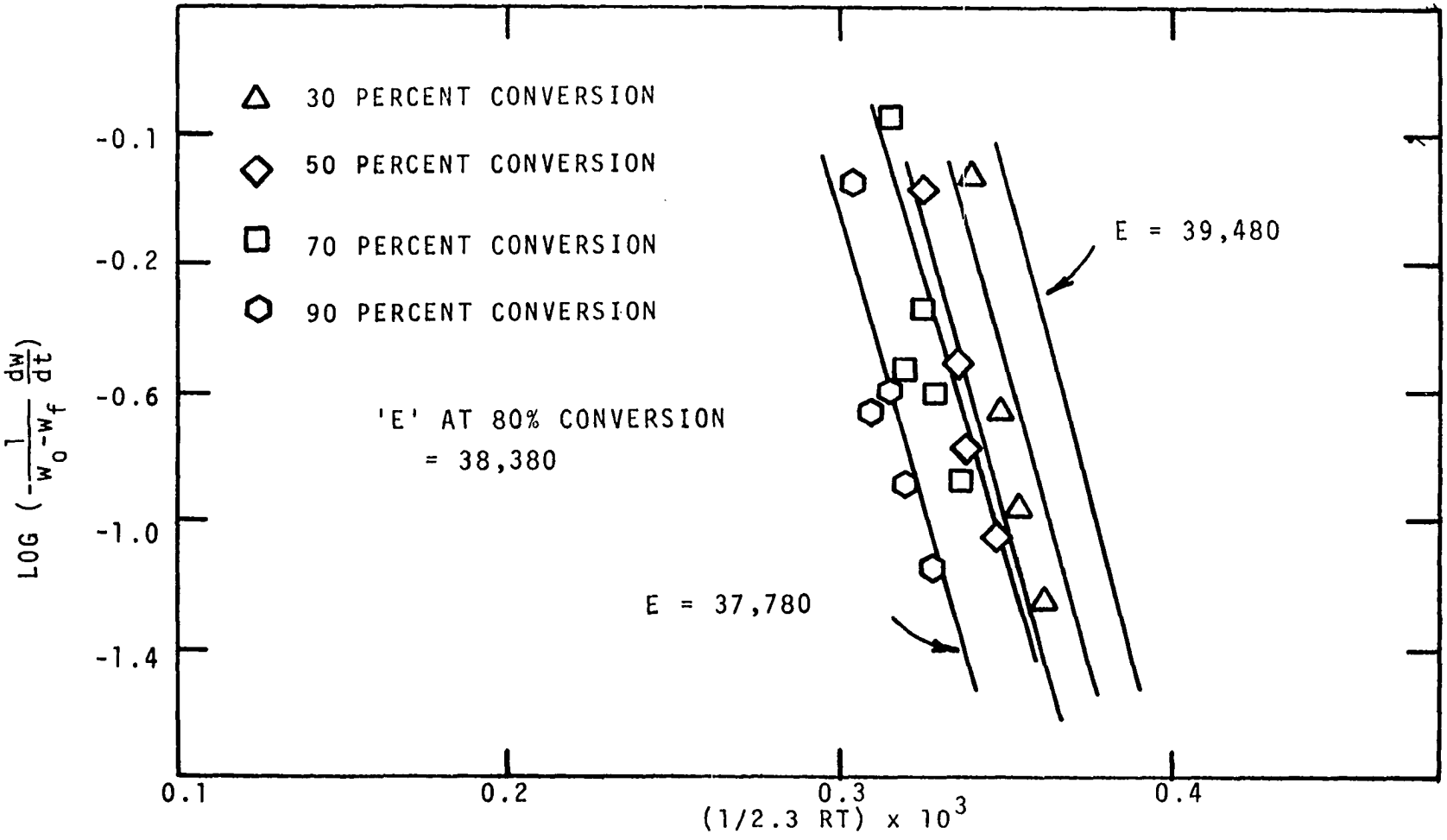

Figure IV-11. Plot to Obtain Activation Energies Using the Method of Friedman. Extracted Excelsior Decomposition.

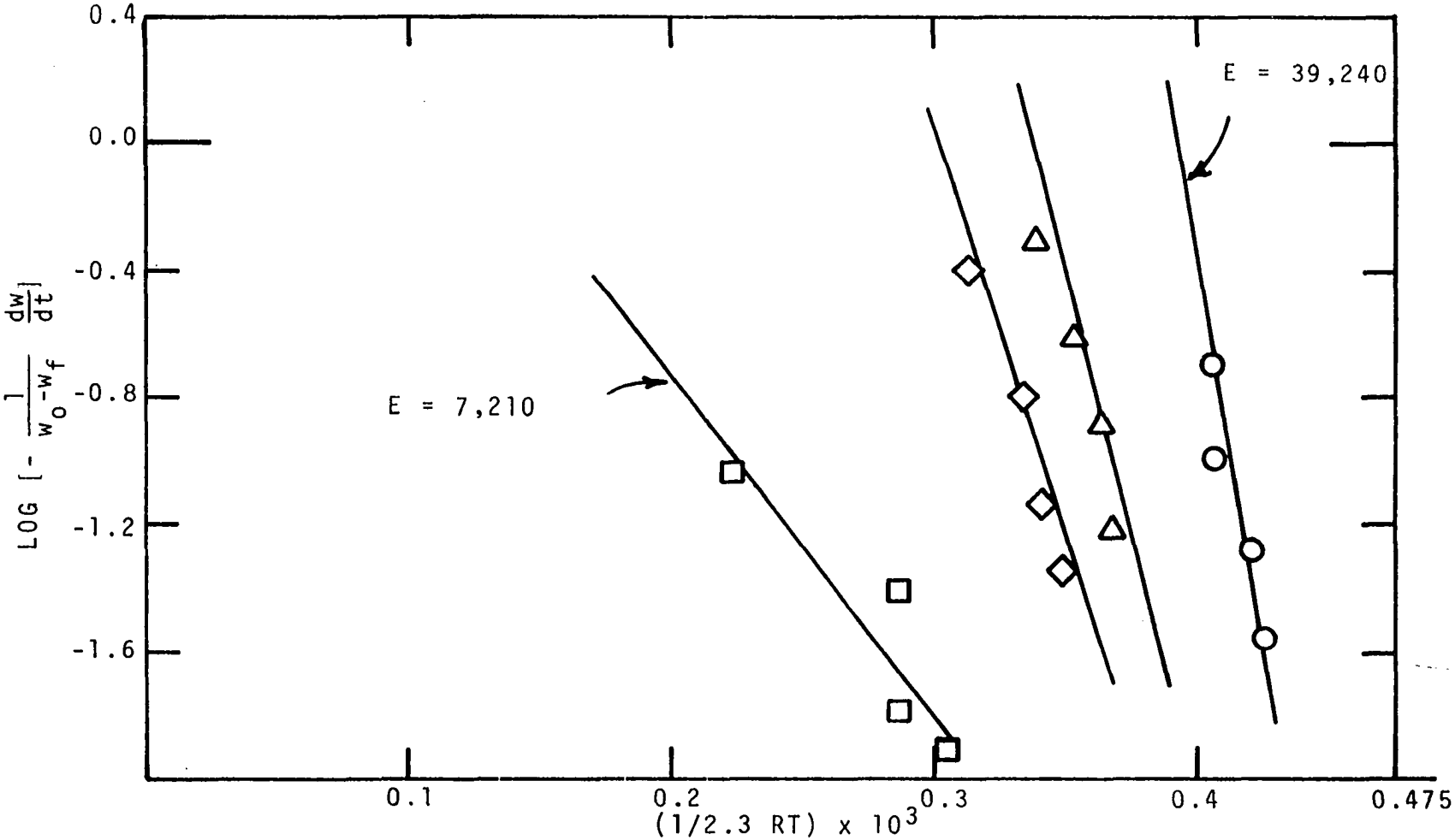

Figure IV-12. Plot to Obtain Activation Energies Using the Method of Friedman. Saltbush Leaves Decomposition.

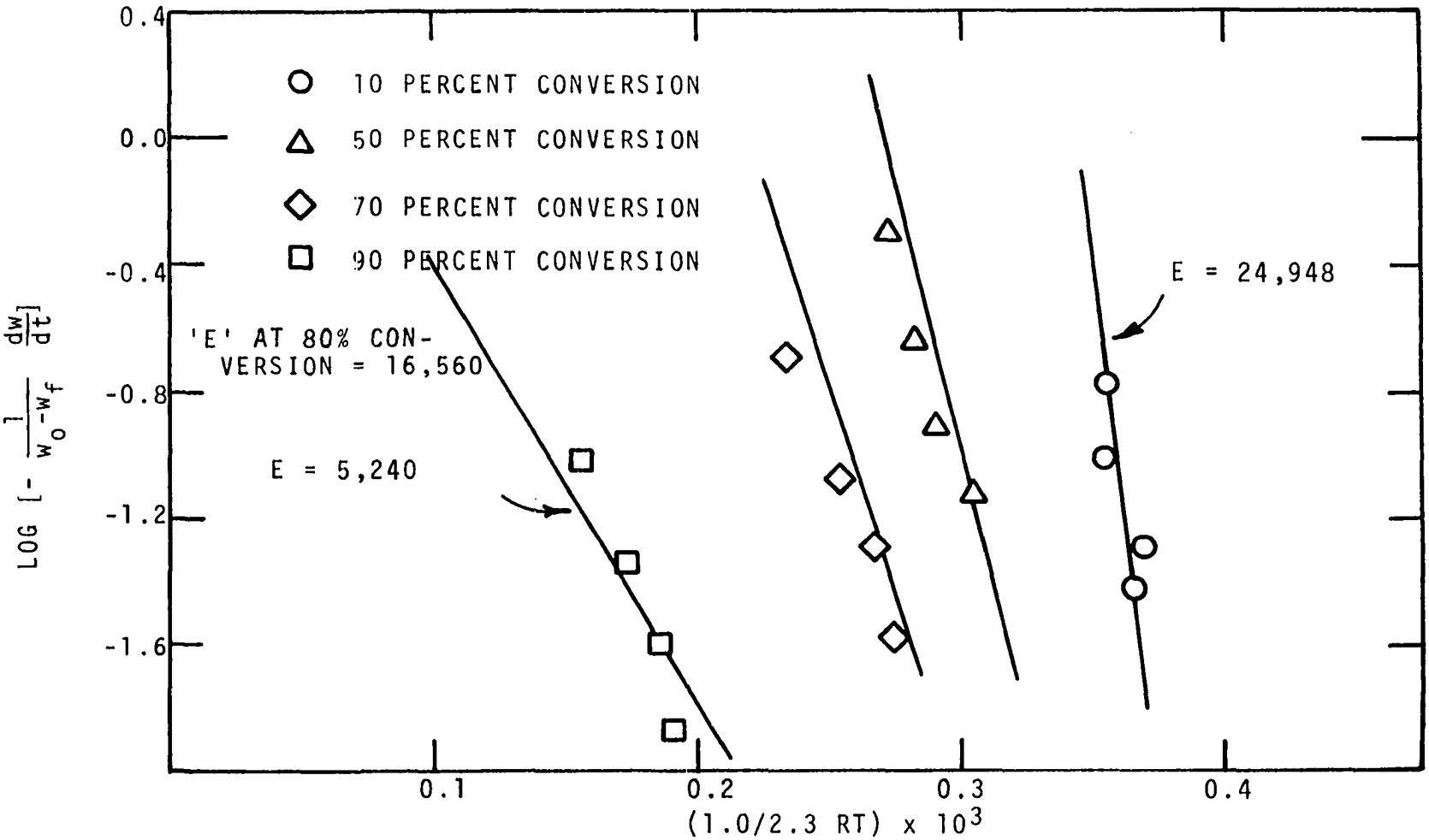

Figure IV-13. Plot to Obtain Activation Energies Using the Method of Friedman. Punky Wood (From Douglas-Fir Snags) Decomposition.

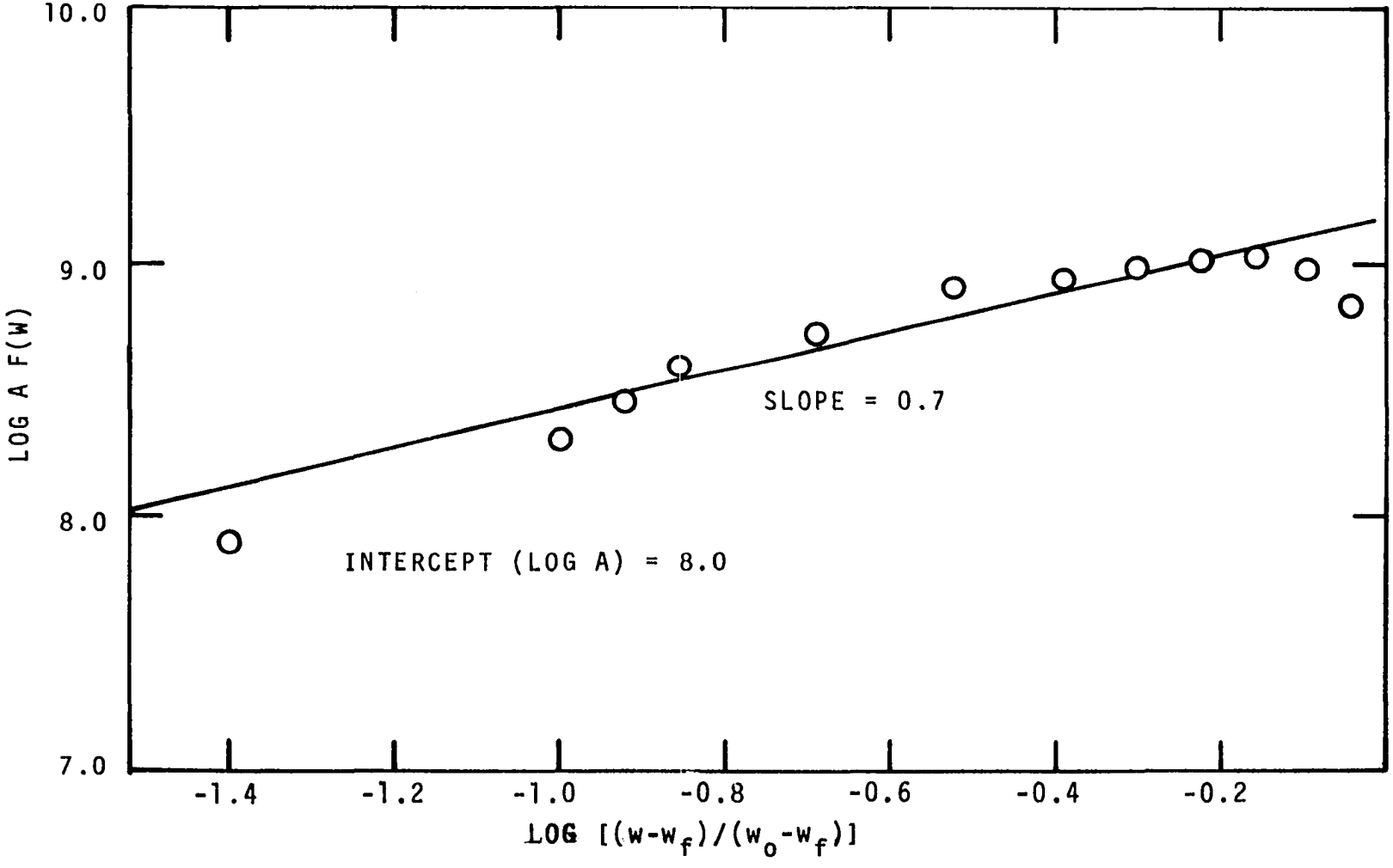

Figure IV-14. Determination of Frequency Factor and Order of Reaction for Cellulose Decomposition Using Friedman's Method of Analysis.

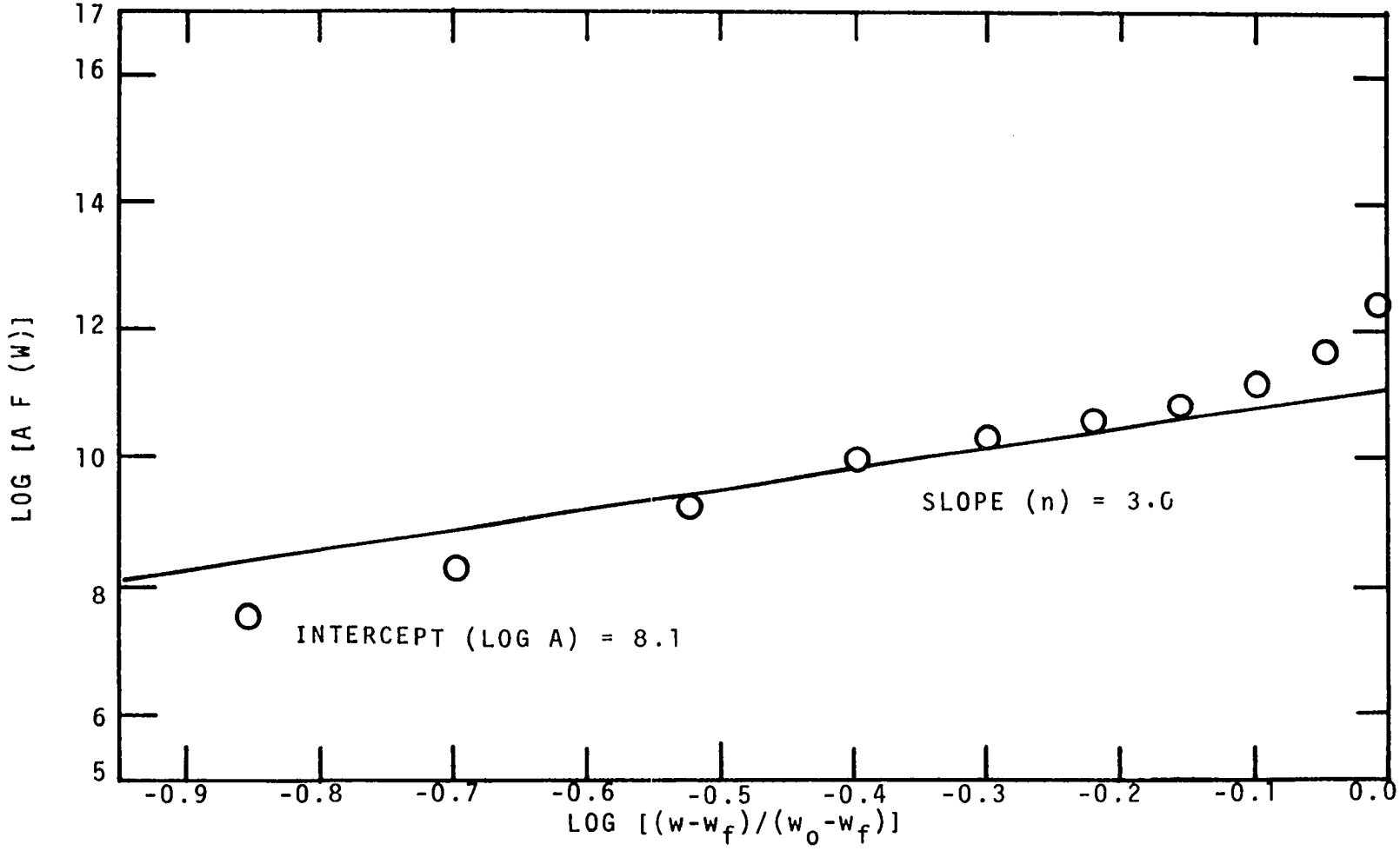

Figure IV-15. Determination of Frequency Factor for Punky Wood Decomposition by Friedman's Method of Analysis.

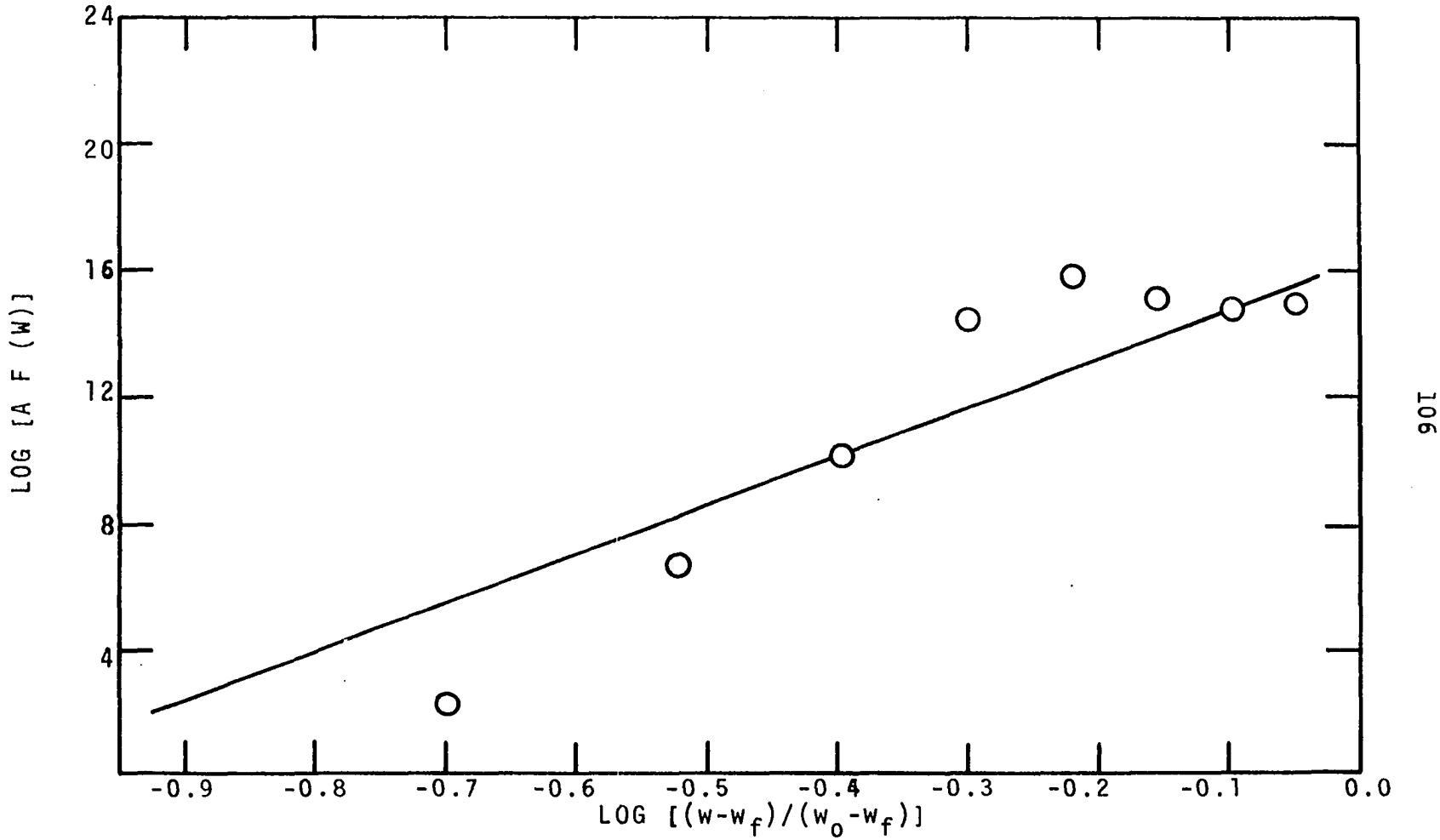

Figure IV-16. Determination of Frequency Factor for Cellulose Decomposition Using Individual Activation Energies. Friedman's Method of Analysis.

linear fit. The intercept obtained from Figure IV-14 yields an order of reaction of 0.7 and a frequency factor of 1.0×10^8 for cellulose decomposition. Woodard (77) plotted activation energy versus weight fraction remaining for clear polystyrene, white polystyrene, polymethyl methacrylate and clear PVC, which clearly shows that the application of the Friedman technique is not meaningful up to the initial 25 to 30 percent and above 90 percent of decomposition for those materials. Sardesai (62) obtained an order of reaction (n) of 0.972, a pre-exponential factor (A) of 8.6×10^{12} (sec^{-1}) and an activation energy (E) of 28.61 kcal/g-mole for Whatman 54 filter paper which is essentially pure cellulose.

Akita (1) proposed a first order kinetic equation involving the summation of the decomposition rates of the individual wood components,

$$\frac{dw}{dt} = \Sigma_i \, k_i \, (w_i - w_{f_i}) \qquad \text{(IV-8)}$$

where $k_i = A_i e^{-E_i/RT}$ (min^{-1})

A_i = pre-exponential factor (min^{-1})

E_i = activation energy (cal/g-mole)

T = absolute temperature (°K)

R = universal gas constant = 1.987 cal/gm-mole-°K

w_{f_i} = final weight of component i (mg)

w_i = weight of component i at time t (mg)

t = time (min)

He reported that when isolated wood components were recombined and tested, the thermal reaction appeared to be the same as that for natural wood. The decomposition, however, was explained by a two-step mechanism; the first was a zero order reaction for the initial stages of reaction followed by the second which was a first order reaction in the final stages of reaction.

Burningham and Seader (17) proposed a quasi-linearization technique to optimize the kinetic parameters as was discussed in Chapter II.

In both the studies mentioned above the reaction order was assumed. In addition, Burningham and Seader also assumed initial guessed values of A, the pre-exponential factor, and E, the activation energy. They had to resort to graphical methods for obtaining the initial values and then to constrain one of the parameters for a positive rapid convergence of the computer results (refer to Equation II-20).

Woodard (77) made a one-dimensional search over an assumed range of values of n, the reaction order, to best fit his data using Friedman's technique for each heating rate. Such a procedure required considerable computer time and close "guesses" on the range of the reaction order to result in convergence.

A simple approach using the data obtained at all heating rates for cellulose and punky wood is proposed in this thesis. Its advantage over the other methods is that no

assumptions are made for any of the kinetic parameters in the equation used, which is

$$-\frac{dW}{dt} = Ae^{-E/RT}(W)^n \qquad \text{(IV-9)}$$

where $W = (w-w_f)/(w_o-w_f)$ (dimensionless)

A = pre-exponential factor (min^{-1})

E = activation energy (kcal/mole)

R = universal gas constant = 1.987 cal/mole-°K

T = absolute temperature (°K)

n = kinetic order of reaction

t = time (min)

w = weight of the sample at time t (gm)

w_f = weight of the residue (gm)

w_o = initial weight of the sample (gm)

Since a dimensionless quantity for W (fraction of volatiles) is being considered, it does not matter what weight units are used for w, w_o and w_f as long as all the three are expressed in the same units. Rewriting Equation IV-9 gives

$$\frac{dW}{dt} = \frac{d}{dt}\left[\frac{w - w_f}{w_o-w_f}\right] = \left[\frac{1}{w_o-w_f}\right]\frac{dw}{dt}$$

or

$$\left[-\frac{1}{w_o-w_f}\frac{dw}{dt}\right] = Ae^{-E/RT}\left[\frac{w - w_f}{w_o-w_f}\right]^n$$

Taking logarithms yields,

$$\log\left[-\frac{1}{w_o-w_f}\frac{dw}{dt}\right] = \log A - \frac{E}{2.3RT} + n \log\left[\frac{w - w_f}{w_o-w_f}\right] \qquad \text{(IV-10)}$$

With the data obtained, a linear regression analysis using the method of least squares was performed with the left hand side of Equation IV-10 as the dependent variable and $1/(2.3RT)$ and $\log [(w-w_f)/(w_o-w_f)]$ as independent variables. The results of the least square analysis of cellulose and punky wood data are shown in Table IV-1. A comparison of the kinetic parameters thus obtained with those found by the method proposed by Goldfarb, et al., can also be seen in this table.

TABLE IV-1

RESULTS OF LEAST SQUARE ANALYSIS ON CELLULOSE AND PUNKY WOOD DATA. COMPARISON WITH THE RESULTS OF GOLDFARB'S TECHNIQUE

Kinetic Parameter	Cellulose		Punky Wood	
	Least Square Technique	Goldfarb's Technique	Least Square Technique	Goldfarb's Technique
Activation Energy (cal/gm-mole)	29,270	27,980	21,290	32,270
Frequency Factor (A) (1/min)	5.0×10^9	2.3×10^8	3.1×10^7	3.5×10^8
Order of Reaction n	0.79	0.7	3.2	3.0

As could be seen from Table IV-1, the values for A, E and n obtained in the present work compare reasonably well with those obtained by Goldfarb's technique except for the

activation energy of punky wood. Due to an uneven scatter in the data in the initial 30 percent and the final 10 percent of the reaction, the straight line drawn using Goldfarb's technique is likely to be in error. In fact, the inherent weakness of Goldfarb's method of analysis lies in the contention that the uncertainty in the decomposition data obtained in the initial 35 percent and the final 10 percent of the reaction requires that these portions of the reaction be neglected in determining the kinetic parameters. None of the data obtained was neglected in the least-squares method of analysis proposed in this thesis.

The results of the regression analysis (the method of least-squares) are plotted in Figures IV-17 and IV-18. It could be noticed from these figures that there exists some scatter in the data. This scatter is probably due to experimental inaccuracies in the initial and final portions of the data. The inaccuracy is also evident from the deviation of the calculated weight loss and rate of weight loss curves from the experimental curves for pure cellulose and punky wood (assumed to be pure lignin) shown in Figures IV-19 through IV-28.

The model proposed in this thesis for the degradation of wood is the first of its kind, although, as mentioned earlier, Akita (1) did suggest a similar approach as given in Equation IV-8. The chief difference is that Akita used the difference in the initial and final weights of a component

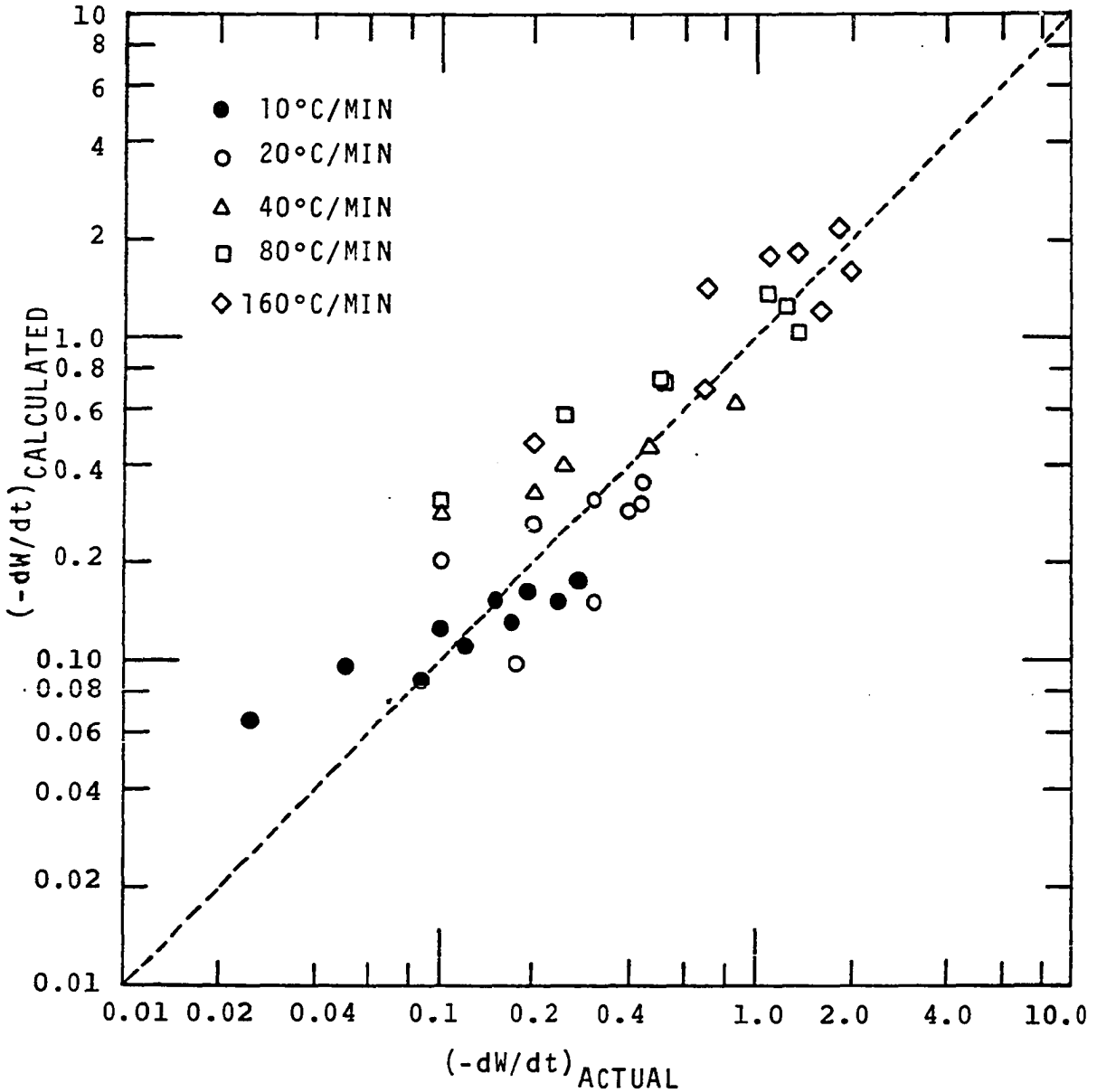

Figure IV-17. Least Square Technique Applied to Data for all Heating Rates. Cellulose Decomposition.

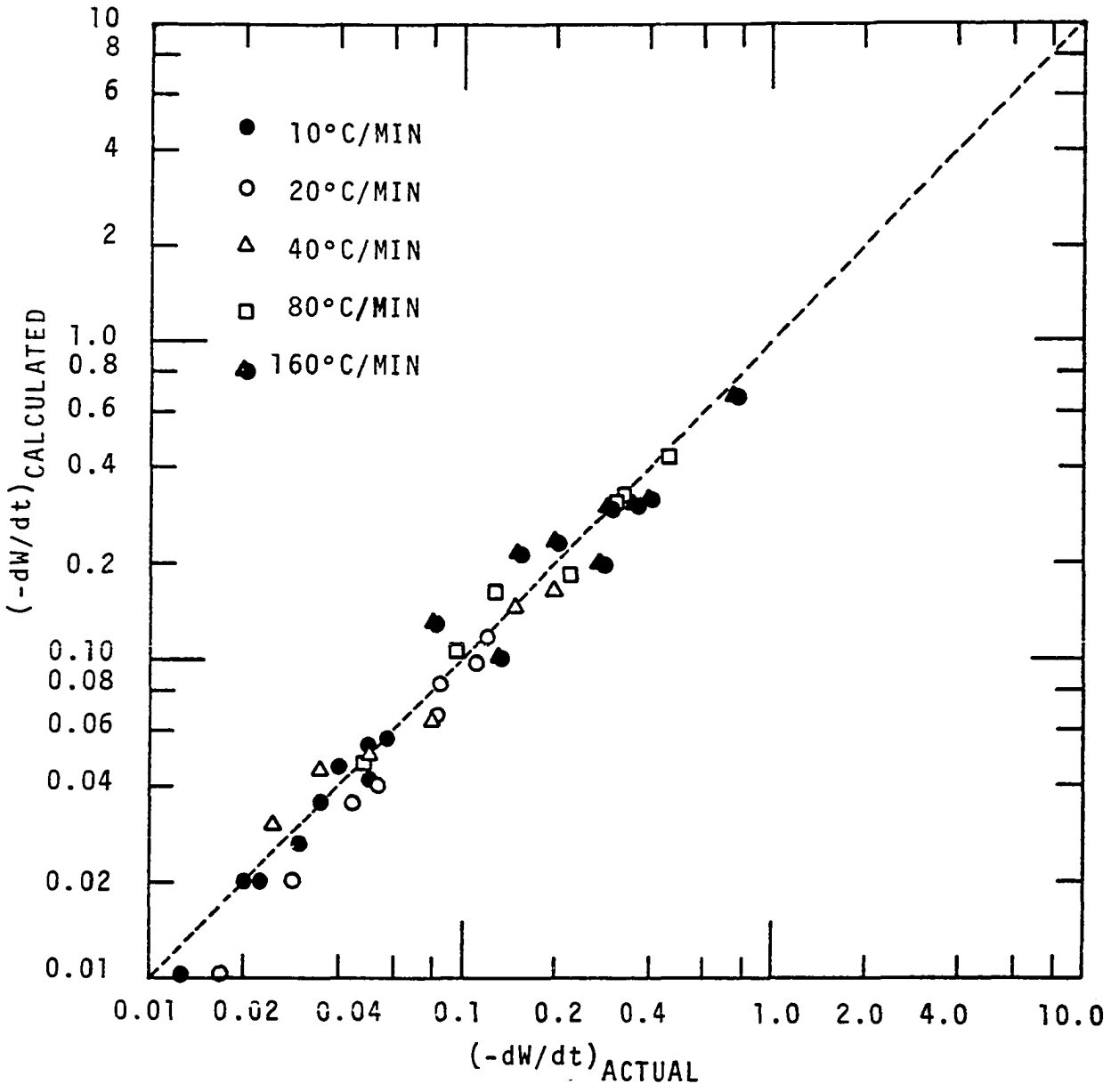

Figure IV-18. Least Square Technique Applied to Data for all Heating Rates. Lignin Decomposition.

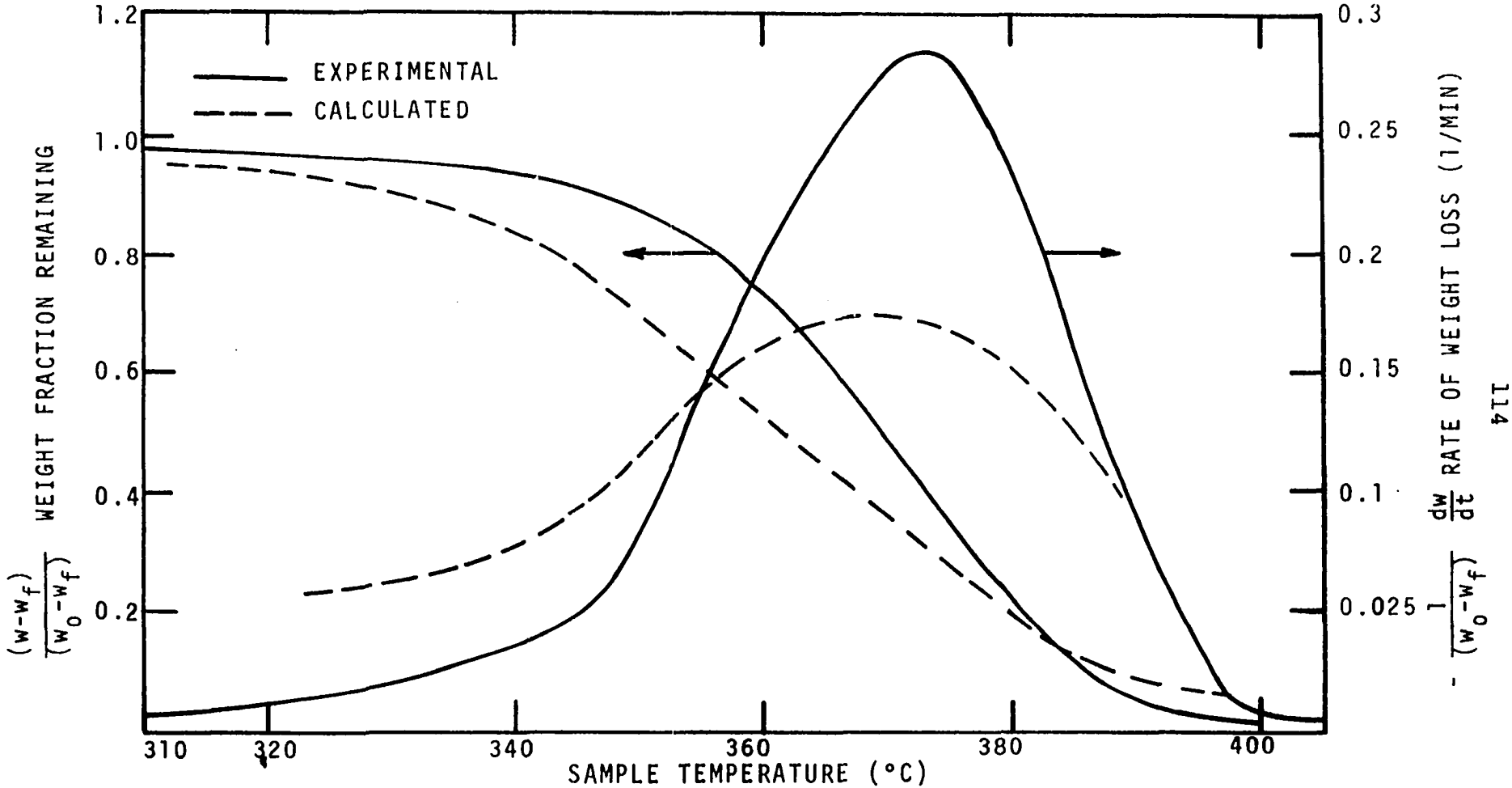

Figure IV-19 Weight Loss and Rate of Weight Loss for Munktell's Cellulose. Heating Rate - 10°C/MIN.

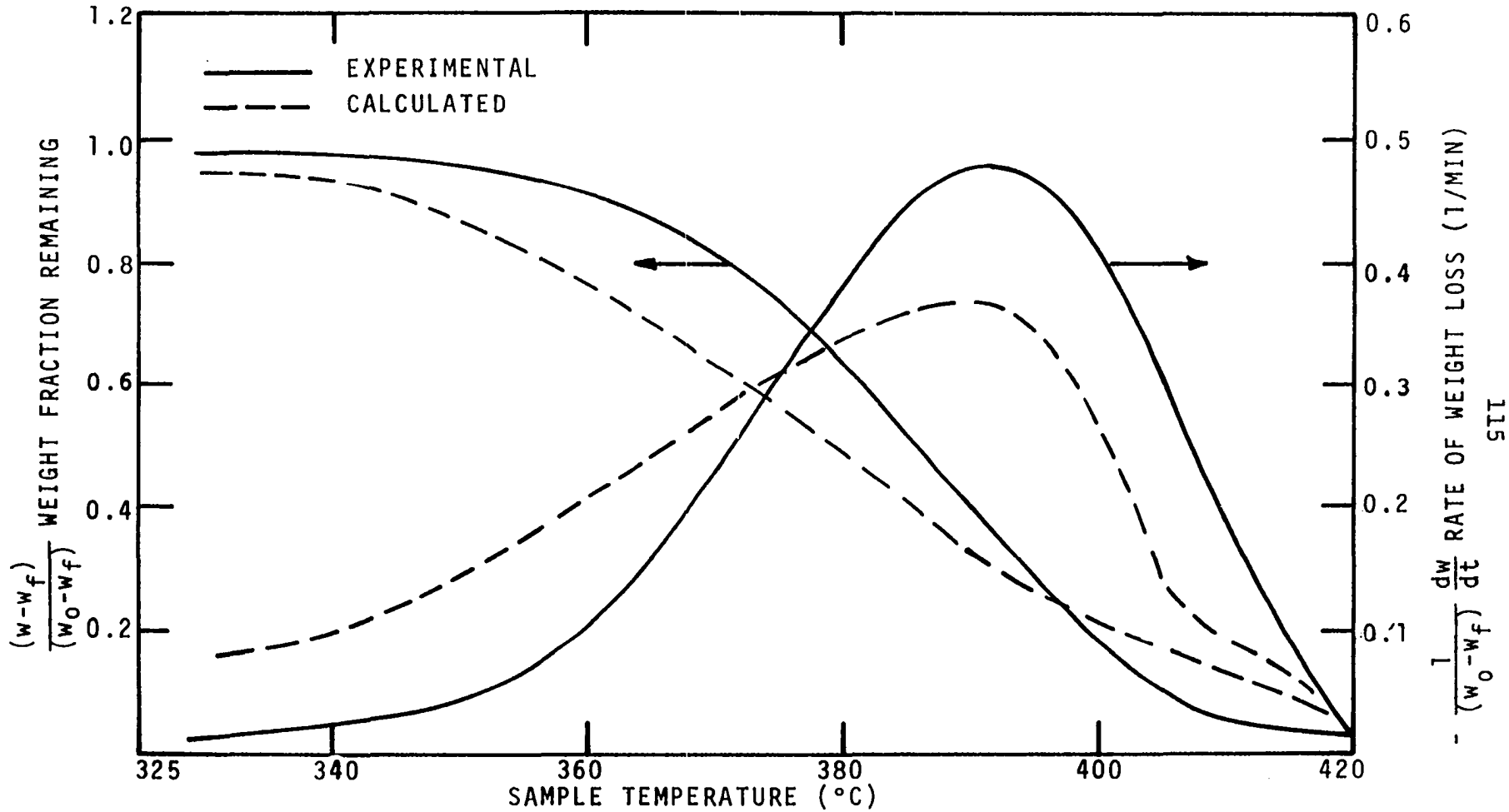

Figure IV-20. Weight Loss and Rate of Weight Loss for Munktell's Cellulose. Heating Rate - 20°C/MIN.

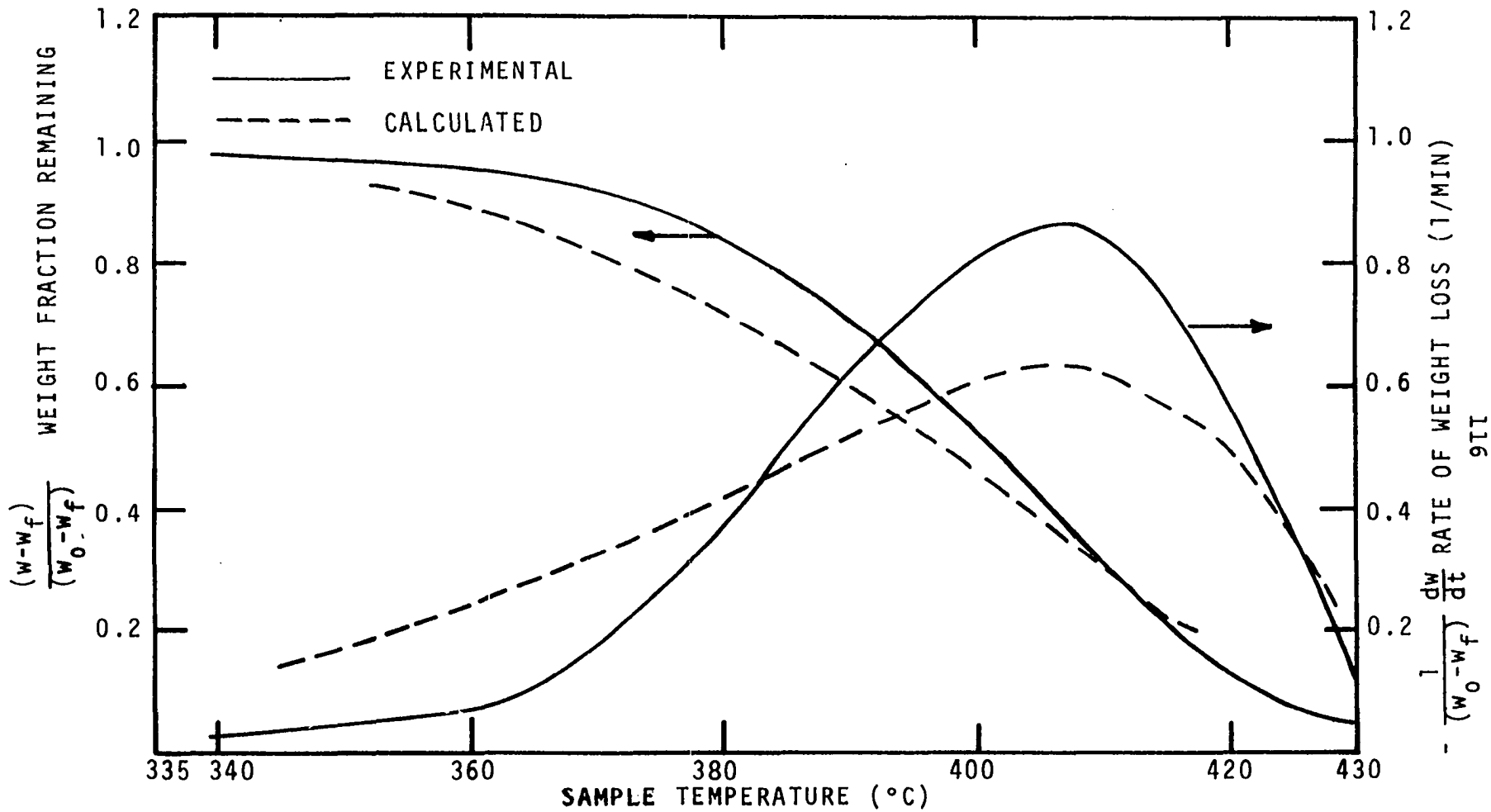

Figure IV-21. Weight Loss and Rate of Weight Loss for Munktell's Cellulose. Heating Rate - 40°C/MIN.

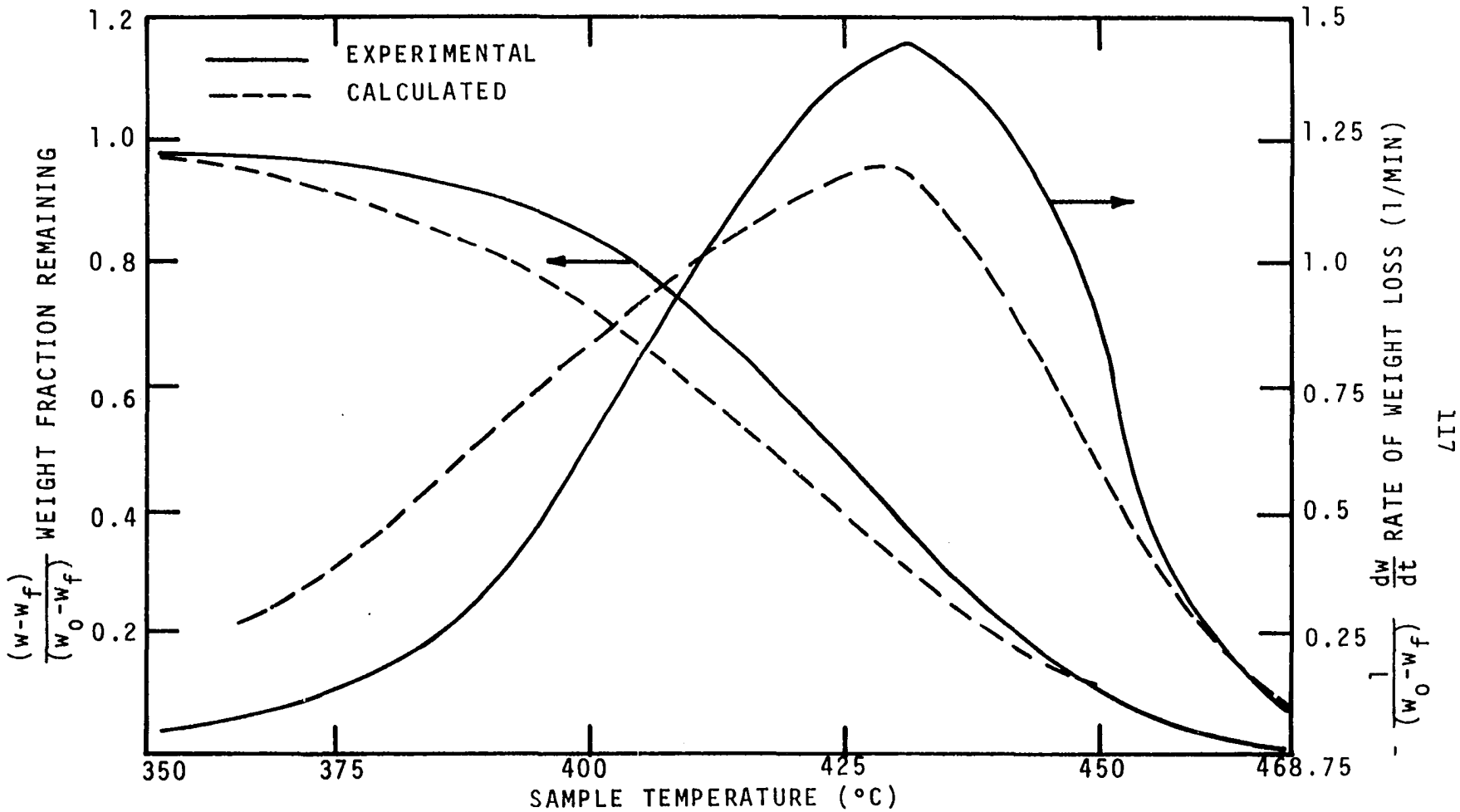

Figure IV-22. Weight Loss and Rate of Weight Loss for Munktell's Cellulose. Heating Rate - 80°C/MIN.

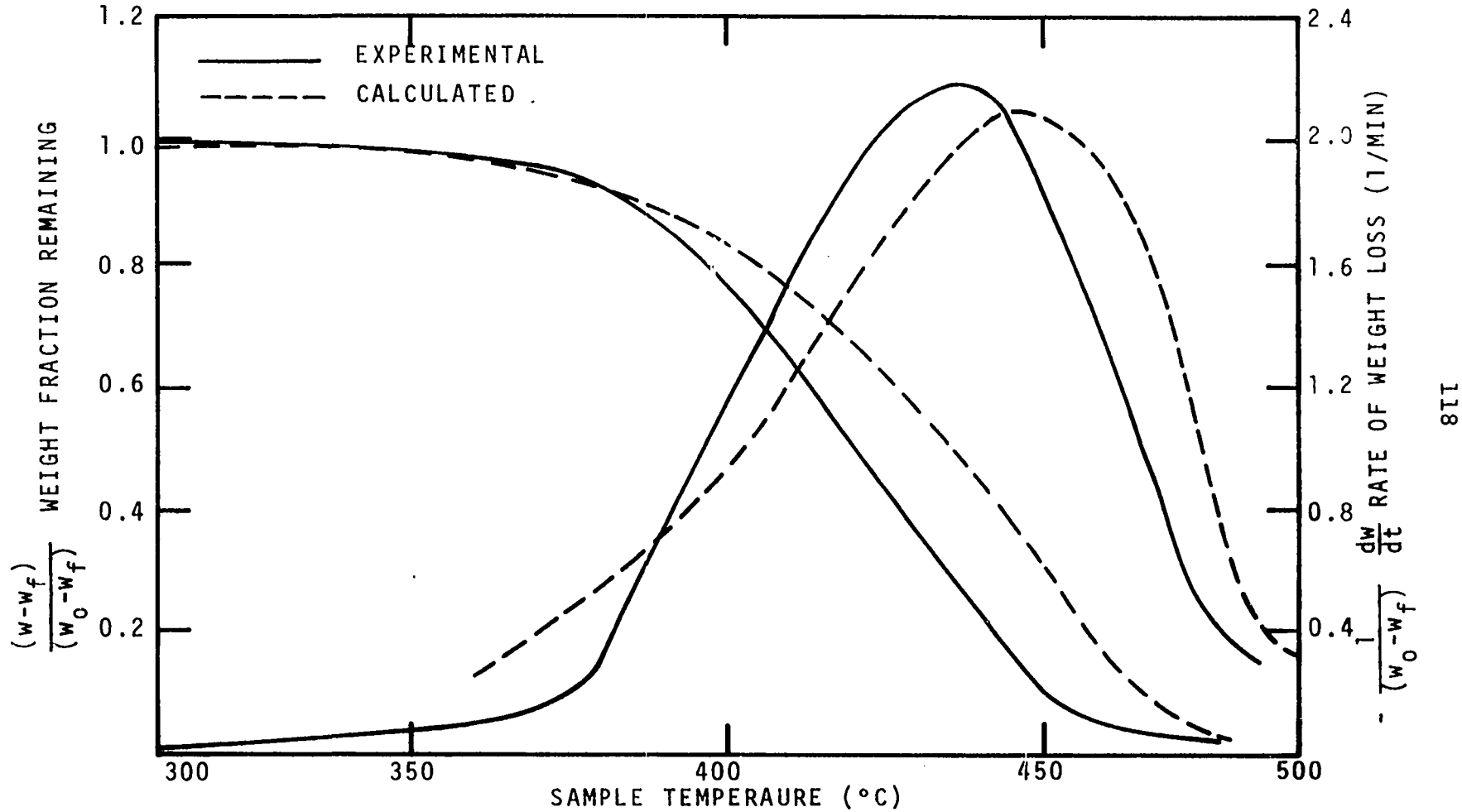

Figure IV-23. Weight Loss and Rate of Weight Loss for Munktell's Cellulose. Heating Rate - 160°C/MIN.

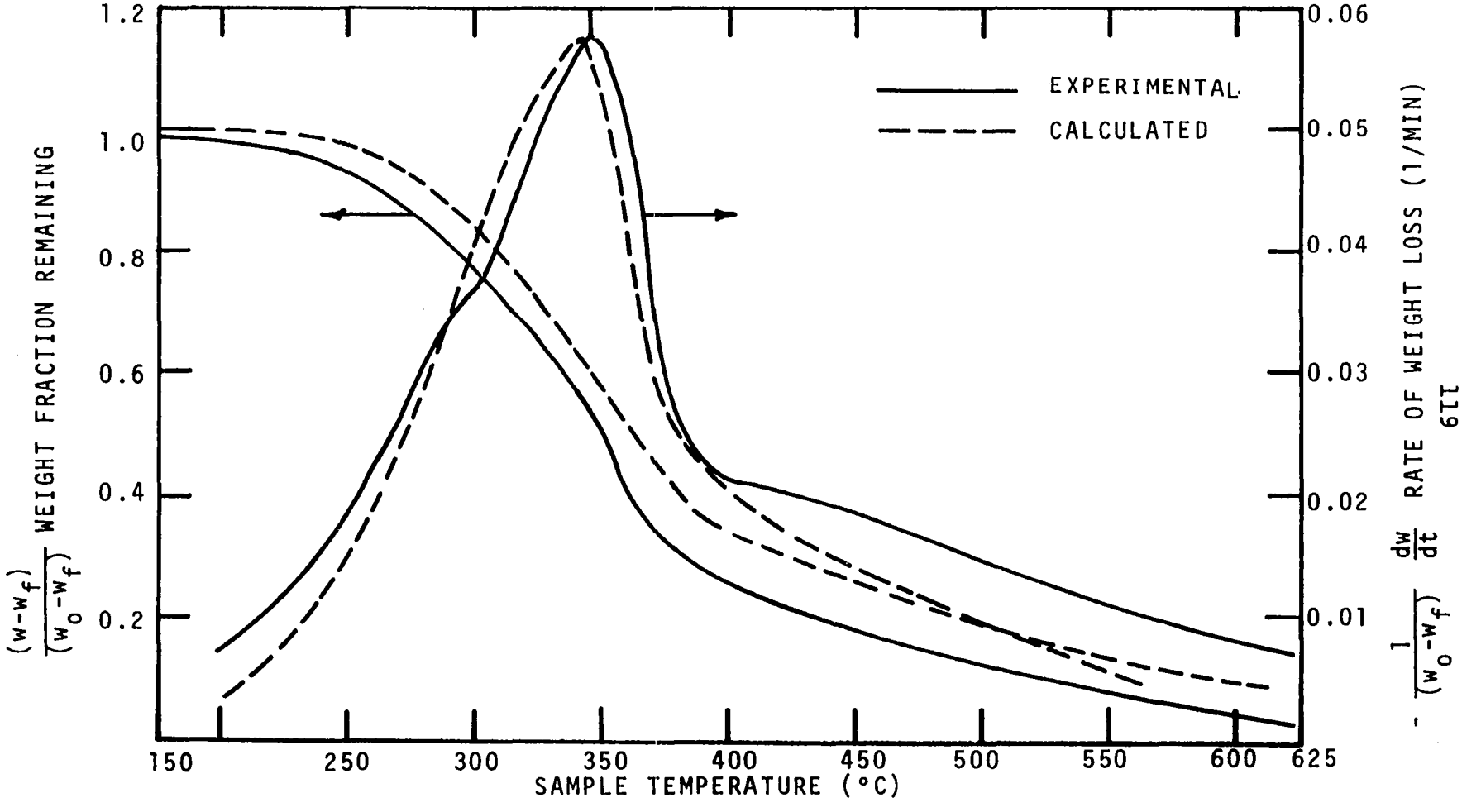

Figure IV-24. Weight Loss and Rate of Weight Loss for Punky Wood from Douglas-Fir Snags. Heating Rate - 10°C/MIN.

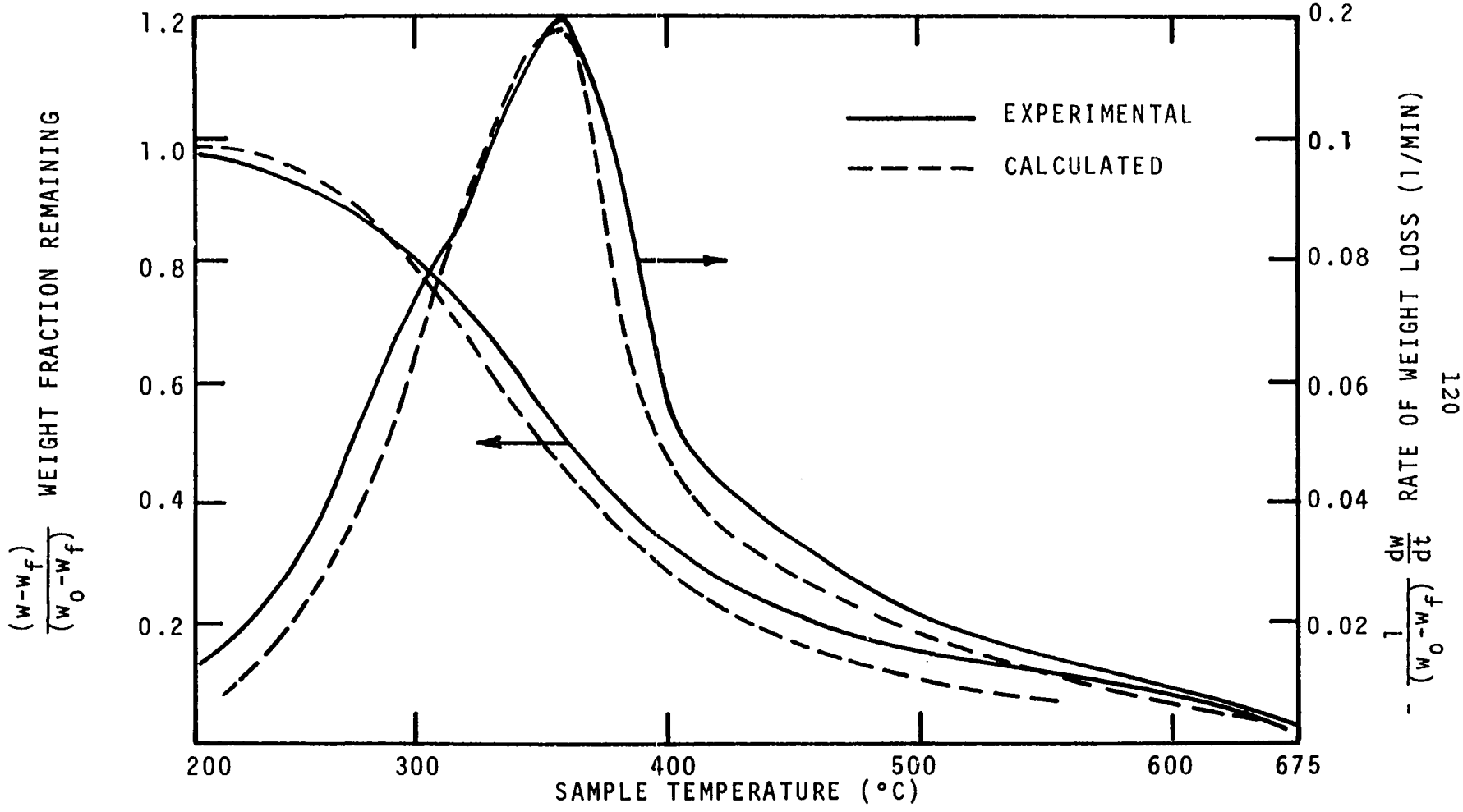

Figure IV-25. Weight Loss and Rate of Weight Loss for Punky Wood from Douglas-Fir Snags. Heating Rate - 20°C/MIN.

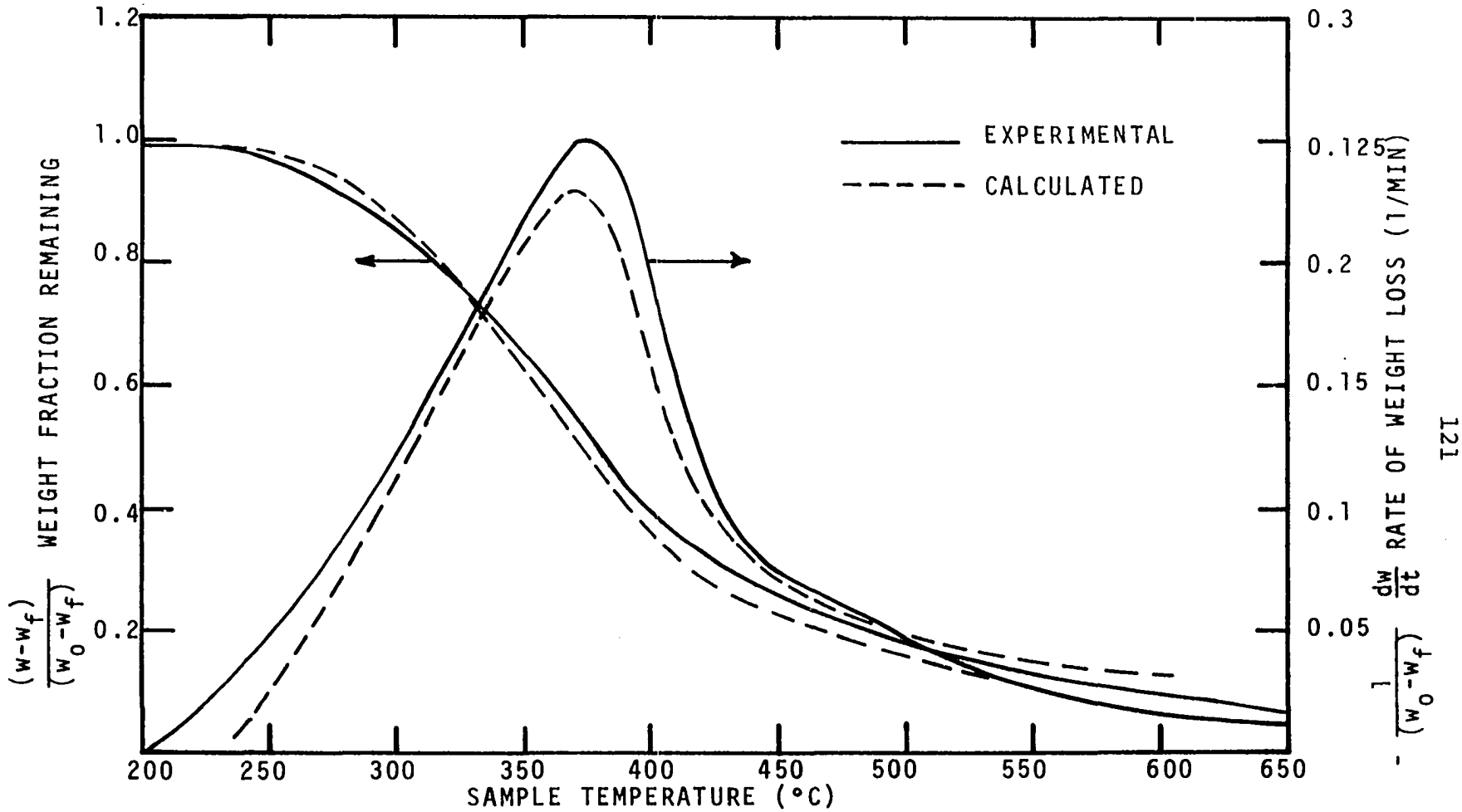

Figure IV-26. Weight Loss and Rate of Weight Loss for Punky Wood from Douglas-Fir Snags. Heating Rate - 40°C/MIN.

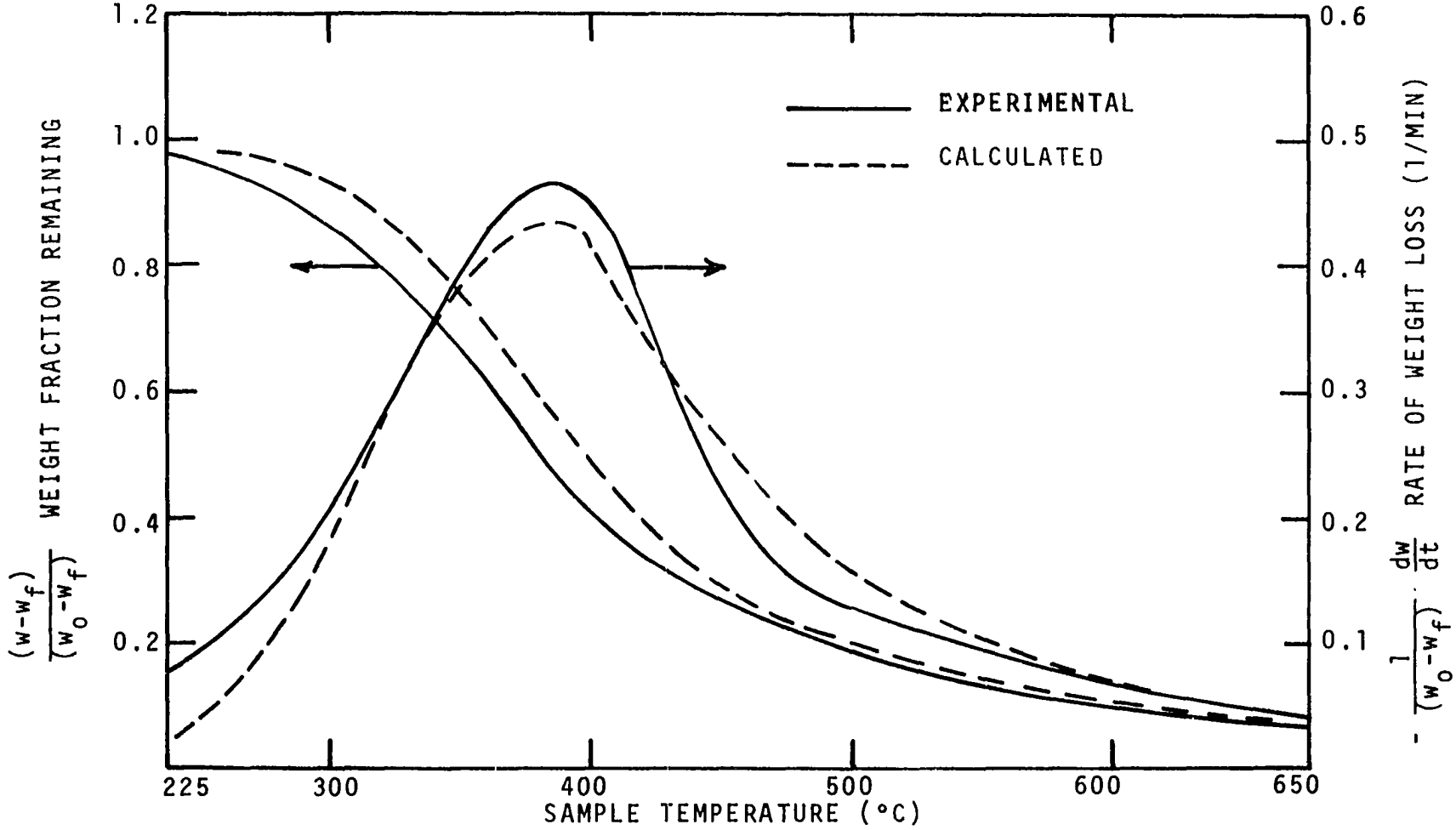

Figure IV-27. Weight Loss and Rate of Weight Loss for Punky Wood from Douglas-Fir Snags. Heating Rate - 80°C/MIN.

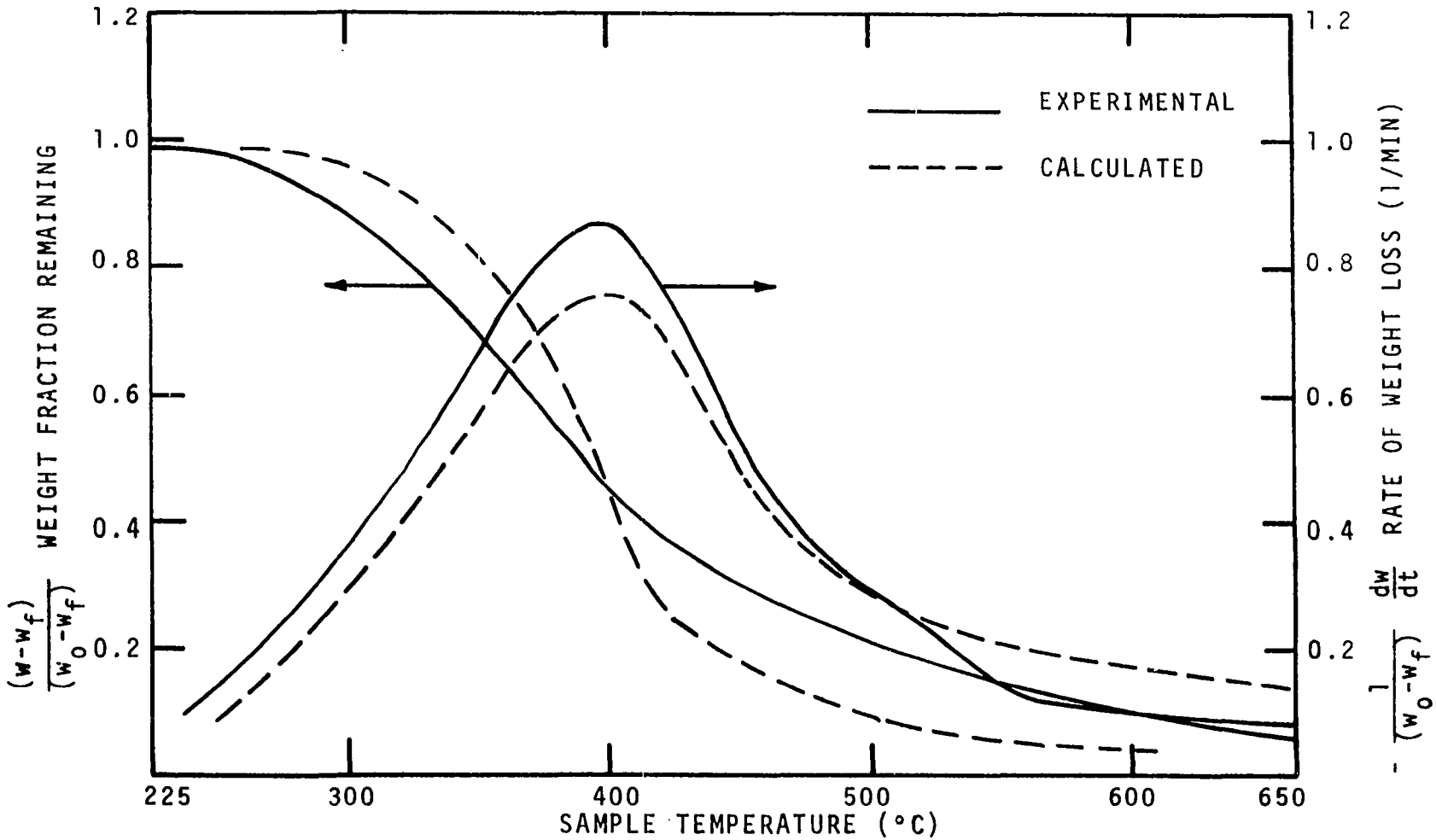

Figure IV-28. Weight Loss and Rate of Weight Loss for Punky Wood from Douglas-Fir Snags. Heating Rate - 160°C/MIN.

for the weight function and an assumed reaction order of unity while the present thesis used a dimensionless function of volatile weight fraction and reaction orders computed directly from the data obtained for cellulose and lignin.

The chief constituents of wood are assumed to be the cellulose and lignin fractions. It is also assumed that when wood pyrolyzes these two essential ingredients decompose in parallel reactions which are non-interacting. The result is that the individual reaction mechanisms of pure cellulose and pure lignin can be combined so as to yield not only a qualitative picture of the degradation of wood but even a quantitative insight into the rate of pyrolysis. In other words the kinetic parameters of any wood can be related to the kinetic parameters of cellulose and lignin.

Two Arrhenius-type terms, one for cellulose and one for lignin, are combined to yield the model

$$-\frac{dW}{dt} = A_c\, e^{-E_c/RT} (W_c)^{n_c} + A_L\, e^{-E_L/RT} (W_L)^{n_L} \qquad \text{(IV-11)}$$

where $W = (w-w_f)/(w_o-w_f)$, the fraction of the wood that will pyrolyze (dimensionless)

w = weight of wood sample remaining at time t (mg)

w_f = final weight of the residue (mg)

w_o = initial sample weight (mg)

A_c = frequency factor of cellulose (min^{-1})

E_c = activation energy of cellulose (cal/g-mole)

n_c = order of reaction of cellulose (dimensionless)

A_L = frequency factor of lignin (min^{-1})

E_L = activation energy of lignin (cal/g-mole)

n_L = order of reaction of lignin (dimensionless)

R = universal gas constant = 1.987 cal/g-mole-°K

T = absolute temperature (°K)

t = time (min)

$W_c = (w_c - w_{c,f})/(w_{c,o} - w_{c,f})$ (dimensionless)

w_c = weight of cellulose remaining in the wood at time t (mg)

$w_{c,o}$ = initial weight of cellulose in the wood (mg)

$w_{c,f}$ = weight of cellulose in the residue of wood (mg)

$W_L = (w_L - w_{L,f})/(w_{L,o} - w_{L,f})$ (dimensionless)

w_L = weight of lignin remaining in the wood at time t (mg)

$w_{L,o}$ = initial weight of lignin in the wood (mg)

$w_{L,f}$ = weight of lignin in the residue of wood (mg)

Since programmed heating rates were used the temperature in Equation IV-11 was more conveniently expressed in units of time as $T = T_o + \beta t$ where T_o is the initial temperature and β is the heating rate. The final form of the model used was

$$-\frac{dw}{dt} = (5.0 \times 10^9)\, e^{-29,740/1.987(T_o+\beta t)}\, (W_c)^{0.79} + (3.1 \times 10^7)\, e^{-21,290/1.987(T_o+\beta t)}\, (W_L)^{3.2} \qquad \text{(IV-12)}$$

A computer program was developed using the fourth order Runge-Kutta technique to solve Equation IV-12. A knowledge of the initial temperature, the heating rate, and the composition of the wood are needed to compute the rate of weight loss and the weight remaining. Figures IV-29 through IV-31 show the computed curves using the proposed model, Equation IV-12, for excelsior decomposition. The compositions of dead Ponderosa pine needles and four wing saltbush leaves were not available during the course of this study for comparing the computed and experimental curves. Larch composition, however, was available. The data on larch were taken expressly for the purpose of verifying the model. The results of larch analysis are given in Figures IV-32 through IV-34. The woods chosen for verifying the model provided a good range of composition, with a lignin content of 16 percent for excelsior and 39 percent for larch. The amount of cellulose was taken to be 84 percent for excelsior and 61 percent for larch, by difference.

The literature abounds with information on the effect of inorganic chemicals on the pyrolysis of wood. The studies of Tang (65, 66), Tang and Neill (70), Brenden (9), Browne and Brenden (16), and Browne and Tang (67, 68) are important in this respect, to name a few. The addition of as little as 2 percent of some inorganic salts could cause a considerable deviation in pyrolysis behavior between the unextracted and extracted wood, judging from the thermograms obtained by these

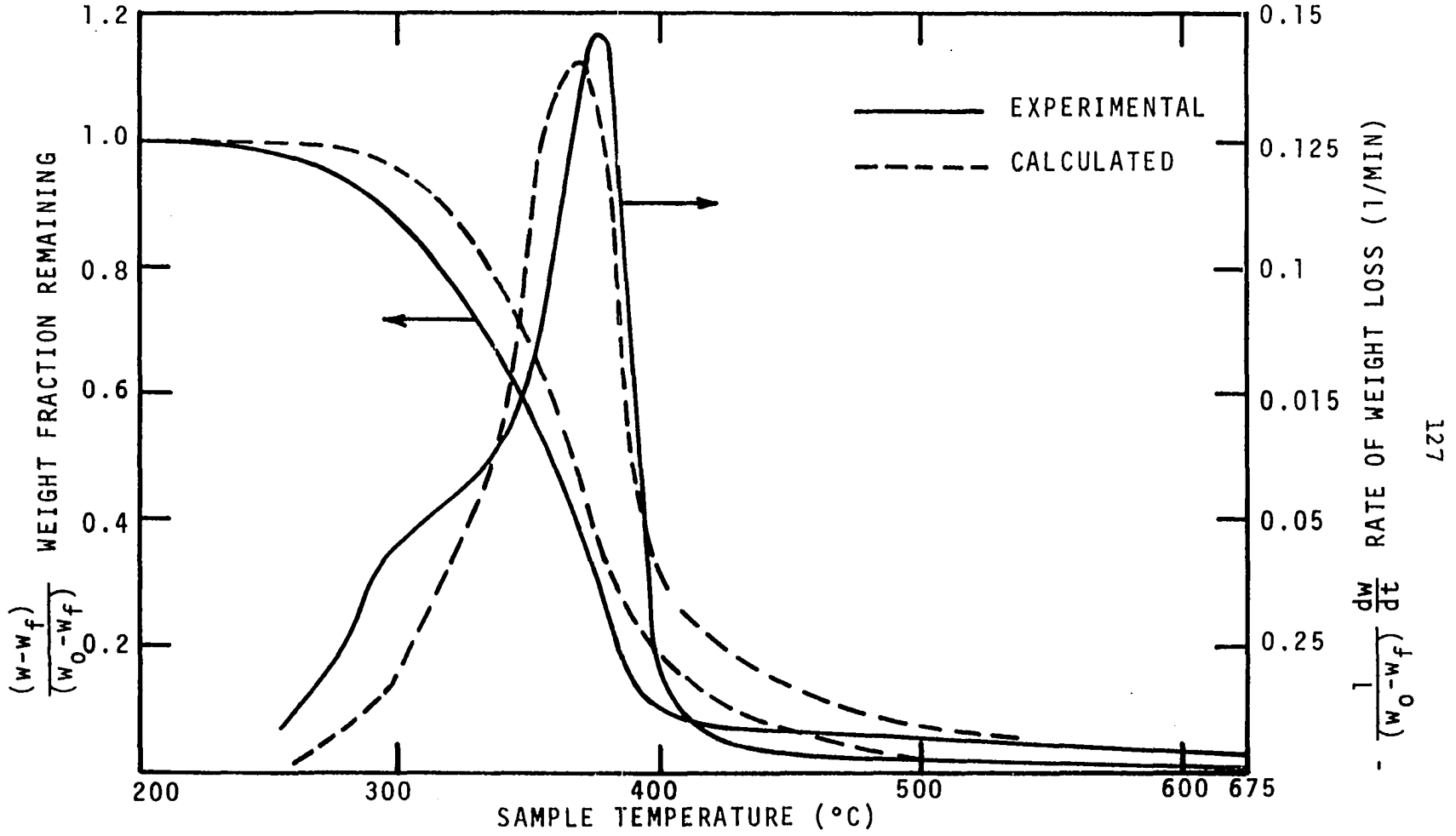

Figure IV-29. Weight Loss and Rate of Weight Loss for Excelsior. Heating Rate - 10°C/MIN.

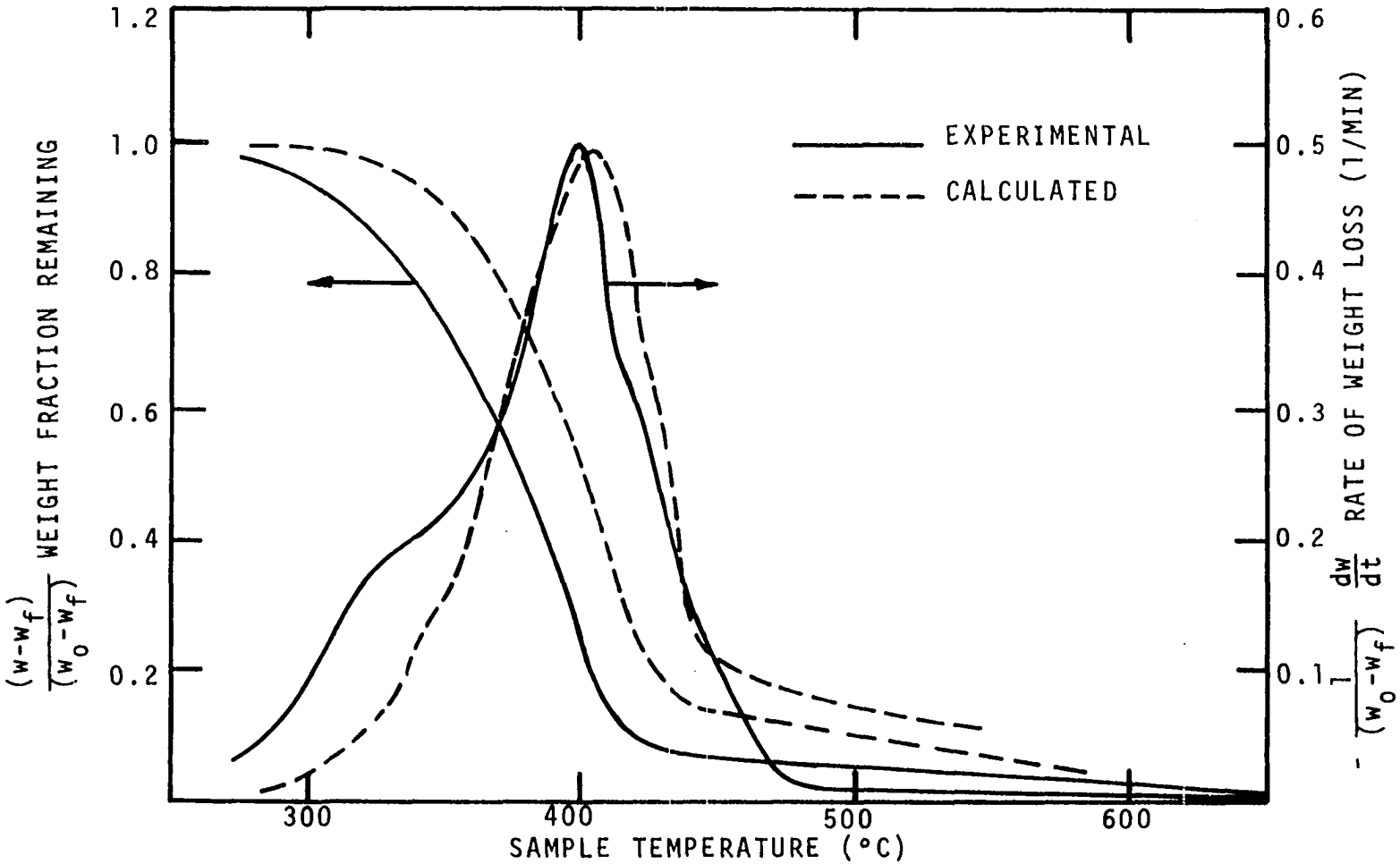

Figure IV-30. Weight Loss and Rate of Weight Loss for Excelsior. Heating Rate - 40°C/MIN.

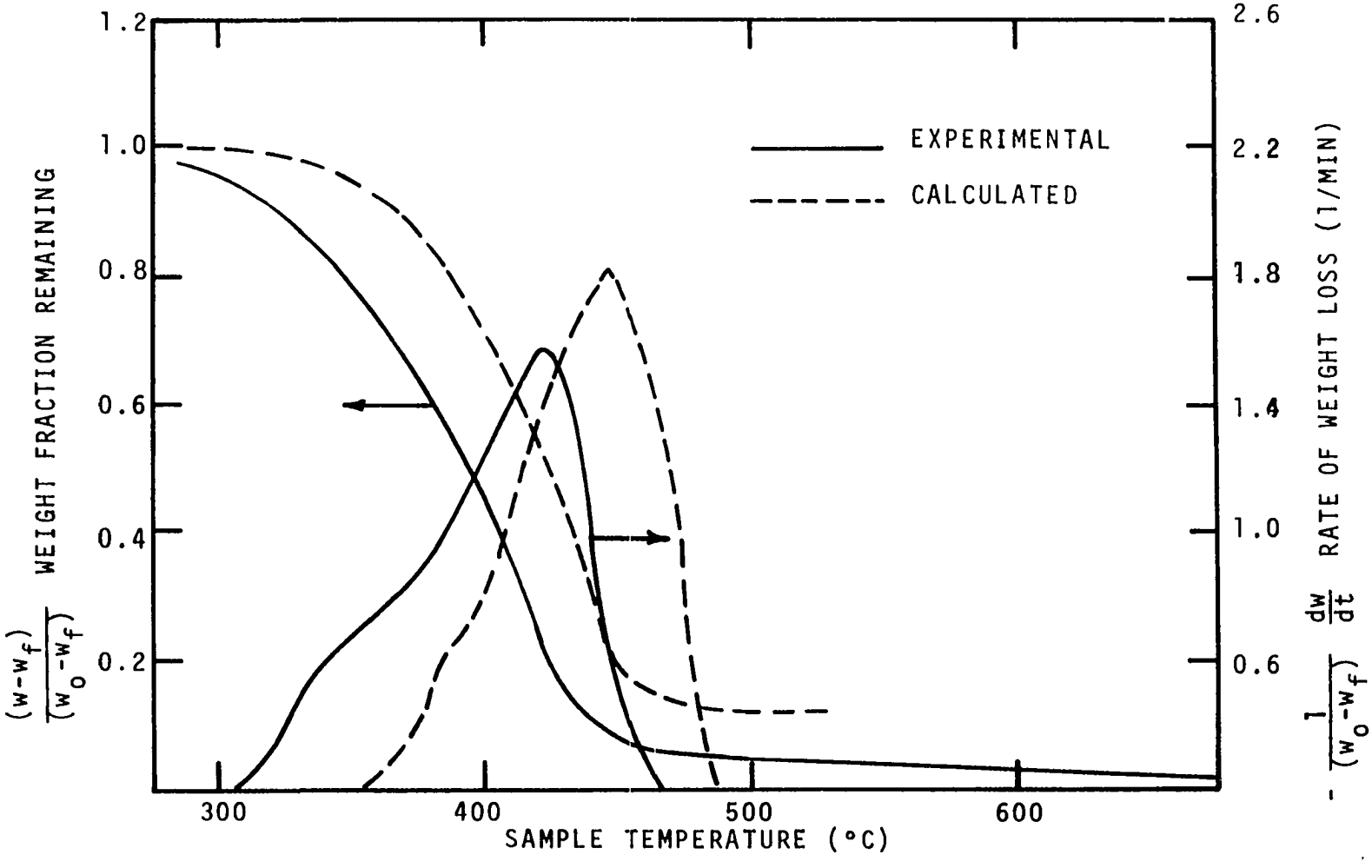

Figure IV-31. Weight Loss and Rate of Weight Loss for Excelsior. Heating Rate - 160°C/MIN.

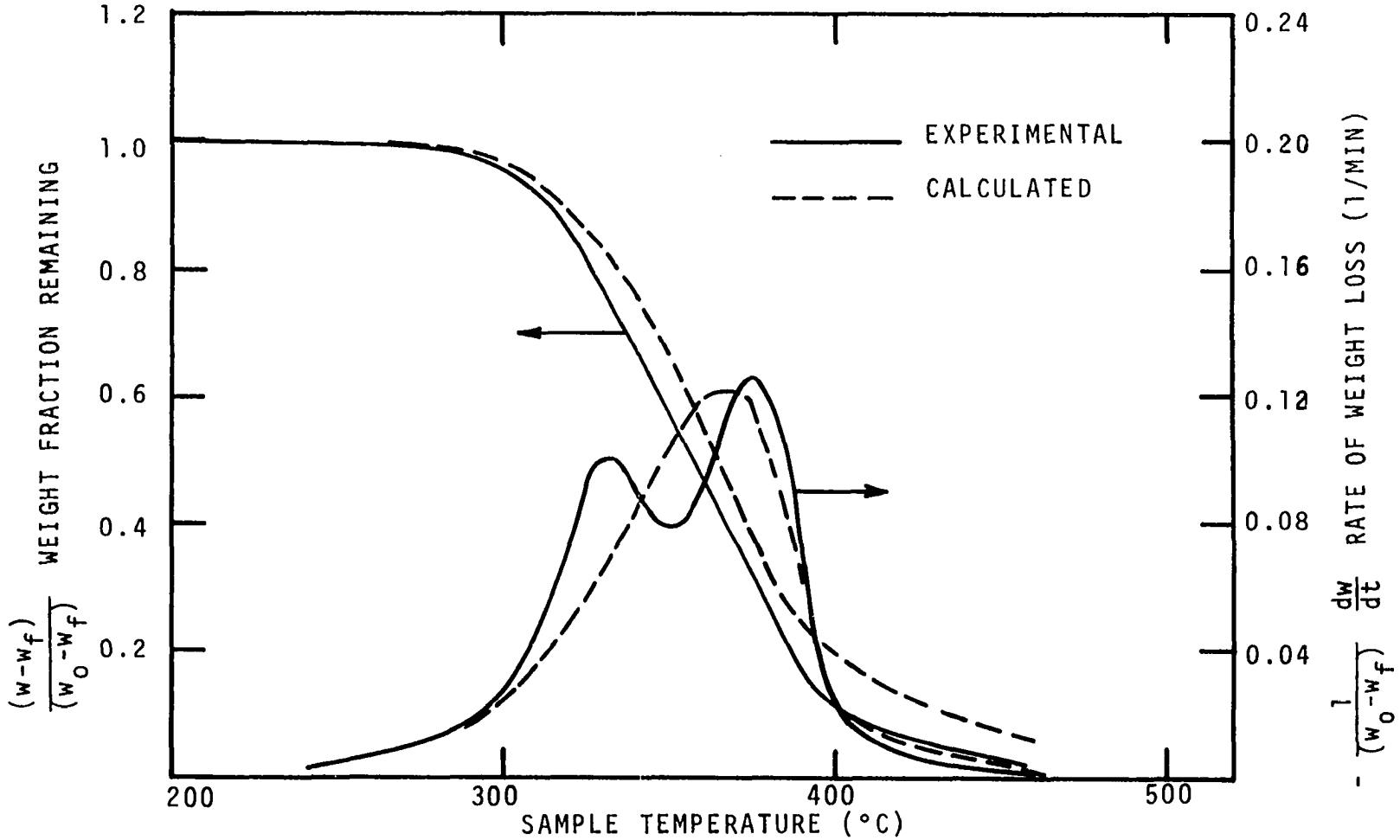

Figure IV-32. Weight Loss and Rate of Weight Loss for Larch. Heating Rate - 10°C/MIN.

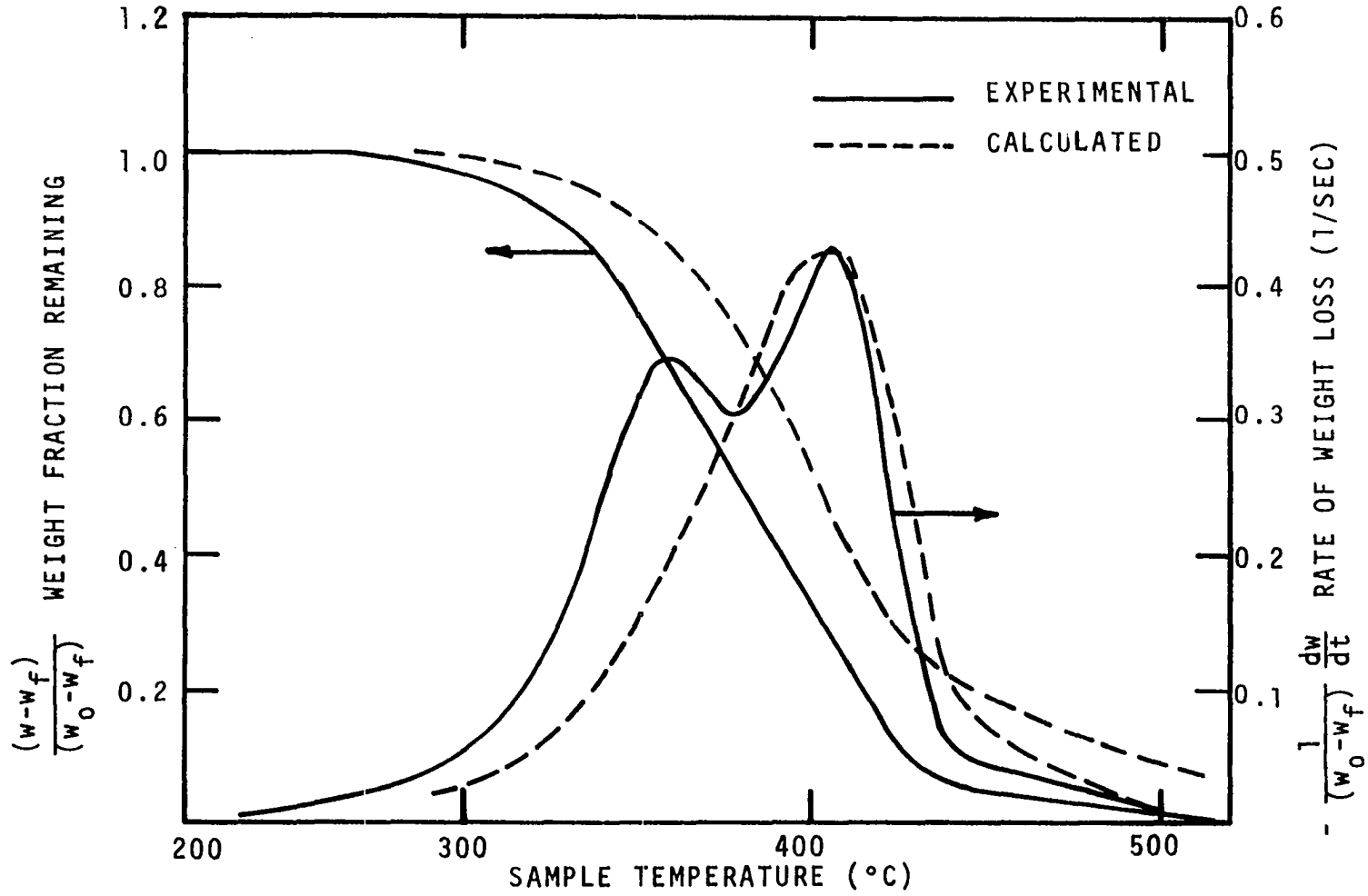

Figure IV-33. Weight Loss and Rate of Weight Loss for Larch. Heating Rate - 40°C/MIN.

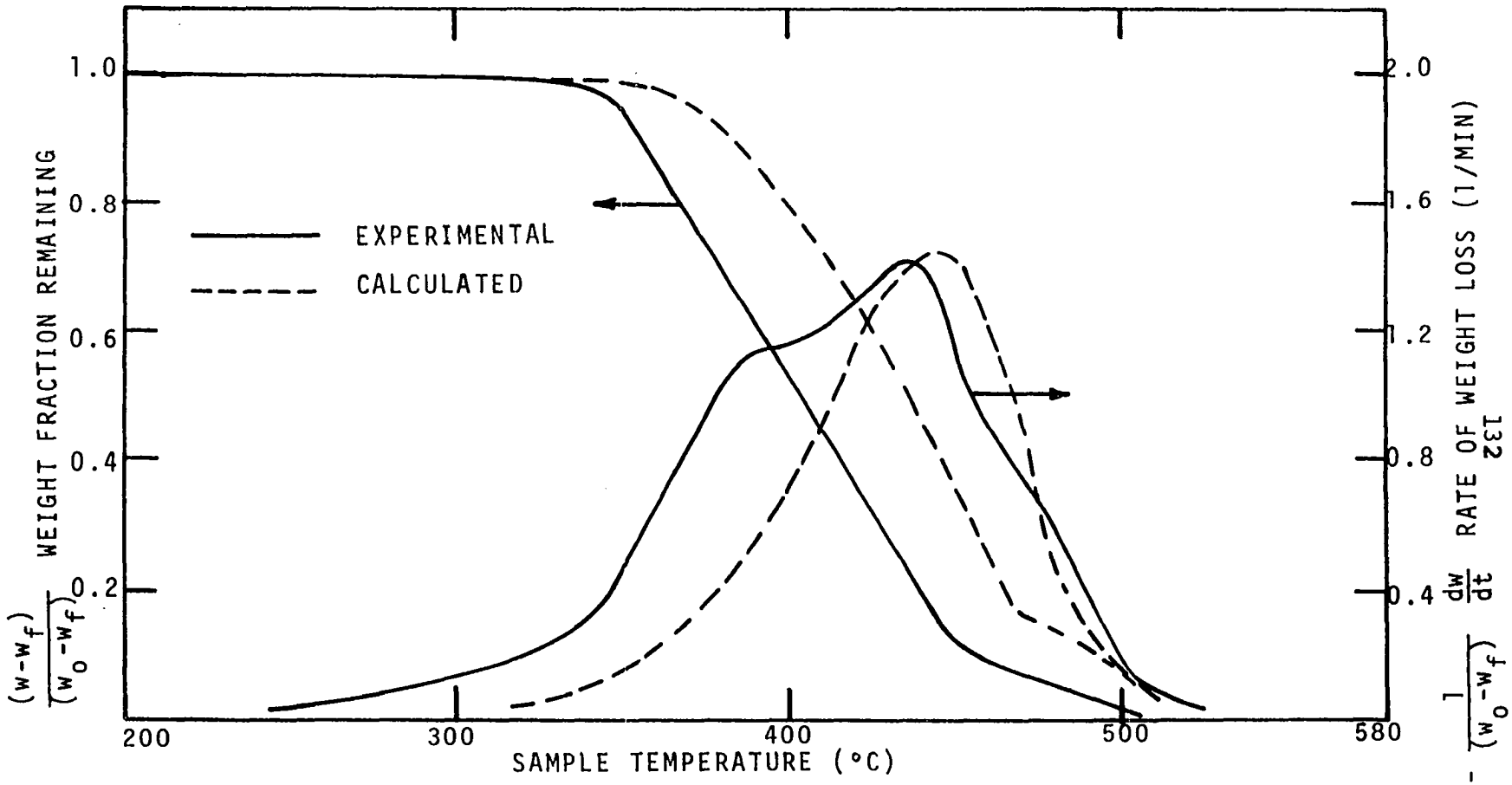

Figure IV-34. Weight Loss and Rate of Weight Loss for Larch. Heating Rate - 160°C/MIN.

investigators. The model proposed in the present study does not take into account the effect of inorganic salts or extractives that are present in the woods. This simplification is part of the reason for the discrepancies in the calculated and experimental curves.

Several investigators (4, 19, 20, 63) observed that there are significant differences in structure and properties of different kinds of cellulose. Hemicelluloses and holocelluloses are two types of wood ingredients frequently referred to other than normal cellulose. The cellulose used as reference in this study is not necessarily any of these constituents and probably has different structure and properties from any other kind mentioned above. This could very well be another reason for the deviations observed in the experimental and calculated curves for both excelsior and larch decomposition.

The decomposition of larch is marked by two distinct peaks at the heating rate of 10°C/min. (At the heating rate of 160°C/min the first peak became less distinct than at lower heating rates.) The calculated curves on the other hand had only one peak at all three heating rates examined. In this case the difference in the behavior between calculated and experimental curves could be attributed to the presence of extractives and minerals in larch which were not considered in the proposed model. It is suggested that inclusion of more Arrhenius type terms to account for the decomposition of

extractives, minerals, etc., could result in an improvement of the calculated curves.

The Texas Instrument Servowriter-II recorder used to record data was equipped with an event marker that is actuated only up to 80°C/min. For 160°C/min runs the indicated temperature had to be marked on the chart paper (running at a speed of 8.0 in/min) by visual observation. This procedure probably caused some error in recording the temperature with respect to weight loss and rate of weight loss during weight loss runs.

The punky wood considered to be pure lignin contained minor quantities of organic material. There exists the possibility that the behavior of punky wood could have a difference, even though slight, from pure lignin normally obtained from spruce by a sulphuric acid process.

For the reasons mentioned in the preceding paragraphs some chemical and some experimental in nature, some scatter in the data is inevitable. The strength of the proposed model in predicting ignition behavior will be brought forth later in this chapter.

A fourth-order Runge-Kutta technique was used for calculating the weight loss and rate of weight loss using the proposed model of Equation IV-12 with the intervals shown in Table IV-2.

The DSC results of the runs on dry and wet samples for cellulose at the heating rates of 40° and 160°C/min are

TABLE IV-2

INTERVAL OF TIME USED FOR RUNGE-KUTTA TECHNIQUE

Heating Rate °C/min	Time Interval (Δt) for Successive Iterations min
10	0.08
20	0.04
40	0.02
80	0.01
160	0.005

shown in Figures IV-35 through IV-40. The results of the runs on other materials studied are presented in Appendices F, G and H. The baseline separates the sensible energy part of the decomposition from the energy effects due to transition alone. The stepwise integration of the differential energy curves is rather difficult if the differential energy value is taken per unit time, $d\dot{E}/dt$ (cal/gm original wt-min) rather than per unit temperature, $d\dot{E}/dT$, along the ordinate. Hence, the ordinate was chosen as $d\dot{E}/dT$ (cal/gm original wt-°C). This selection also helps in choosing a single scale to represent data obtained at both 40° and 160°C/min. The difficulty in integrating $d\dot{E}/dt$ versus T curves is obvious from Figure IV-41, for extracted excelsior.

The energy data obatined in this thesis differ from those of Tang and Eickner (69) both qualitatively and quantitatively except in the case of cellulose. A comparison of the data is presented in Table IV-3.

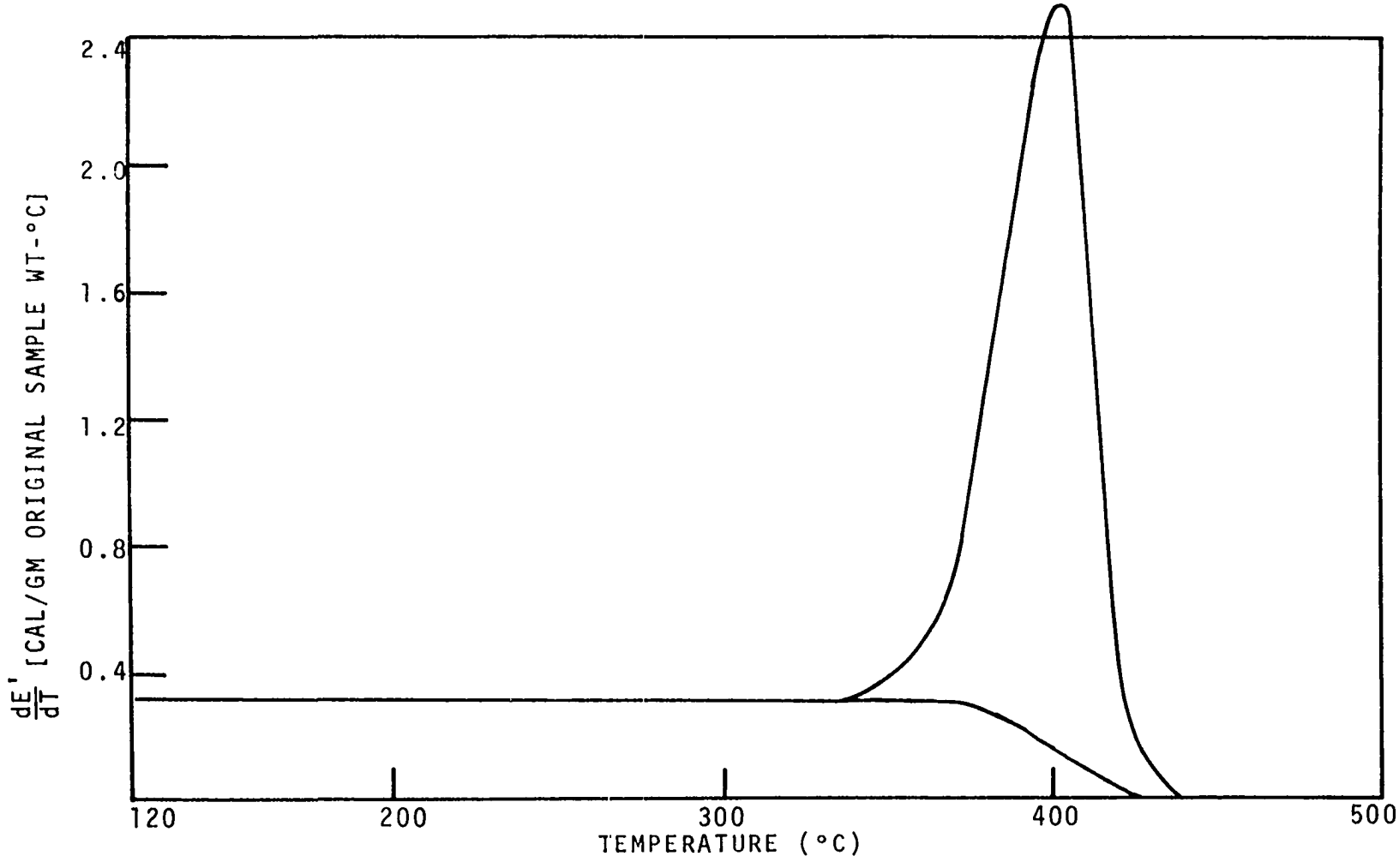

Figure IV-35. Differential Energy Curve for Dry Cellulose Decomposition. Heating Rate - 40°C/MIN.

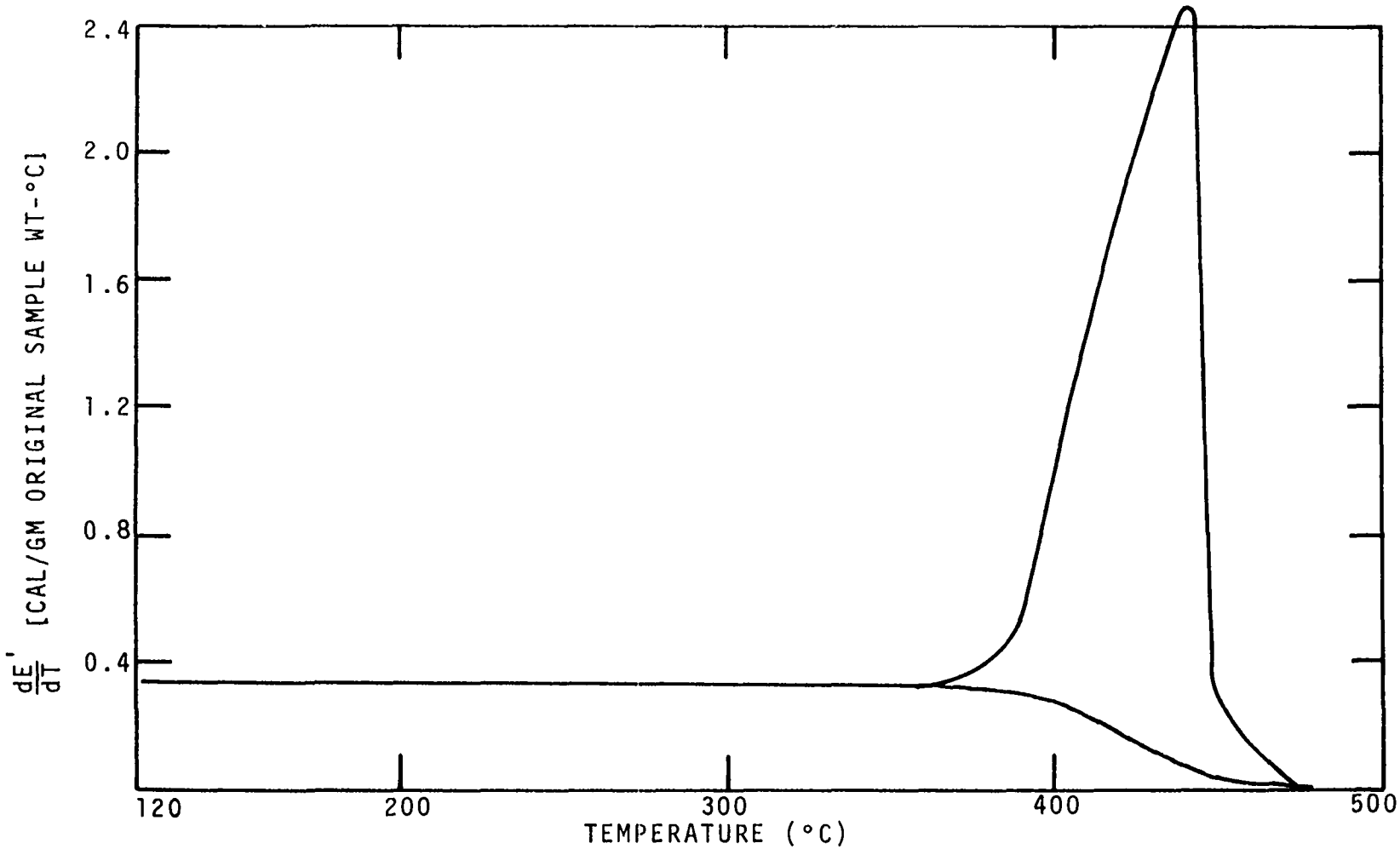

Figure IV-36. Differential Energy Curve for Cellulose Decomposition. Heating Rate - 160°C/MIN.

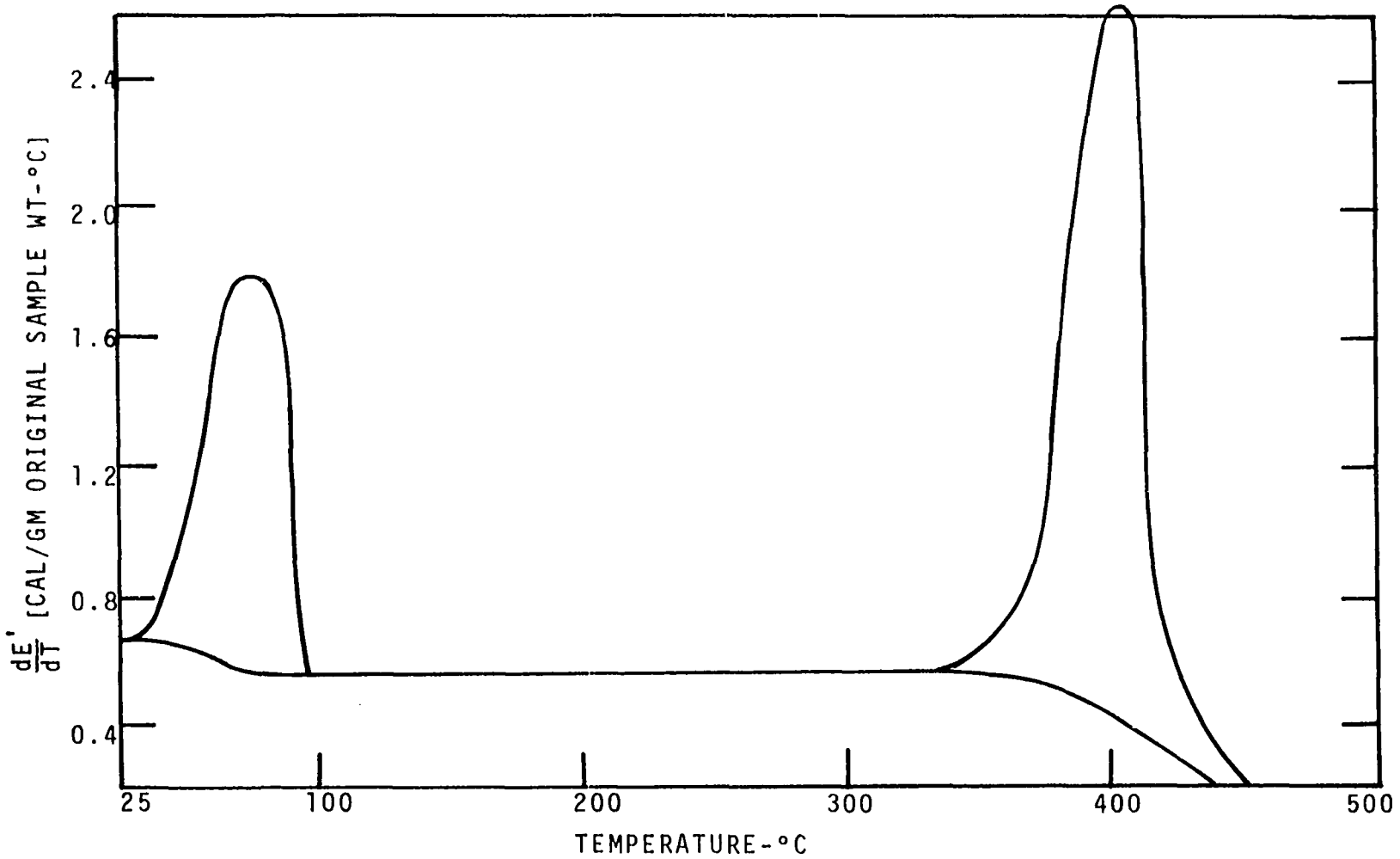

Figure IV-37. Differential Energy Curve for Moist Cellulose. Heating Rate - 40°C/MIN.

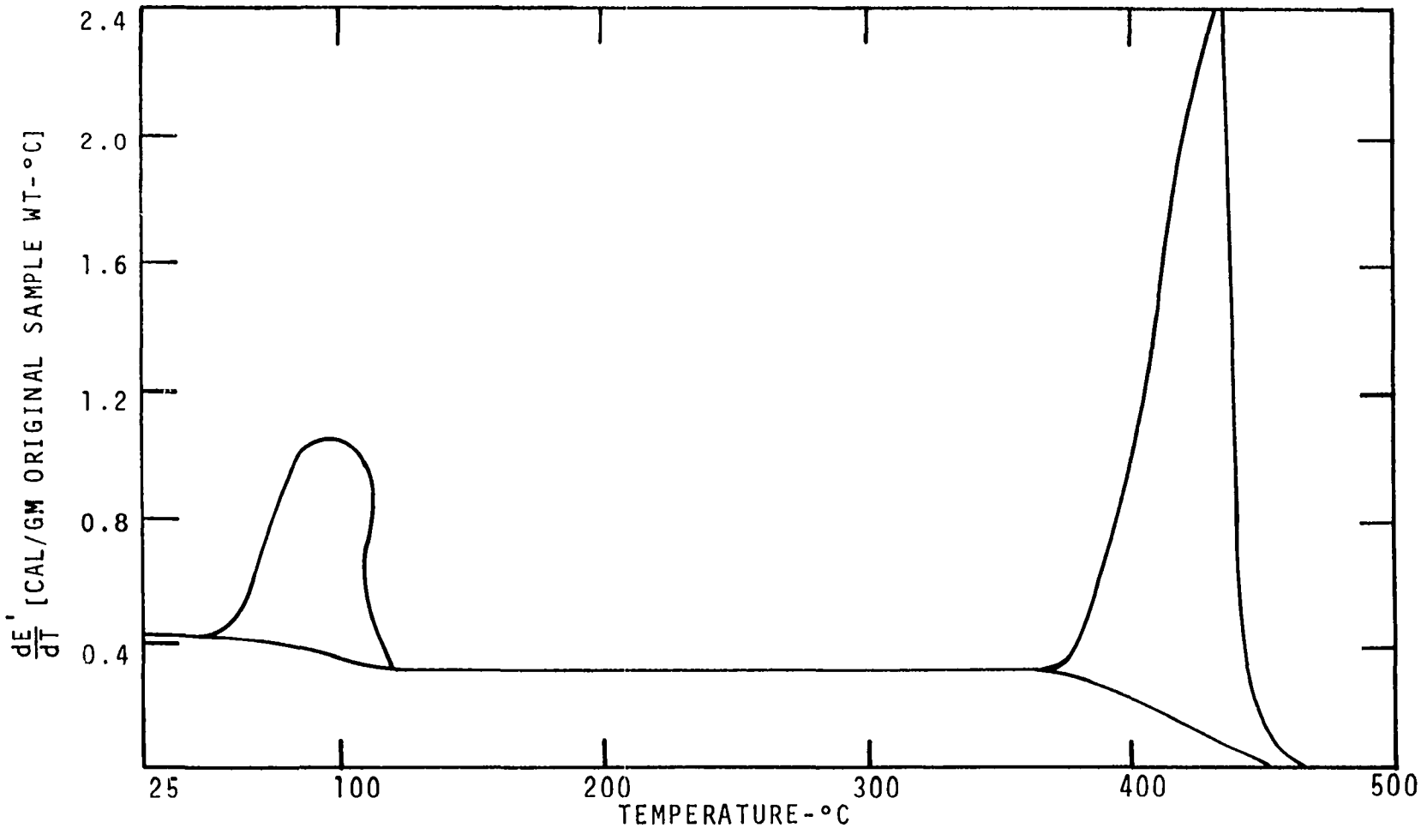

Figure IV-38. Differential Energy Curve for Moist Cellulose. Heating Rate - 160°C/MIN.

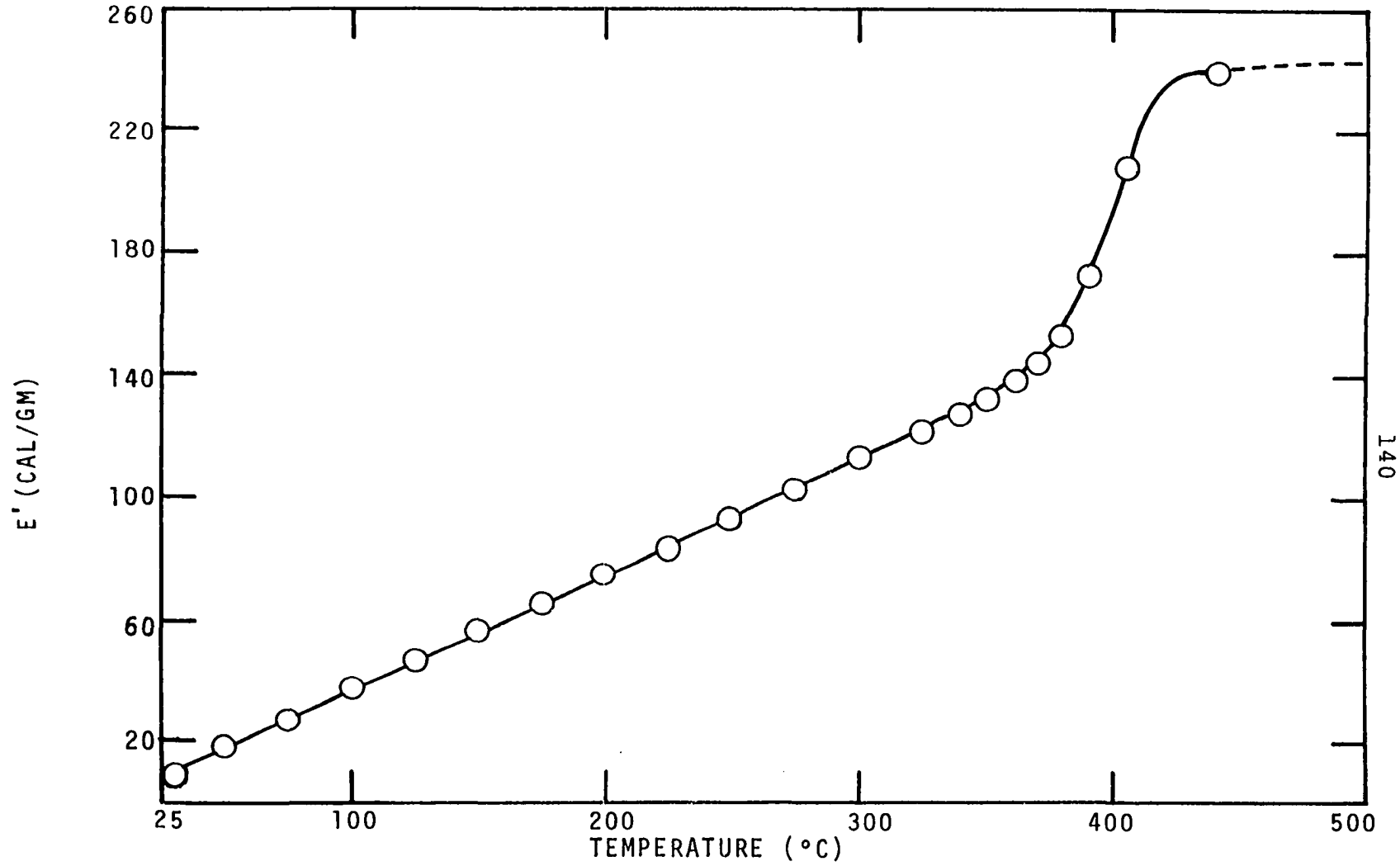

Figure IV-39. Total Energy of Pyrolysis versus Temperature Curve for Cellulose. Heating Rate - 40°C/MIN.

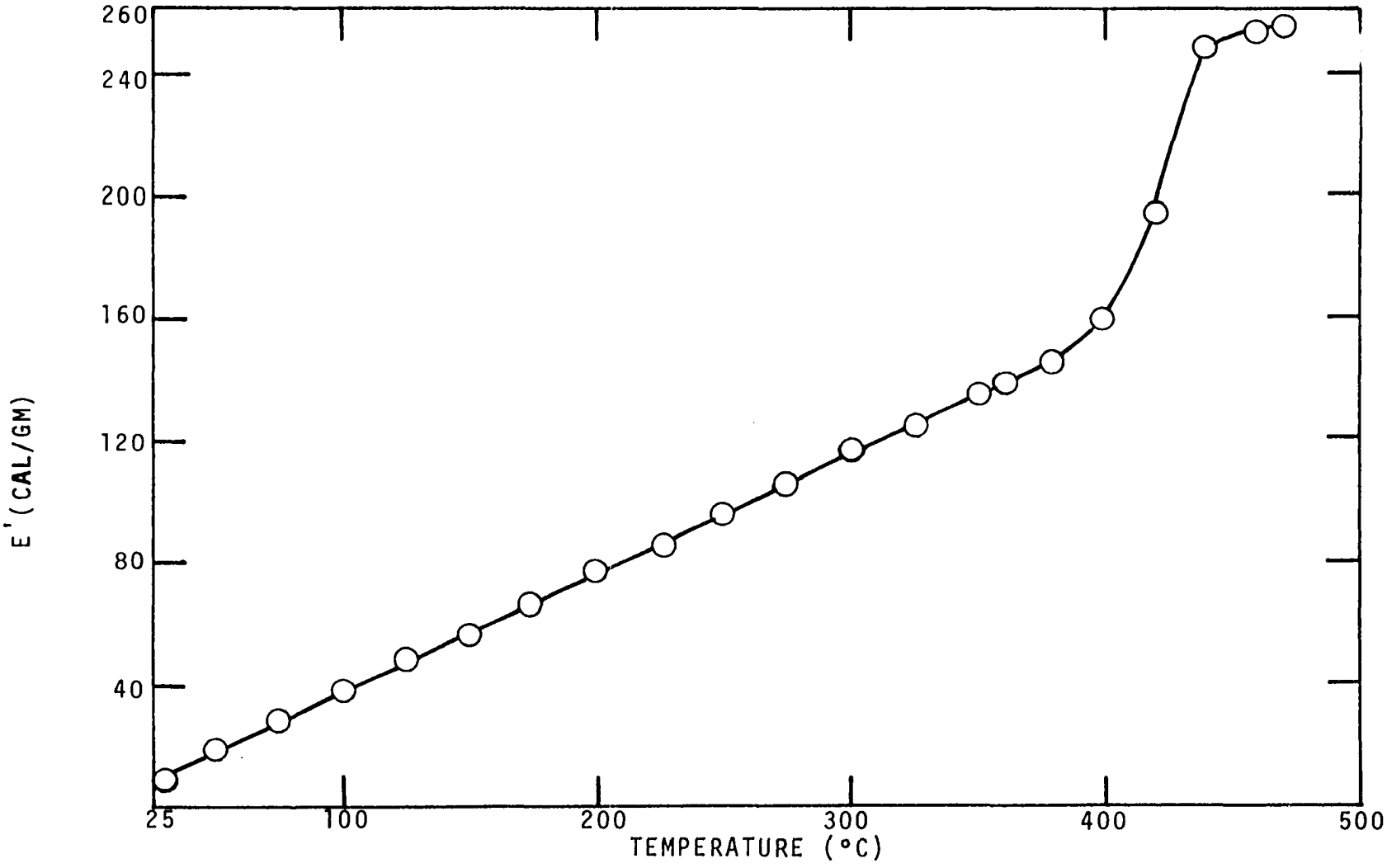

Figure IV-40. Total Energy of Pyrolysis versus Temperature Curve for Cellulose. Heating Rate - 160°C/MIN.

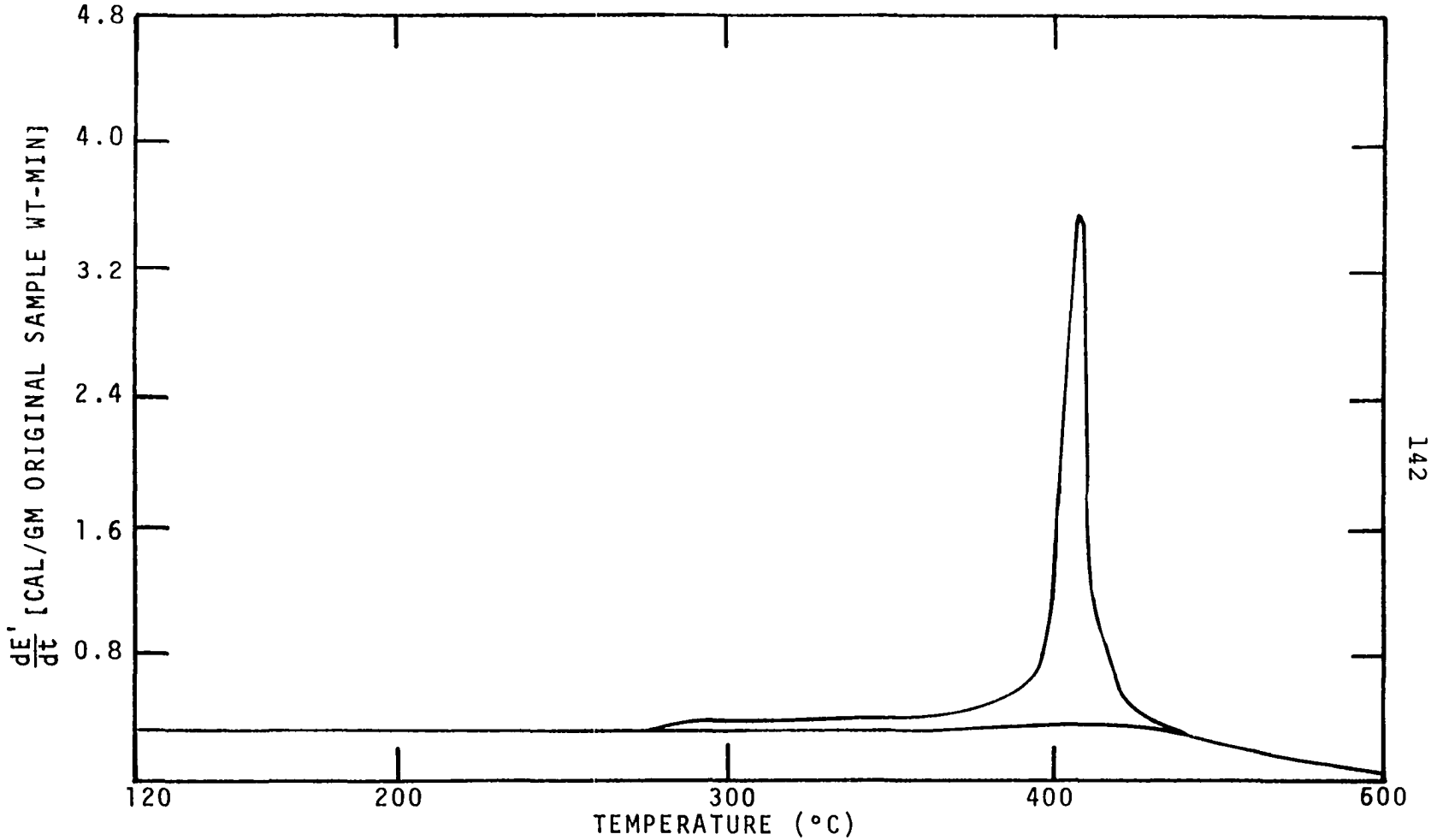

Figure IV-41. A Curve of the Differential Energy of Extracted Excelsior with Respect to Time. Heating Rate - 160°C/MIN.

TABLE IV-3

COMPARISON OF THE PYROLYSIS ENERGY DATA OF THE PRESENT WORK WITH THAT OF TANG AND EICKNER (69)

Investigators	Material	Exothermic cal/gm	Endothermic cal/gm
Tang & Eickner	Ponderosa pine sapwood	31	77
Present study	Dead Ponderosa pine needles	--	76
Tang & Eickner	Cellulose	--	88
Present study	Cellulose	--	86
Tang & Eickner	Lignin	40	19
Present study	Punky wood	--	37

As could be noticed in Table IV-3, the present study observed no exothermic effects with any of the three materials compared. Tang and Eickner used lignin obtained by the sulfuric acid process from spruce while the punky wood tested in this thesis was a decayed form of wood which might not be pure lignin. The major reason for the discrepancies are believed to be in the manner of experimentation. Tang and Eickner used 120 mg samples with thickness of 0.45 mm packed in pyrex capsules in an American Instrument Company "Thermograv" which has a relatively large volume to be purged before a test run, compared to DSC-2 sample holder assembly. The maximum sample size in the present work was 4 mg powder of 20 mesh size.

The samples of Tang and Eickner were also conditioned at 30 percent relative humidity before testing. Kung and Kalelkar (46) suggested the phenomenon of "thermal explosion" as explained in Chapter II for samples with dimensions on the order of those used by Tang and Eickner. Bamford, et al., (5) have observed exothermic reactions with moist wood slabs. The physical dimensions of the samples used in the present study were much smaller (powdered wood of 20 mesh size) compared to those of Bamford, et al. This difference in sample contributed to the difference in heat transfer characteristics. The samples used in this study were either oven-dry or deliberately enriched with moisture. The observations of the present study differed from those of Britton, et al. (12) in that the moisture loss rate in the samples tested never stabilized to the exponential decay. The probable cause of this difference is the difference in both the heating rate and the sample physical dimensions.

The temperature at which moisture was totally driven from the wood was also reported to be in the range of 150° to 200°C by Tang and Eickner with a heating rate of 12°C/min and a 600-mg sample. In this investigation the maximum temperature reached by the time moisture was totally driven off was found to be 100°C at the heating rate of 40°C/min and 120° to 130°C at 160°C/min. This discrepancy in temperature observations for moisture loss is due to the difference in moisture absorption and heat transfer characteristics of

powdered wood (as used in the present work) and the cylindrical or rectangular slabs of wood (as used by Tang and Eickner and most other investigators). The moist sample total energy data for cellulose is presented in Figures IV-42 and IV-43. The energy data for all other moist samples tested are presented in Appendix I.

One area in which accurate data could not be obtained from the DSC chart output is wet wood specific heat. A combination of factors is responsible for this lack of accuracy. It is best explained by considering an experimental condition. At a heating rate of 160°C/min the chart speed used was 4.0 in/min with DSC runs. At the start of the programmed heating rate the recorder pen was displaced from the initial isothermal baseline for a distance that depends upon the weight of the sample and its specific heat. A steady reading was reached a few seconds after the start. At the end of this run the char baseline run was repeated over the chart output of the sample run. When the programmed heating was started and the baseline displacement was obtained it took a few seconds to adjust the chart paper position to match the indicated temperature for the baseline run with that of the (previously marked) sample run. This procedure was particularly difficult at a high heating rate like 160°C/min. With dry samples the displacement of the sample thermogram was fairly steady until the temperature of the onset of pyrolysis was reached, which is normally well over 200°C for any wood. This longer steady

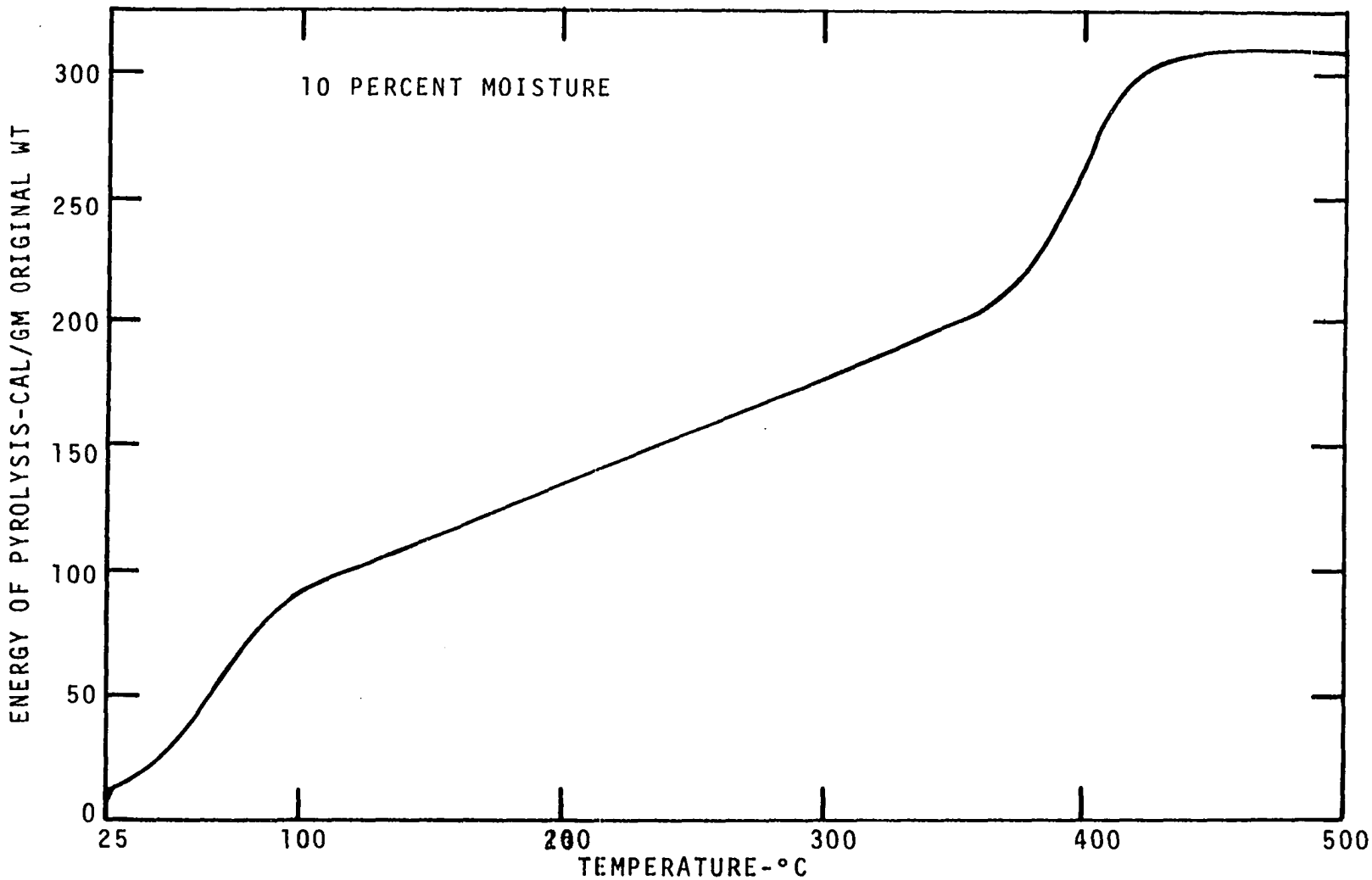

Figure IV-42. Total Energy of Pyrolysis versus Temperature Curve for Moist Cellulose. Heating Rate - 40°C/MIN.

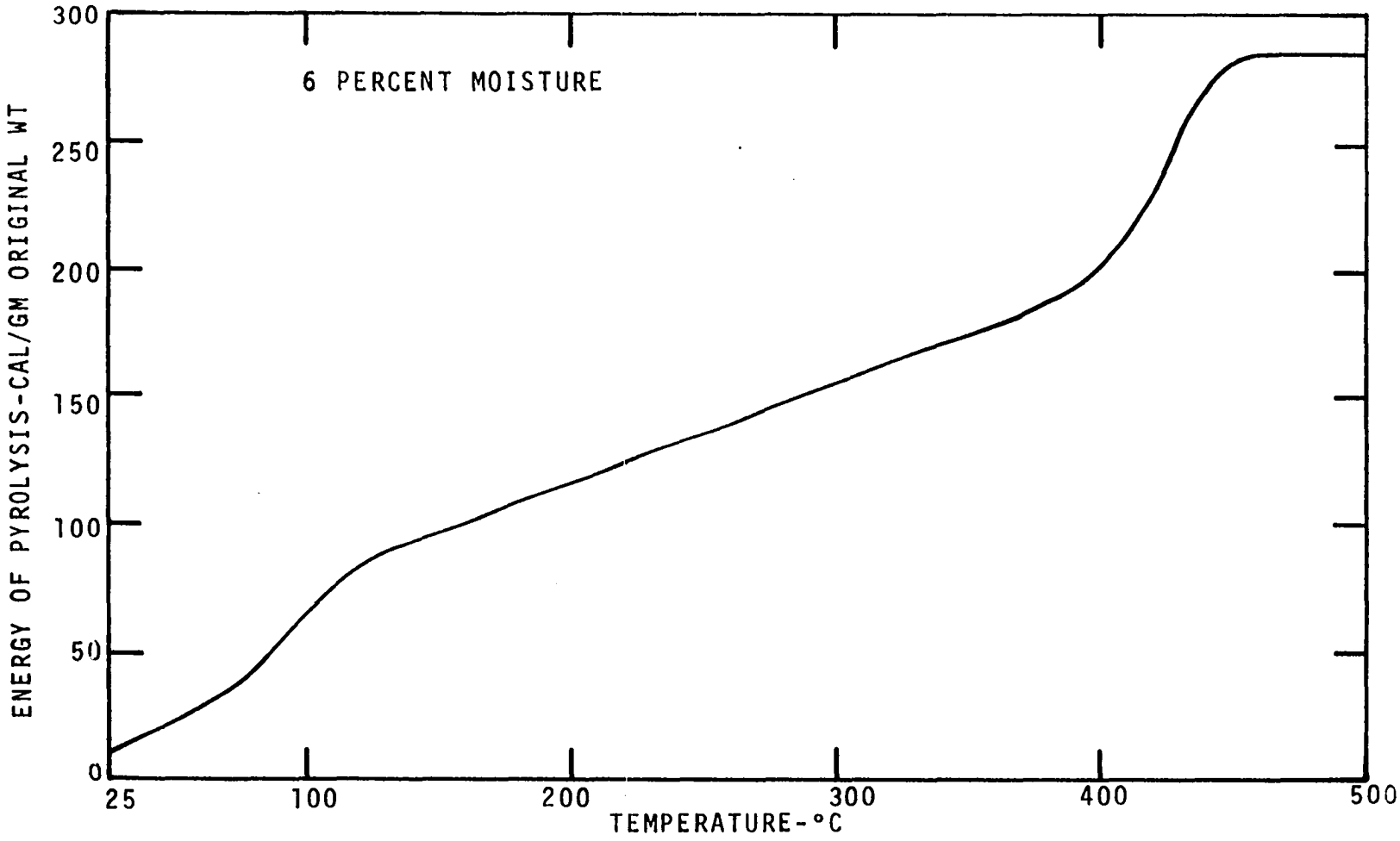

Figure IV-43. Total Energy of Pyrolysis versus Temperature Curve for Moist Cellulose. Heating Rate - 160°C/MIN.

period provides enough time to match the indicated temperatures of sample and baseline thermograms. However, with wet samples the onset of evaporation of water usually occurs near 40° to 50°C so that the "temperature-matching" of sample and baseline runs could not be accurately achieved before the onset of evaporation of water. This experimental limitation is the reason for the difference in the present values of the experimental wet wood specific heat and those obtained using Kollman's relation as shown in Table IV-4.

TABLE IV-4

COMPARISON OF COMPUTED AND MEASURED VALUES OF SPECIFIC HEAT

Material	$C_{computed}$	$C_{experimental}$
Cellulose	0.46	0.46
Dead Ponderosa pine needles	0.57	0.54
Extracted Ponderosa pine needles	0.61	0.53
Excelsior	0.47	0.45
Extracted excelsior	0.50	0.47
Four wing saltbush leaves	0.55	0.50
Punky wood (lignin)	0.53	0.54

Wangaard, et al. (74) observed that woods of different species vary in the nature and amount of extractives with a resultant variation in the absorption characteristics. This was found to be true in the present study also. Samples of the same particle size (40 mesh screen size) of different species of wood maintained at the same environment absorbed different

amounts of moisture ranging from 15 to 45 percent based on dry weight. However, at the onset of the programmed temperature rise the moisture content decreased to a range of 6 to 18 percent. This was due to purging with dry nitrogen at 30°C at a gas rate of 120 cc/min, in addition to the delay involved in weighing the sample accurately in the sample pan before placing the sample pan in the DSC sample holder.

The specific heat of dry samples was observed to be fairly constant over the temperature range studied. The char specific heat obtained in this study (0.34 to 0.40) for different samples is comparable to the value reported by Havens (37) of 0.36 cal/gm-°C.

The model developed for the prediction of the weight loss and rate of weight loss was extended to energy measurements by calculating energy requirements of each component. The total energy of decomposition at any temperature in the range of 0 to 500°C is given by the equation

$$E' = \int_0^{500} Wc_p \, dT + \int_0^{500} \Delta H_p \frac{dW}{dT} \, dT \qquad \text{(IV-13)}$$

or

$$E' = \int_0^{500} Wc_p \, dT + \int_0^{500} \Delta H_p \frac{dW}{dt} \frac{dt}{dT} \, dT$$

The wood could be separated into individual cellulose and lignin terms in the following manner:

$$E' = \left(\int_0^{500} Wc_p \, dT + \int_0^{500} \Delta H_p \frac{dW}{dt} \frac{dt}{dT} \, dT \right)_c$$

$$+ \left(\int_0^{500} Wc_p \, dT + \int_0^{500} \Delta H_p \frac{dW}{dt} \frac{dt}{dT} \, dT \right)_L \qquad \text{(IV-14)}$$

where $W = (w-w_f)/(w_o-w_f)$ = weight fraction remaining at time t, or temperature T (calculated)

c_p = specific heat of the sample measured at temperature T (cal/gm original wt-°C)

ΔH_p = measured heat of transition without the sensible heat effects at temperature T (cal/gm original sample wt)

dW/dt = calculated rate of weight loss (1/min)

dt/dT = reciprocal of heating rate (min/°C)

c and L refer to cellulose and lignin, respectively.

The total energy over the range of interest computed by Equation IV-14 using the values of W and dW/dt obtained from the proposed model (IV-12) is in fair agreement with the experimentally measured values in the case of excelsior for the heating rates of 40°C/min and 160°C/min as shown in Figures IV-44 and IV-45. The deviation of the computed curves from the experimental curves at 500°C is 11.7 percent at the heating rate of 40°C/min and 18 percent at 160°C/min.

It is thus established in this thesis that in spite of the probable differences that exist between the cellulose

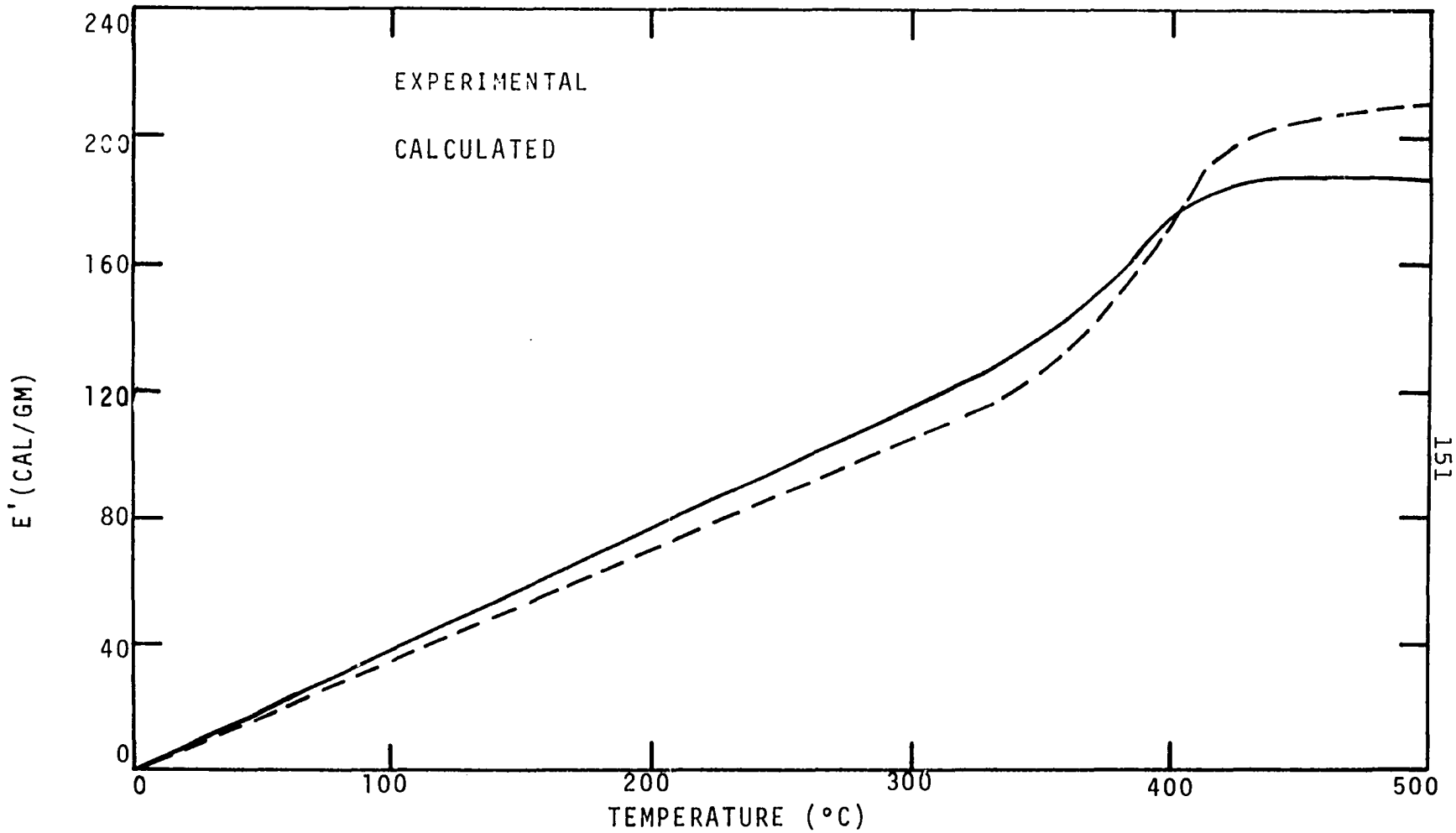

Figure IV-44. Calculated and Experimental Total Energy for Dry Excelsior. Heating Rate - 40°C/MIN.

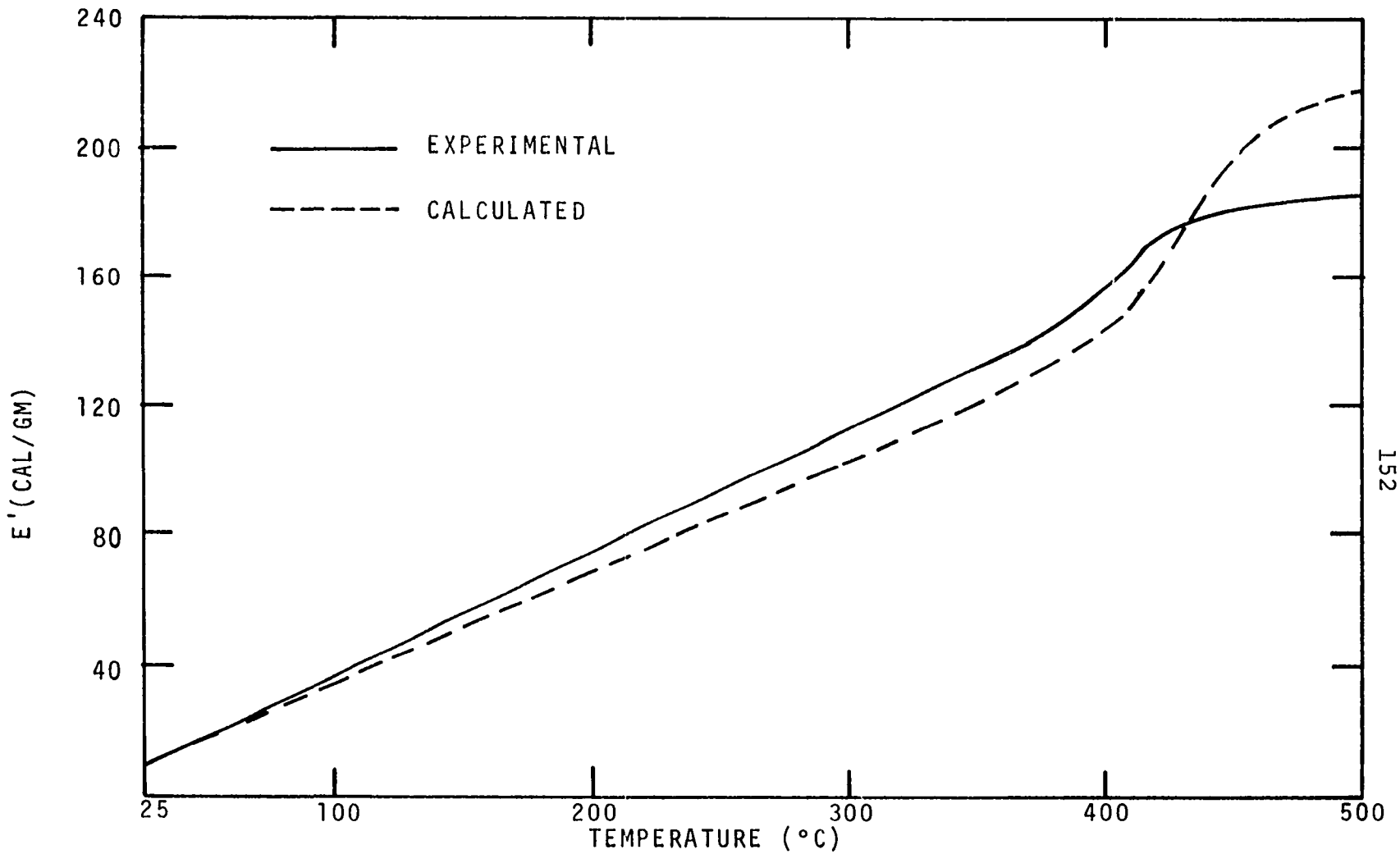

Figure IV-45. Calculated and Experimental Total Energy for Excelsior. Heating Rate - 160°C/MIN.

fraction of the woods and the cellulose used in the runs (which caused some deviations in the calculated weight loss and rate of weight loss curves from the experimental curves), the results of the proposed model could be used to predict the total energy of pyrolysis at any needed temperature fairly closely. All that is needed for this prediction is a knowledge of the composition of the wood as described earlier.

In the range of the heating rates (10°-160°C/min) considered the results of the regression analysis technique on cellulose data obtained show a certain amount of scatter. If kinetic parameters were obtained for each individual heating rate rather than a single set of kinetic parameters for all the heating rates, the scatter in the log $-(dW/dt)$ calculated versus log $-(dW/dt)_{actual}$ might be less. However, it is felt that in the range of heating rates studied in this thesis, the difference in the calculated weight loss and the rate of weight loss curves by using these two different approaches is small. Therefore, in the range of heating rates studied in this thesis, the chemistry of decomposition is considered to be independent heating rate. As was shown earlier in this chapter, weight loss and rate of weight loss profiles are merely shifted to a higher temperature with increase in heating rate. It could well be seen from Appendices G and I that for a given species of wood, the same is true of total energy versus temperature profiles.

CHAPTER V

CONCLUSIONS

It has been observed by Brown (14) and Havens (37) in connection with studies on the pyrolysis of oak and white pine that up to a heating rate of 80°C/min, the chemistry of decomposition is independent of heating rate. From the findings of this thesis, this conclusion can be extended up to a heating rate of 160°C/min for all the seven species studied. The total heat of transition involved in the process of pyrolysis is found to be very nearly the same for heating rates of 40°C/min and 160°C/min for each wood studied in this work, namely, cellulose, dead Ponderosa pine needles, extracted dead Ponderosa pine needles, excelsior, extracted excelsior, fourwing saltbush leaves and punky wood (lignin). However, the onset of pyrolysis is found to shift to higher temperature with increase in heating rate and the peak rate of volatile weight fraction loss with respect to temperature (dW/dT) progressively decreased with increase in heating rate. This decrease is shown in Figure IV-6 . The peak rate of energy of pyrolysis with respect to temperature (dE/dT) is also observed to shift to higher temperature with an increase in heating rate.

Cellulose pyrolysis is observed to occur primarily in the range of 340°C to 440°C at the heating rate of 40°C/min. For the same heating rate the lignin pyrolysis range is 200°C to 470°C. The fact that the threshold temperature of pyrolysis is lower for lignin than for cellulose seems at first to conflict with much of the literature (15), which holds that in wood hemicellulose pyrolyzes most readily, cellulose less so, and lignin least readily. The apparent conflict, however, is easily reconciled because lignin is still undergoing active pyrolysis after cellulose is already completely pyrolyzed.

The rate expressions for pure cellulose and lignin have been combined to yield a model that gives a good qualitative picture of the decomposition mechanism--the weight loss and the rate of weight loss profiles. Quantitatively, energy predictions obtained from the proposed model at 40°C/min are within 12 percent of the total energy obtained experimentally, The deviations are attributed to the probable discrepancies that exist in the cellulose and lignin used in the model and the cellulose and lignin fractions of the wood, the unaccounted for extractives, etc., in the wood, and the experimental errors.

The wet wood analysis confirms that the sample physical dimensions do have an effect on the qualitative as well as quantitative aspects of the absorption characteristics of the wood. If samples of the size used in this thesis (20 mesh size) are considered the analysis is simple in that the

moisture present in the wood is completely lost by the time the wood is heated to 100°C at the rate of 40°C/min or 120° and 130°C at the rate of 160°C/min, and the excess energy required to drive the moisture off is equal to the latent heat of vaporization for an equivalent quantity of water as present in the wood. There are no exothermic degradation reaction effects noticed for any of the woods. This result is quite certainly attributable to the sample particle size as well as the experimental conditions.

Woodard (77), Brown (14), and Havens (37) suggested that the baseline drift could be minimized by minimizing the sample size. The supposed reduction in the volatiles emitted made it possible for the volatiles to be swept away by the purge gas before condensation on the dome. With a proper purge rate and even more importantly, with an optically black sample holder cover (which has been successfully utilized for the first time in this thesis), it is possible to minimize the baseline drift to workable limits for larger samples than used in earlier studies. The purge gas rate limitation inherent in the DSC-1B used by the above mentioned three investigators is not as restrictive in the DSC-2 used in this study. The darkening of the sample holder was suggested by Rogers (55) but was not previously applied in practice.

The linear regression analysis applied to cellulose and lignin data did show some scatter in the data. However,

the kinetic parameters evaluated by this method compare closely to those obtained by the widely used method of Goldfarb, et al. (32) and Burningham and Seader (17). The advantages in the use of the least squares technique are that no assumptions are required (other than the form of the equation) and the method is simple, direct and run through only once to yield all the kinetic parameters. Other methods call for some initial assumptions or "guesses" of the order of reaction which is required to be quite close to the actual order to evaluate successfully the other kinetic parameters; in short, they are trial-and-error methods requiring considerable computer time.

Qualitatively, the decomposition process does not vary widely among wood species. The maximum deviation of the extrapolated sensible heat curves from the actual total heat curves is perhaps 25 percent at the peak rate of reaction (or weight loss) but at 500°C the deviation reduces a little (15 to 20 percent). Therefore, a fair estimate of the total heat of reaction at 500°C can be made by merely extrapolating the sensible energy curve up to 500°C. The transition energy is typically in the range of 25 to 35 percent of the total energy required for pyrolysis. Above 500°C most of the differential energy curves leveled off almost parallel to the abscissa indicating negligible increment in the transition energy.

Specific heats of all the oven-dry woods studied fall in the range of 0.33 to 0.40 cal/gm-°C. The char specific

heat is in the same range. There is hardly any change in the specific heat of wood with increase in the temperature of wood taken on the basis of the weight of unpyrolyzed material at any temperature. Thus, fairly accurate estimation of pyrolysis energy can be made by extrapolating the sensible energy curve.

The data on the extracted Ponderosa pine needles and extracted excelsior do not show any significant difference in behavior from the corresponding unextracted samples except for a slight indication of decrease in the energy of pyrolysis following extraction. The difference in the behavior is small probably because of the relatively minor role the extractives play in dead fuels as compared to living foliage (greens) in which the role of extractives could be considerably more significant. The data obtained from dead fuels could be significantly different from those of living foliage.

CHAPTER VI

SUGGESTIONS FOR FURTHER STUDIES

Extensive TG and DSC data were taken during the course of this study for all seven species of materials studied, namely cellulose, excelsior, extracted excelsior, dead Ponderosa pine needles, extracted Ponderosa pine needles, saltbush leaves and punky wood (lignin). Tests on wet wood were limited to one moist sample per wood in the range of 6 to 18 percent moisture based on dry weight. Some of the tested wet samples contained only as much moisture as they might under ambient conditions. It is therefore necessary to conduct more runs with wet woods conditioned to hold far higher moisture contents. In doing so, the problem of holding the moisture (at least a large part of it) in the sample during weighing and purging the sample pan in the DSC before the start of programmed heating needs to be solved. One possibility to overcome this problem would be to use a heat transfer fluid in the DSC circulating system that holds the lower isothermal at 5°C (e.g., acetone-ethanol mixture).

As mentioned earlier, the woods studied were assumed to consist of only cellulose and lignin for modeling purposes.

To some extent, the deviations of the proposed model from the actual (experimental) TG data was attributed to this approximation. The extent to which minerals and extractives are present in the woods or their effect on the process of pyrolysis is not known at this time. From the investigations of Tang (65), Tang and Neill (70), Tang and Browne (67, 68), Browne and Brenden (16) and Brenden (9) it could be seen that relatively small quantities of some chemicals could affect the pyrolysis to a considerable extent. Therefore, there is a need for a systematic study of the quantitative effects of minerals and extractives on pyrolysis. The fact that the effect of extractives was not significant in dead Ponderosa pine needles and excelsior decomposition studied here is no guarantee that this conclusion would be a general case. In fact, the effect is felt to be fairly significant with living foliage. For this reason some living fuels need to be tested.

REFERENCES

1. Akita, K. "Studies on the Mechanism of Igniiton of Wood." Report of Fire Research Institute of Japan, No. 9 (1959).

2. Akita, K., and Kase, M. "Determination of Kinetic Parameters for Pyrolysis of Cellulose and Cellulose Treated with Ammonium Phosphate by Differential Thermal Analysis and Thermal Gravimetric Analysis." J. of Polymer Science, Part A-1, 5 (1967):833-848.

3. Anderson, D. A., and Freeman, E. S. "The Kinetics of the Thermal Degradation of Polystyrene and Polyethylene." Journal of Polymer Science, 54 (1961):253-260.

4. Arseneau, D. F. "The Differential Thermal Analysis of Wood." Canadian Journal of Chemistry, 39 (1961): 1915-1919.

5. Bamford, C. H.; Crank, J.; and Malan, D. H. "The Combustion of Wood, Part I." Proc. of Cambridge Phil. Soc., 42 (1946):166.

6. Beall, F. C. "Differential Calorimetric Analysis of Wood and Wood Components." Forest Products Laboratory, Madison, Wisconsin, Wood Science and Technology, 5 (1971):159-175.

7. Beall, F. C. "Thermogravimetric Analysis of Wood Lignin and Hemicelluloses." Forest Products Laboratory, Forest Service, USDA, Wood and Fiber, 1, 3 (Fall 1969).

8. Blackshear, P. L., Jr., and Kanury, A. Murty. "An X-Ray Photographic Study of the Reaction Kinetics of α-Cellulose Decomposition." Pyrodynamics, 4 (1968): 285-298.

9. Brenden, John J. "Effect of Fire-Retardant and Other Inorganic Salts on Pyrolysis Products of Ponderosa Pine at 250°C and 350°C." U.S. Forest Service Research Paper FPL 80, October 1967.

10. Brennan, W. P.; Miller, B.; and Whitwell, J. C. "An Improved Method of Analyzing Curves in Differential Scanning Calorimetry." I&EC Fundamentals, 8, 2 (May 1969):314-318.

11. Brennan, W. P.; Miller, B.; and Whitwell, J. C. "Thermal Conductivity Measurements with the Differential Scanning Calorimeter." Journal of Applied Polymer Science, 12 (1968):1800-1802.

12. Britton, C. M.; Countryman, C. M.; Wright, H. A.; and Walvekar, A. G. "The Effect of Humidity, Air Temperature, and Wind Speed on Fire Fuel Moisture Content." Fire Technology, February 1973, p. 46.

13. Broido, A. "Thermogravimetric and Differential Thermal Analysis of Potassium Bicarbonate Contaminated Cellulose." WSCI Paper No. 66-20. 1966 Spring Meeting, Western States Section, The Combustion Institute, Denver Research Institute, April 1966.

14. Brown, L. E. "An Experimental and Analytic Study of Wood Pyrolysis." Ph.D. dissertation, University of Oklahoma, Norman, Oklahoma, 1972.

15. Browne, F. L. "Theories of the Combustion of Wood and Its Control." U.S. Forest Products Laboratory, Report 2136, 1958, p. 69.

16. Browne, F. L., and Brenden, J. J. "Heat of Combustion of the Volatile Pryolysis Products of Fire Retardant-Treated Ponderosa Pine." U.S. Forest Service Research Paper, FPL 19, December 1964.

17. Burningham, N. W., and Seader, J. D. "Determination of Kinetic Parameters for the Thermal Degradation of Polymers by the Quasi-Linearization Technique." Paper presented at 161st Meeting, American Chemical Society, 1971.

18. Chung, P. K., and Jackson, M. L. "Thermal Diffusivity of Low Conductivity Materials." Industrial & Engineering Chemistry, 46, 12 (1954):2563-2566.

19. Domansky, Radislov; and Rendos, Frantisek. "Zum Studium der Pyrolysis des Holzes und Seiner Komponenten." Holz Als Roh-Und Werkstoff, 20 (1962):473-476.

20. Domburgs, G., and Sergeeva, V. N. "Thermographic Method for Studying the Pyrolysis of Wood and Its Components." Latvijas PSR Zinatsu. Akad. Vestis Kim. Ser. (Russian), 5 (1964):625-632.

21. Domburgs, G.; Sergeeva, V. N.; Kalnins, A. I.; and Kiselis, O. "Thermal Analysis in the Chemistry of Wood." Latv. PSR Zinat. Akad. Vestis (Russian), 12 (1966):52-57.

22. Dunlap, F. "The Specific Heat of Wood." U.S. Department of Agriculture, Forest Service Bulletin No. 110 (1912).

23. Fire Research Board. Report of Fire Research Board, Dept. of Scientific and Industrial Research and Fire Offices' Commission (Great Britain). "Prolonged Heating of Wood." 1948, pp. 8-10.

24. Fons, Wallace. "Heating and Ignition of Small Wood Cylinders." Industrial and Engineering Chemistry, 42 (1950):2130-2133.

25. Forest Products Laboratory. "Ignition and Charring Temperatures of Wood." USDA Forest Service Report No. 1464, January 1958.

26. Forest Products Laboratory. "Theories of the Combustion of Wood and Its Control." Forest Products Laboratory, Madison, Wisconsin. Report No. 2136 (1963).

27. Fosberg, Michael A. "Prediction of Pre-Pyrolysis Temperature Rise in Dead Forest Fuels." Fire Technology, August 1973, p. 182.

28. Fosberg, Michael A., and Schroeder, Mark T. "Fire Herbaceous Fuels in Fire Danger Rating." USDA Forest Service Research Note RM-185, 1971, p. 7.

29. Frandsen, W. H. "Fire Spread Through Porous Fuels from the Conservation of Energy." Combustion and Flame, 16 (1971):9-16.

30. Freeman, Eli S., and Carroll, Benjamin. "The Application of Thermoanalytical Techniques to Reaction Kinetics: The Thermogravimetric Evaluation of the Kinetics of the Decomposition of Calcium Oxalate Monohydrate." Journal of Physical Chemistry, 62 (1958):394.

31. Ginnings, D. C., and Furukawa, T. "Heat Capacity Standards for the Range 14 to 1200°K." J. Amer. Chem. Soc., 75 (1953):522-524.

32. Goldfarb, I. J.; McGuchan, R.; and Meeks, A. C. "Kinetic Analysis of Thermogravimetry. Part II. Programmed Temperatures." Air Force Materials Laboratory, Wright-Patterson Air Force Base, Ohio. ARML-TR-68-181, Part 2 (1968).

33. Griffiths, Ezer, and Kaye, G. W. "The Measurement of Thermal Conductivity." Proceedings of the Royal Society of London, Series A, 104 (1923):71-98.

34. Guttman, Charles M., and Flynn, H. J. "On the Drawing of the Baseline for Differential Scanning Calorimetric Calculation of Heats of Transition." Analytical Chemistry, 45, 2 (February 1973):408-410.

35. Hall, J. Alfred. "Forest Fuels, Prescribed Fire, and Air Quality." USDA, Portland, Oregon, 1972.

36. Hashemi, H. T. "Heat Conduction with Change of Phase." Ph.D. dissertation, University of Oklahoma, Norman, Oklahoma, 1965.

37. Havens, J. A. "Thermal Decomposition of Wood." Ph.D. dissertation, University of Oklahoma, Norman, Oklahoma, 1969.

38. Hawley, Lee F. "Combustion of Wood." Chapter 19 in Wood Chemistry, by Louis E. Wise and Edwin C. Jahn. New York: Reinhold, 2nd ed.

39. Heinrich, H. J., and Kaesche-Kriescher, B. "Contributions to the Explanation of Self-Ignition of Wood." Brennstoff-Chemie, 43, 5:142-148

40. Jones, G. W., and Scott, G. S. U.S. Bureau of Mines, Report of Investigations 3468 (1939).

41. Kanury, A. Murty. "An Evaluation of the Physico-Chemical Factors Influencing the Burning Rate of Cellulosic Fuels and a Comprehensive Model for Solid Fuel Pyrolysis and Combustion." Ph.D. dissertation, University of Minnesota, Minneapolis, Minnesota, 1969.

42. Keylwerth, R., and Christoph, N. "Contributions to the Study of Thermal Decomposition of Wood by Means of Differential Thermal Analysis." Deutscher Verband fur Materials Prufung Dvm, 2, 8 (20 August 1960): 281-288.

43. Koch, Peter. "Specific Heat of Spruce Pine Wood and Bark." Wood Science, 1, 4 (1969):203-214.

44. Kollman, F. Technologie Des Holzes und der Holzwerkstoffs, Vol. 1. 2nd ed. Berlin: Julius Springer, 1936.

45. Koohyar, A. "The Ignition of Wood by Flame Radiation." Ph.D. dissertation, University of Oklahoma, Norman, Oklahoma, 1967.

46. Kung, H. C., and Kalelkar, Ashok S. "On the Heat of Reaction in Wood Pyrolysis." Combustion and Flame, 20 (1973):91-103.

47. Lawson, D. T., and Simms, D. L. "The Ignition of Wood by Radiation." British J. of Applied Physics, 3, (1952):288-292, 394-396.

48. MacLean, J. D. "Thermal Conductivity of Wood." Heating, Piping and Air Conditioning, July 1940, pp. 459-464.

49. McMillin, Charles W. "Specific Heat of Oven-Dry Loblolly Pine Wood." Wood Science, 2, 2 (1969):107-111.

50. McMillin, Charles W. "Specific Heat of Some Oven-Dry Chemical Constituents of Loblolly Pine Wood." Wood Science, 2, 1 (1970).

51. Mita, I.; Imai, I.; and Kambe, H. "Determination of Heat of Mixing and Heat of Vaporization with a Differential Scanning Calorimeter." Thermochimica Acta, 2 (1971):337-344.

52. O'Neill, M. J. "Measurement of Specific Heat Function by Differential Scanning Calorimetry." Analytical Chemistry, 38, 10 (September 1966):1331-1336.

53. Panton, R. L., and Rittman, J. G. "Analytical Study of Combustion." Final Report to Air Force Armament Laboratory Ballistics Division, Elgin Air Force Base, Florida.

54. Roberts, A. F., and Clough, G. "Thermal Decomposition of Wood in an Inert Atmosphere." Ninth Symposium (International) on Combustion. New York: Academic Press, 1963.

55. Rogers, R. N. "Simplified Determination of Rate Constants by Scanning Calorimetry." Analytical Chemistry, 44, 7 (June 1972):1336-1337.

56. Rogers, R. N., and Morris, E. D., Jr. "Determination of Emissivities with a Differential Scanning Calorimeter." Analytical Chemistry, 38, 3 (March 1966):410-412.

57. Rogers, R. N., and Morris, E. D., Jr. "On Estimating Activation Energies with a Differential Scanning Calorimeter." Analytical Chemistry, 38, 3 (March 1966):412-414.

58. Rogers, R. N., and Smith, L. C. "Estimation of Pre-exponential Factor from Thermal Decomposition Curve of an Unweighed Sample." Analytical Chemistry, 39, 8 (July 1967):1024-1025.

59. Rothermel, Richard C. "A Mathematical Model for Predicting Fire Spread in Wildland Fuels." Intermountain Forest and Range Experiment Station, Ogden, Utah. USDA Research Paper INT-115 (1972).

60. Rowley, F. B. "The Heat Conduction of Wood at Climatic Temperature Differences." Transactions, Am. Soc. of Heating and Ventilating Engineers, 39 (1933):313-323.

61. Sandermann, W., and Augustin, Hans. "Chemische Untersuchungen Uber Die Thermische Fersetzung of Holz Erste Metteilung: Stand der Forschung, Zwerte Metteilung: Unterschungen mit Hilte der DTA." Holz Als Ruh-Und-Werkstoff, 21 (1963):305-315.

62. Sardesai, U. V. "Thermogravimetric Analysis of Cellulose." M.S. Thesis, University of Oklahoma, Norman, Oklahoma, 1973.

63. Sergeeva, V. N., and Vaivads, A. "Thermographic Study of the Pyrolysis of Wood and Its Components." Latvijas PSR Zinatner Akad. Vertis (Russia), 86 (1954):102-108.

64. Stamm, A. J. "Thermal Degradation of Wood and Cellulose." Industrial and Engineering Chemistry, 48 (1956):413-417.

65. Tang, W. K. "Effect of Inorganic Salts on Pyrolysis of Wood, Alpha-Cellulose, and Lignin Determined by Dynamic Thermogravimetry." U.S. Forest Service Research Paper FPL 71, January 1967.

66. Tang, W. K. "Study of the Effect of Chemical Treatment of the Thermal Decomposition of Wood." Forest Products Laboratory Report 1960.

67. Tang, W. K., and Browne, F. L. "Effect of Various Chemicals on Thermogravimetric Analysis of Ponderosa Pine." U.S. Forest Service Research Paper FPL-6, June 1963.

68. Tang, W. K., and Browne, F. L. "Thermogravimetric and Differential Thermal Analysis of Wood and of Wood Treated with Inorganic Salts During Pyrolysis." Forest Products Laboratory, Forest Service, USDA, Madison, Wisconsin, May 1962.

69. Tang, W. K., and Eickner, H. W. "Effect of Inorganic Salts on Pyrolysis of Wood, Cellulose, and Lignin Determined by Differential Thermal Analysis." U.S. Forest Service Research Paper FPL-82, January 1968.

70. Tang, W. K., and Neill, W. K. "Effects of Flame Retardants on Pyrolysis and Combustion of α-Cellulose." J. Polymer Science, Part C, 6 (1964):65-81.

71. Vyas, R. J. "End-Grain Piloted Ignition of Wood by Flame Radiation." M.S. thesis, University of Oklahoma, Norman, Oklahoma, 1973.

72. Wangaard, F. F. "Transverse Heat Conductivity of Wood." Heating, Piping and Air-Conditioning, July 1940, pp. 459-464.

73. Wangaard, F. F. "The Transverse Conductivity of Wood.": Ph.D. dissertation, NY State College of Forestry, Syracuse, New York, 1948.

74. Wangaard, F. F., and Granados, L. A. "The Effect of Extractives on Water Vapor Sorption by Wood." Wood Science and Technology, 1 (1967):253-277.

75. Weatherford, W. D., Jr., and Shappard, D. M. "Basic Structure of the Mechanism of Ignition of Cellulosic Materials." Tenth Symposium (International) on Combustion. New York: Academic Press, 1965, pp. 897-910.

76. Widell, Torsten. "Thermal Investigation into Carbonization of Wood." Acta Polytechnica, Chemical and Metallurgical Series 1, 6 (1949):35.

77. Woodard, W. M. "Thermal Decomposition of Synthetic Polymers." Ph.D. dissertation, University of Oklahoma, Norman, Oklahoma, 1973.

APPENDICES

APPENDIX A

DATA FROM WOOD TGA STUDIES

Run No.	Heating rate (°C/min)	Initial weight (mg)	Final weight (mg)	Maximum rate of wt loss (Normalized)*	Temp at max. rate of wt loss (°C)
Cellulose					
1	10	3.89	0.0610	0.28	373
2	10	2.9	0.0537	0.28	373
3	10	3.38	0.0659	0.28	371
4	20	3.5	0.0710	0.47	389
5	20	4.33	0.0761	0.47	390
6	20	4.01	0.075	0.47	384
7	40	3.46	0.070	0.87	402
8	40	2.24	0.036	0.86	406
9	40	3.91	0.070	0.84	403
10	80	3.9	0.061	1.43	430
11	80	3.84	0.056	1.46	430
12	80	3.22	0.052	1.44	430
13	160	3.34	0.06	2.23	443
14	160	3.84	0.046	2.20	441
15	160	3.92	0.073	2.17	447
Dead Ponderosa Pine Needles					
1	10	2.96	0.5743	0.08	376
2	10	3.17	0.6352	0.08	374
3	10	3.41	0.6770	0.08	373
4	20	2.83	0.5360	0.14	382
5	20	2.90	0.5954	0.13	383
6	20	2.73	0.5460	0.13	382
7	40	2.84	0.5260	0.27	394

*min^{-1}

Run No.	Heating rate (°C/min)	Initial weight (mg)	Final weight (mg)	Maximum rate of wt loss (Normalized)*	Temp at max. rate of wt loss (°C)
Dead Ponderosa Pine Needles, Continued					
8	40	2.91	0.5426	0.26	394
9	40	2.73	0.5341	0.26	395
10	80	3.21	0.6251	0.50	417
11	80	3.21	0.6280	0.50	418
12	80	3.05	0.5800	0.49	417
13	160	2.98	0.5775	0.92	421
14	160	3.07	0.6123	0.94	428
15	160	3.07	0.6015	0.91	428
Extracted Ponderosa Pine Needles					
1	10	3.9	0.4033	0.08	366
2	10	3.92	0.4120	0.08	367
3	10	4.14	0.4200	0.08	370
4	20	3.56	0.348	0.14	379
5	20	3.72	0.384	0.16	376
6	20	3.53	0.362	0.15	378
7	40	3.65	0.3712	0.27	382
8	40	3.56	0.326	0.27	384
9	40	3.35	0.342	0.27	383
10	80	3.36	0.339	0.58	391
11	80	3.10	0.314	0.54	392
12	80	3.87	0.401	0.53	393
13	160	3.44	0.341	1.01	413
14	160	3.23	0.302	0.99	413
15	160	3.19	0.322	1.00	413
Excelsior					
1	10	2.99	0.2360	0.14	375
2	10	3.38	0.2419	0.14	376
3	10	3.64	0.2744	0.14	377
4	20	3.46	0.2689	0.25	392
5	20	3.35	0.2604	0.25	392
6	20	3.38	0.2438	0.26	393
7	40	3.44	0.2524	0.48	403
8	40	2.95	0.2152	0.49	402

Run No.	Heating Rate (°C/min)	Initial weight (mg)	Final weight (mg)	Maximum rate of wt loss (Normalized)*	Temp at max. rate of wt loss (°C)
Excelsior, Continued					
9	40	3.18	0.2387	0.50	401
10	80	3.08	0.2623	0.87	410
11	80	3.26	0.2353	0.89	412
12	80	2.98	0.2241	0.86	413
13	160	3.14	0.2119	1.53	420
14	160	3.10	0.2242	1.55	422
15	160	3.10	0.2165	1.56	422
Extracted Excelsior					
1	10	3.44	0.2508	0.13	378
2	10	3.92	0.2553	0.13	379
3	10	3.64	0.2576	0.14	381
4	20	3.25	0.2518	0.25	394
5	20	3.17	0.2481	0.25	395
6	20	3.37	0.2540	0.26	396
7	40	3.11	0.2410	0.47	402
8	40	3.46	0.2520	0.52	405
9	40	3.15	0.2391	0.46	405
10	80	3.84	0.2540	0.90	419
11	80	3.30	0.2511	0.89	419
12	80	3.34	0.2489	0.88	420
13	160	3.18	0.2391	1.55	430
14	160	3.61	0.2532	1.54	433
15	160	3.89	0.2548	1.54	433
Saltbush Leaves					
1	10	3.31	0.7117	0.08	341
2	10	3.42	0.7523	0.08	338
3	10	3.48	0.7330	0.07	336
4	20	3.76	0.7525	0.16	349
5	20	3.15	0.7065	0.16	346
6	20	3.48	0.7264	0.13	346
7	40	3.55	0.7363	0.31	360
8	40	3.56	0.7230	0.30	362

Run No.	Heating rate (°C/min)	Initial weight (mg)	Final weight (mg)	Maximum rate of wt loss (Normalized)*	Temp at max. rate of wt loss (°C)
Saltbush Leaves, Continued					
9	40	3.28	0.7131	0.27	358
10	80	3.56	0.7317	0.59	368
11	80	3.86	0.7729	0.53	367
12	80	3.83	0.7654	0.61	371
13	160	3.55	0.7289	1.21	380
14	160	3.65	0.7441	1.14	381
15	160	3.50	0.7205	1.17	382
Punky Wood					
1	10	3.52	0.9176	0.06	343
2	10	3.28	0.8426	0.06	345
3	10	3.43	0.8510	0.05	342
4	20	3.98	1.0571	0.12	356
5	20	3.06	0.7721	0.12	360
6	20	3.88	1.0282	0.12	364
7	40	3.96	0.9370	0.21	375
8	40	3.56	0.9256	0.25	375
9	40	3.69	0.9539	0.22	376
10	80	3.82	0.9875	0.47	388
11	80	3.82	0.9860	0.46	385
12	80	3.85	0.9865	0.46	388
13	160	3.14	0.8085	0.87	406
14	160	3.22	0.8262	0.89	403
15	160	3.24	0.8290	0.88	405
Larch Wood					
1	10	4.13	0.9525	0.12	375
2	10	4.04	0.9514	0.13	376
3	10	3.92	0.9462	0.14	376
4	20	--	--	--	--
5	20	--	--	--	--
6	20	--	--	--	--
7	40	4.10	1.0587	0.42	407
8	40	3.74	0.9021	0.48	410
9	40	4.21	1.1234	0.52	409
10	80	--	--	--	--
11	80	--	--	--	--
12	80	--	--	--	--
13	160	3.60	0.8013	1.40	435
14	160	3.82	0.8764	1.56	437
15	160	4.06	0.9293	1.62	436

APPENDIX B

DRY WOOD DSC DATA

Run No.	Heating Rate °C/min	C_p 25°C cal/gm-°C	Initial Sample Weight mg	Final Sample Weight mg	Temp Max PYR*	ΔH_t Wood cal/gm-sam	ΔH Sensible cal/gm-sam
Cellulose							
1	40	0.33	0.83	0.01	405	86	121
2	40	0.33	1.22	0.024	404	85	122
3	80	0.34	1.31	0.025	428	86	120
4	80	0.33	1.05	0.021	429	84	123
5	160	0.34	1.39	0.026	441	87	121
6	160	0.33	1.26	0.024	440	86	122
Dead Ponderosa Pine Needles							
1	40	0.44	0.99	0.20	398	73	129
2	40	0.43	1.34	0.26	395	76	130
3	80	0.44	1.27	0.18	414	78	131
4	80	0.45	1.06	0.15	416	71	127
5	160	0.45	1.56	0.18	426	79	129
6	160	0.43	1.38	0.16	427	75	130
Extracted Ponderosa Pine Needles							
1	40	0.43	1.16	0.12	388	64	119
2	40	0.43	1.28	0.13	386	65	123
3	80	0.44	1.43	0.14	394	62	122

* Temperature at the maximum rate of pyrolysis, °C.

APPENDIX B--Continued

Run No.	Heating Rate °C/min	C_p 25°C cal/gm-°C	Initial Sample Weight mg	Final Sample Weight mg	Temp Max PYR*	$\Delta H_{t_{Wood}}$ cal/gm-sam	$\Delta H_{Sensible}$ cal/gm-sam
4	80	0.43	1.36	0.14	395	66	126
5	160	0.43	1.41	0.14	414	67	122
6	160	0.43	1.18	0.12	412	69	126
Excelsior							
1	40	0.38	1.14	0.09	402	45	106
2	40	0.37	1.4	0.11	400	47	108
3	80	0.36	1.21	0.09	414	52	104
4	80	0.38	1.31	0.10	412	48	110
5	160	0.35	1.35	0.12	423	49	106
6	160	0.345	1.3	0.097	424	50	101
Extracted Excelsior							
1	40	0.34	0.96	0.07	405	44	101
2	40	0.34	1.32	0.086	404	43	102
3	80	0.35	1.13	0.08	419	45	100
4	80	0.34	1.09	0.078	418	46	108
5	160	0.355	1.24	0.074	434	47	112
6	160	0.345	1.40	0.086	433	46	110
Saltbush Leaves							
1	40	0.39	1.2	0.26	360	42	108
2	40	0.39	1.31	0.29	359	43	109
3	80	0.40	1.11	0.22	368	41	112

APPENDIX B--Continued

Run No.	Heating Rate °C/min	C_p 25°C cal/gm-°C	Initial Sample Weight mg	Final Sample Weight mg	Temp Max PYR*	$\Delta H_{t_{Wood}}$ cal/gm-sam	$\Delta H_{Sensible}$ cal/gm-sam
Saltbush Leaves--Continued							
4	80	0.39	1.24	0.25	368	45	104
5	160	0.40	1.09	0.125	378	47	110
6	160	0.40	1.37	0.29	380	46	106
Punky Wood							
1	40	0.44	1.04	0.27	372	36	132
2	40	0.43	1.3	0.33	373	38	133
3	80	0.43	1.12	0.29	384	36	140
4	80	0.45	1.28	0.34	385	34	132
5	160	0.42	1.49	0.37	402	38	126
6	160	0.43	1.29	0.33	401	39	133

APPENDIX C

WET WOOD DSC DATA

Run No.	Heating Rate °C/min	C_p 25°C cal/gm-°C	Initial Sample Weight mg	Final Sample Weight mg	Percent Moisture Content (Dry Basis)	Temp Max ML*	Temp Max PYR**	$\Delta H_{t_{water}}$ cal/gm-sam	$\Delta H_{t_{wood}}$ cal/gm-sam	$\Delta H_{sensible}$ cal/gm-sam
Cellulose										
1	40	0.43	1.35	0.16	10	76	405	49	89	159
2	40	0.42	1.0	0.12	10	76	406	49	88	160
3	80	0.44	1.12	0.136	9	85	428	43	87	158
4	80	0.42	0.95	0.101	8	87	431	42	87	161
5	160	0.45	1.39	0.11	6	100	439	30	83	154
6	160	0.44	1.22	0.10	6	102	440	31	84	152
Dead Ponderosa Pine Needles										
1	40	0.53	1.28	0.373	13	74	398	69	62	178
2	40	0.54	1.14	0.34	13	76	396	68	63	180
3	80	0.57	1.32	0.39	13	84	414	67	65	179
4	80	0.55	1.46	0.42	13	85	412	69	63	176
5	160	0.57	1.11	0.33	13	99	420	67	69	184
6	160	0.56	1.21	0.36	13	101	422	68	70	181
Extracted Dead Ponderosa Pine Needles										
1	40	0.53	1.35	0.25	18	77	387	95	53	169
2	40	0.52	1.22	0.33	18	76	384	94	51	172
3	80	0.53	1.41	0.37	18	85	395	93	54	170
4	80	0.53	1.26	0.33	18	87	397	96	56	173
5	160	0.53	1.23	0.33	18	100	412	93	57	174
6	160	0.54	1.15	0.30	18	101	414	95	58	170
Excelsior										
1	40	0.48	1.92	0.35	12	75	398	58	40	152
2	40	0.47	2.01	0.37	12	76	400	59	41	151
3	80	0.44	1.85	0.34	12	87	408	58	43	150
4	80	0.46	1.53	0.28	12	84	410	60	41	152
5	160	0.45	1.42	0.27	12	99	422	58	45	148
6	160	0.46	2.16	0.4	12	101	424	57	44	150

*Temperature at the maximum rate of moisture loss, °C.

**Temperature at the maximum rate of pyrolysis, °C.

APPENDIX C--Continued

Run No.	Heating Rate °C/min	C_p 25°C cal/gm-°C	Initial Sample Weight mg	Final Sample Weight mg	Percent Moisture Content (Dry Basis)	Temp Max ML*	Temp Max PYR**	ΔH_t Water cal/gm-sam	ΔH_t Wood cal/gm-sam	ΔH Sensible cal/gm-sam
Extracted Excelsior										
1	40	0.42	2.09	0.41	13	72	405	67	41	139
2	40	0.43	2.13	0.42	13	75	404	64	41	150
3	80	0.43	2.11	0.41	13	84	416	66	41	147
4	80	0.45	1.92	0.38	13	86	418	64	44	153
5	160	0.45	1.75	0.34	13	101	434	63	42	158
6	160	0.46	2.25	0.45	13	102	435	65	43	149
Saltbush Leaves										
1	40	0.49	3.58	1.16	15	75	362	77	37	157
2	40	0.47	3.24	1.07	15	77	363	78	36	160
3	80	0.46	2.86	0.93	15	85	370	79	39	162
4	80	0.48	3.25	1.06	15	86	369	81	36	159
5	160	0.45	3.3	1.07	15	102	377	80	41	160
6	160	0.45	2.94	1.01	15	100	378	81	40	162
Punky Wood										
1	40	0.54	3.49	1.14	9	77	375	45	32	182
2	40	0.54	3.56	1.15	9	76	376	47	34	179
3	80	0.53	3.22	1.07	9	88	386	44	35	183
4	80	0.54	3.36	1.09	9	85	388	48	32	180
5	160	0.52	2.97	1.0	9	98	400	46	36	180
6	160	0.53	3.15	1.04	9	100	402	45	34	181

*Temperature at the maximum rate of moisture loss, °C.

**Temperature at the maximum rate of pyrolysis, °C

APPENDIX D

ESTIMATED CHEMICAL CONSTITUENTS OF SAMPLES

Samples	Percent Ash	Percent Silica-free Ash	Percent Lignin	Percent Cellulose
Excelsior (Populus spp.)	0.36	0.36	16	--
Ponderosa Pine Needles Dead (Pinus Ponderosa)	3.69	1.53	--	--
Salt Bush Leaves (Atriplex Canescens)	12.89	12.29	--	--
Punky Wood (Pseudotsuga Menzeissii)	0.20	0.20	100	--
Cellulose	0	0	0	100
Larch (Larix Occidentalis)	--	--	39	--

APPENDIX E

WEIGHT LOSS AND RATE OF WEIGHT LOSS CURVES

Weight loss and rate of weight loss curves for dead Ponderosa pine needles (extracted and unextracted), excelsior (extracted and unextracted), fc rwing saltbush leaves, punky wood from Douglas-fir snags, and larch wood.

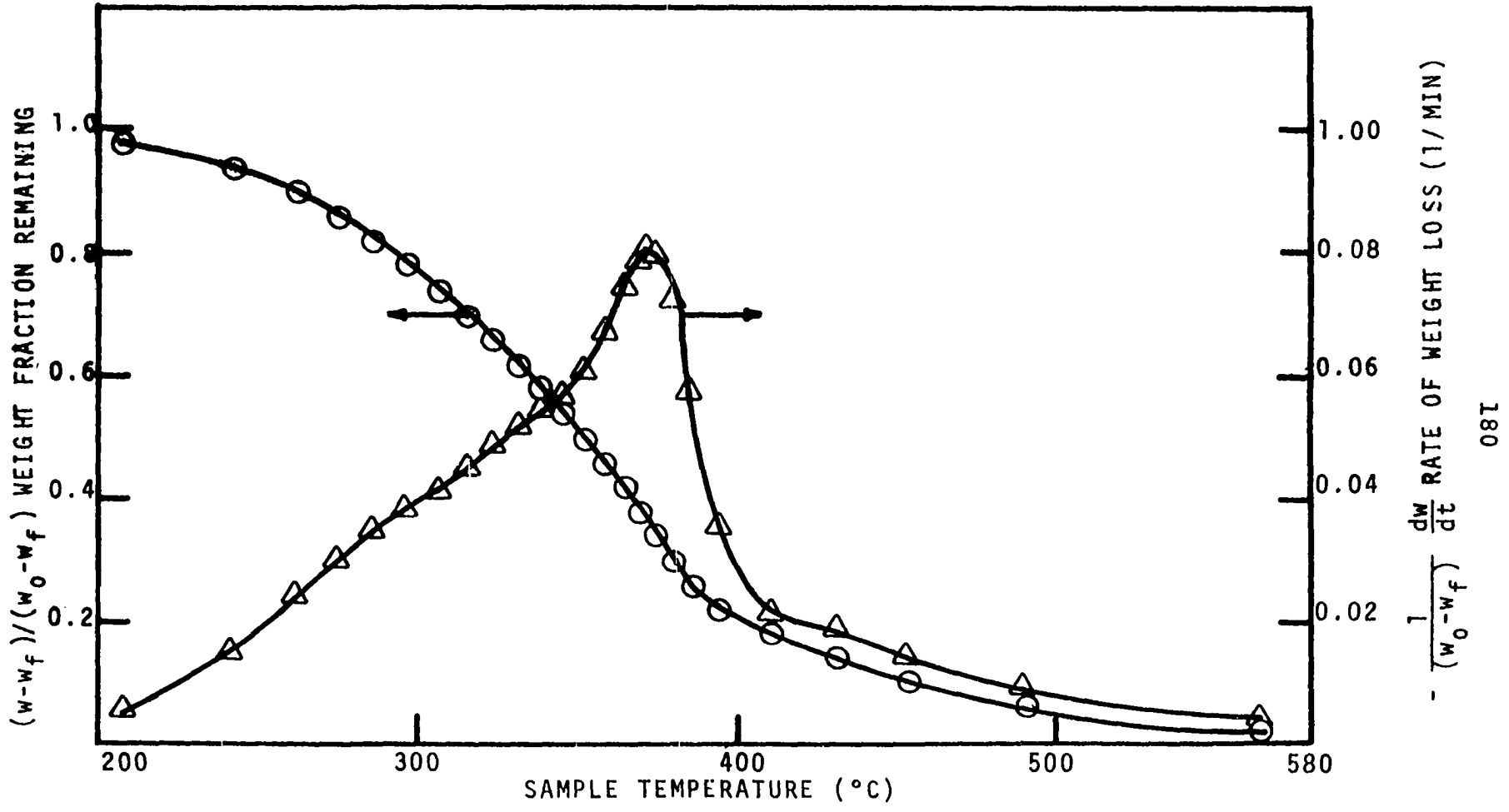

Figure E-1. Weight Loss and Rate of Weight Loss for Dead Ponderosa Pine Needles. Heating Rate - 10°C/MIN.

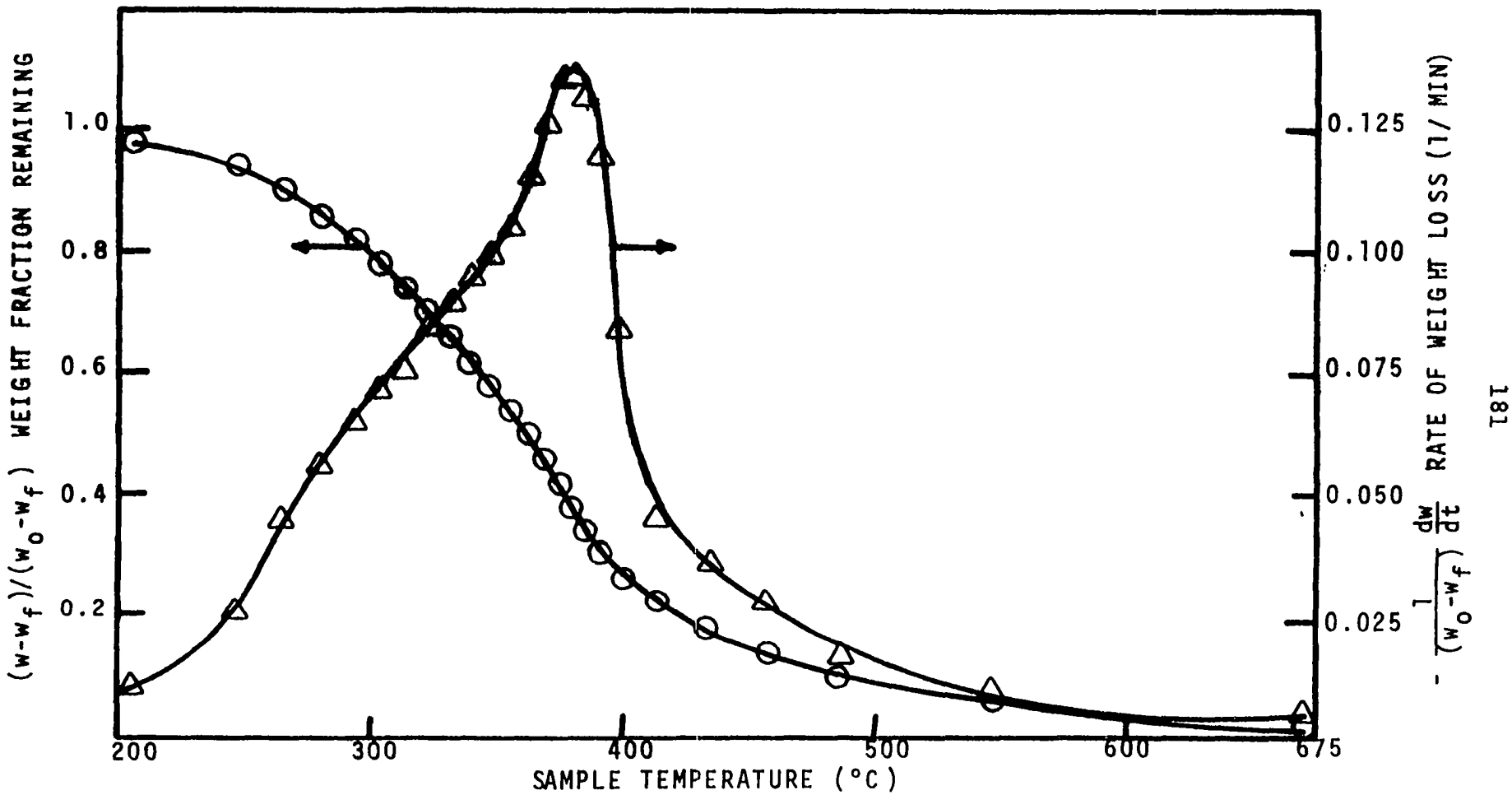

Figure E-2. Weight Loss and Rate of Weight Loss for Dead Ponderosa Pine Needles. Heating Rate - 20°C/MIN.

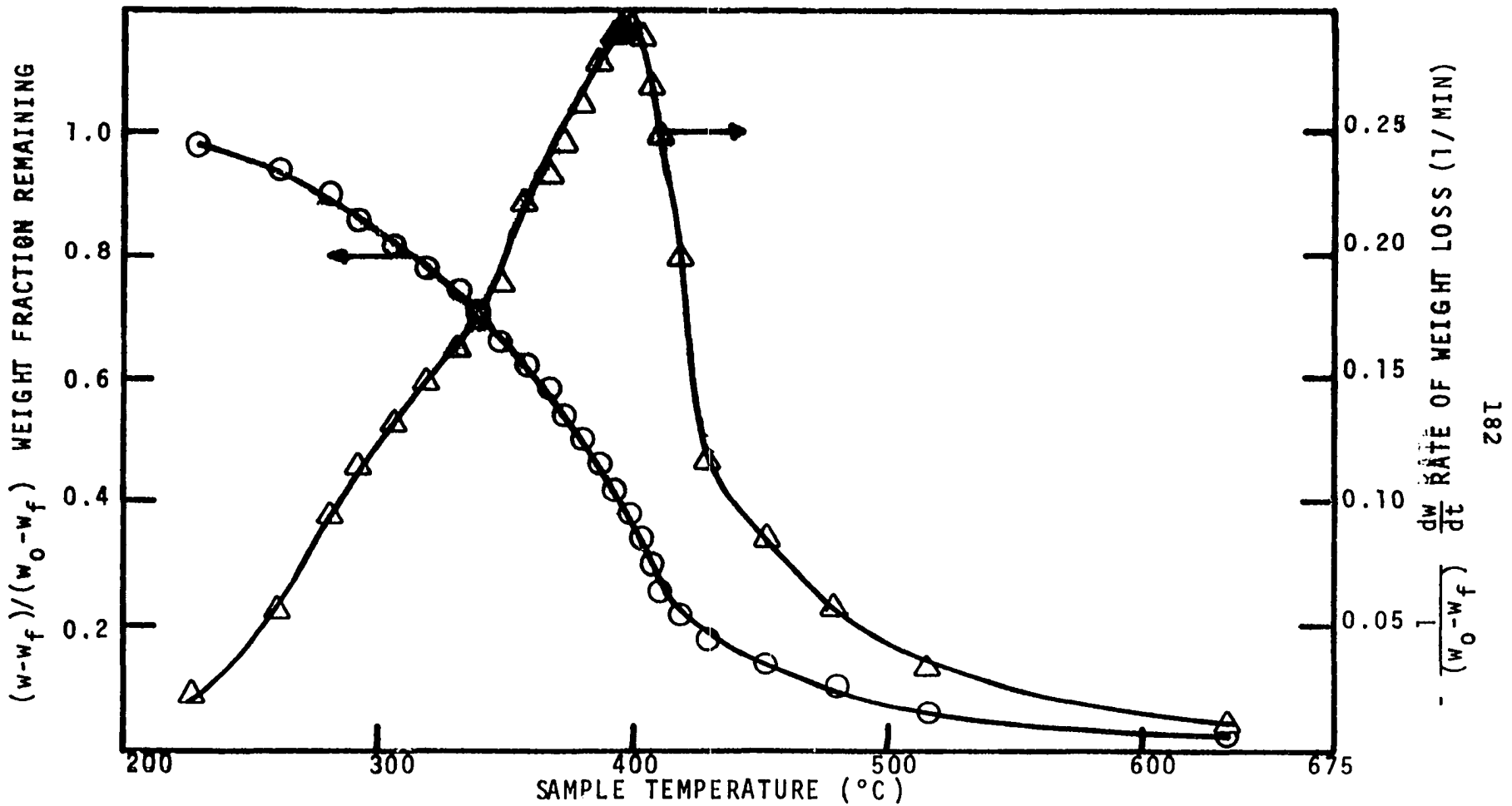

Figure E-3. Weight Loss and Rate of Weight Loss for Dead Ponderosa Pine Needles. Heating Rate - 40°C/MIN.

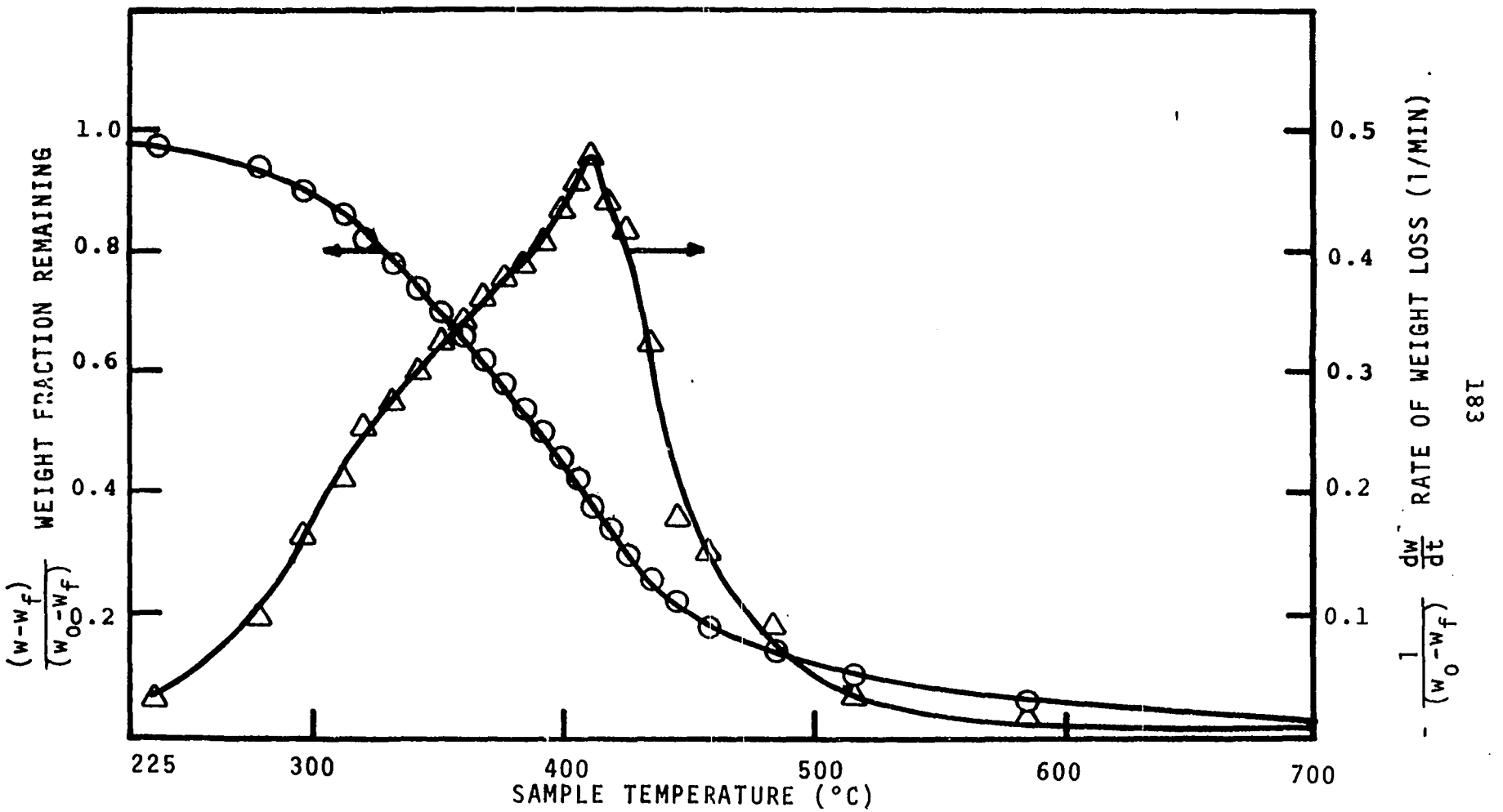

Figure E-4. Weight Loss and Rate of Weight Loss for Dead Ponderosa Pine Needles. Heating Rate - 80°C/MIN.

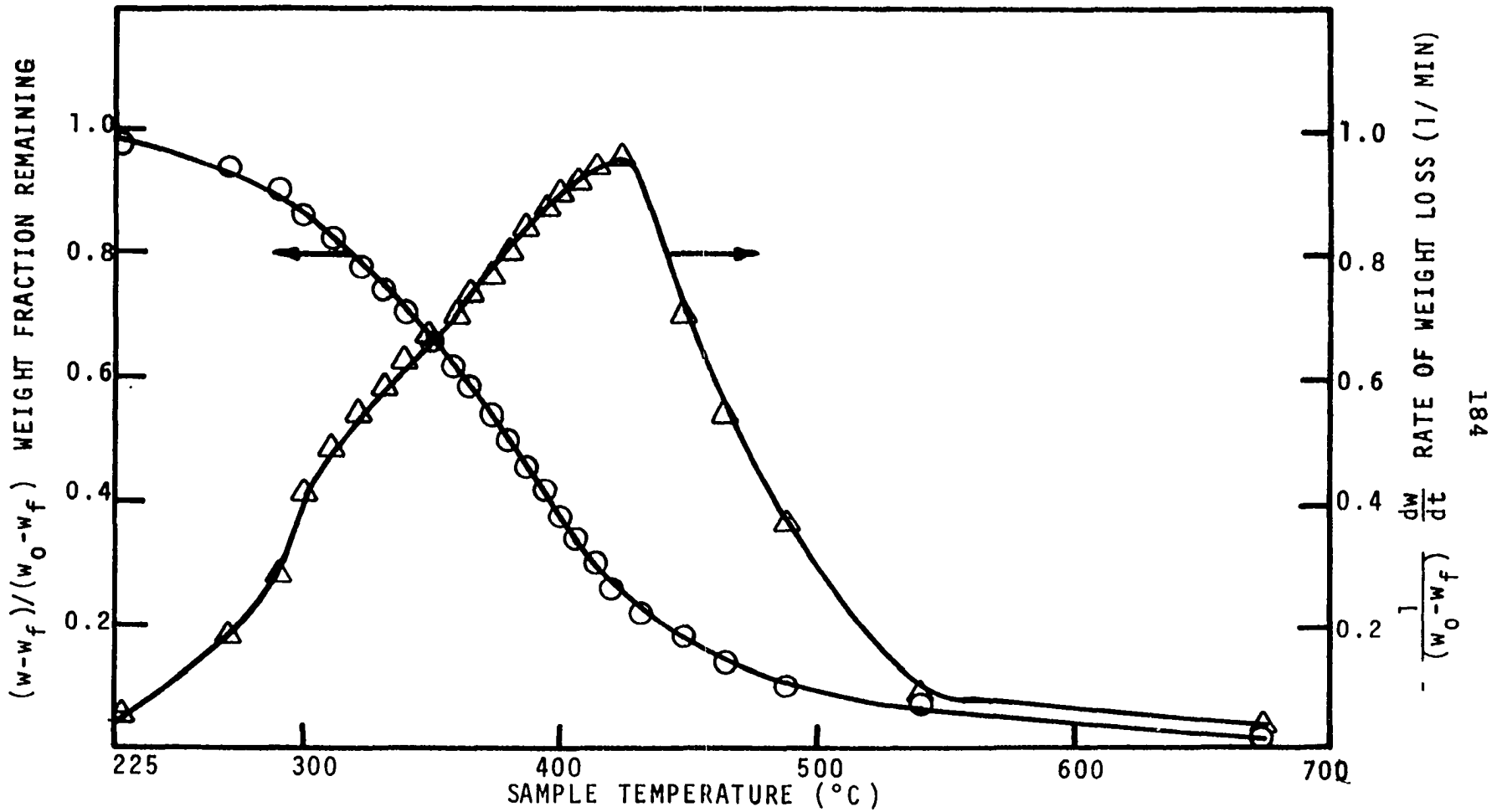

Figure E-5. Weight Loss and Rate of Weight Loss for Dead Ponderosa Pine Needles. Heating Rate - 160°C/MIN.

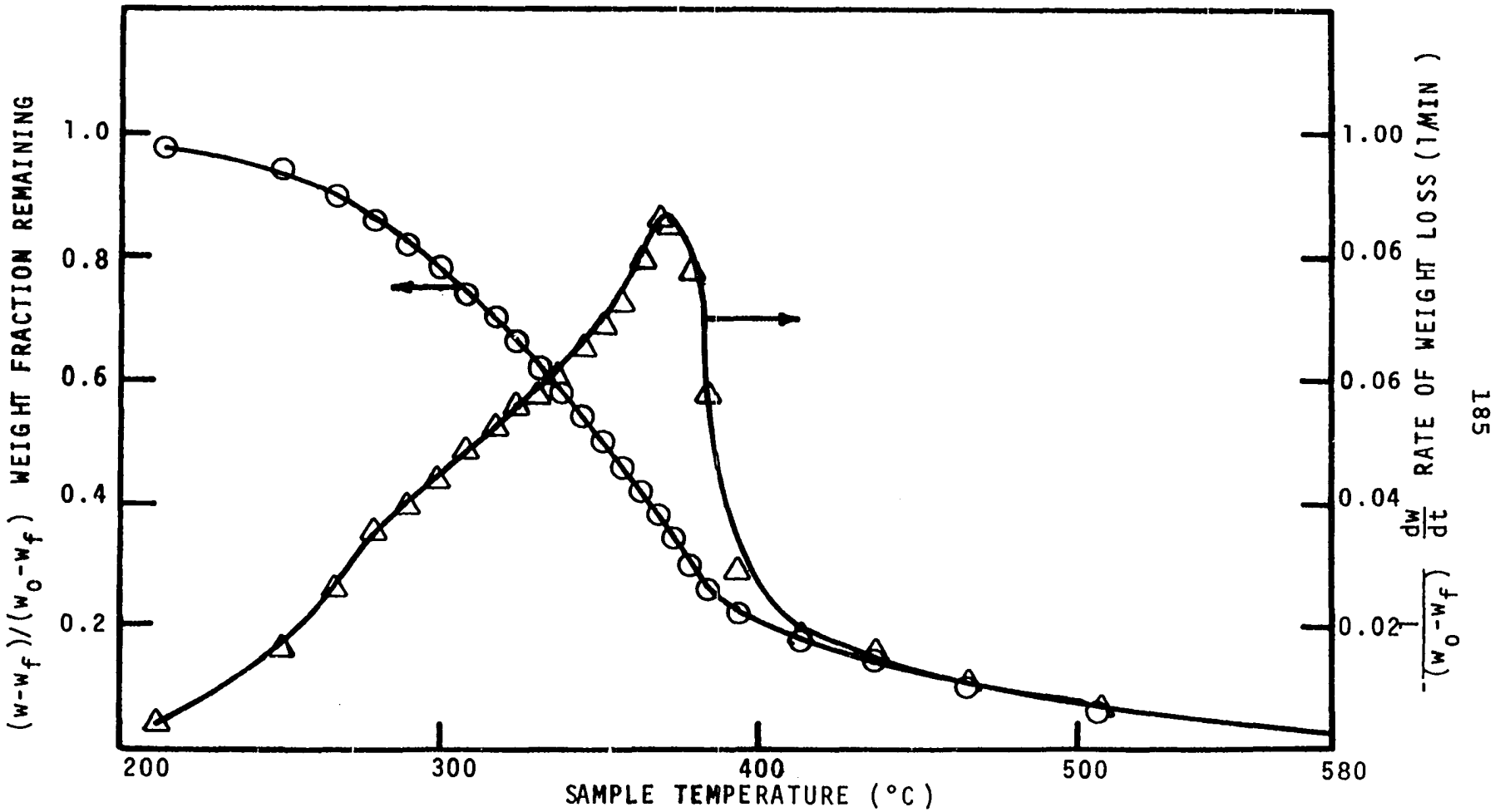

Figure E-6. Weight Loss and Rate of Weight Loss for Dead Ponderosa Pine Needles Extracted with Ether. Heating Rate - 10°C/MIN.

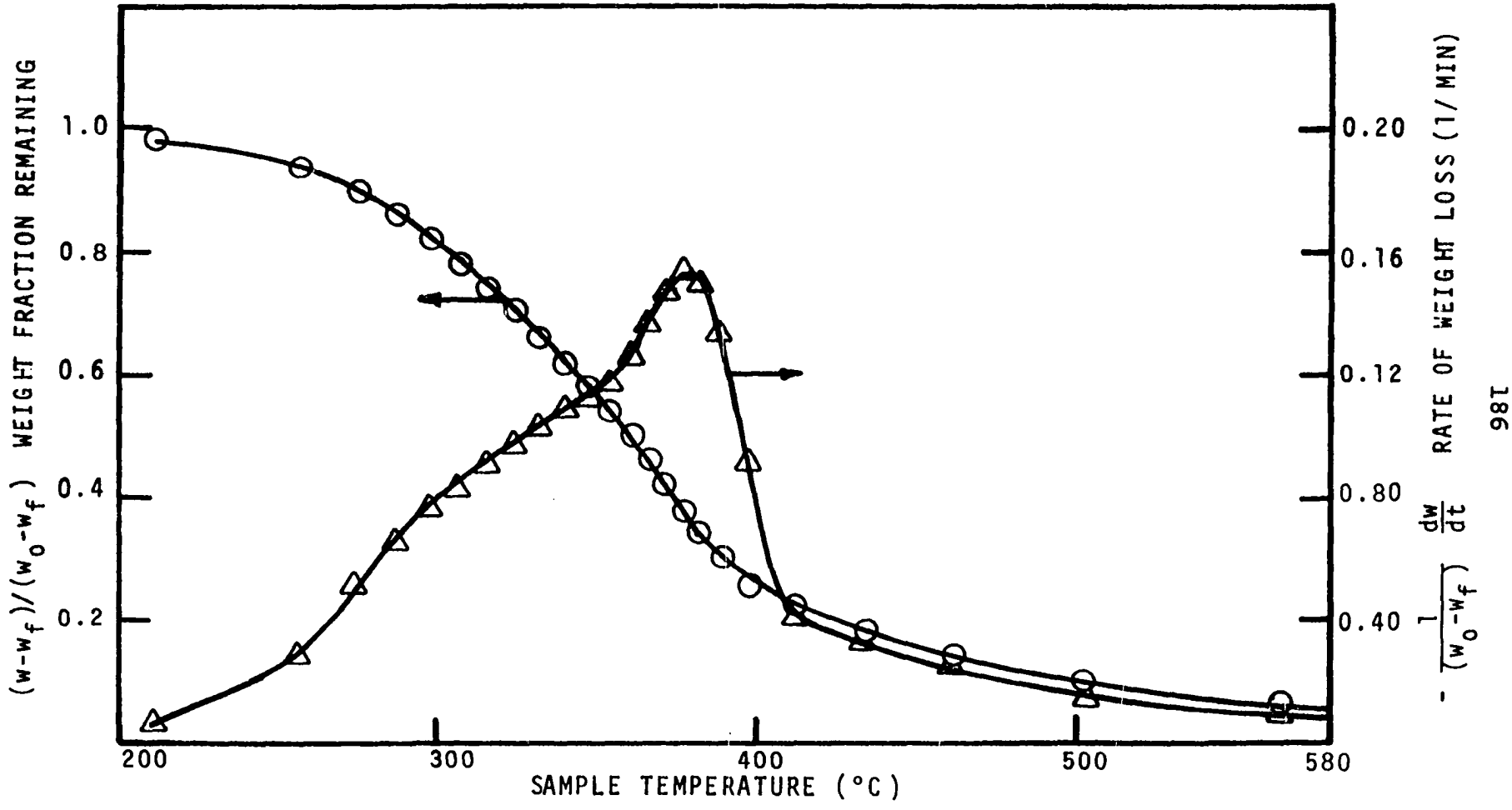

Figure E-7. Weight Loss and Rate of Weight Loss for Dead Ponderosa Pine Needles Extracted with Ether. Heating Rate - 20°C/MIN

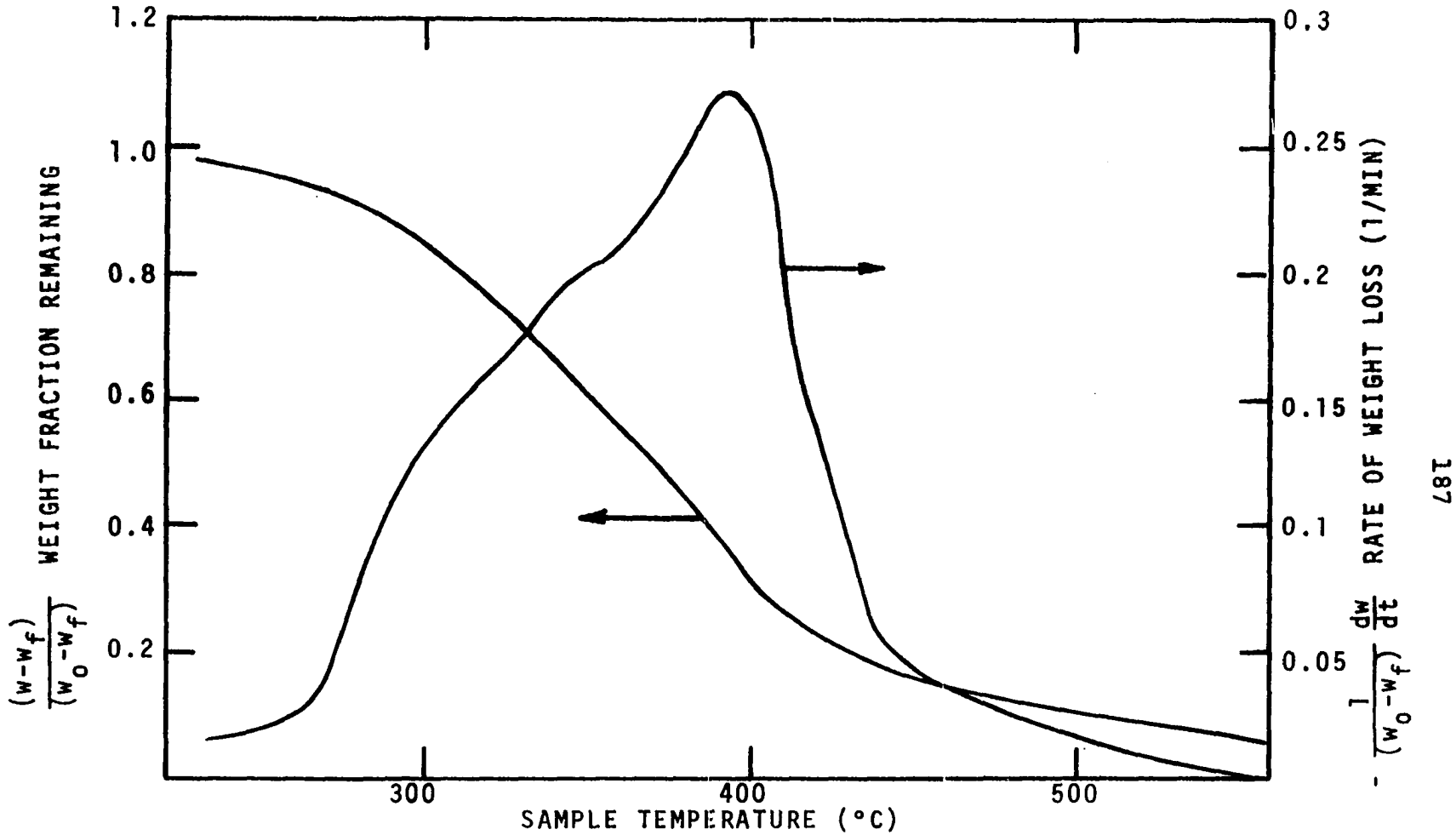

Figure E-8. Weight Loss and Rate of Weight Loss for Dead Ponderosa Pine Needles Extracted with Ether. Heating Rate - 40°C/MIN.

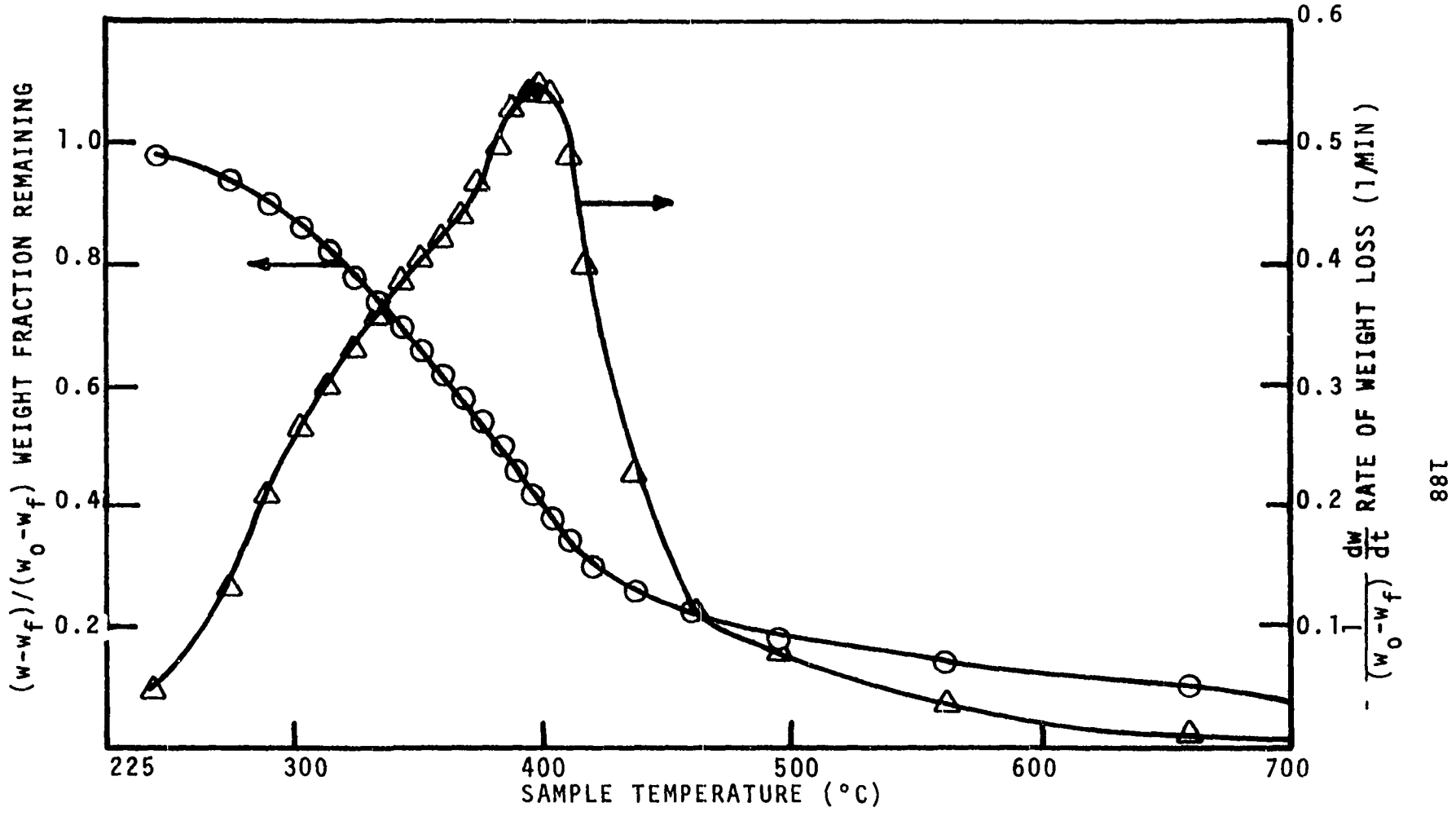

Figure E-9. Weight Loss and Rate of Weight Loss for Dead Ponderosa Pine Needles Extracted with Ether. Heating Rate - 80°C/MIN.

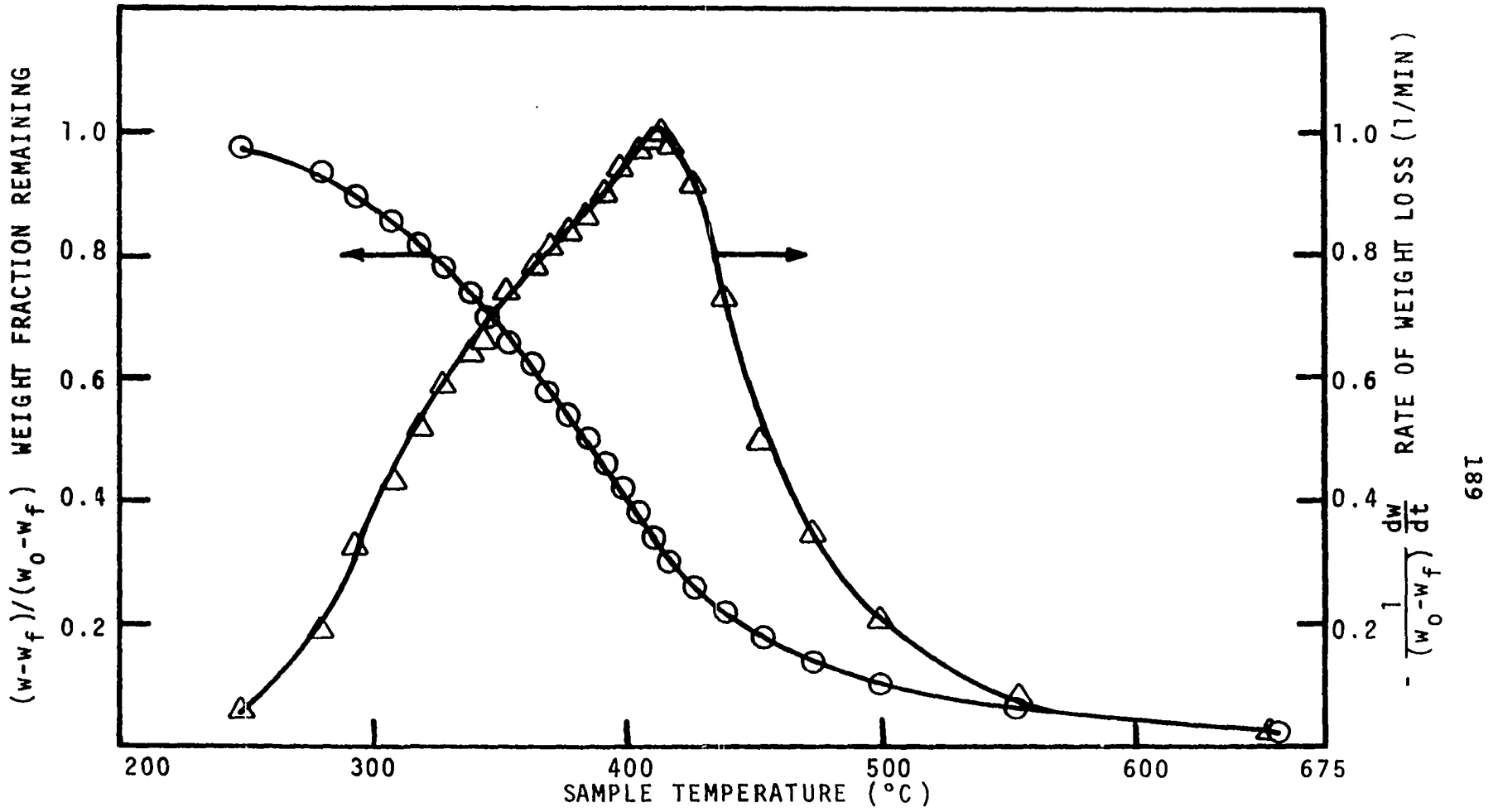

Figure E-10. Weight Loss and Rate of Weight Loss for Dead Ponderosa Pine Needles Extracted with Ether. Heating Rate - 160°C/MIN.

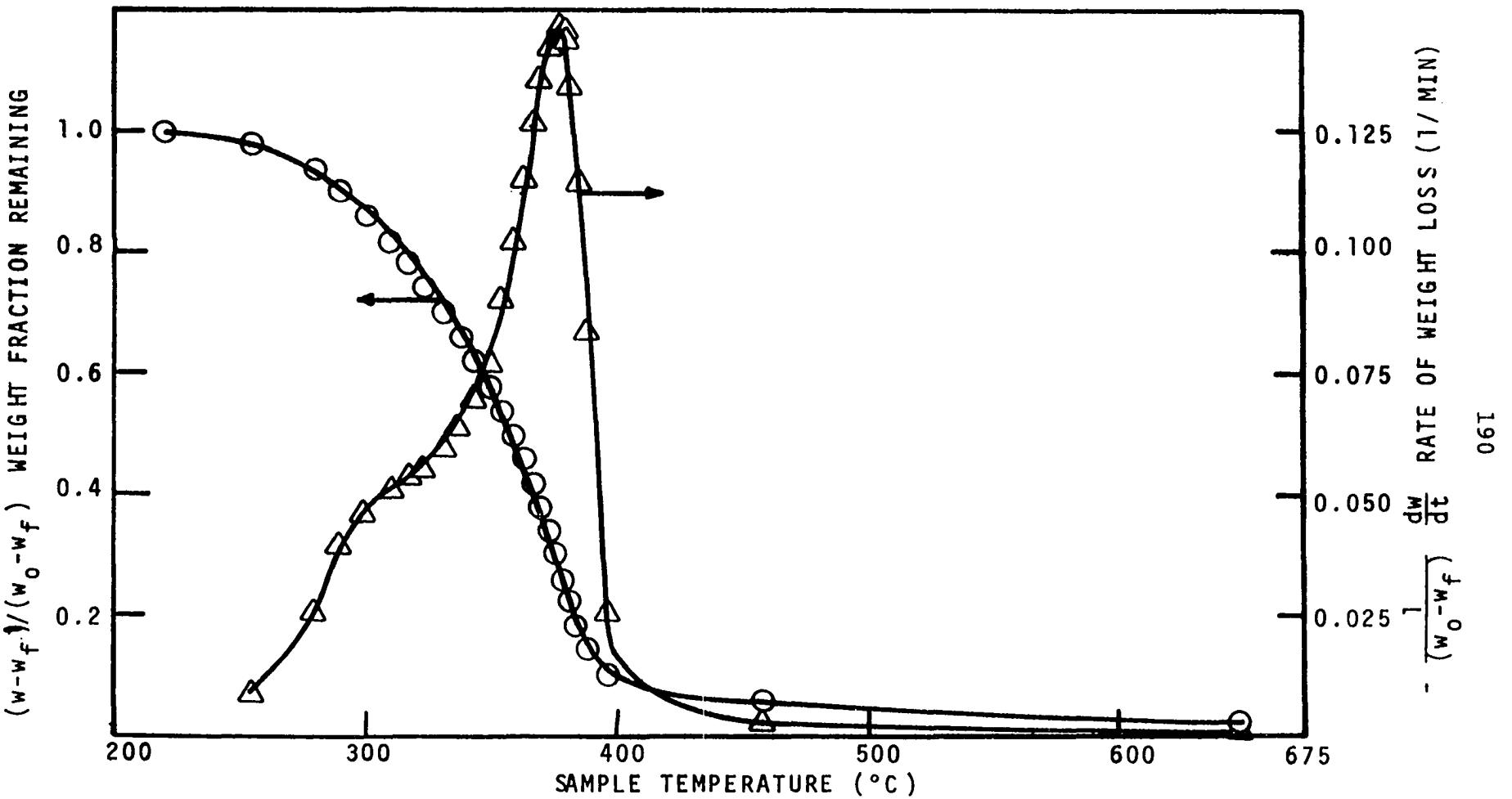

Figure E-11. Weight Loss and Rate of Weight Loss for Excelsior. Heating Rate - 10°C/MIN.

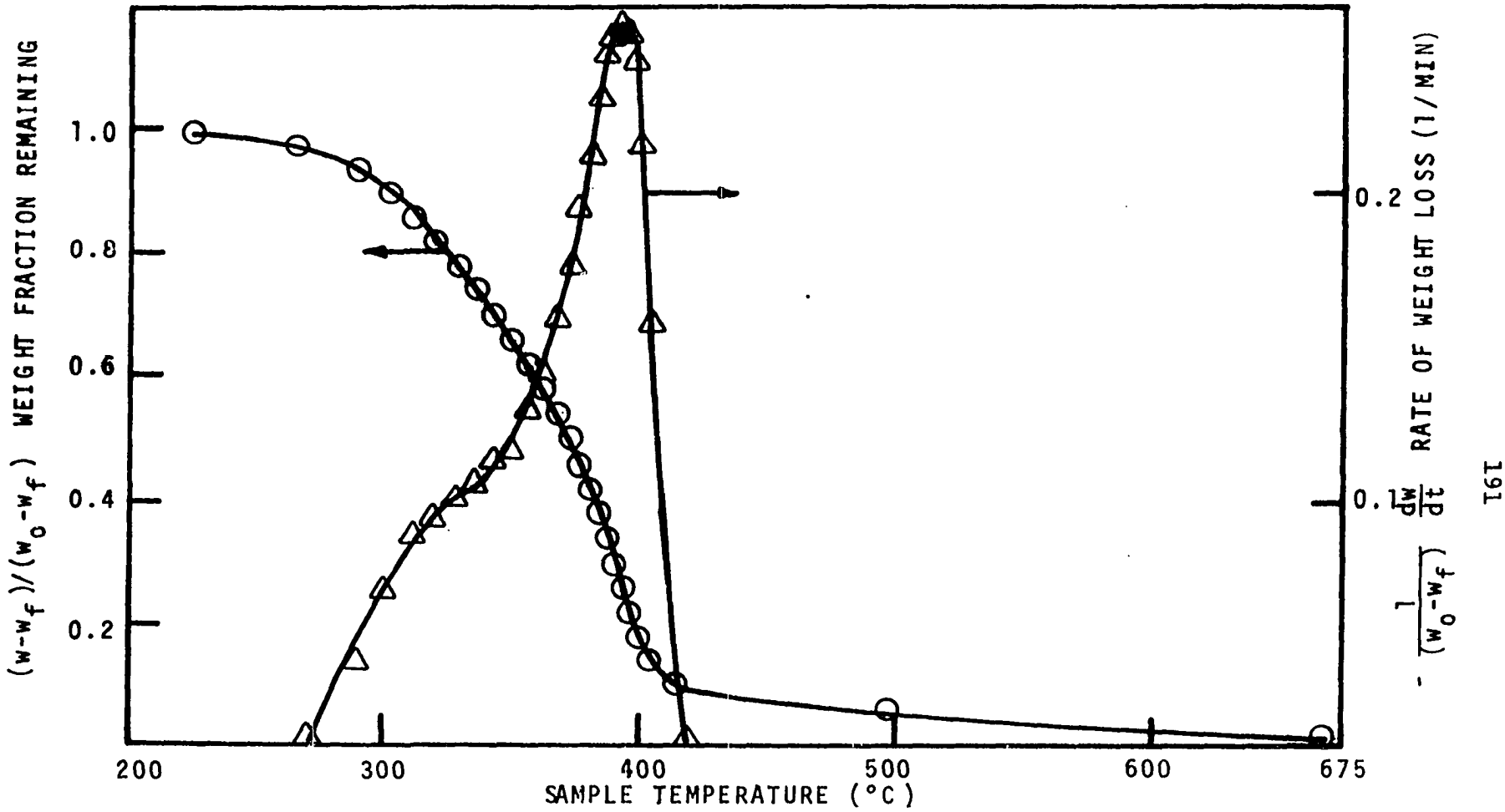

Figure E-12. Weight Loss and Rate of Weight Loss for Excelsior. Heating Rate - 20°C/MIN.

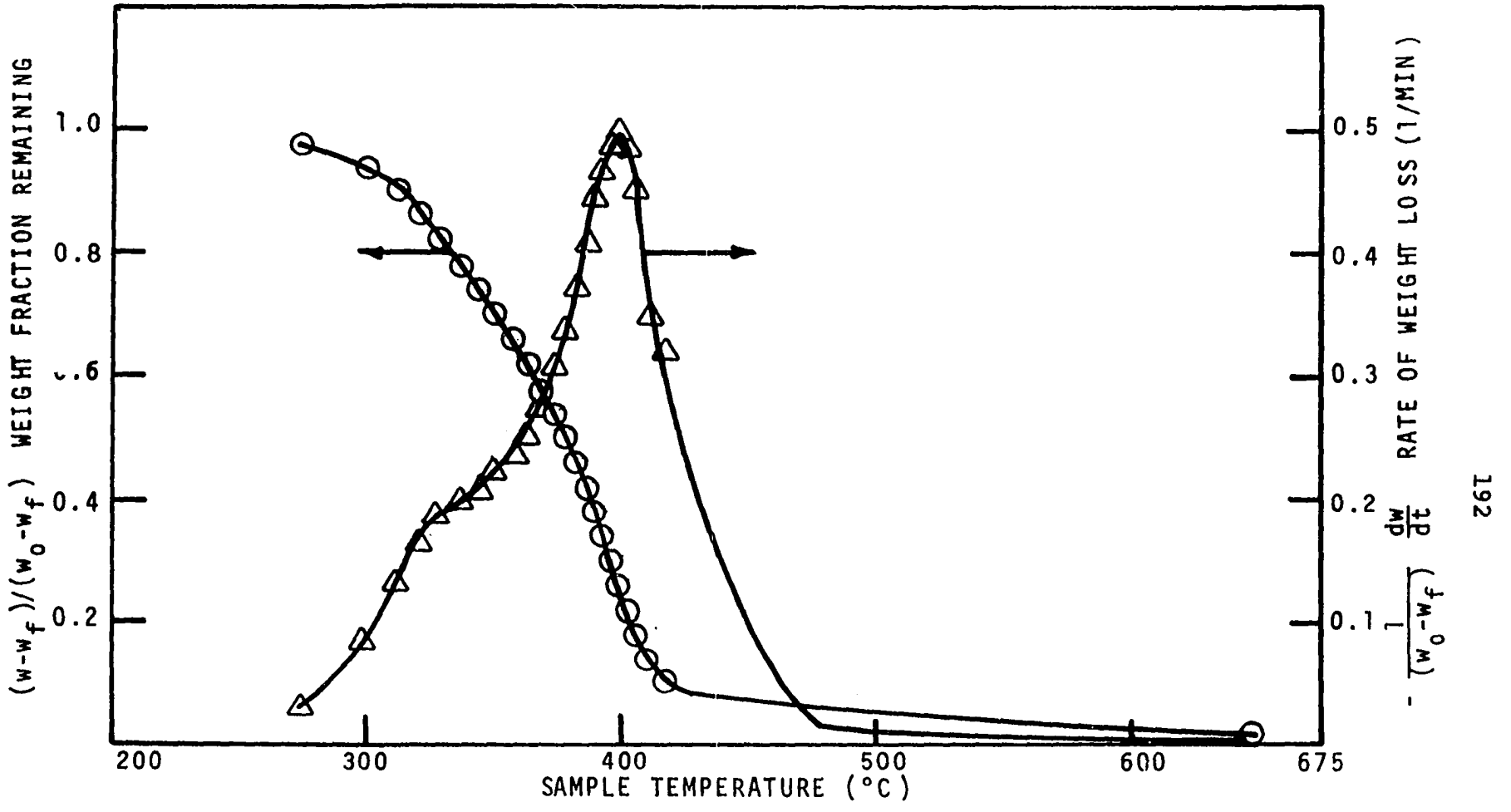

Figure E-13. Weight Loss and Rate of Weight Loss for Excelsior. Heating Rate - 40°C/MIN.

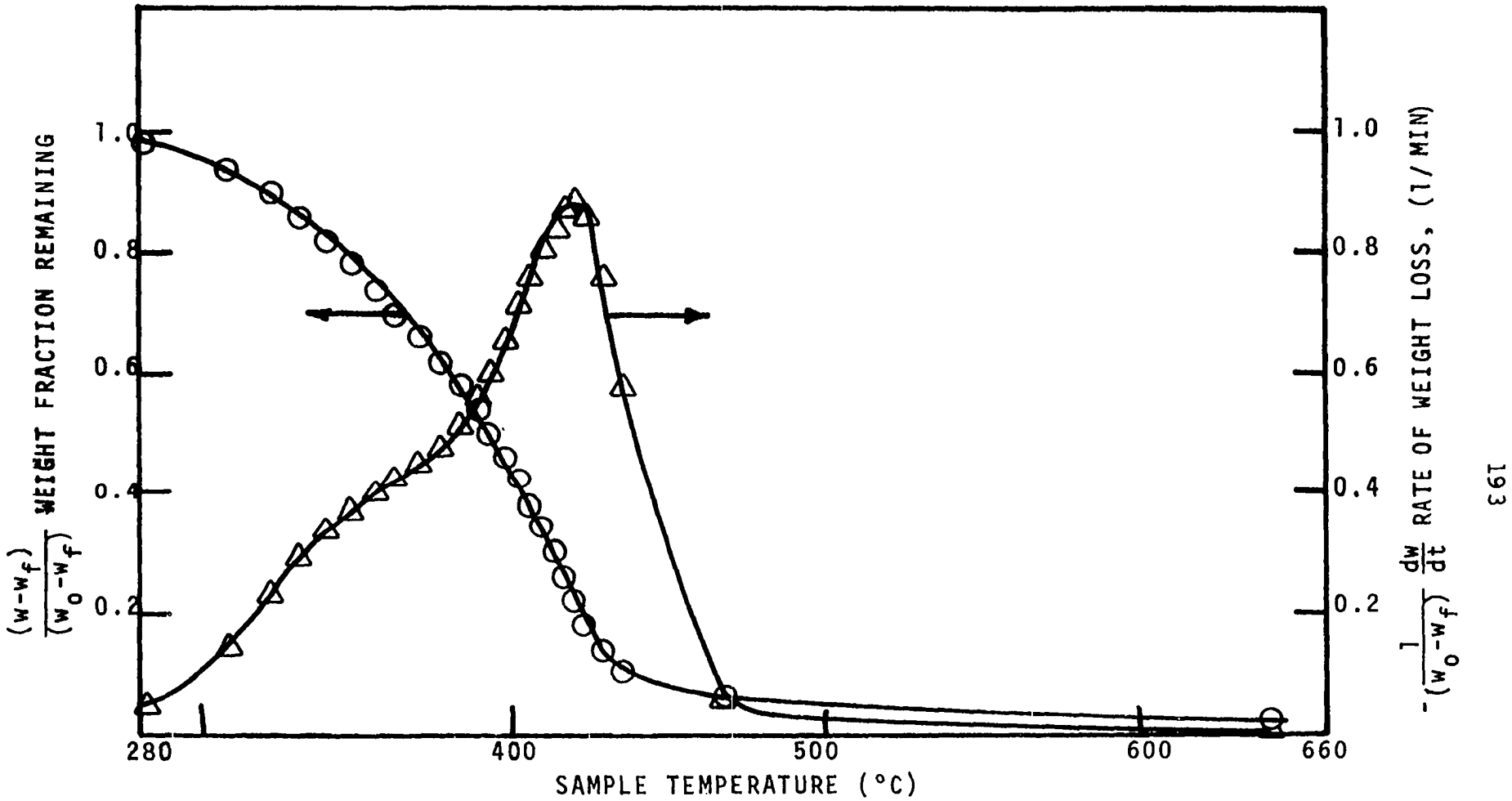

Figure E-14. Weight Loss and Rate of Weight Loss for Excelsior. Heating Rate - 80°C/MIN.

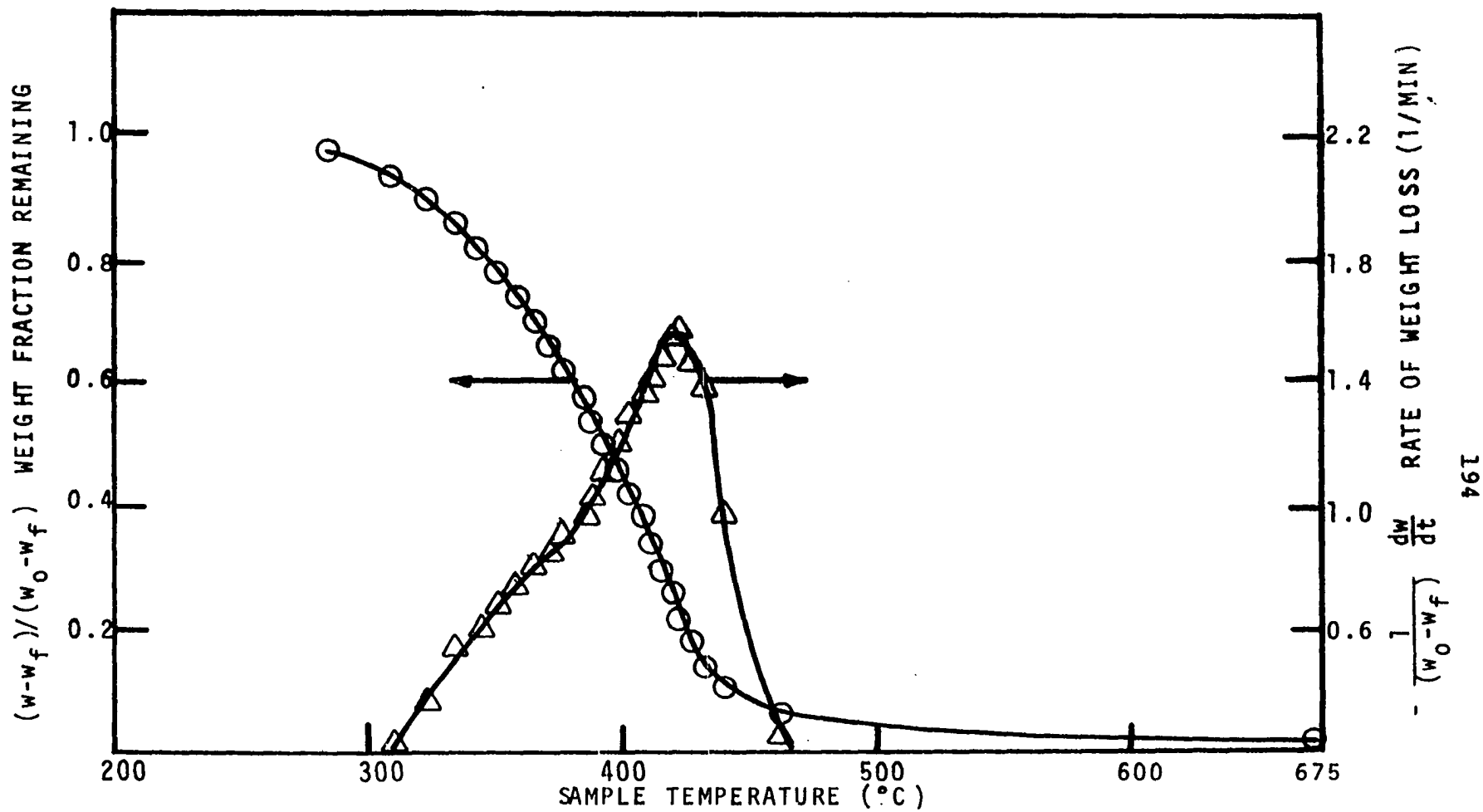

Figure E-15. Weight Loss and Rate of Weight Loss for Excelsior. Heating Rate - 160°C/MIN.

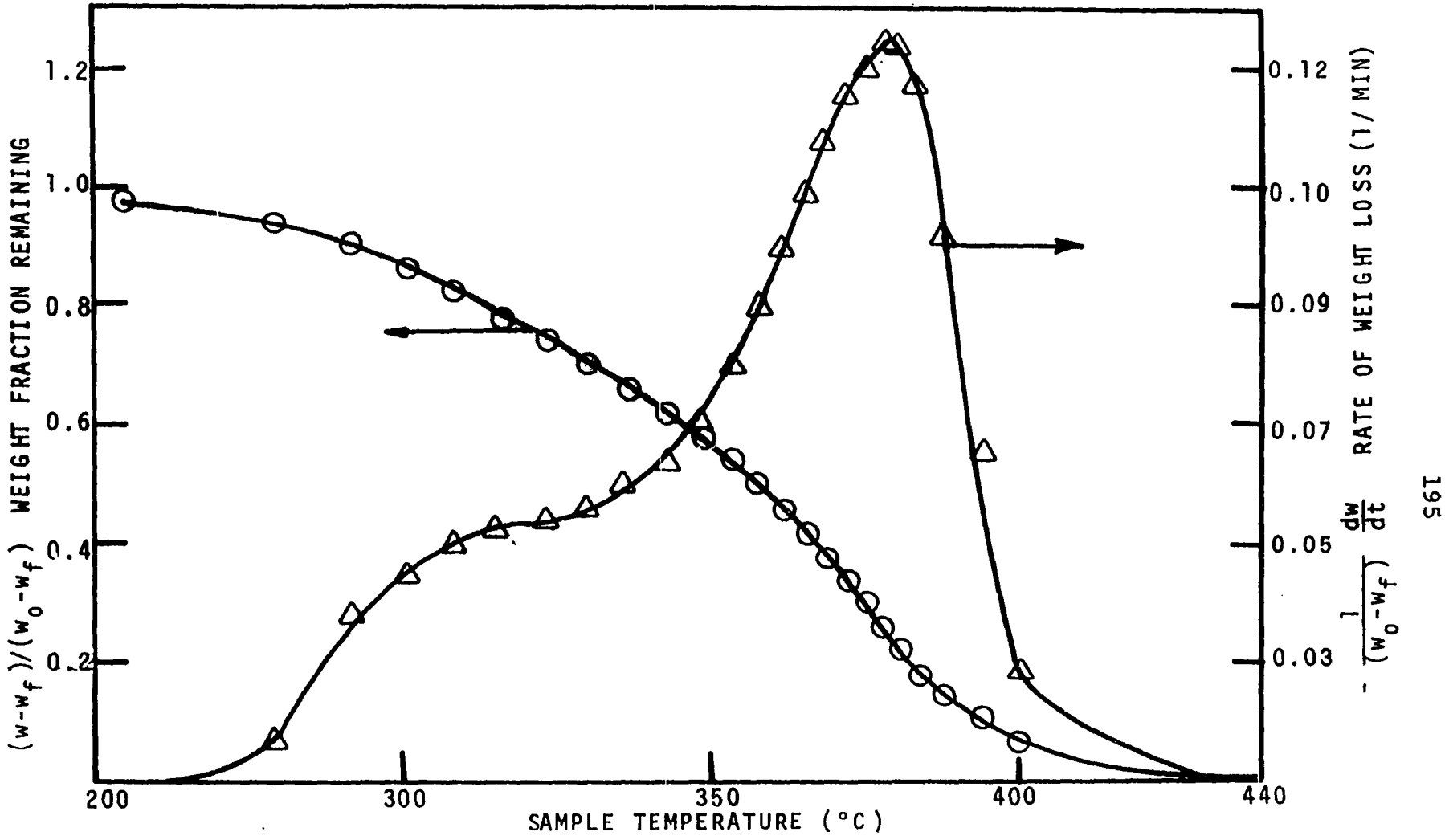

Figure E-16. Weight Loss and Rate of Weight Loss for Excelsior Extracted with Ether. Heating Rate - 10°C/MIN.

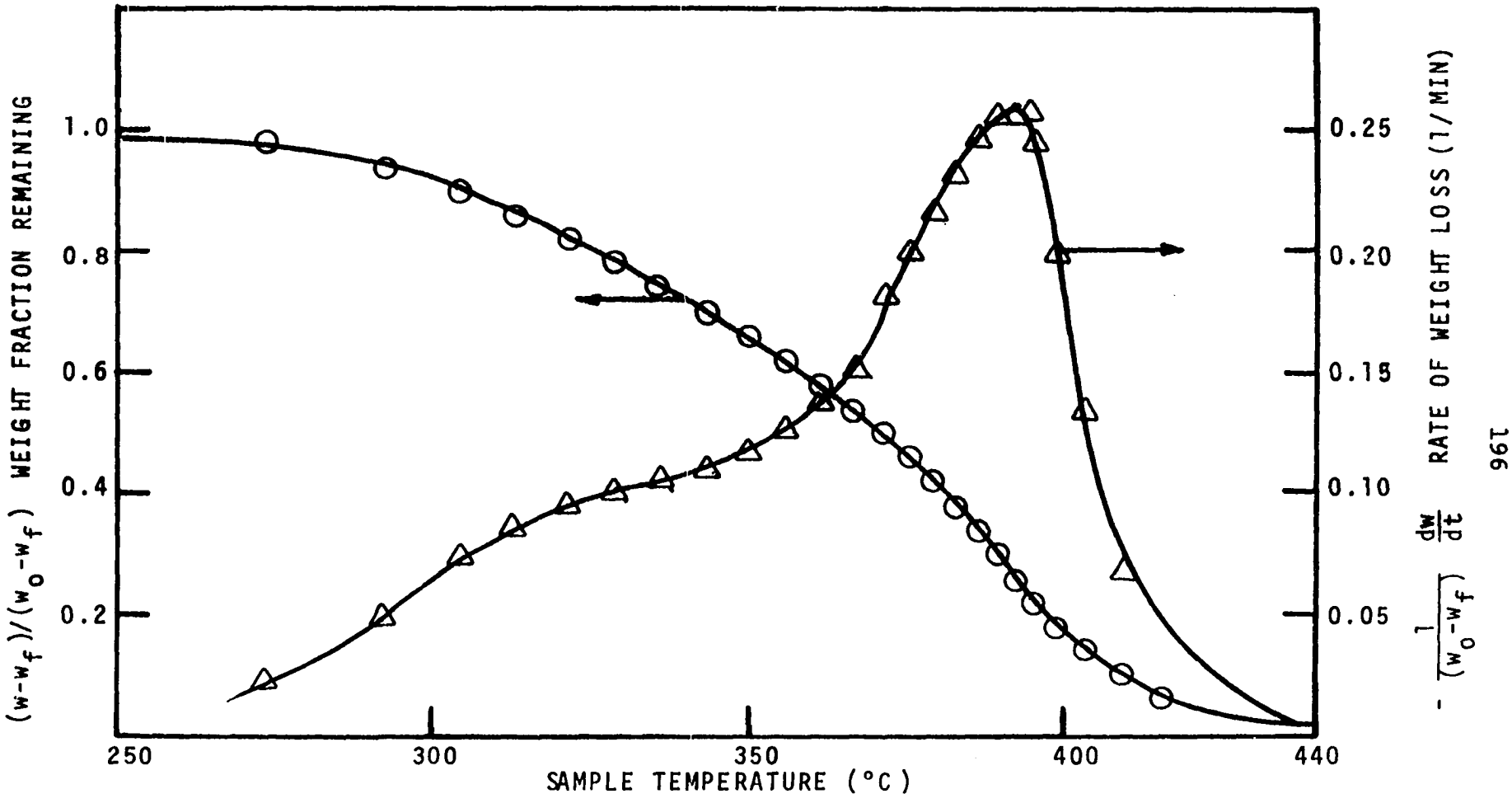

Figure E-17. Weight Loss and Rate of Weight Loss for Excelsior Extracted with Ether. Heating Rate - 20°C/MIN.

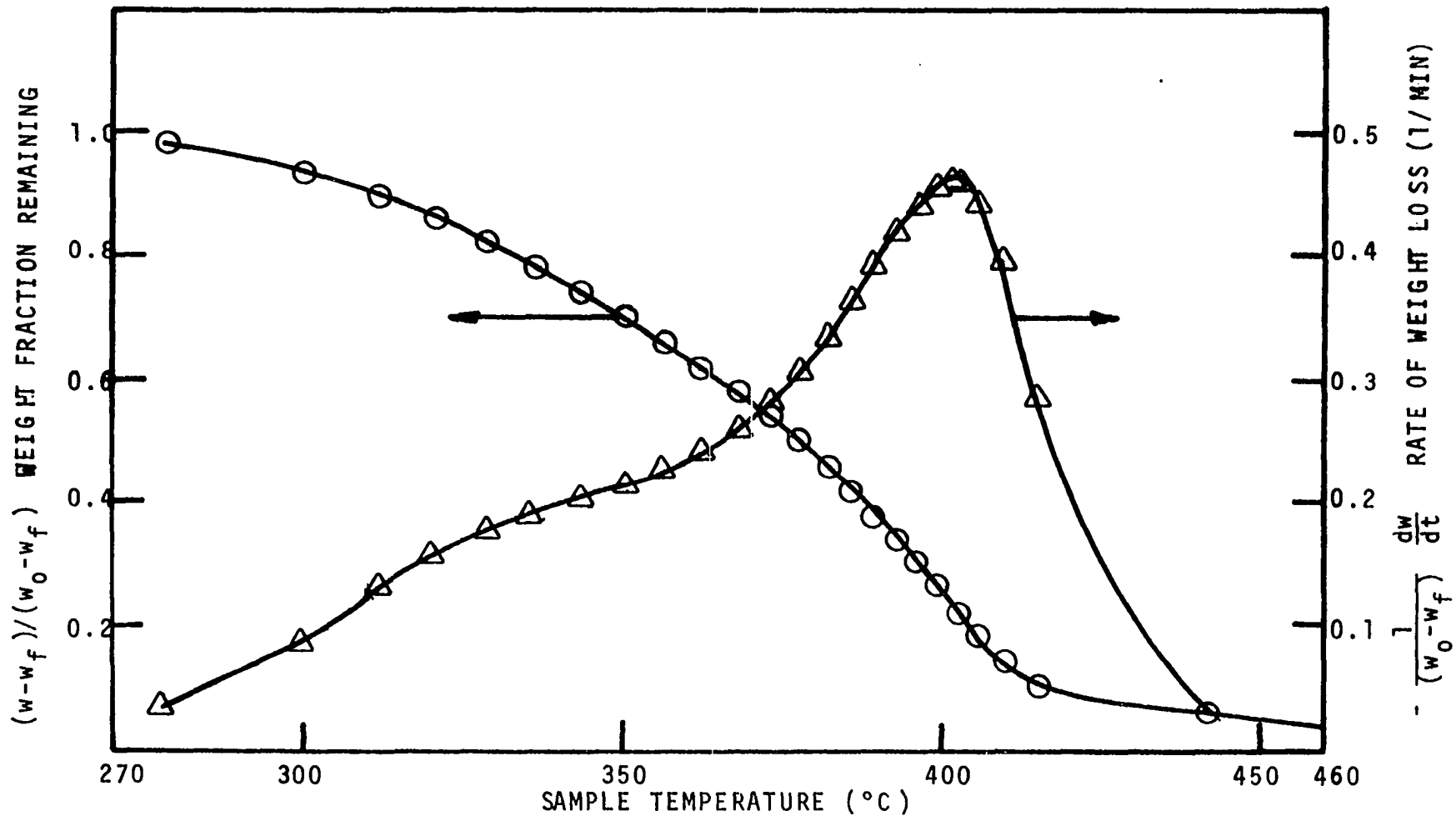

Figure E-18. Weight Loss and Rate of Weight Loss for Excelsior Extracted with Ether. Heating Rate - 40°C/MIN.

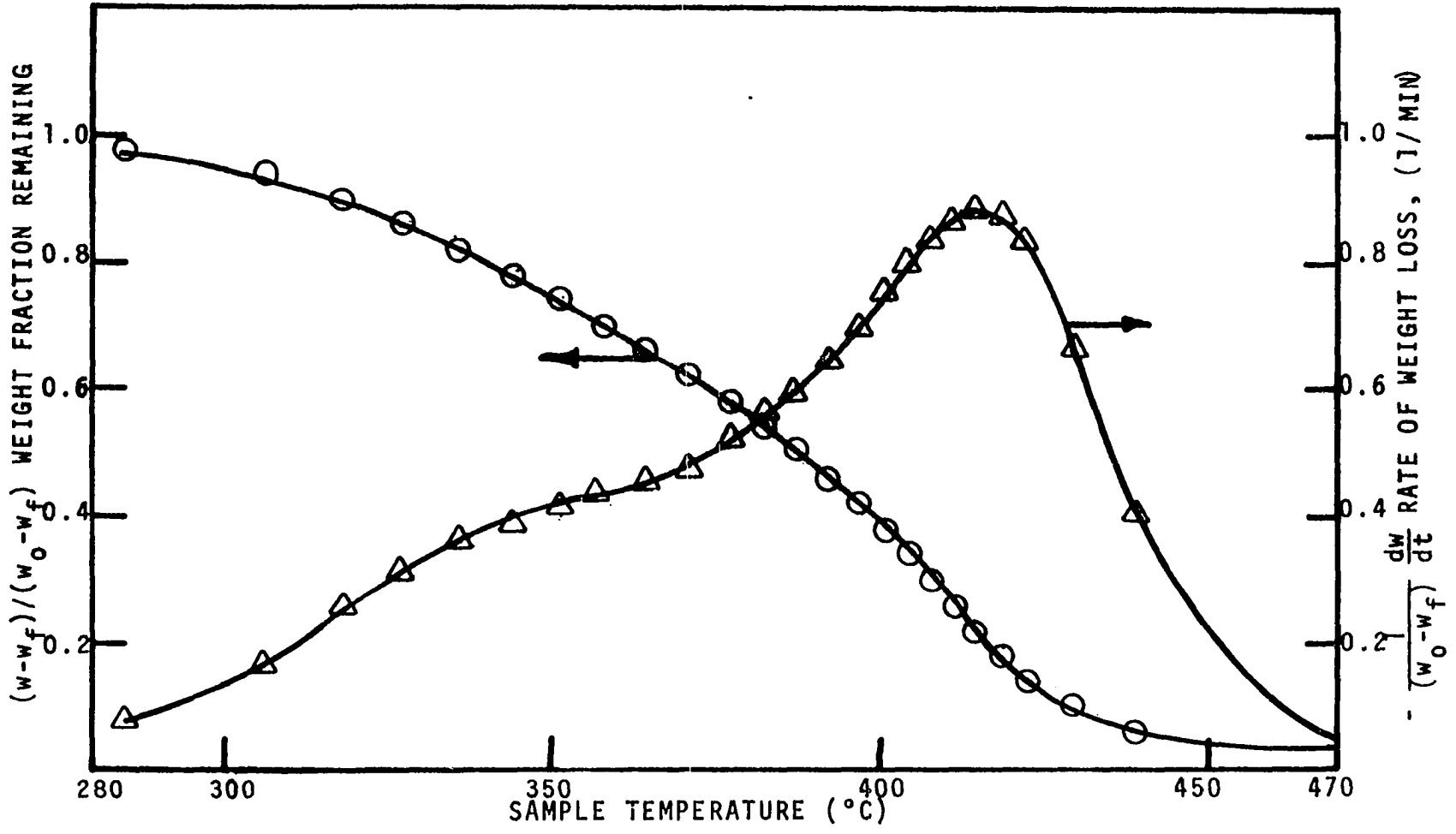

Figure E-19. Weight Loss and Rate of Weight Loss for Excelsior Extracted with Ether. Heating Rate - 80°C/MIN.

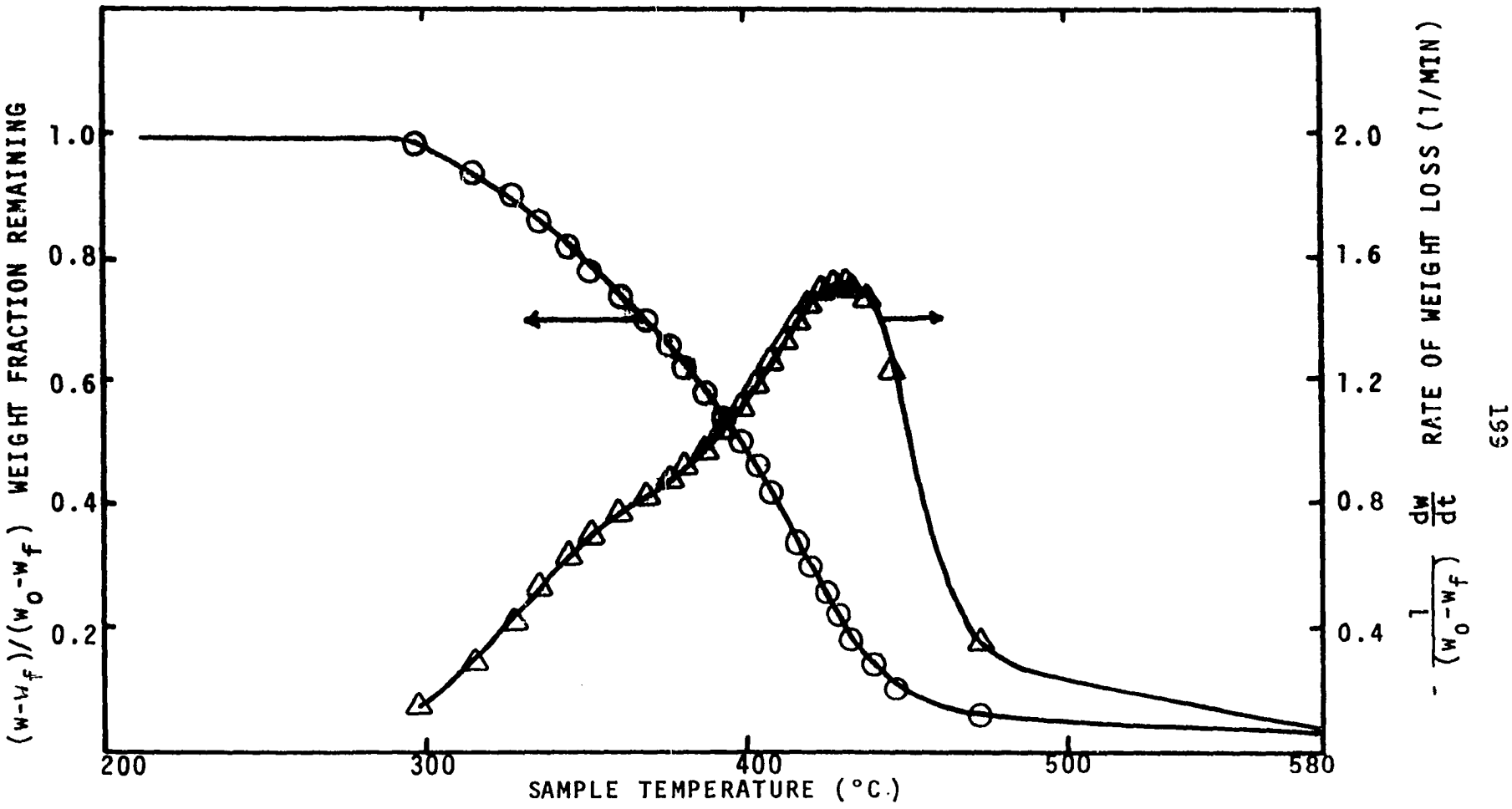

Figure E-20. Weight Loss and Rate of Weight Loss for Excelsior Extracted with Ether. Heating Rate - 160°C/MIN.

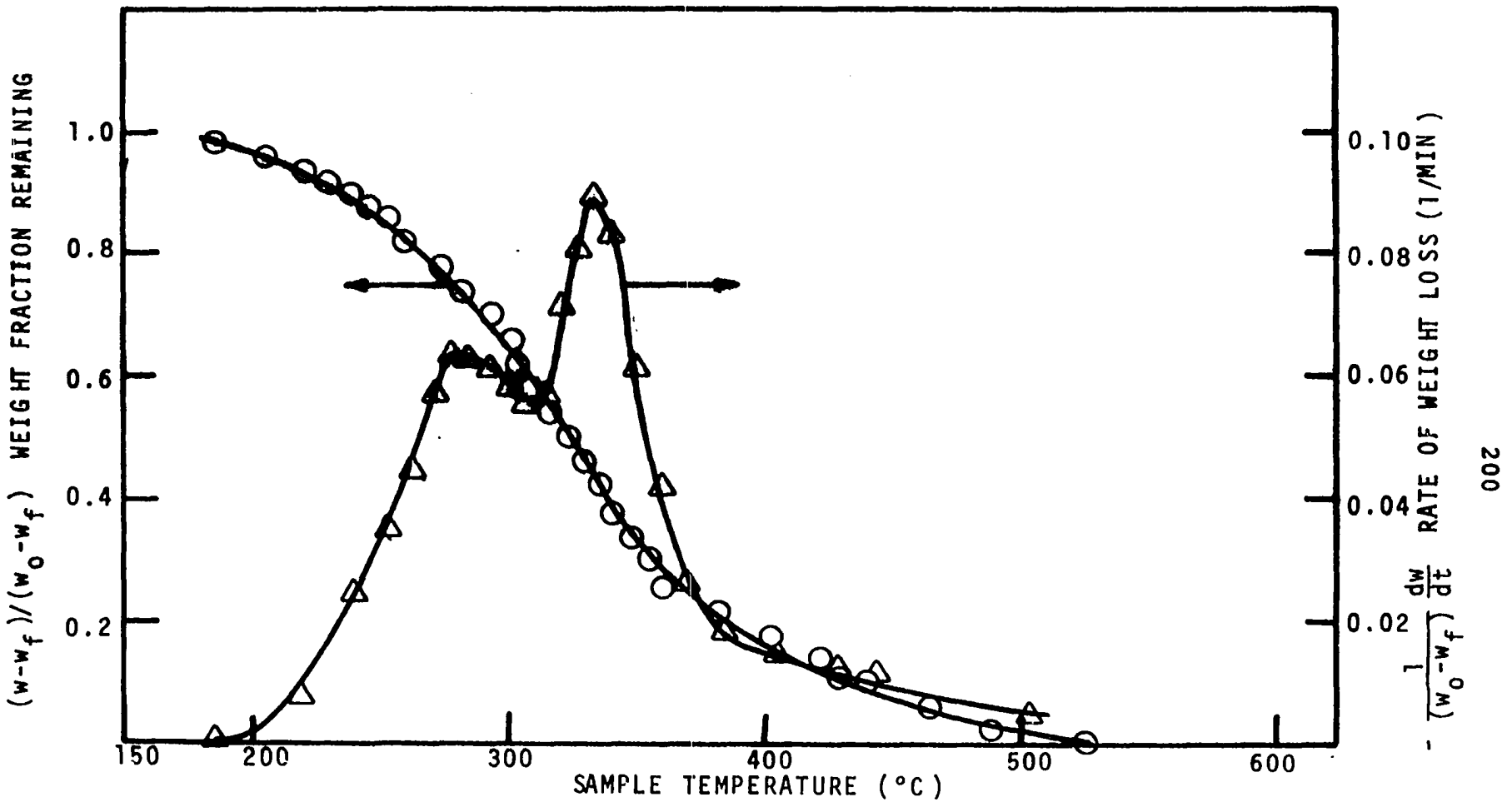

Figure E-21. Weight Loss and Rate of Weight Loss for Saltbush Leaves Heating Rate - 10°C/MIN.

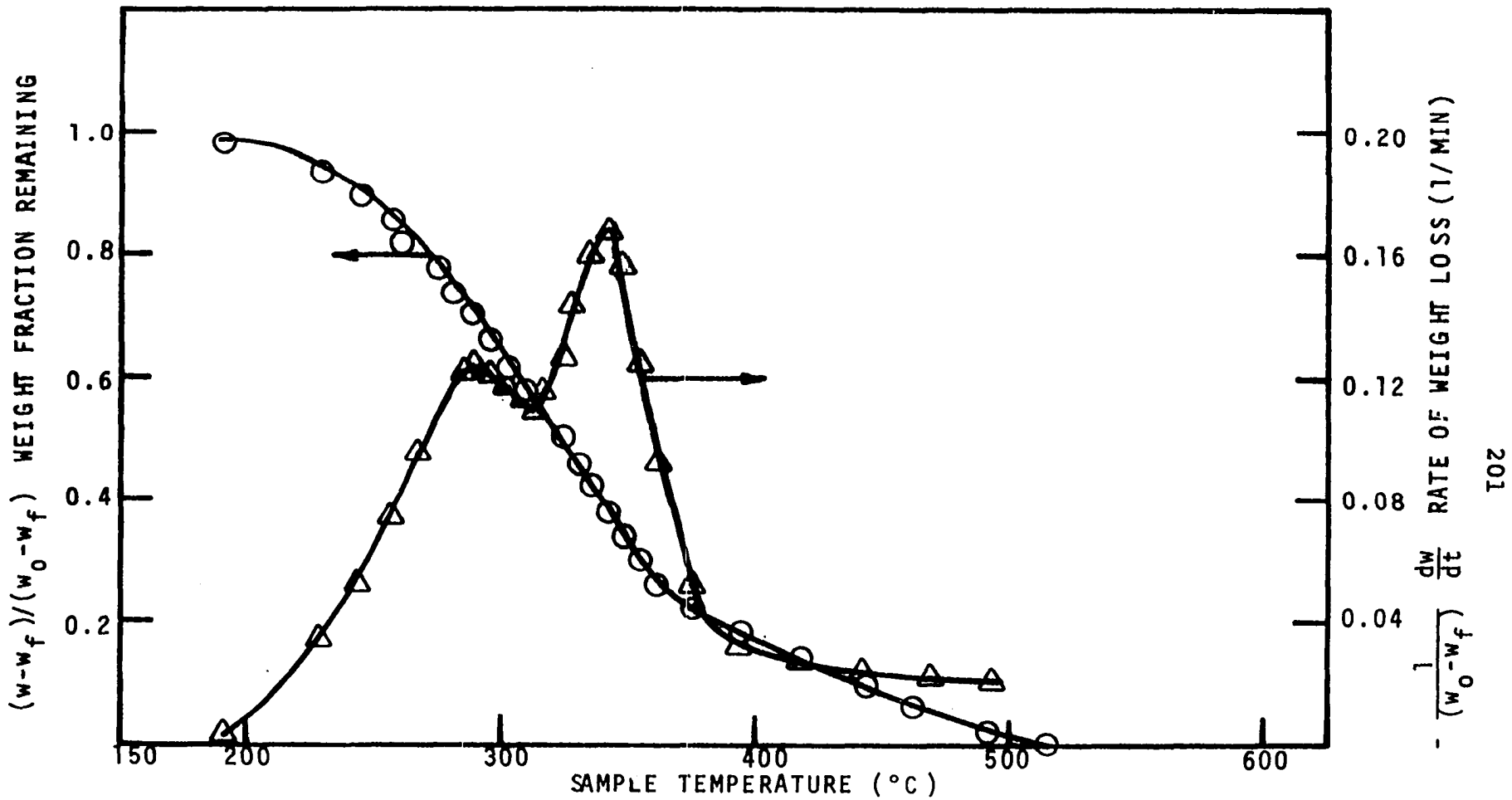

Figure E-22. Weight Loss and Rate of Weight Loss for Saltbush Leaves at the Heating Rate of 20°C/MIN.

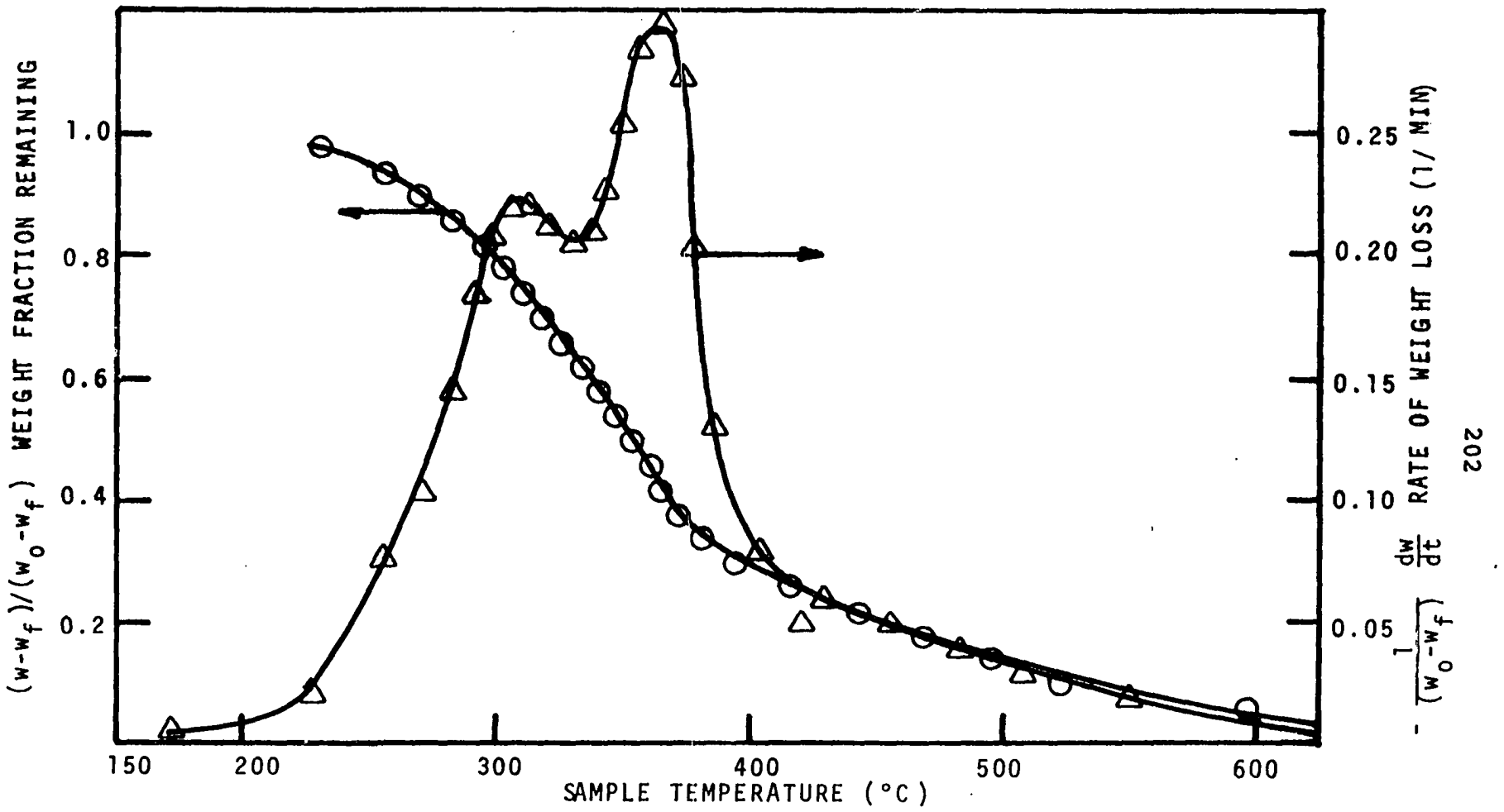

Figure E-23. Weight Loss and Rate of Weight Loss for Saltbush Leaves Heating Rate - 40°C/MIN.

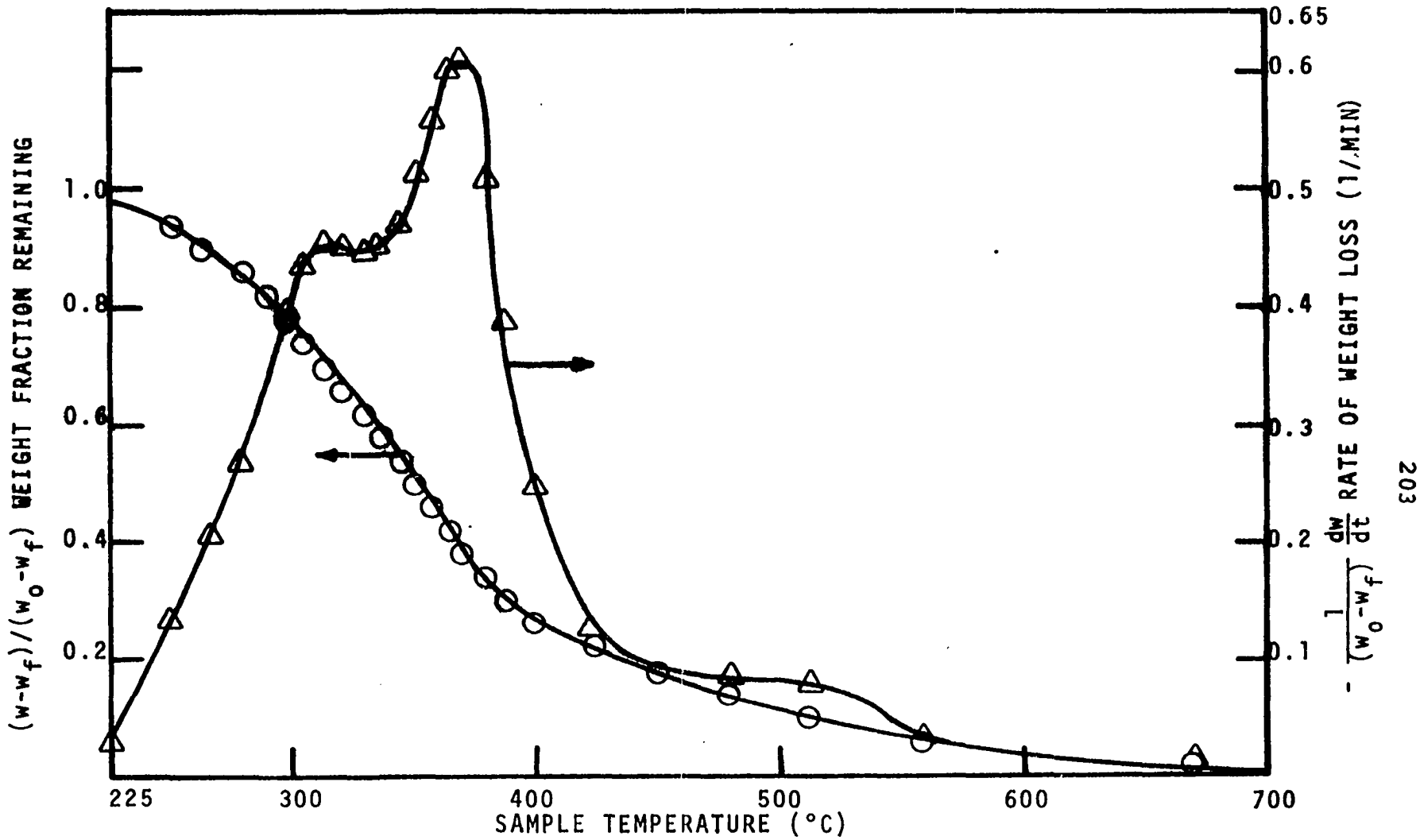

Figure E-24. Weight Loss and Rate of Weight Loss for Saltbush Leaves Heating Rate -- 80°C/MIN.

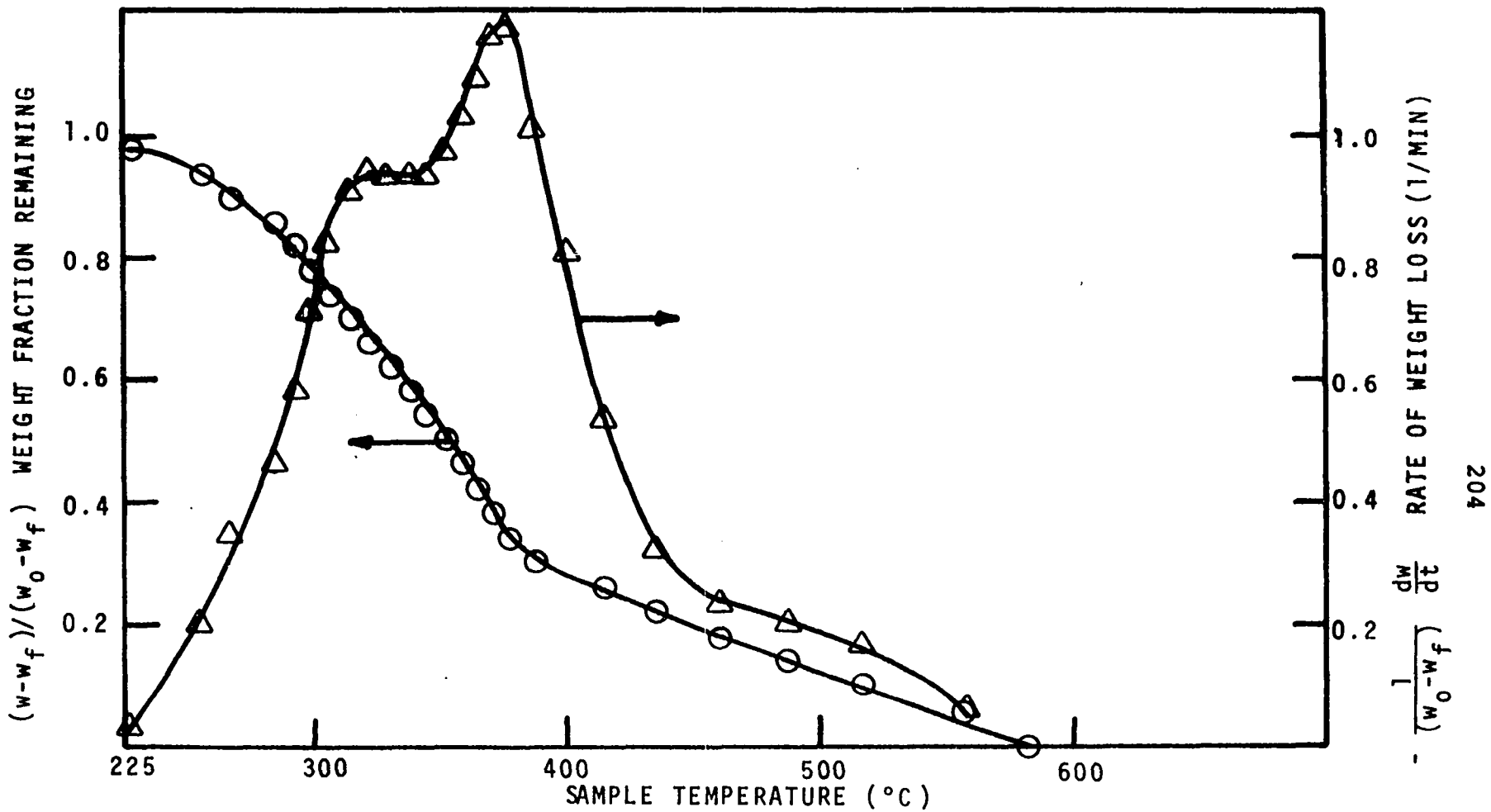

Figure E-25. Weight Loss and Rate of Weight Loss for Saltbush Leaves Heating Rate - 160°C/MIN.

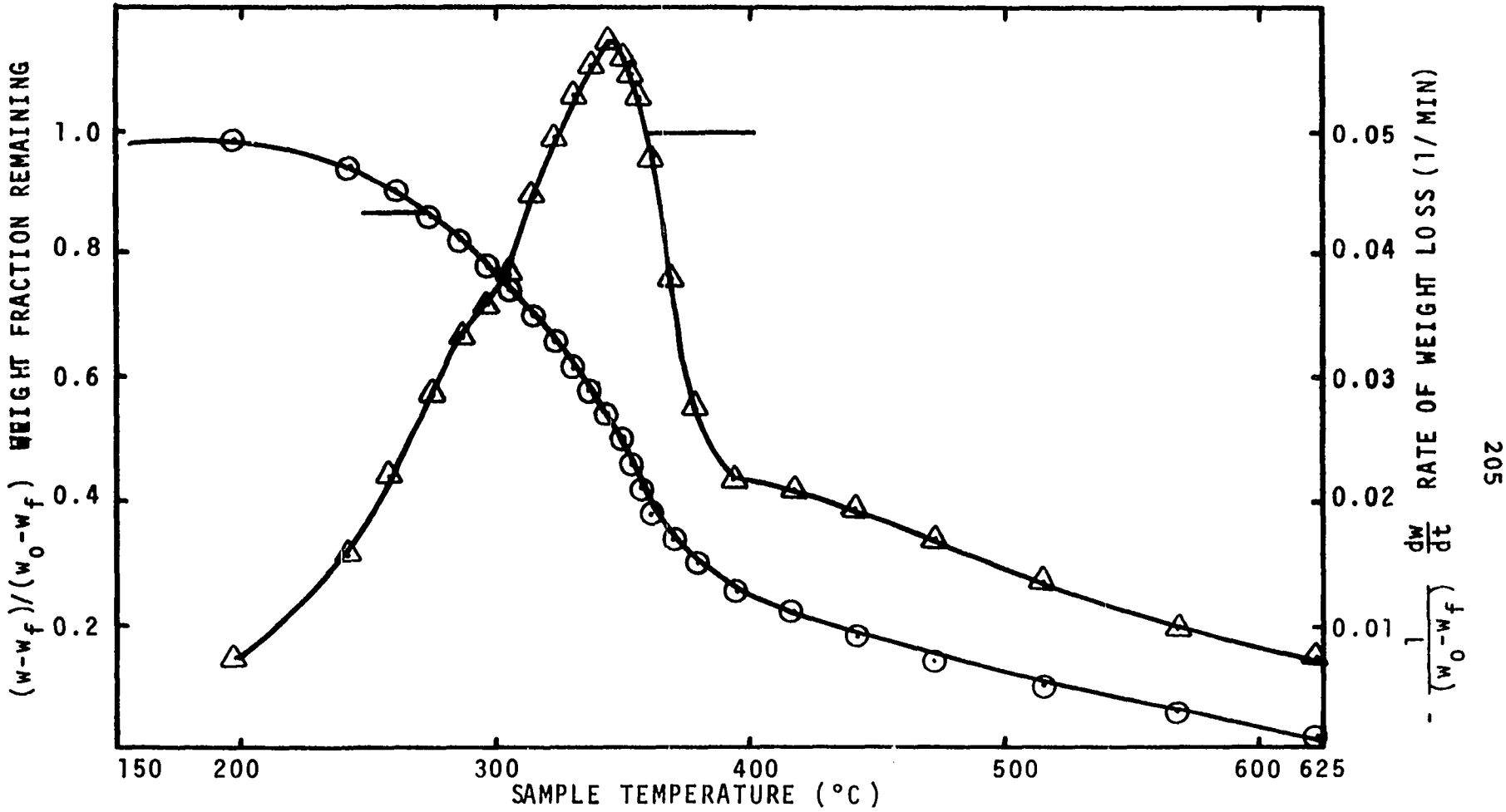

Figure E-26. Weight Loss and Rate of Weight Loss for Punky Wood from Douglas-Fir Snags. Heating Rate - 10°C/MIN.

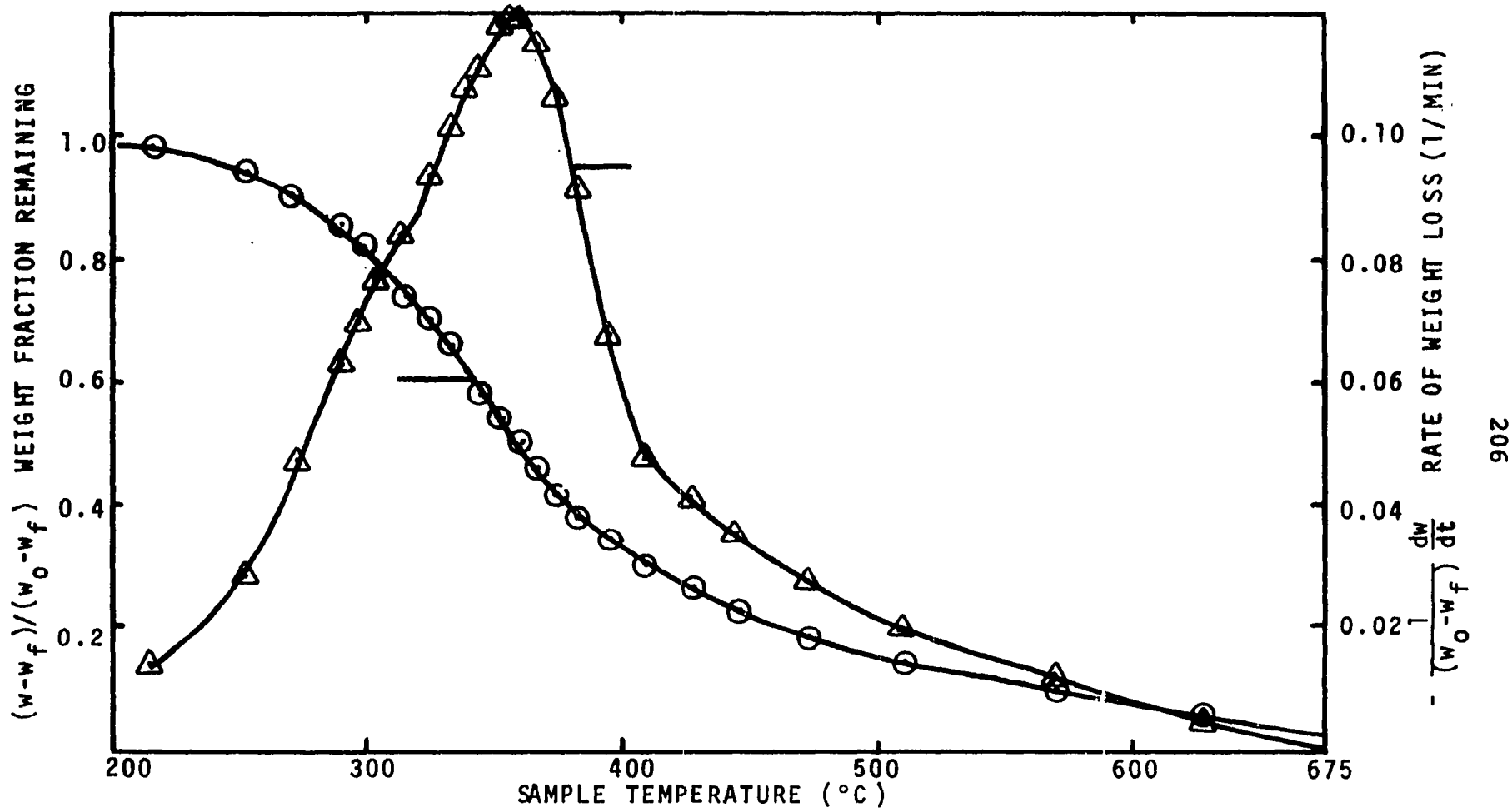

Figure E-27. Weight Loss and Rate of Weight Loss for Punky Wood from Douglas-Fir Snags. Heating Rate - 20°C/MIN.

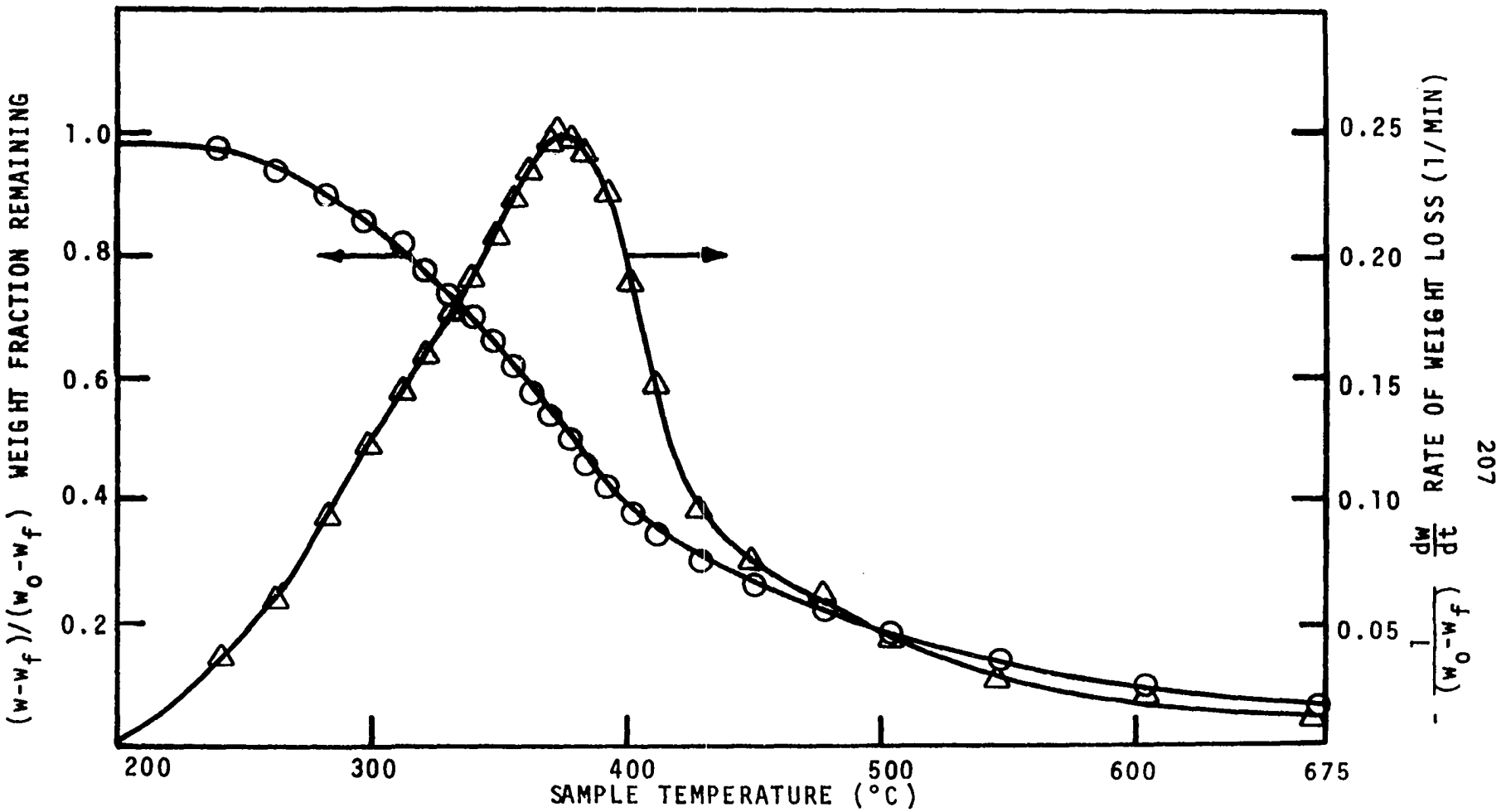

Figure E-28. Weight Loss and Rate of Weight Loss for Punky Wood from Douglas-Fir Snags. Heating Rate - 40°C/MIN.

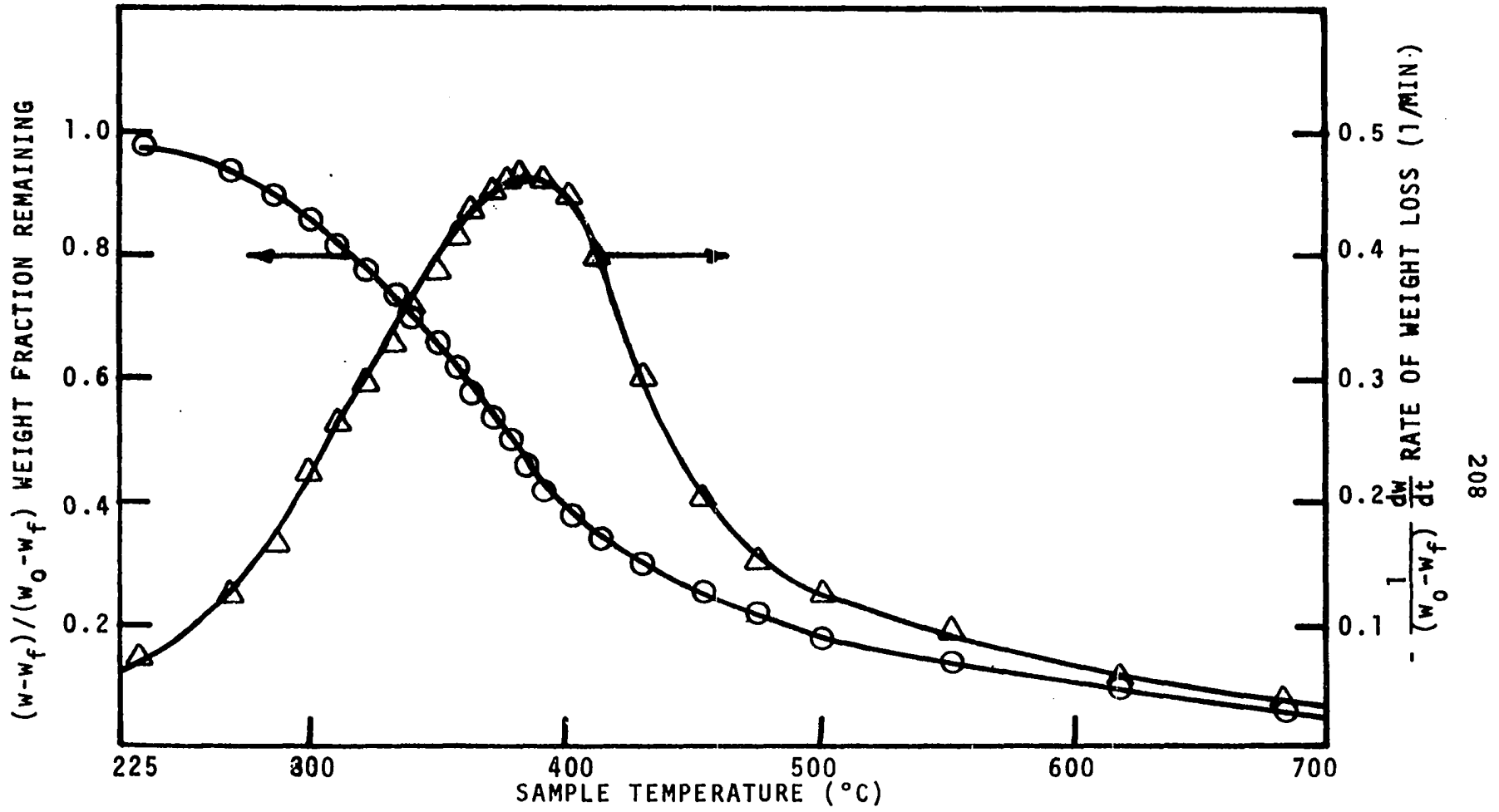

Figure E-29. Weight Loss and Rate of Weight Loss for Punky Wood from Douglas-Fir Snags. Heating Rate = 80°C/MIN.

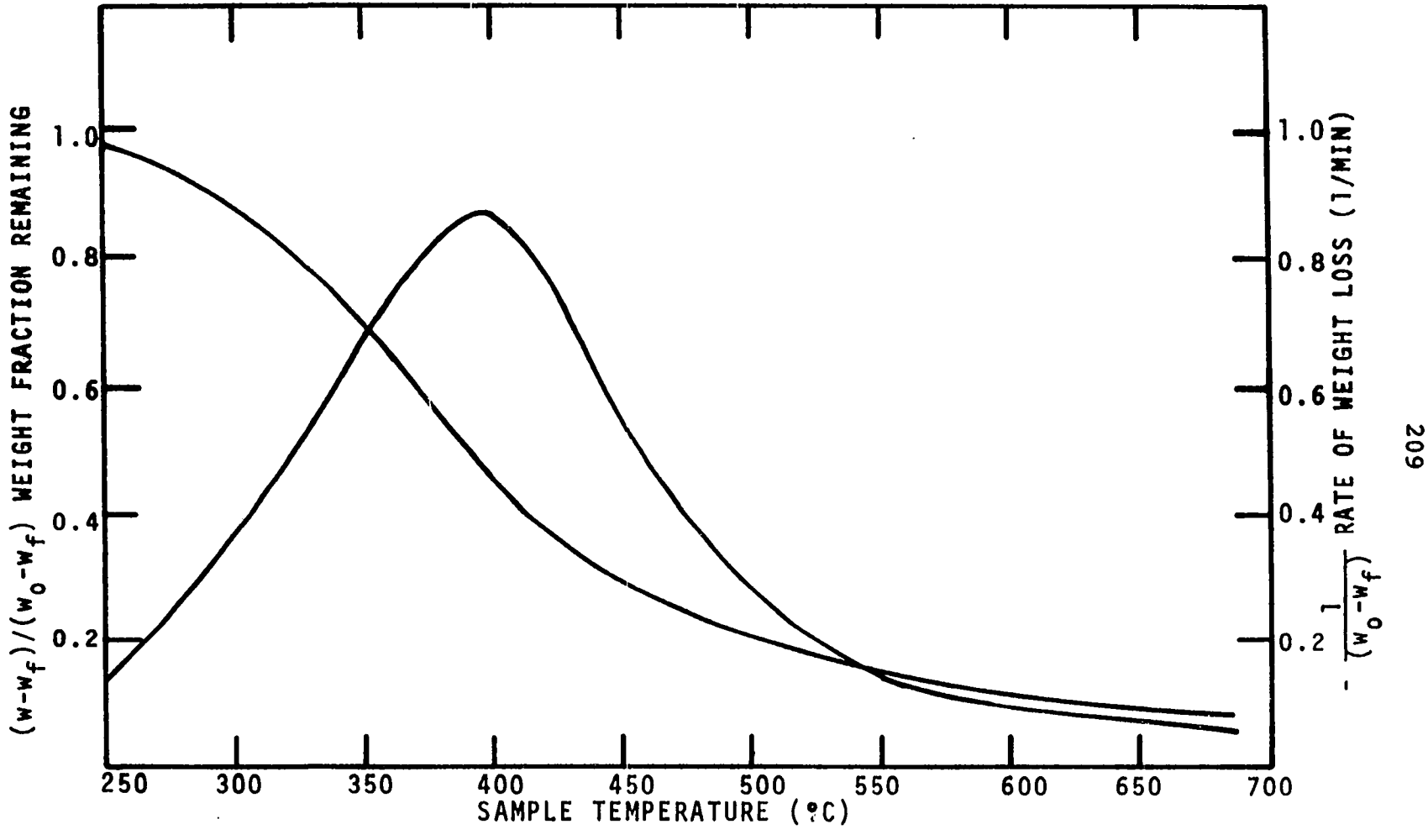

Figure E-30. Weight Loss and Rate of Weight Loss for Punky Wood from Douglas Fir Snags. Heating Rate - 160°C/MIN.

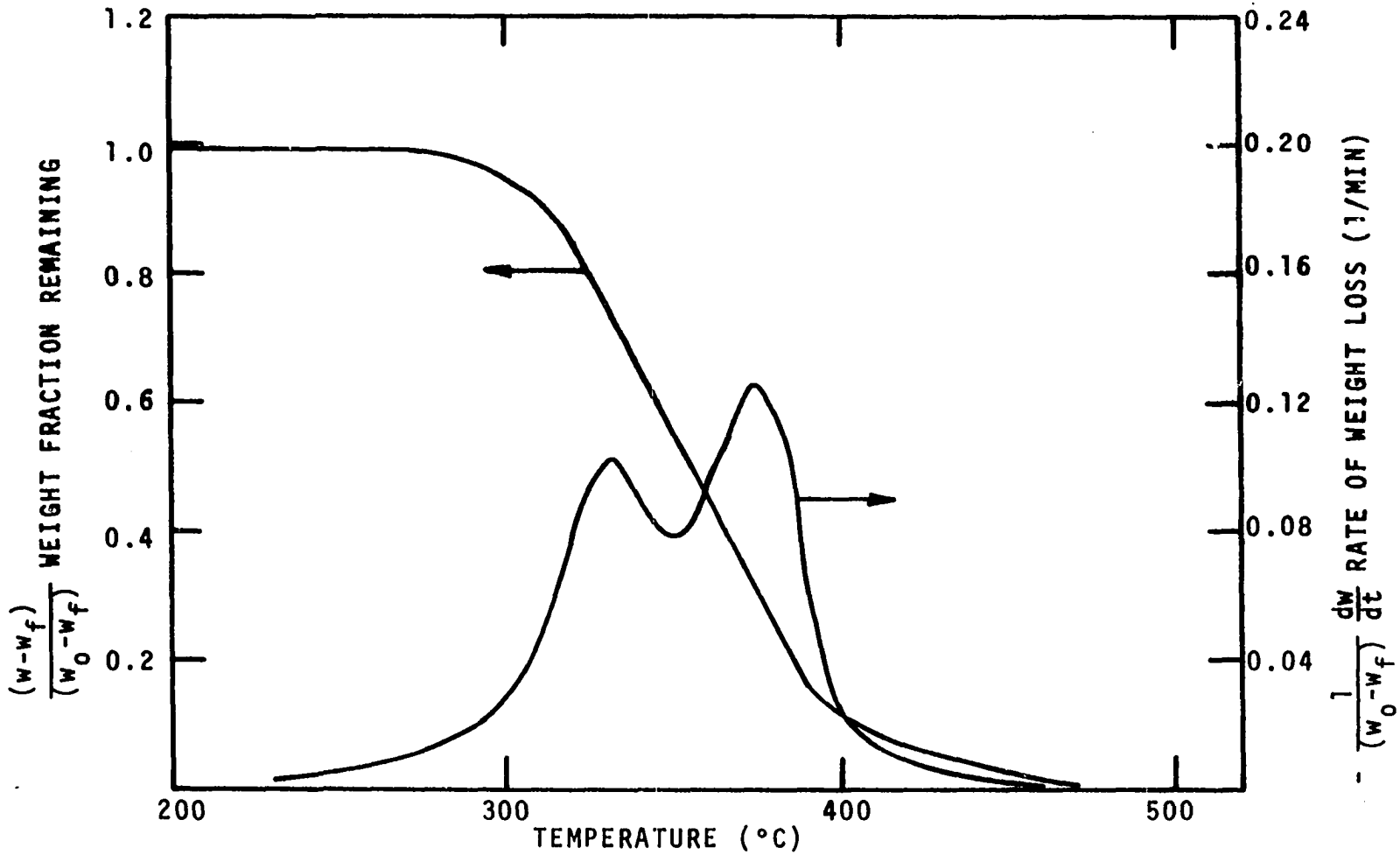

Figure E-31. Weight Loss and Rate of Weight Loss for Larch. Heating Rate - 10°C/MIN.

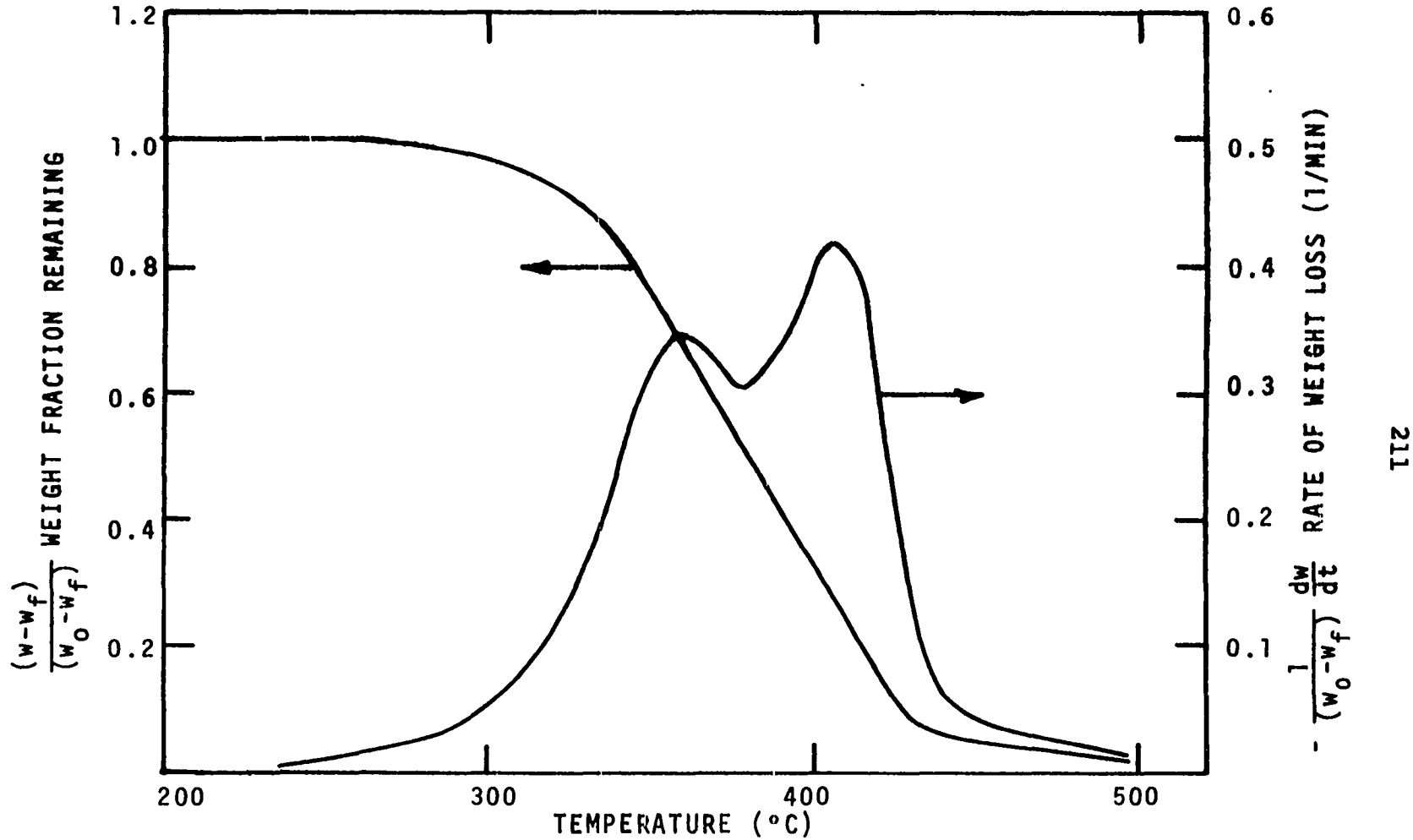

Figure E-32. Weight Loss and Rate of Weight Loss for Larch. Heating Rate - 40°C/MIN.

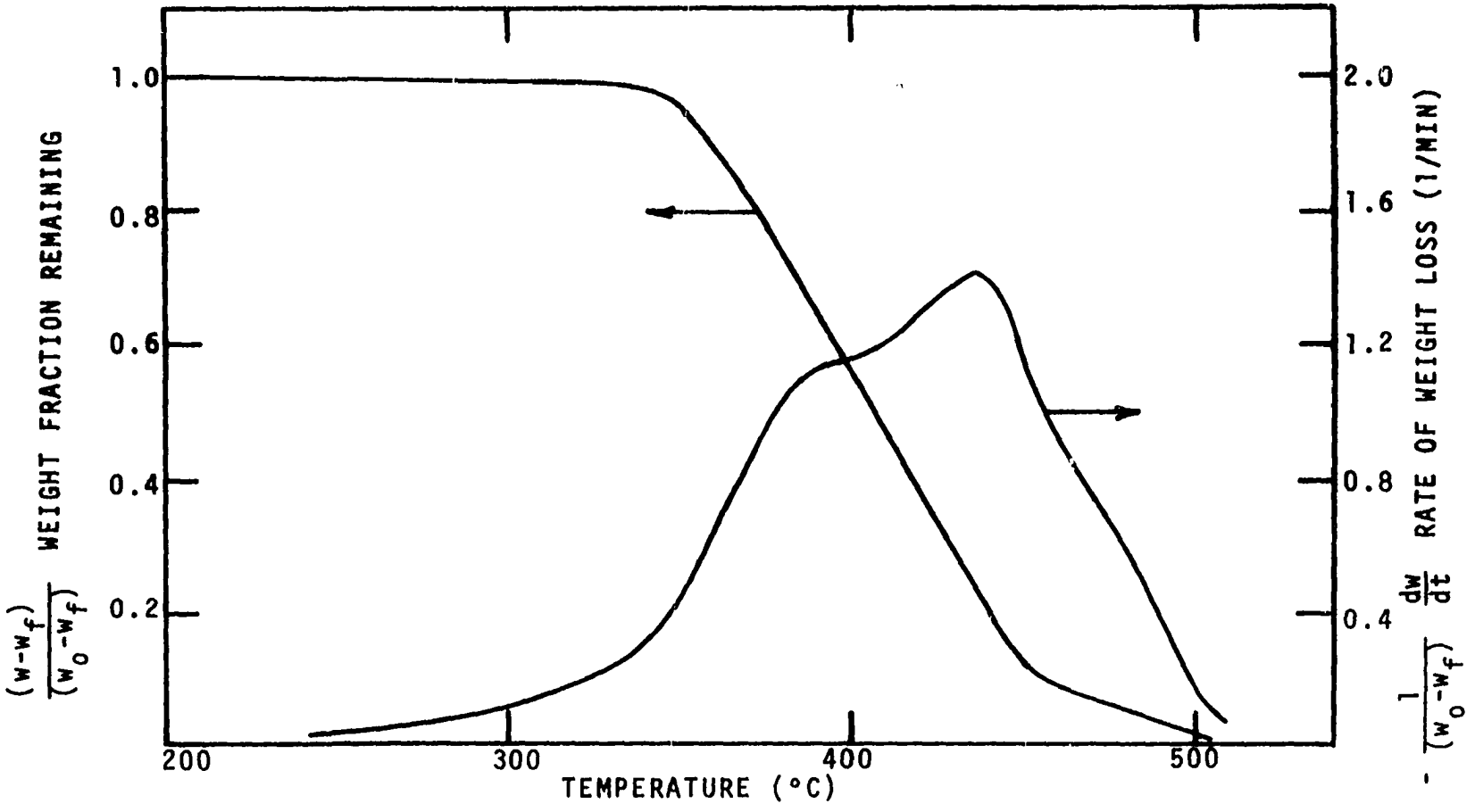

Figure E-33. Weight Loss and Rate of Weight Loss for Larch. Heating Rate - 160°C/MIN.

APPENDIX F

DIFFERENTIAL ENERGY CURVES FOR DRY SAMPLES

Differential energy curves for dry samples of dead Ponderosa pine needles (extracted and unextracted), excelsior (extracted and unextracted), fourwing saltbush leaves, and punky wood at the heating rates of 40° and 160°C/MIN.

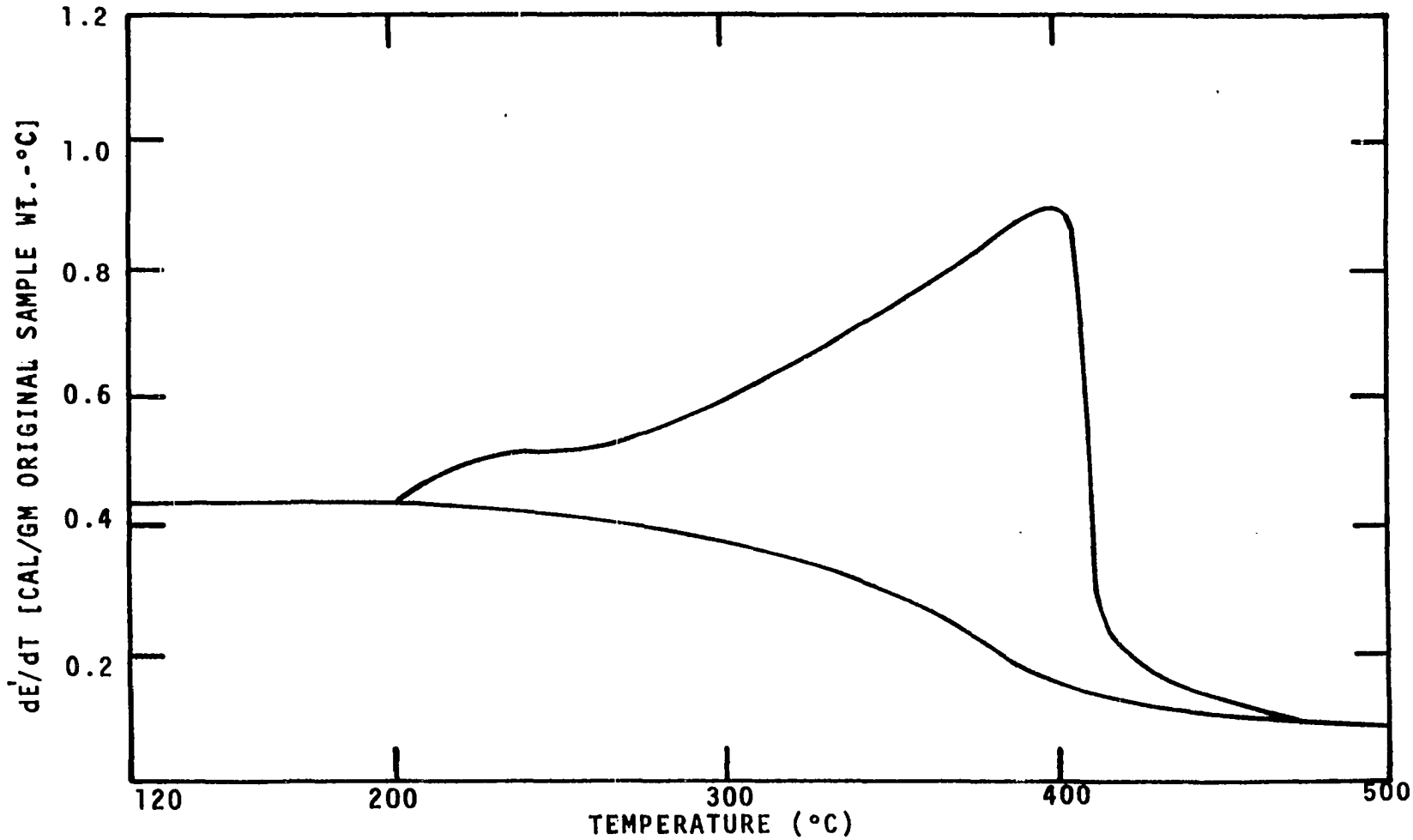

Figure F-1. Differential Energy Curve for Dead Ponderosa Pine Needles Heating Rate - 40°C/MIN.

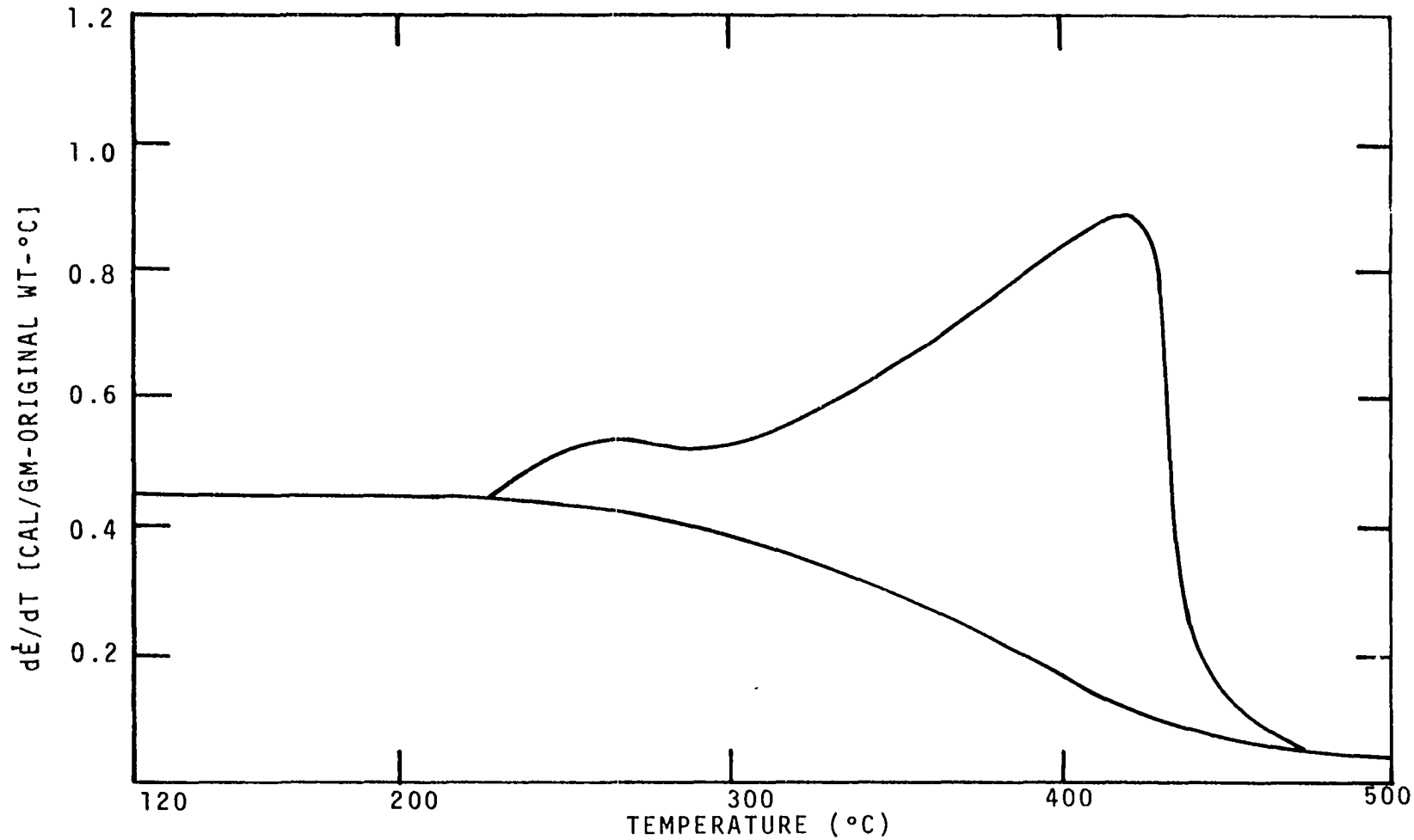

Figure F-2. **Differential Energy** Curve for Dead Ponderosa Pine Needles. Heating Rate - 160°C/MIN.

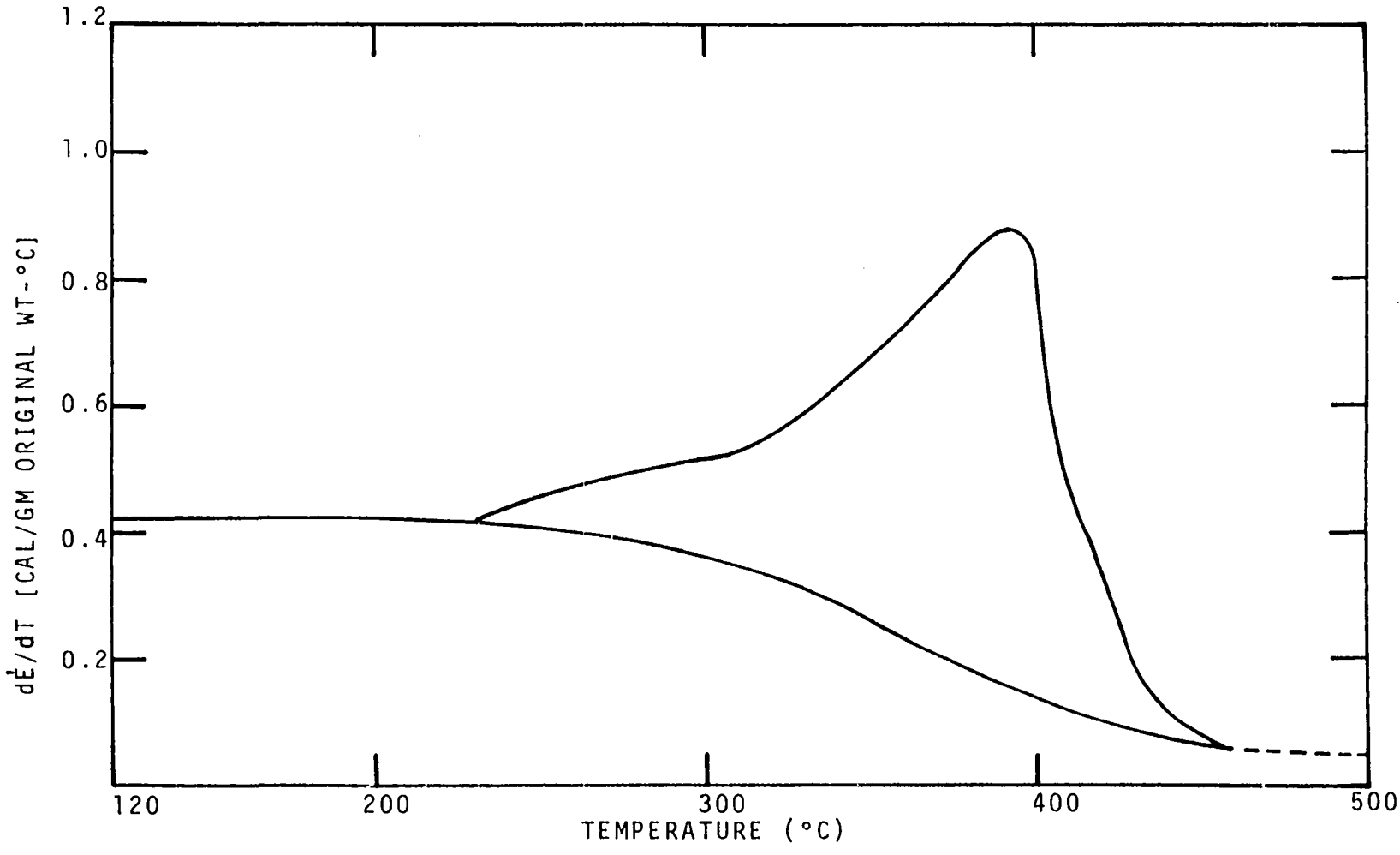

Figure F-3. Differential Energy Curve for Extracted Ponderosa Pine Needles. Heating Rate - 40°C/MIN.

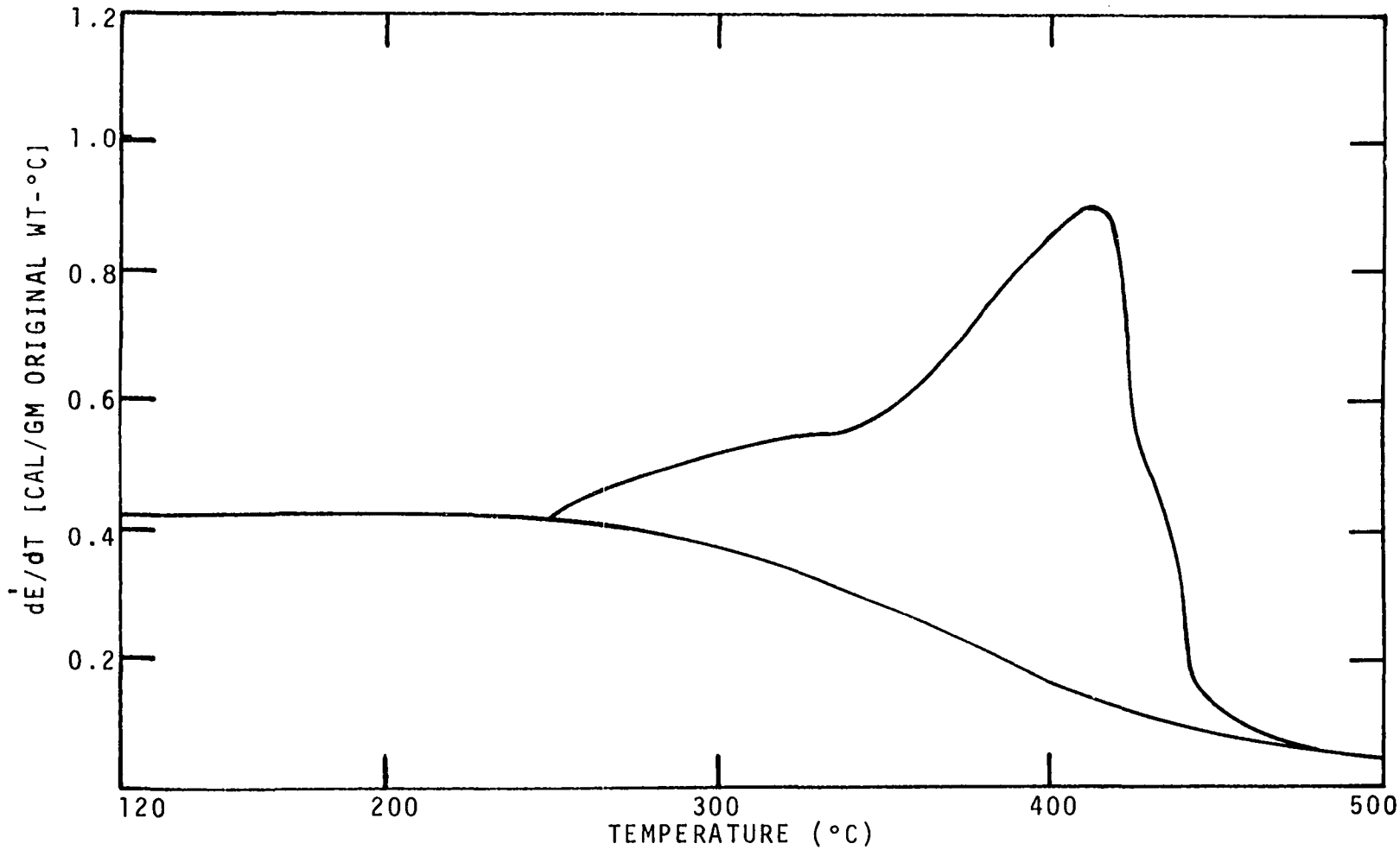

Figure F-4. Differential Energy Curves for Extracted Ponderosa Pine Needles. Heating Rate - 160°C/MIN.

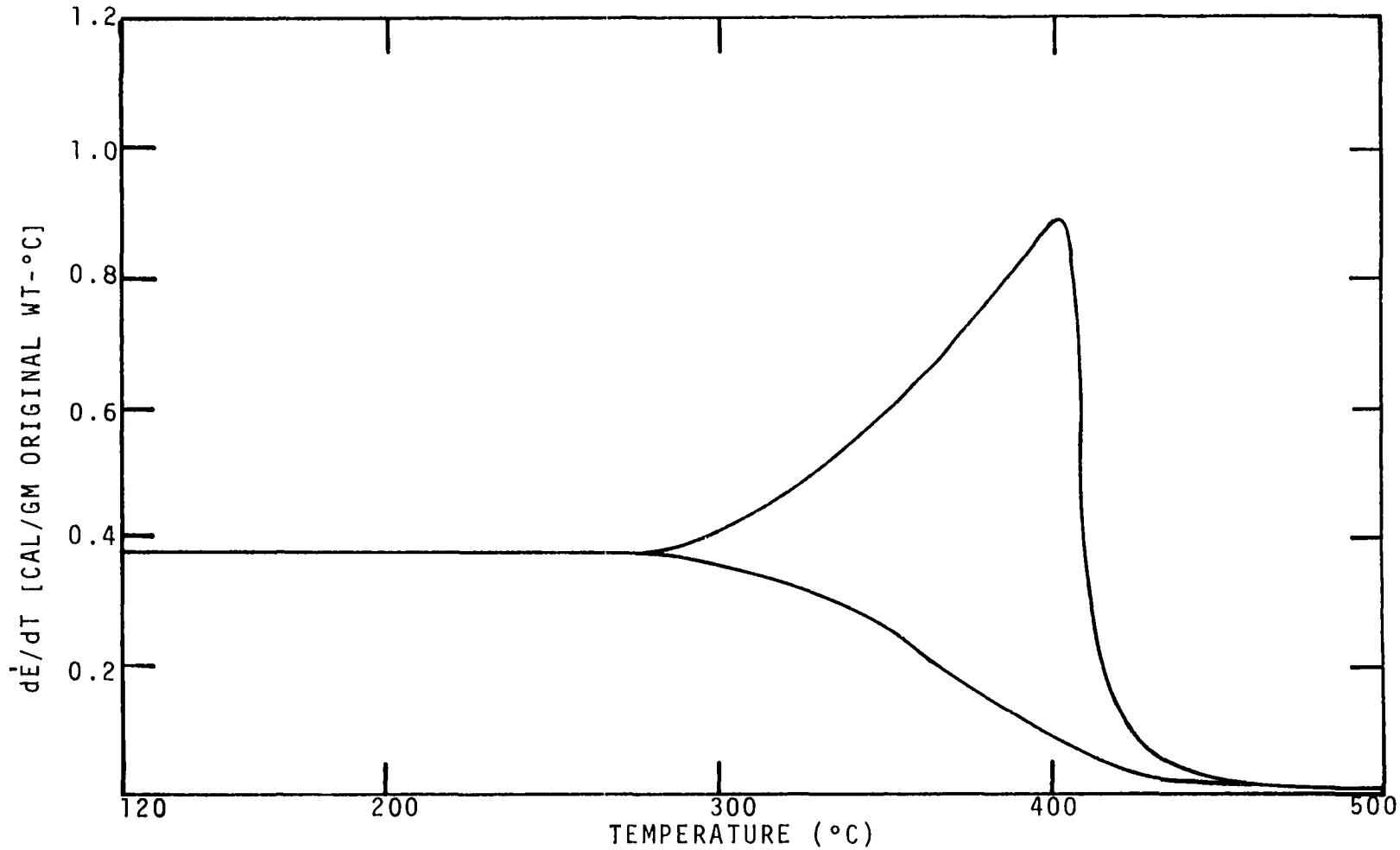

Figure F-5. Differential Energy Curves for Excelsior. Heating Rate - 40°C/MIN.

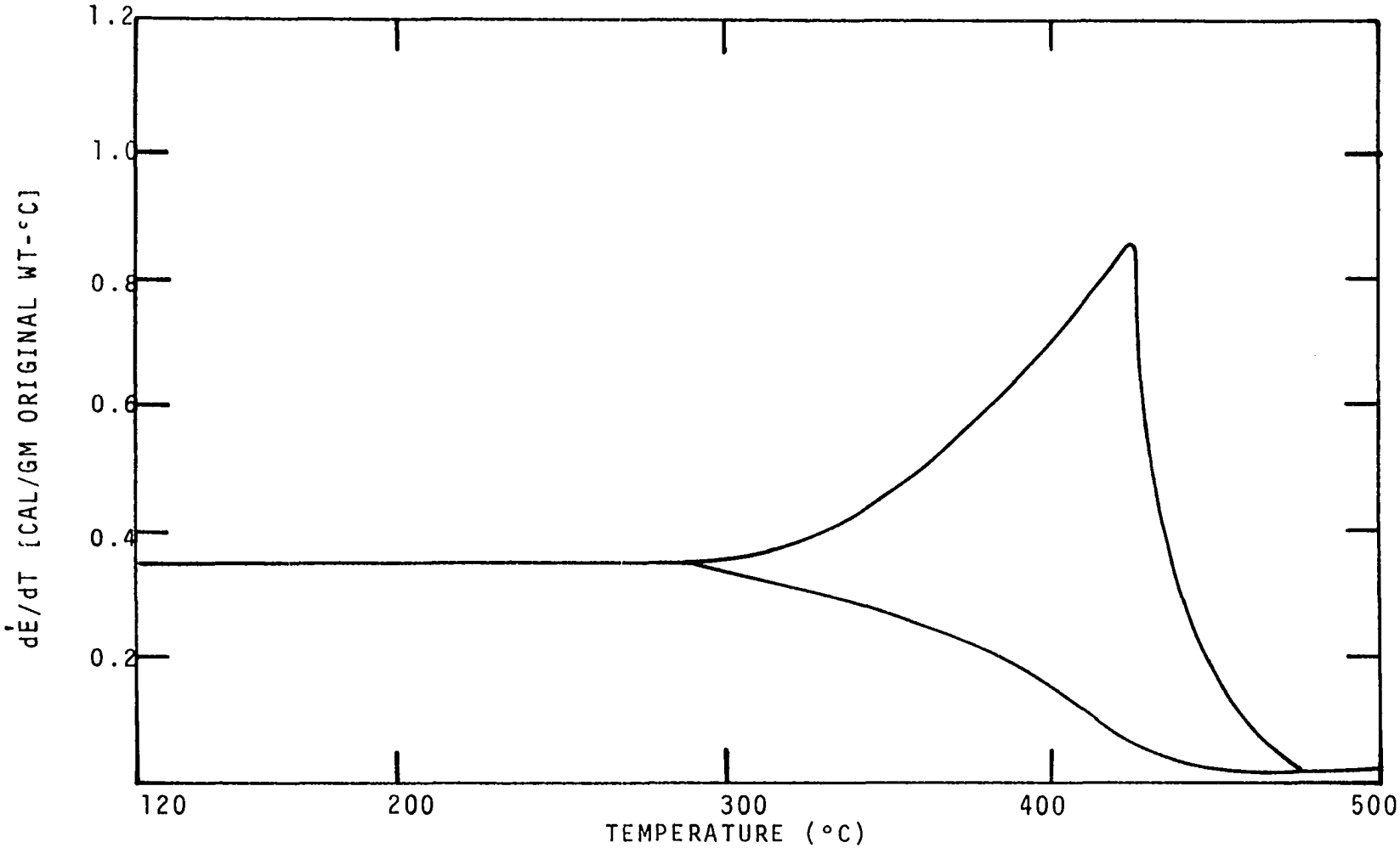

Figure F-6. Differential Energy Curves for Excelsior. Heating Rate - 160°C/MIN.

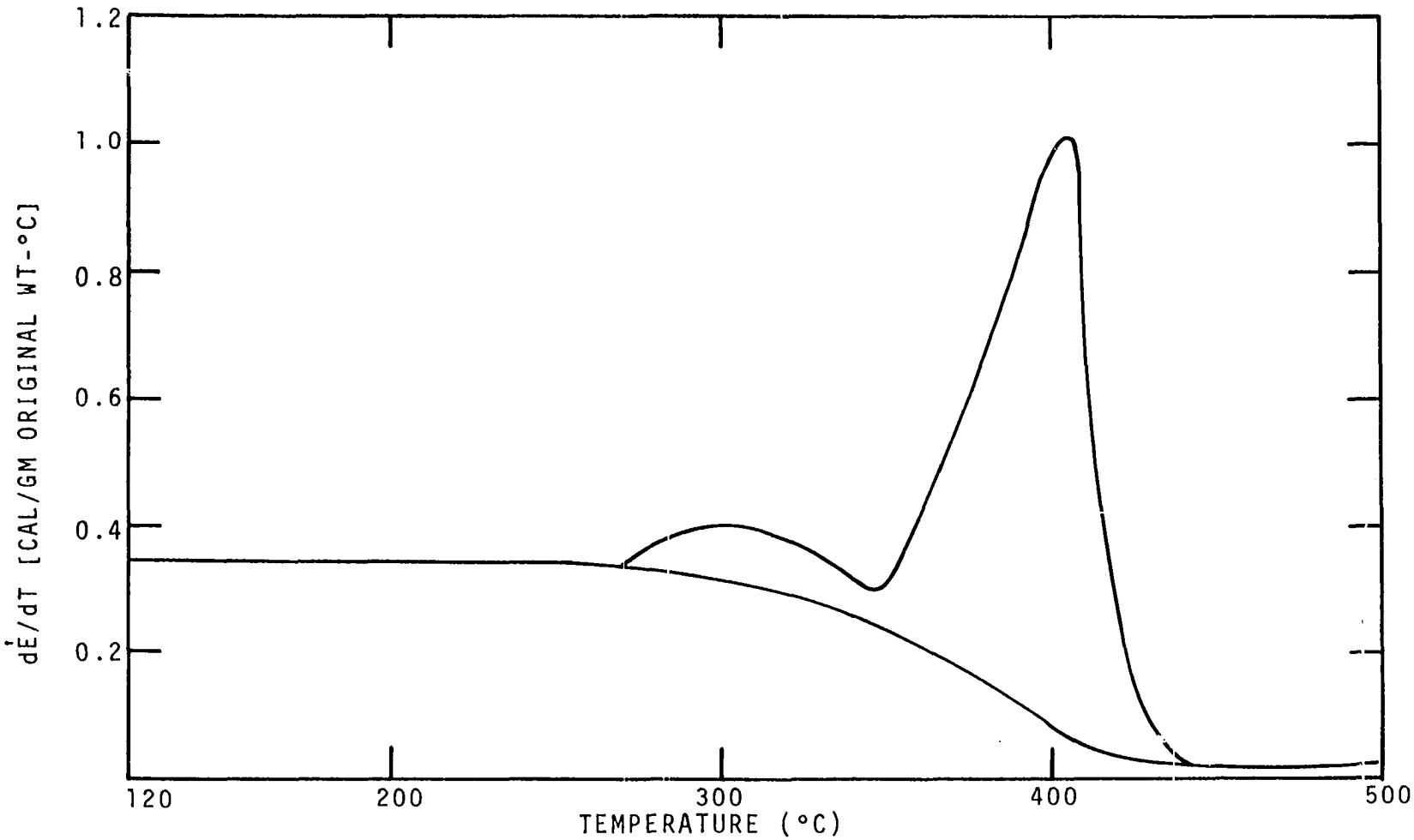

Figure F-7. Differential Energy Curves for Extracted Excelsior. Heating Rate - 40°C/MIN.

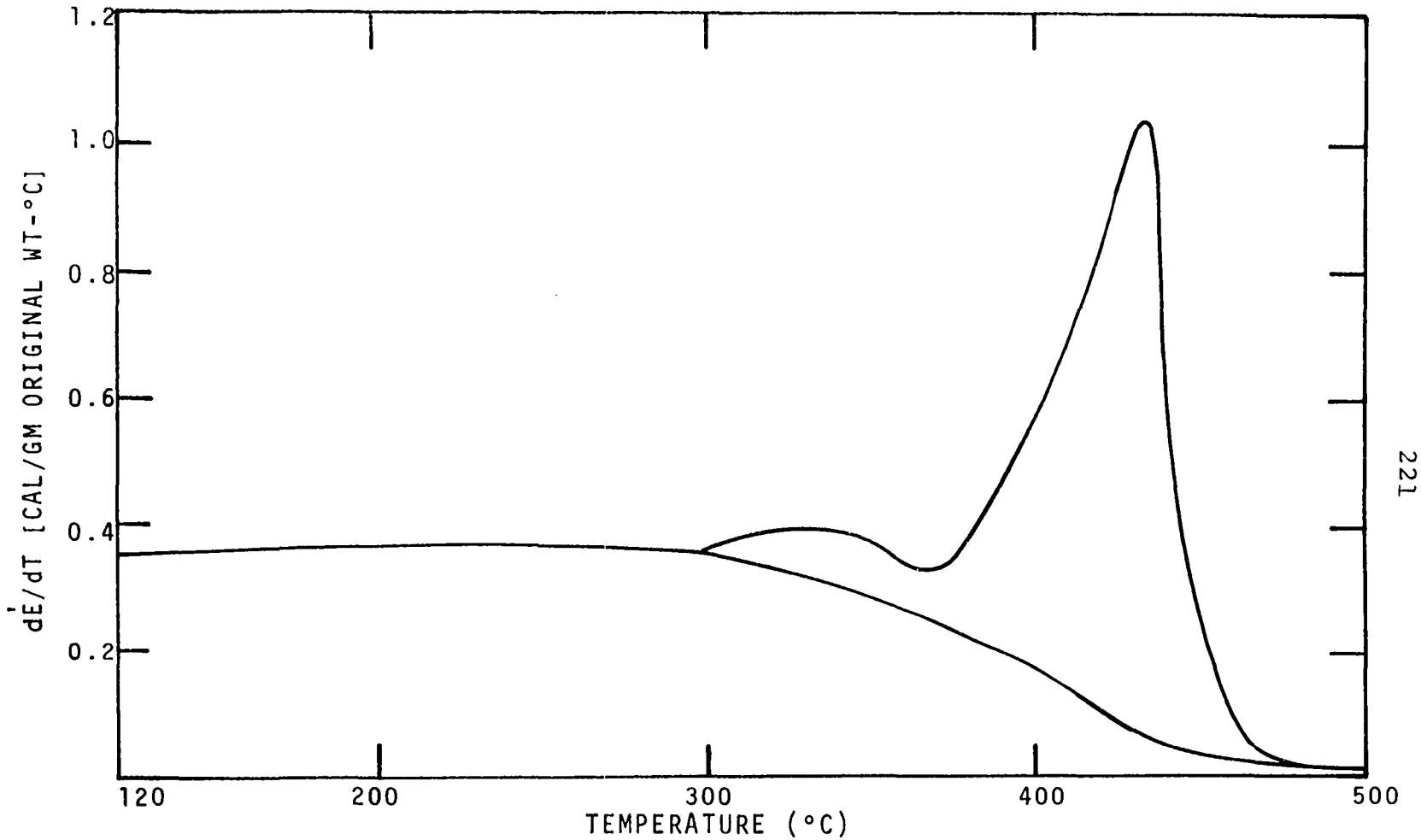

Figure F-8. Differential Energy Curves for Extracted Excelsior. Heating Rate - 160°C/MIN.

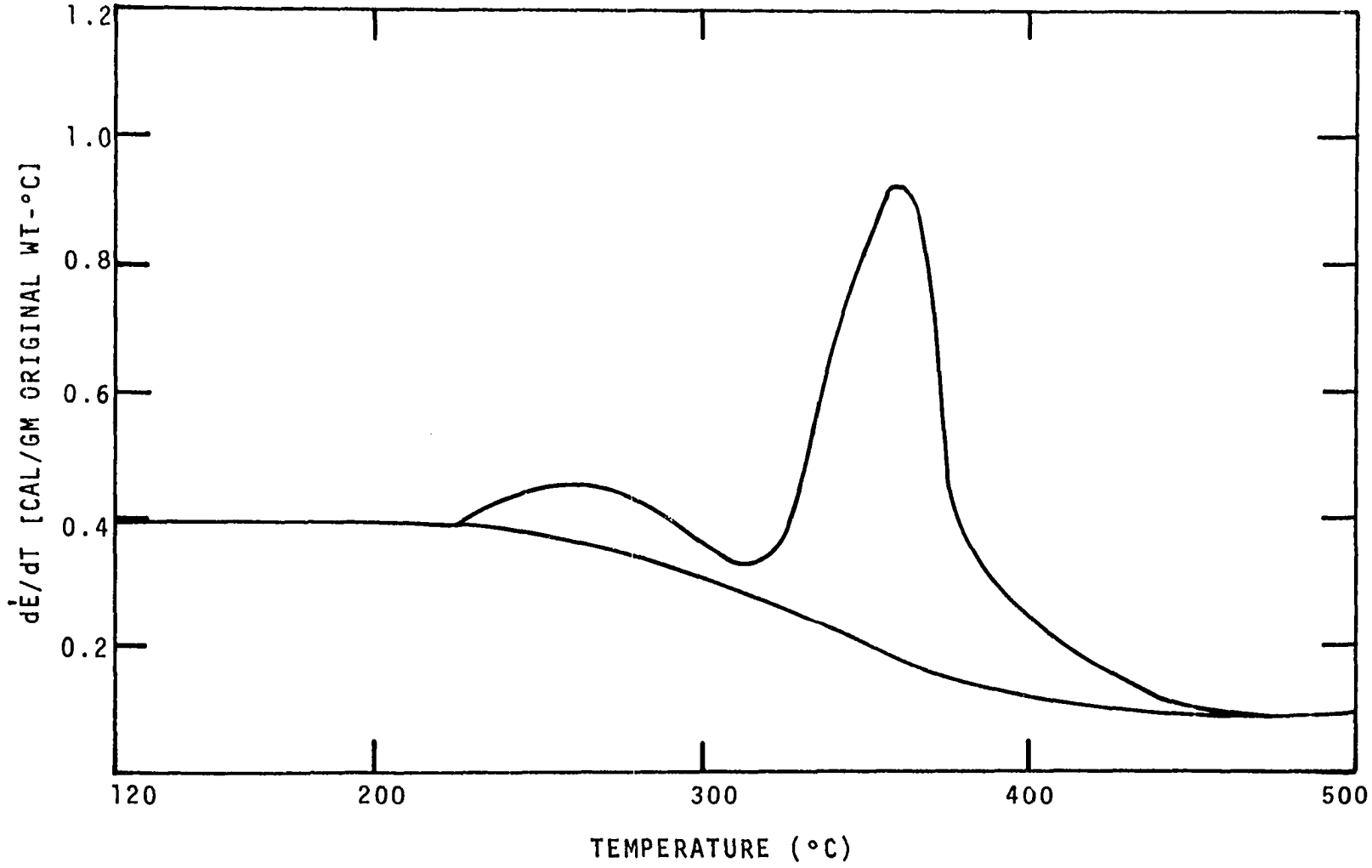

Figure F-9. Differential Energy Curves for Fourwing Saltbush Leaves. Heating Rate - 40°C/MIN.

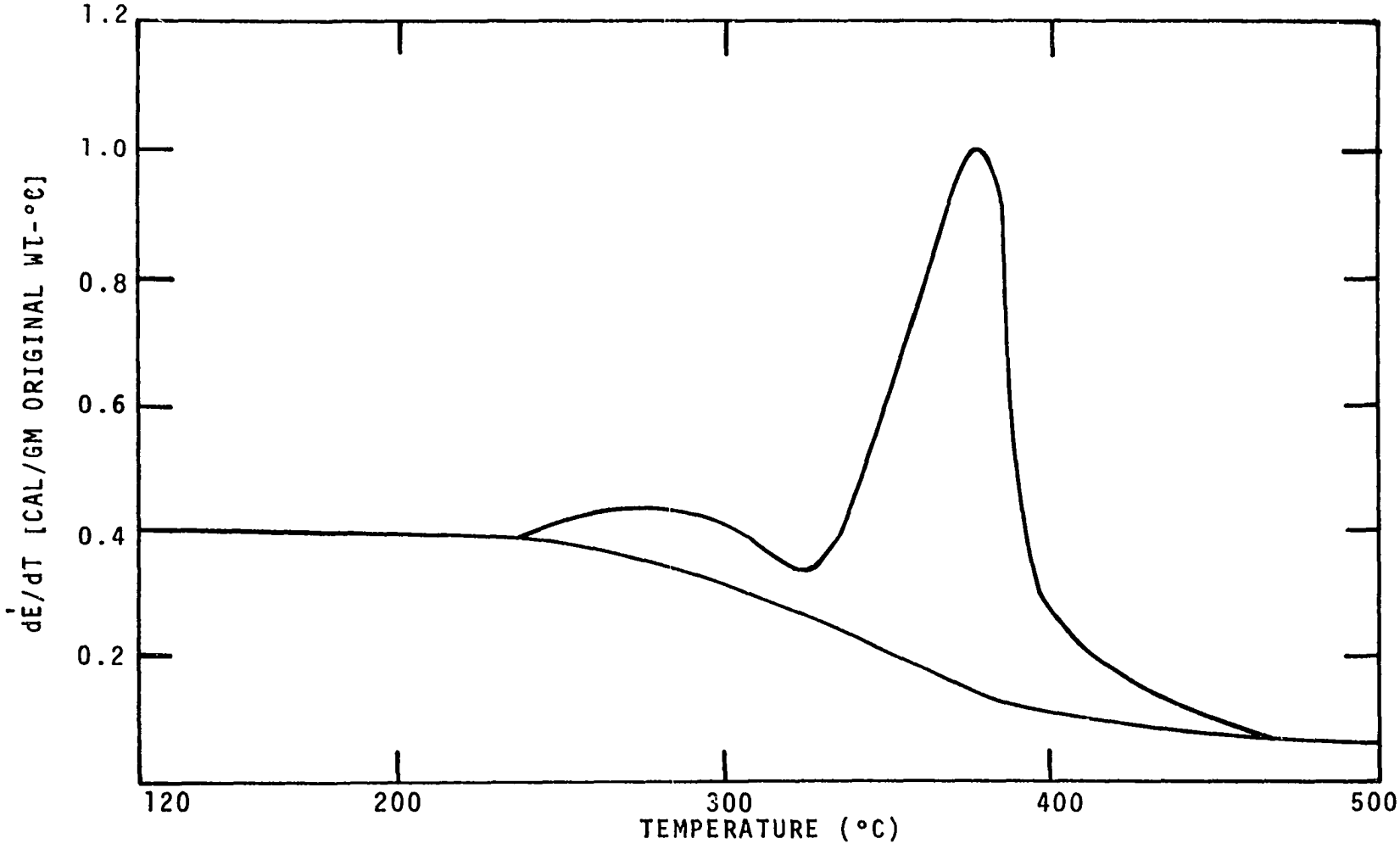

Figure F-10. Differential Energy Curves for Fourwing Saltbush Leaves. Heating Rate - 160°C/MIN.

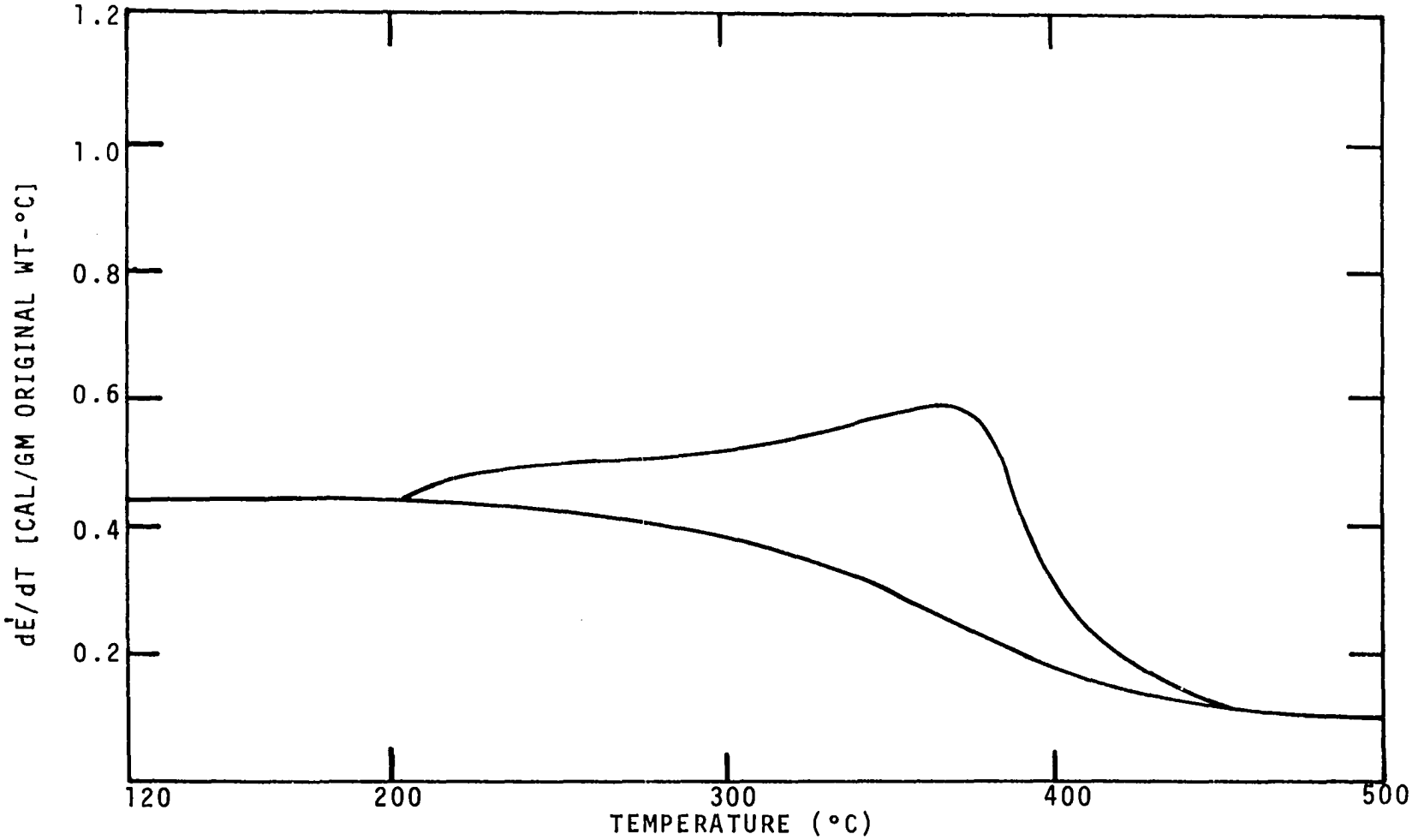

Figure F-11. Differential Energy Curves for Punky Wood. Heating Rate - 40°C/MIN.

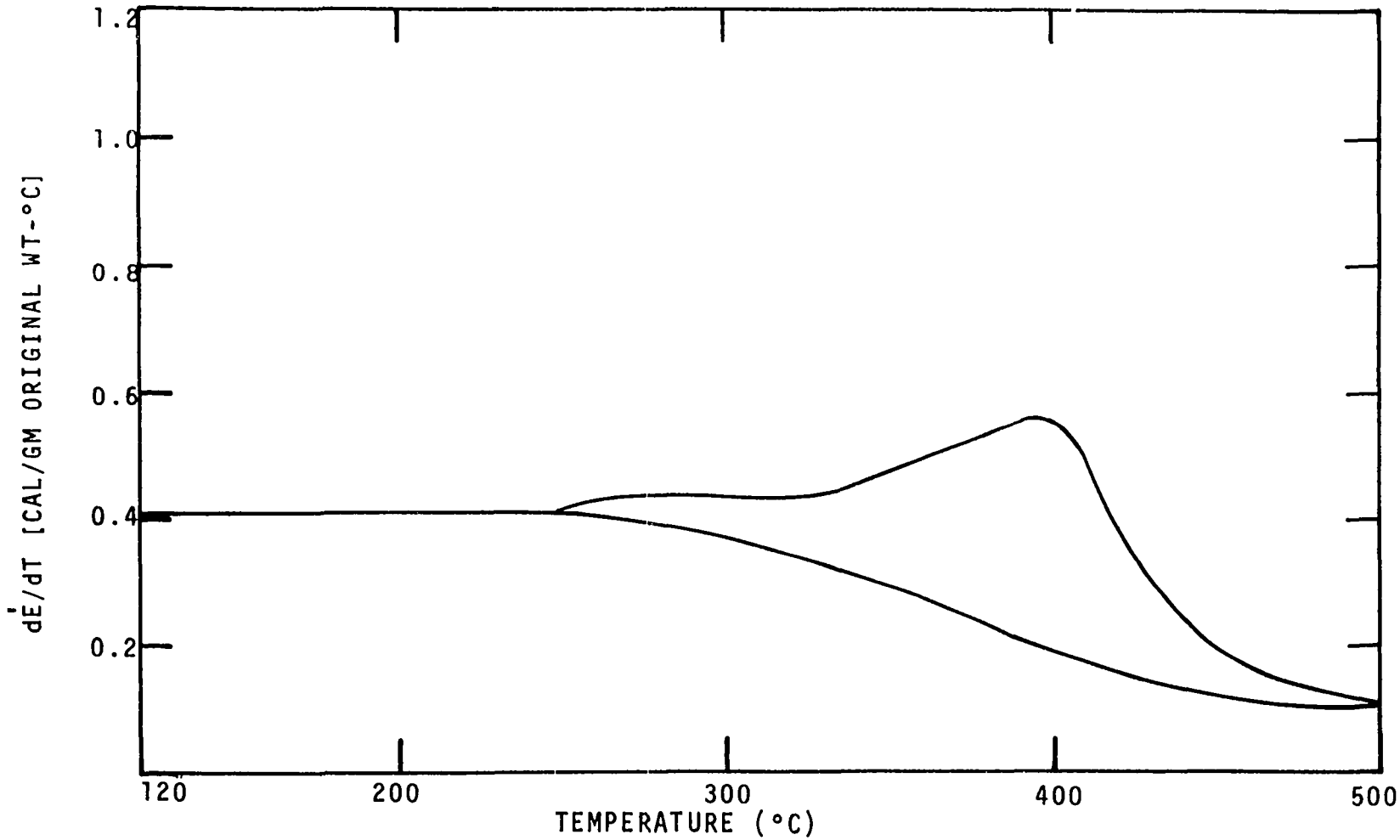

Figure F-12. Differential Energy Curves for Punky Wood. Heating Rate - 160°C/MIN.

APPENDIX G

TOTAL ENERGY VERSUS TEMPERATURE CURVES FOR DRY SAMPLES

Total energy versus temperature curves for dry samples of dead Ponderosa pine needles (extracted and unextracted), excelsior (extracted and unextracted), fourwing saltbush leaves, and punky wood at the heating rates of 40° and 160°C/MIN.

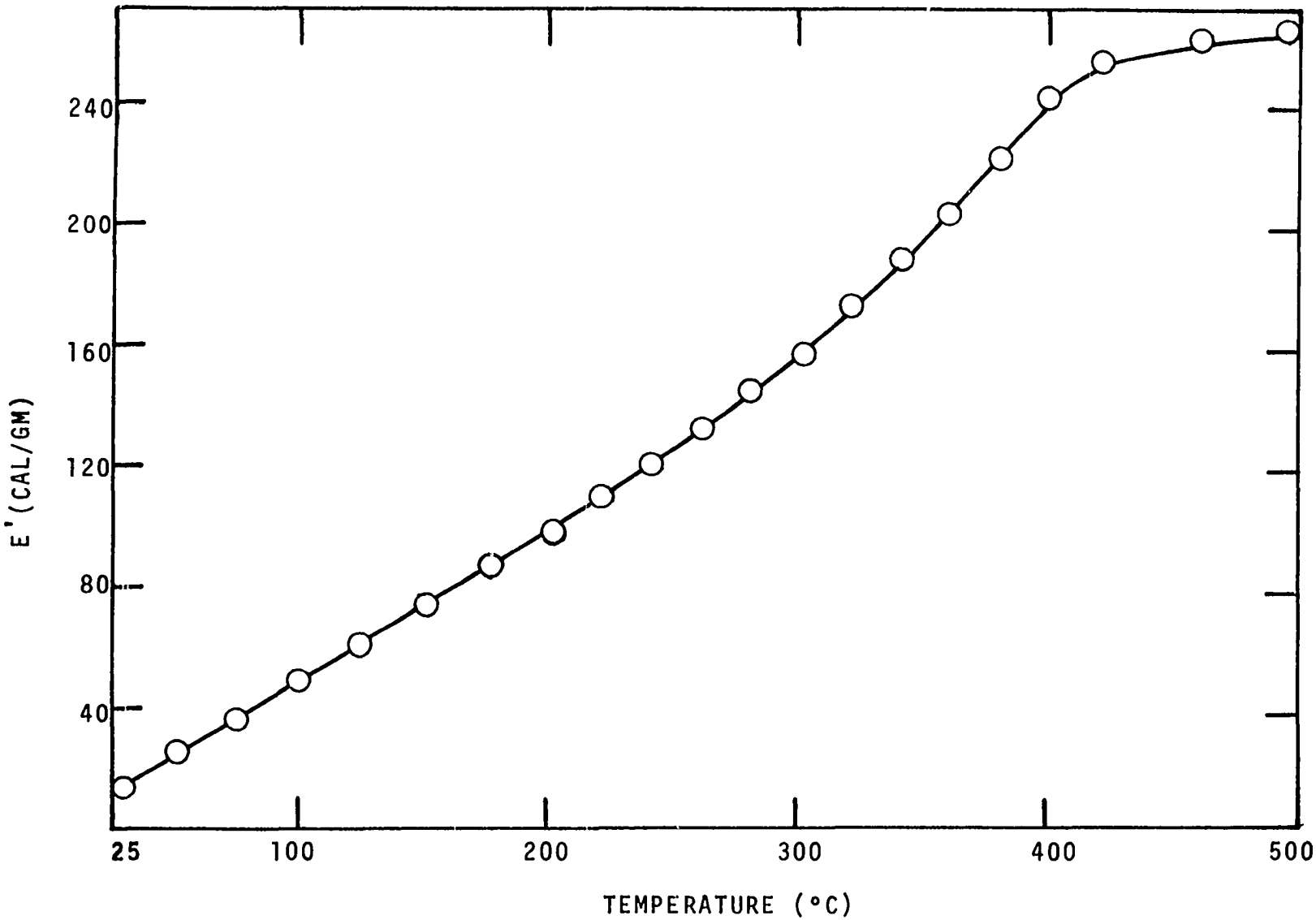

Figure G-1. Total Energy of Pyrolysis versus Temperature Curve for Dead Ponderosa Pine Needles. Heating Rate - 40°C/MIN.

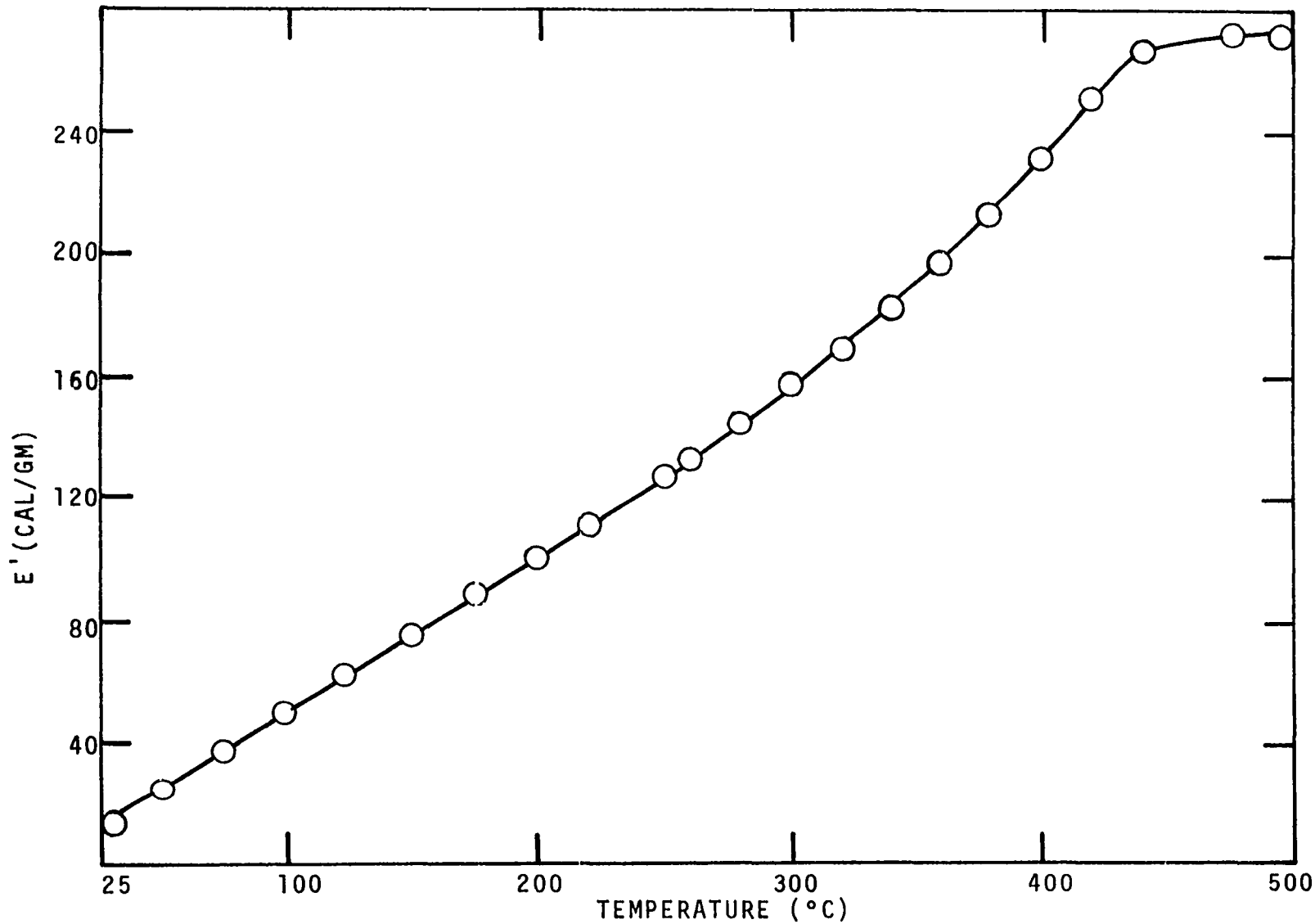

Figure G-2. Total Energy of Pyrolysis versus Temperature Curve for Dead Ponderosa Pine Needles. Heating Rate - 160°C/MIN.

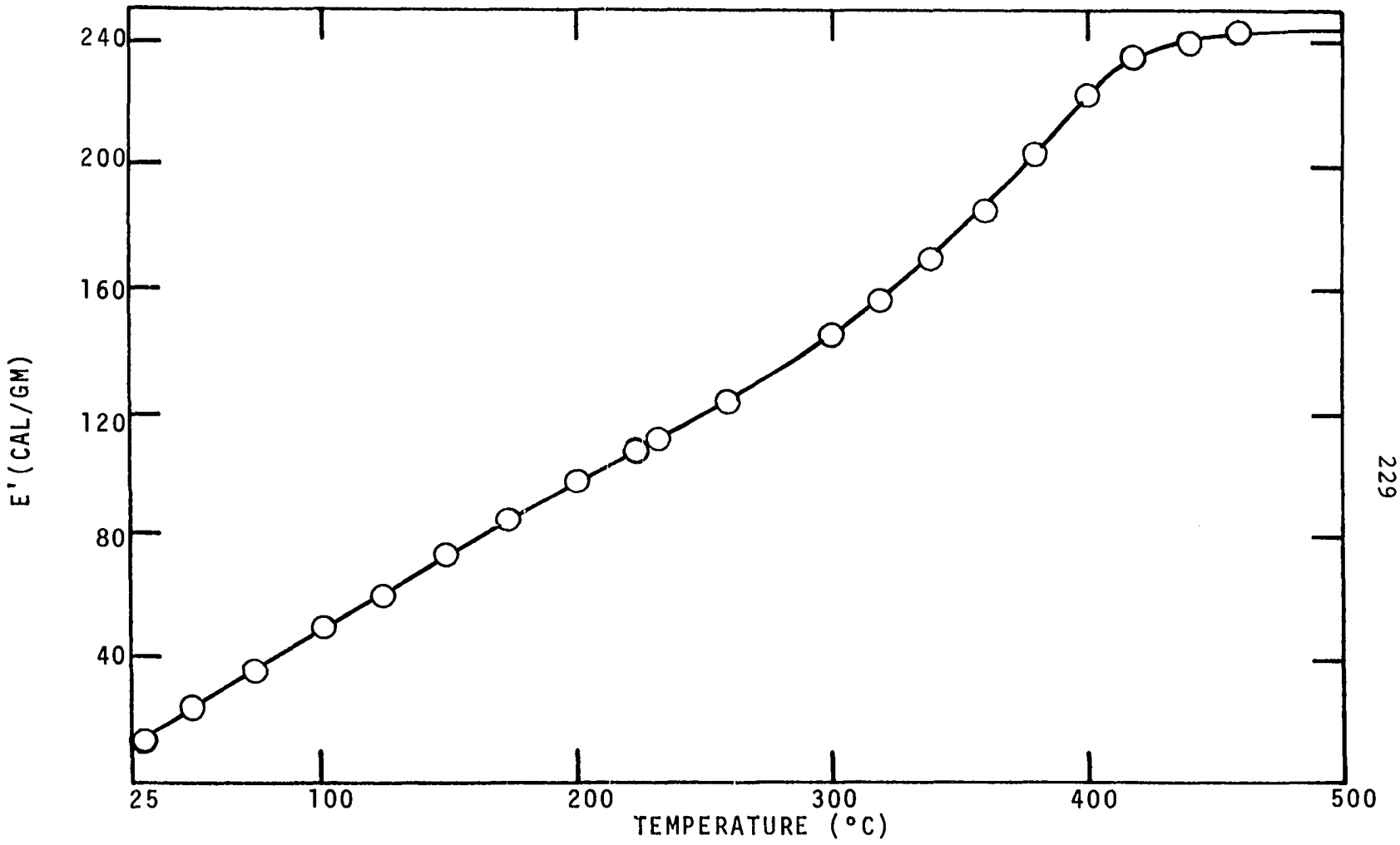

Figure G-3. Total Energy of Pyrolysis versus Temperature Curve for Extracted Ponderosa Pine Needles. Heating Rate - 40°C/MIN.

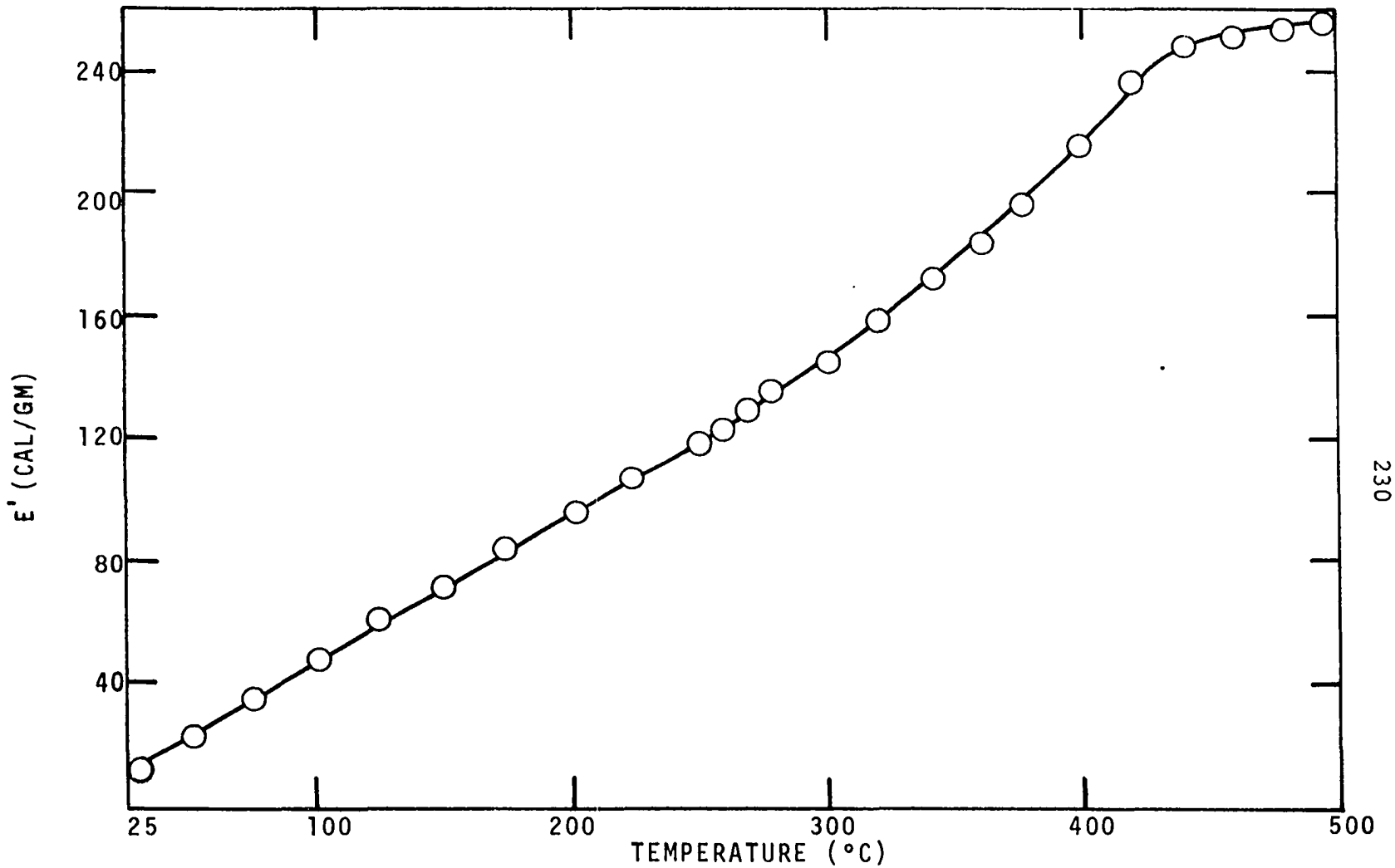

Figure G-4. Total Energy of Pyrolysis versus Temperature Curve for Extracted Ponderosa Pine Needles. Heating Rate - 160°C/MIN.

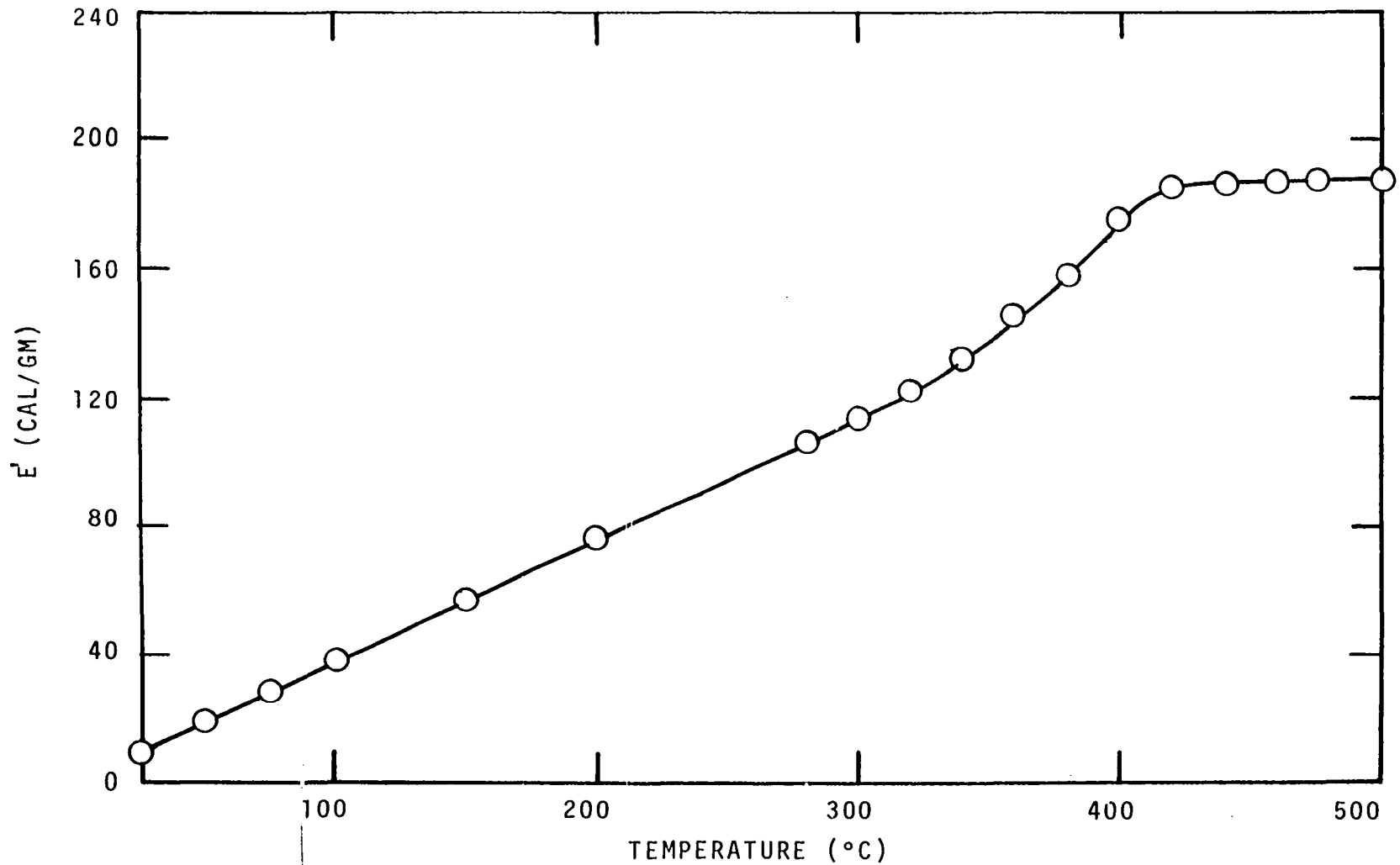

Figure G-5. Total Energy of Pyrolysis versus Temperature Curve for Excelsior. Heating Rate - 40°C/MIN.

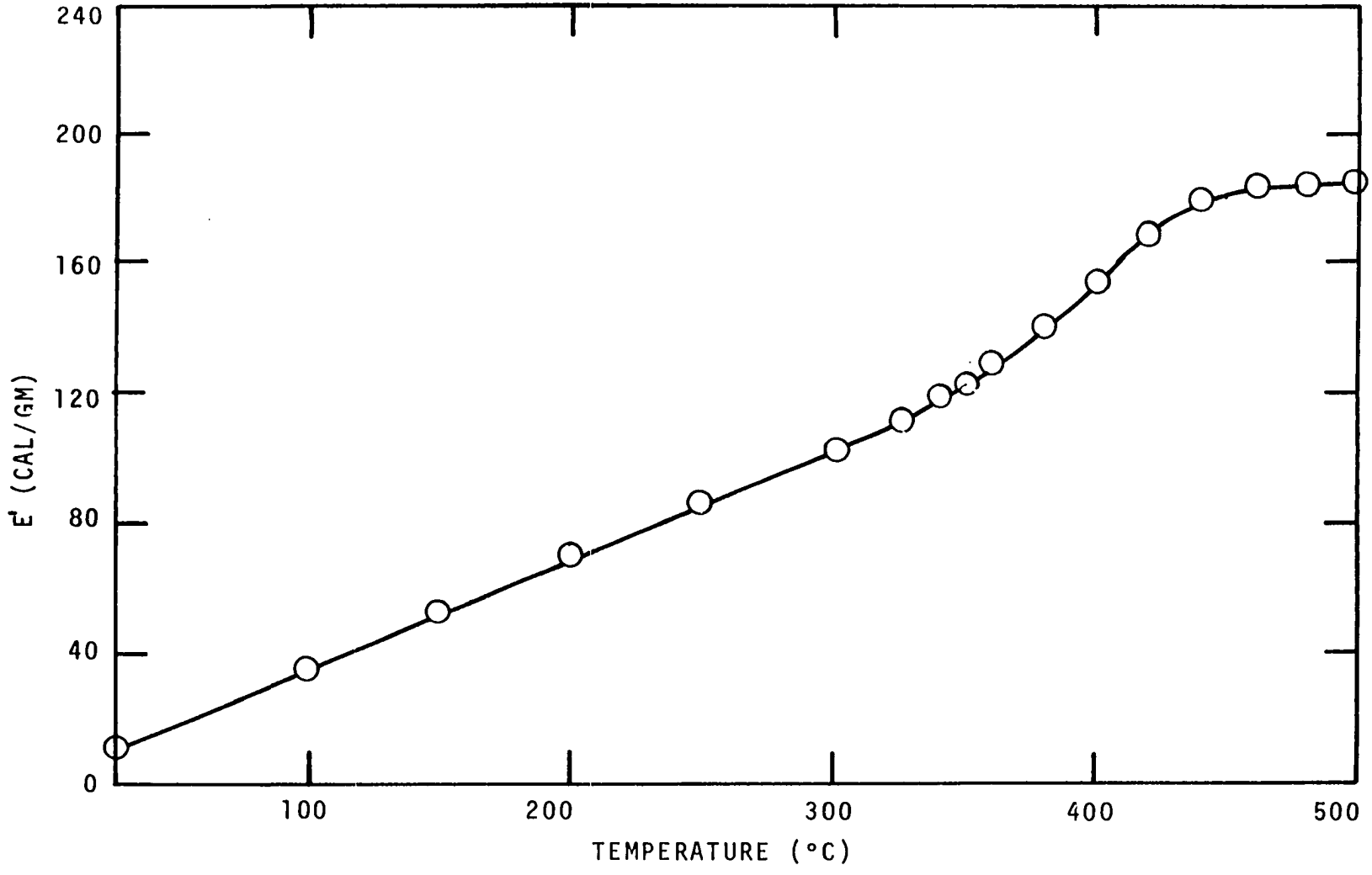

Figure G-6. Total Energy of Pyrolysis versus Temperature Curve for Excelsior. Heating Rate - 160°C/MIN.

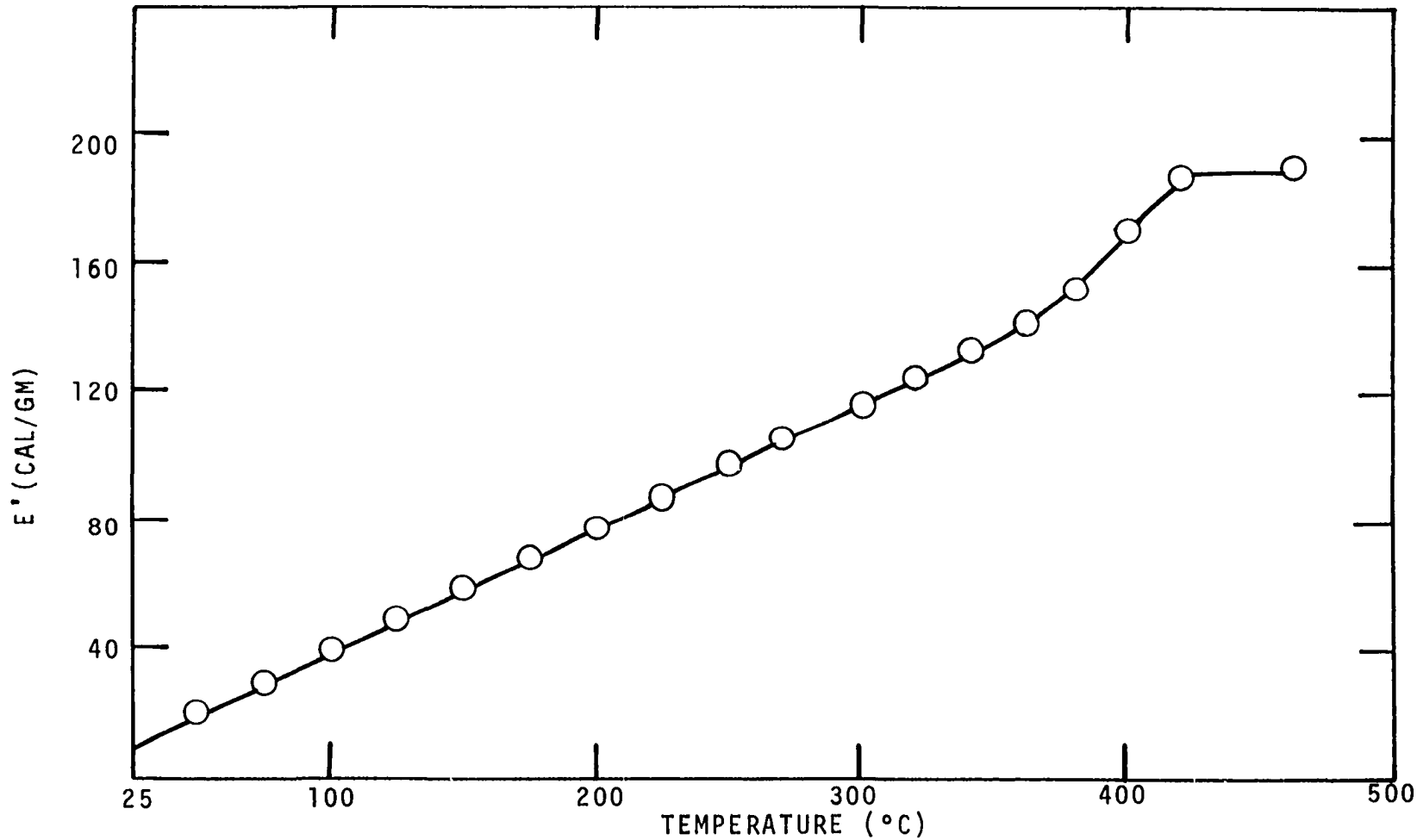

Figure G-7. Total Energy of Pyrolysis versus Temperature Curve for Extracted Excelsior. Heating Rate - 40°C/MIN.

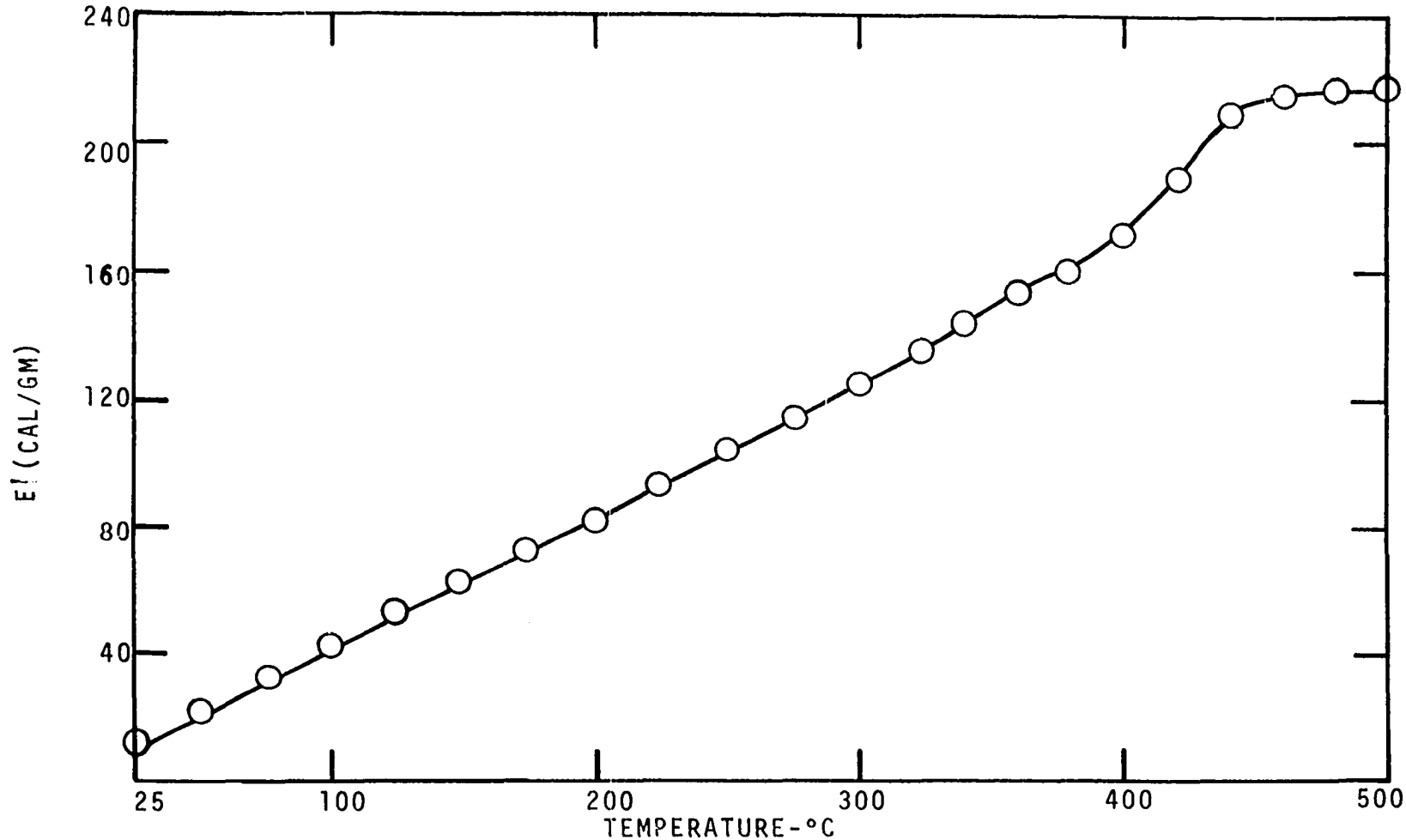

Figure G-8. Total Energy of Pyrolysis versus Temperature Curve for Extracted Excelsior. Heating Rate - 160°C/MIN.

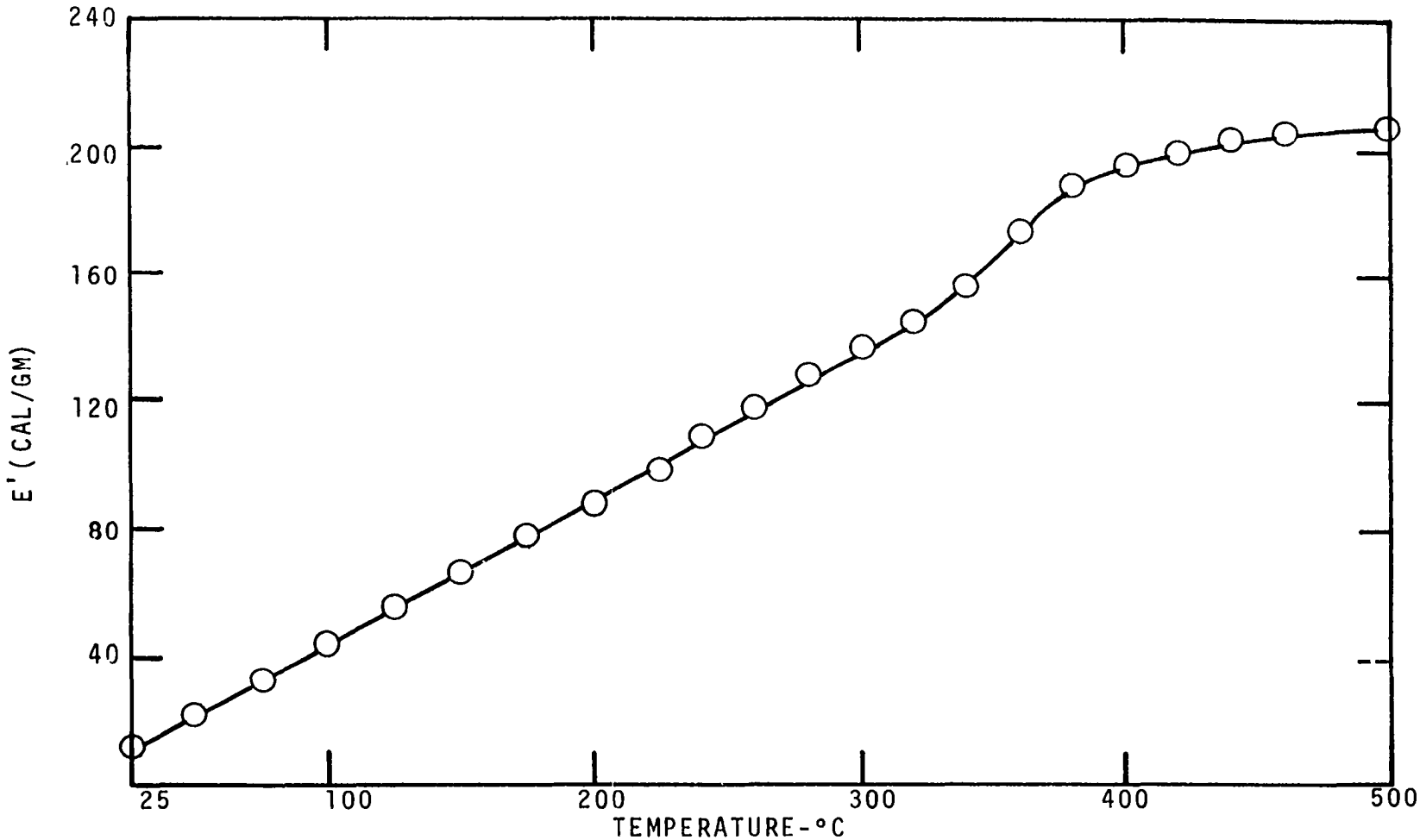

Figure G-9. Total Energy of Pyrolysis versus Temperature Curve for Fourwing Saltbush Leaves. Heating Rate - 40°C/MIN.

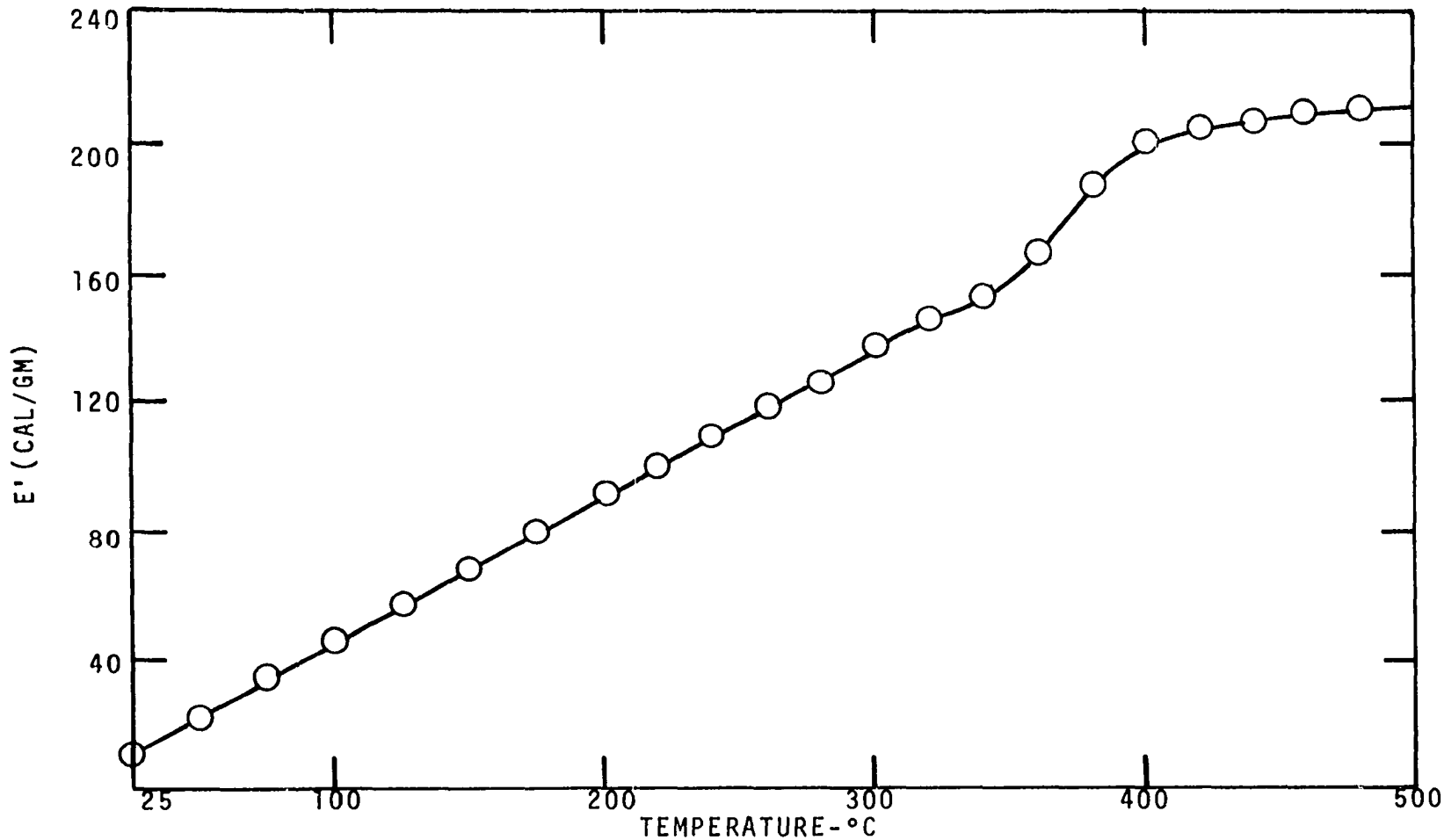

Figure G-10. Total Energy of Pyrolysis versus Temperature Curve for Fourwing Saltbush Leaves. Heating Rate - 160°C/MIN.

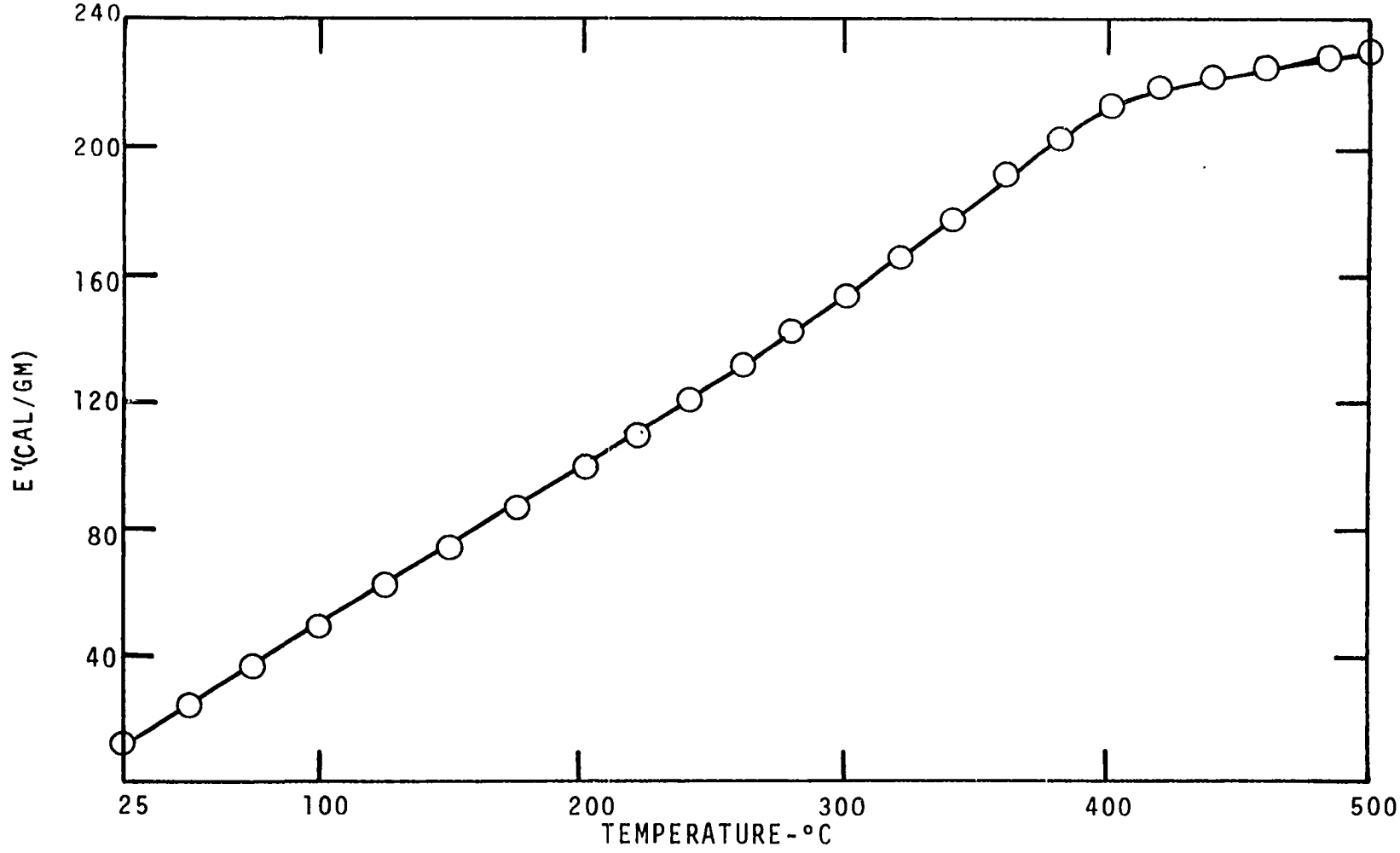

Figure G-11. Total Energy of Pyrolysis versus Temperature Curve for Punky Wood. Heating Rate - 40°C/MIN.

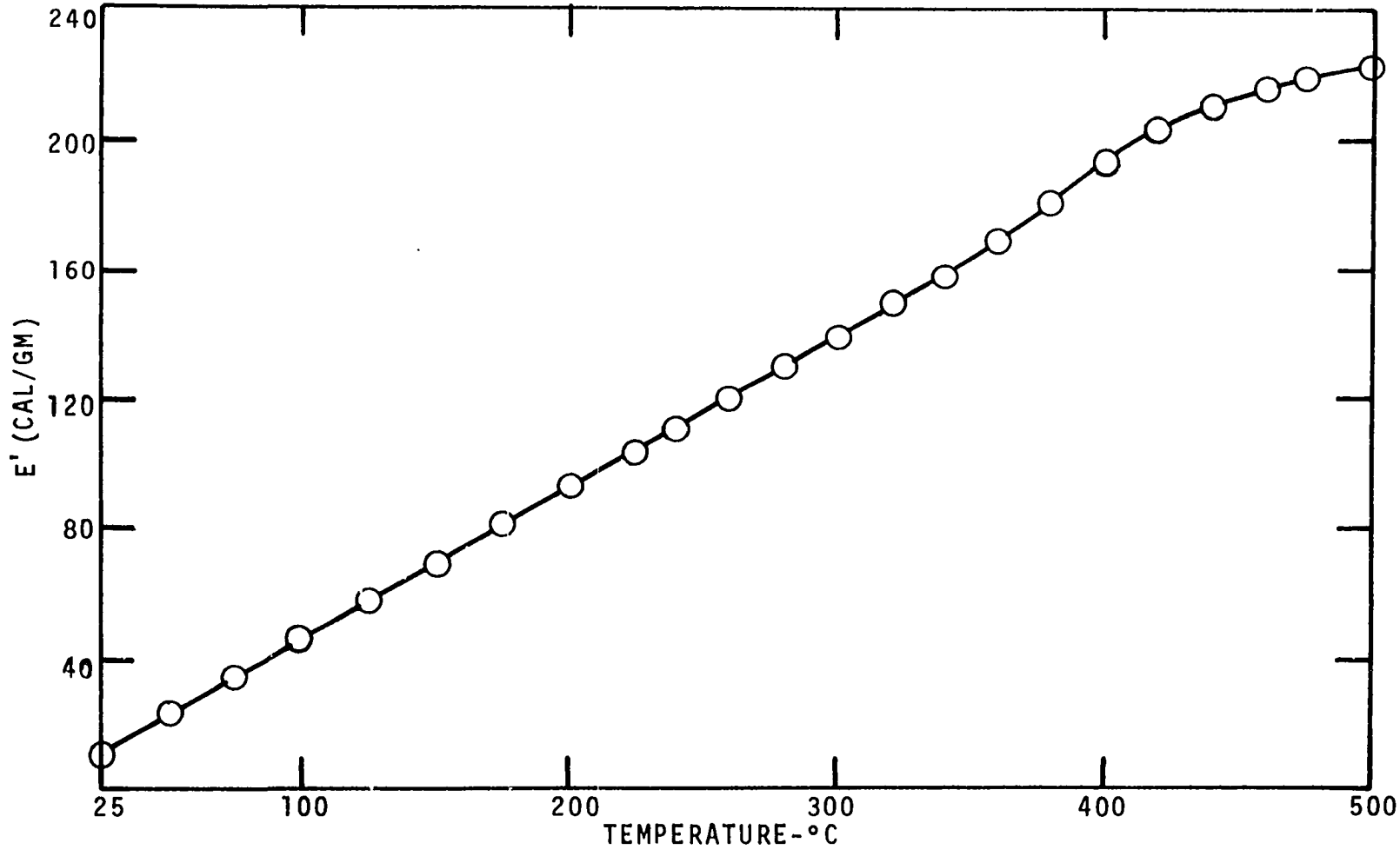

Figure G-12. Total Energy of Pyrolysis versus Temperature Curve for Punky Wood. Heating Rate - 160°C/MIN.

APPENDIX H

WET SAMPLE DIFFERENTIAL ENERGY CURVES

Wet sample differential energy curves [dE'/dT vs T] for dead Ponderosa pine needles (extracted and unextracted), excelsior (extracted and unextracted), fourwing saltbush leaves, and punky wood at the heating rates of 40° and 160°C/MIN.

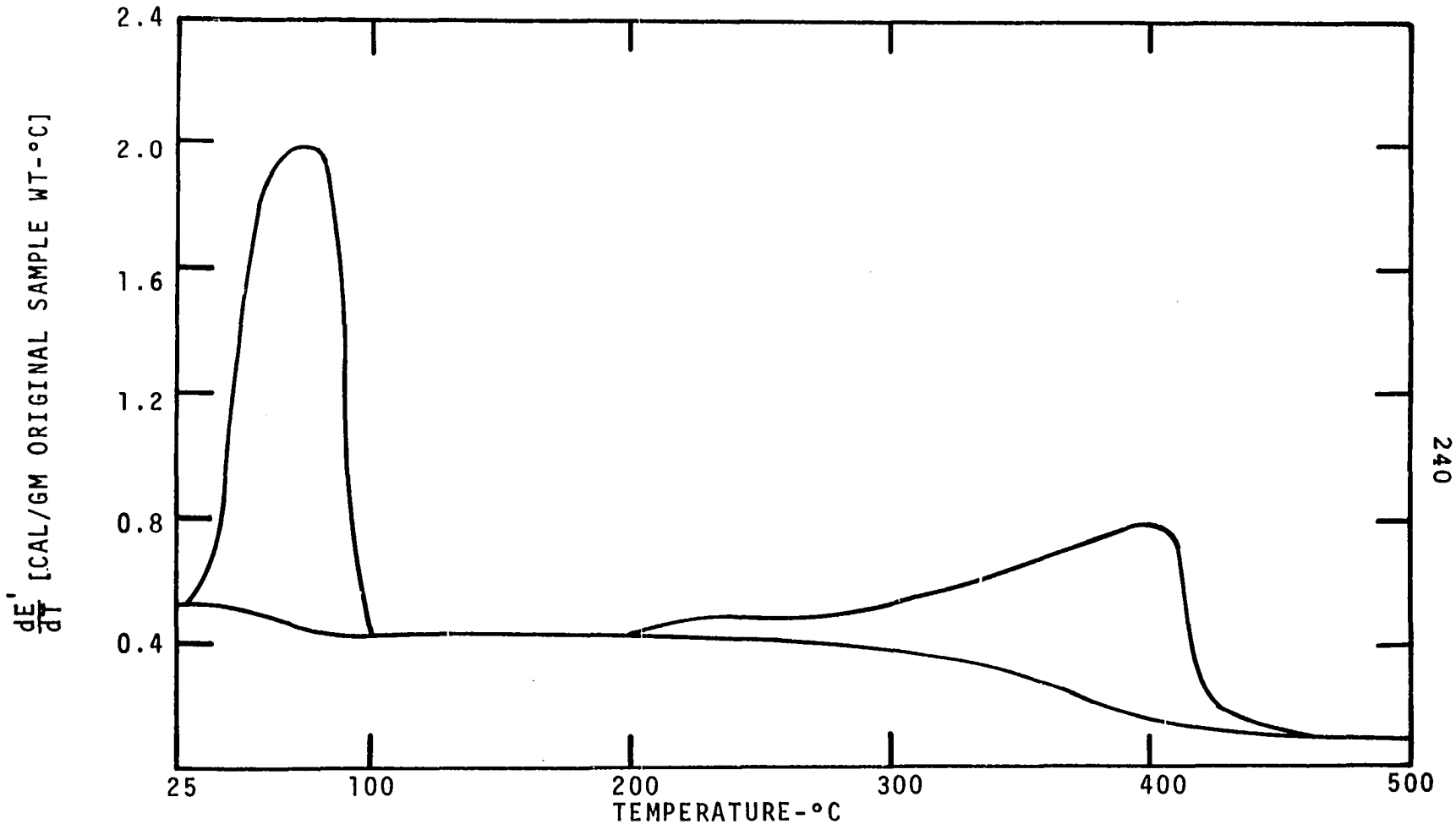

Figure H-1. Differential Energy versus Temperature Curve for Dead Ponderosa Pine Needles. Heating Rate - 40°C/MIN.

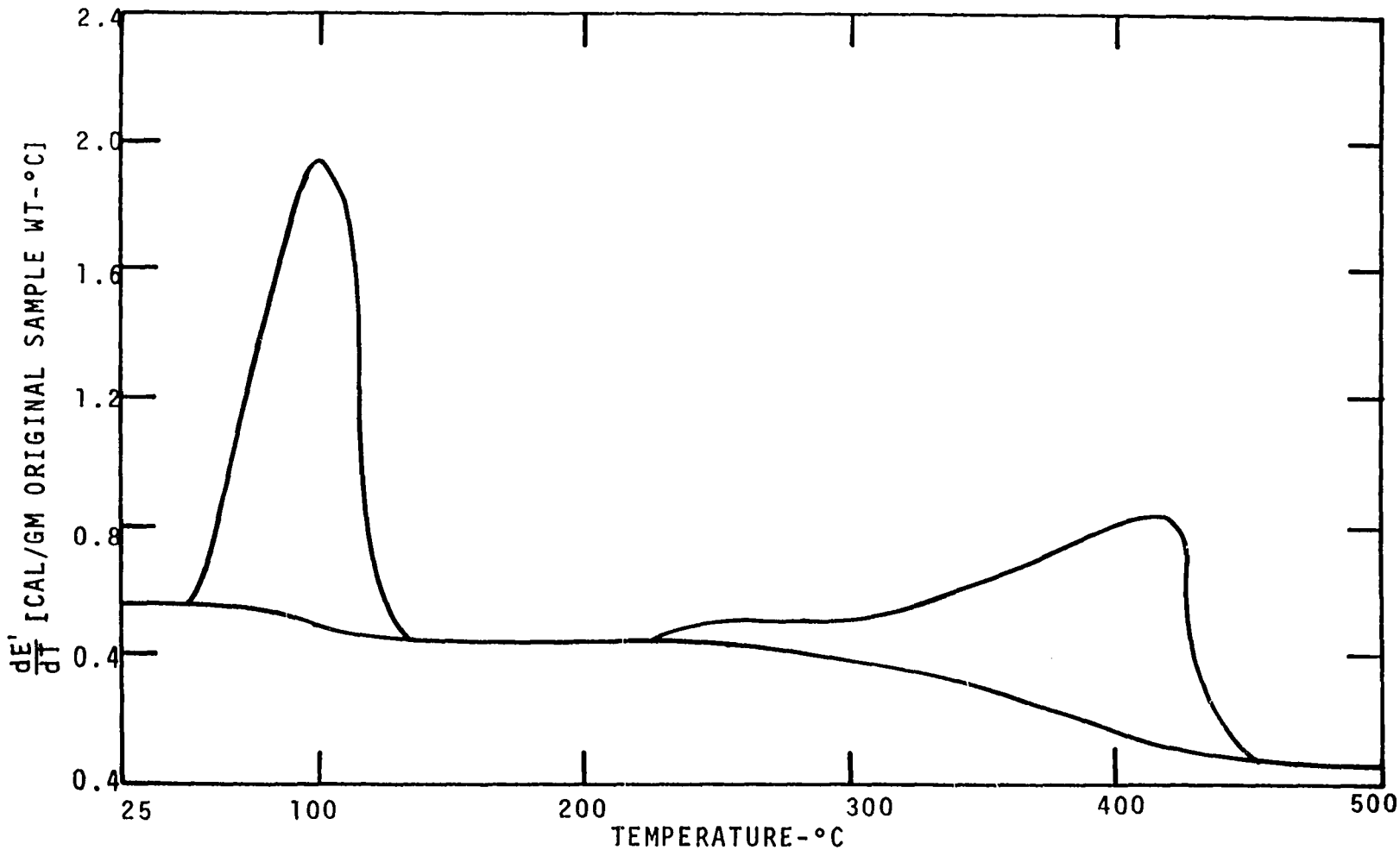

Figure H-2. Differential Energy versus Temperature Curve for Dead Ponderosa Pine Needles. Heating Rate - 160°C/MIN.

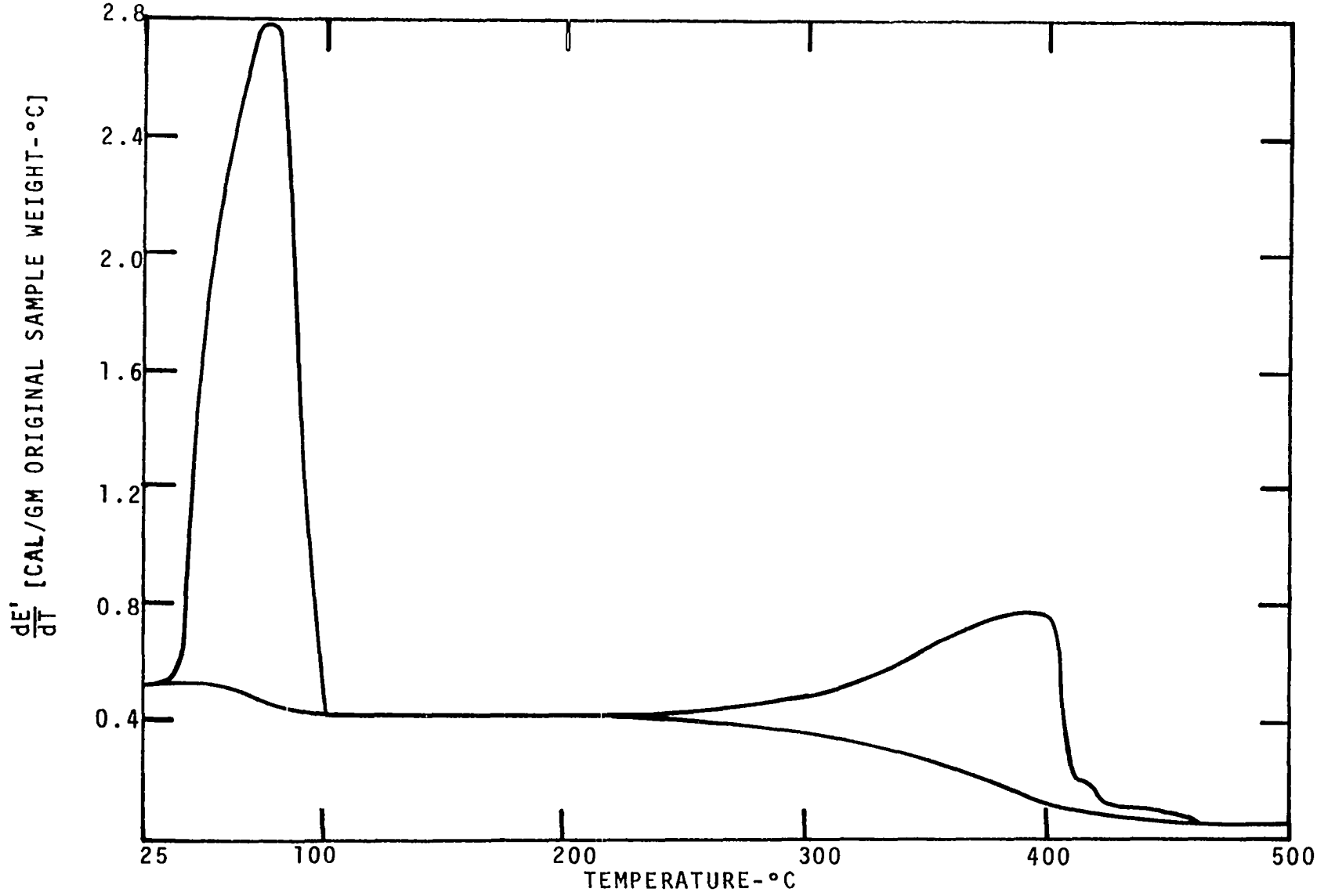

Figure H-3. Differential Energy versus Temperature Curve for Extracted Ponderosa Pine Needles. Heating Rate - 40°C/MIN.

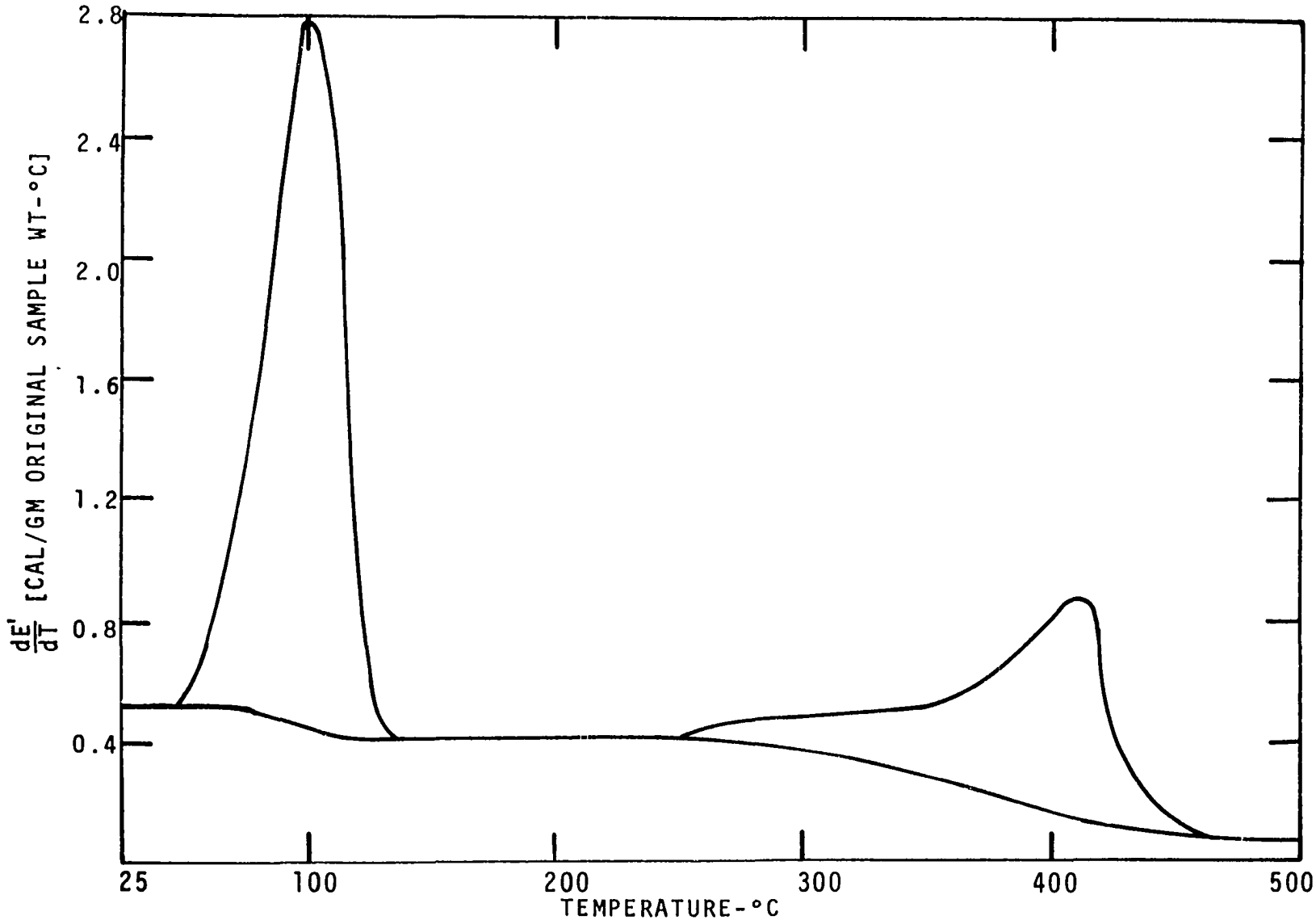

Figure H-4. Differential Energy versus Temperature Curve for Extracted Ponderosa Pine Needles. Heating Rate - 160°C/MIN.

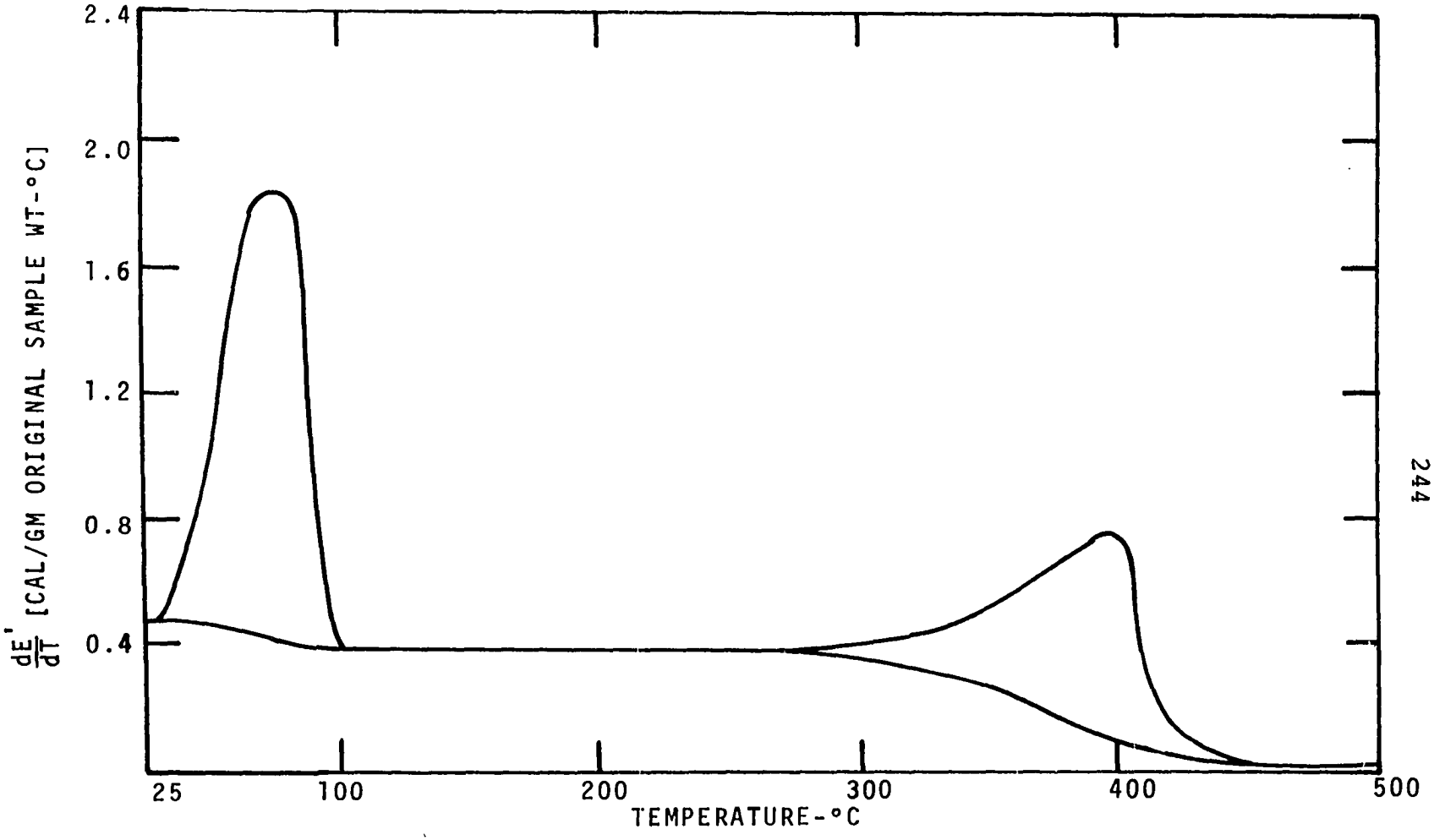

Figure H-5. Differential Energy versus Temperature Curve for Excelsior. Heating Rate - 40°C/MIN.

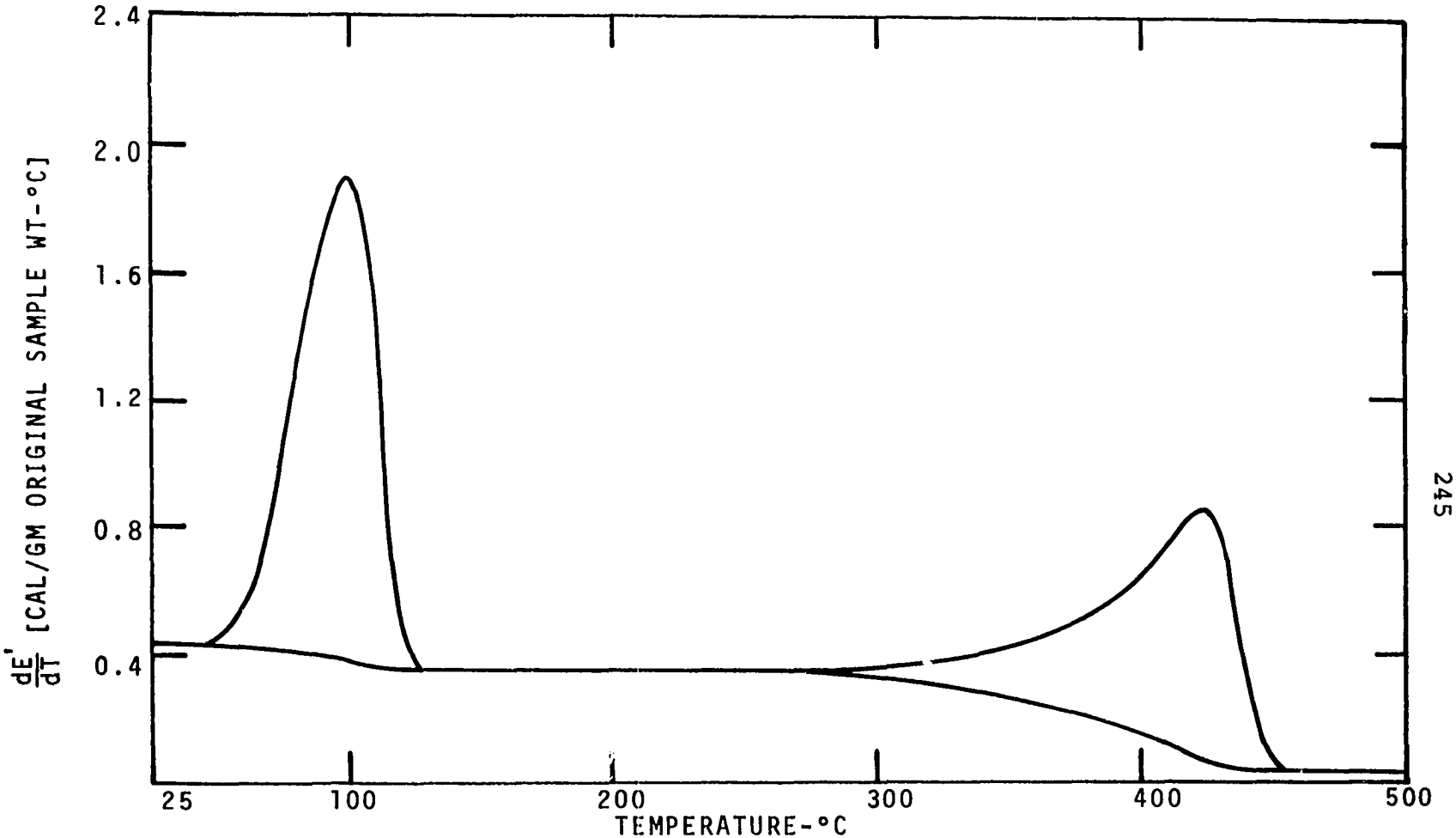

Figure H-6. Differential Energy versus Temperature Curve for Excelsior. Heating Rate - 160°C/MIN.

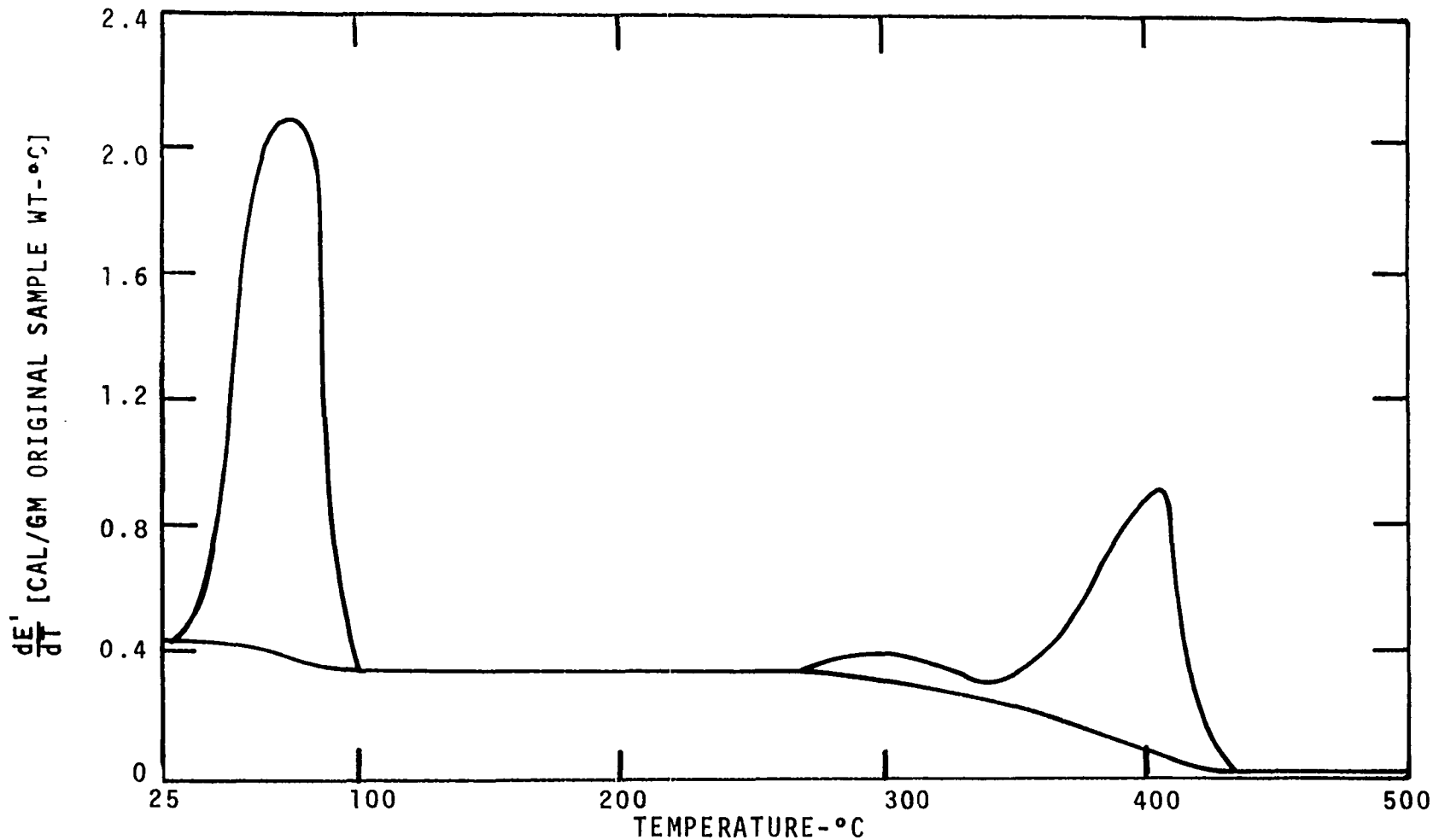

Figure H-7. Differential Energy versus Temperature Curve for Extracted Excelsior. Heating Rate - 40°C/MIN.

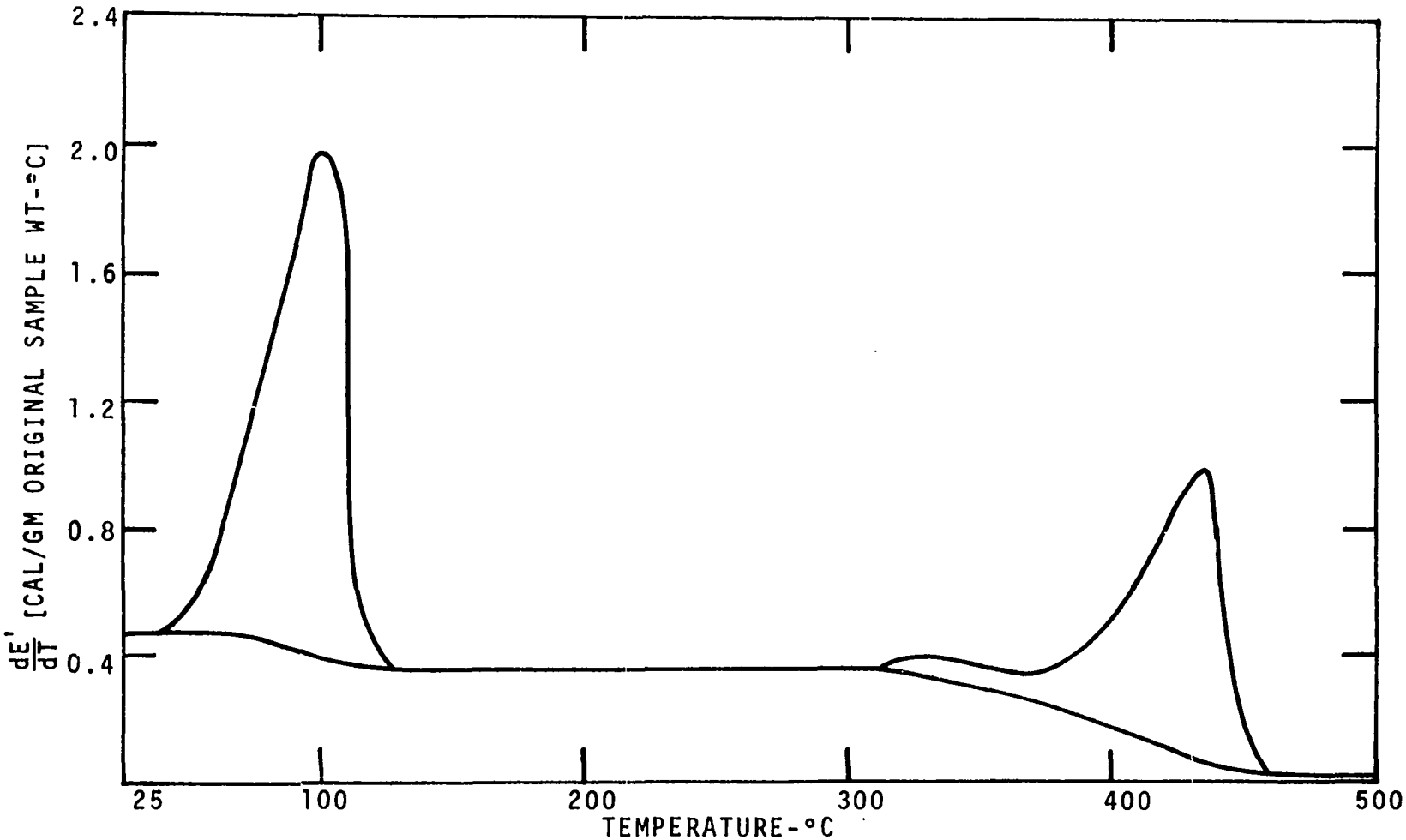

Figure H-8. Differential Energy versus Temperature Curve for Extracted Excelsior. Heating Rate - 160°C/MIN.

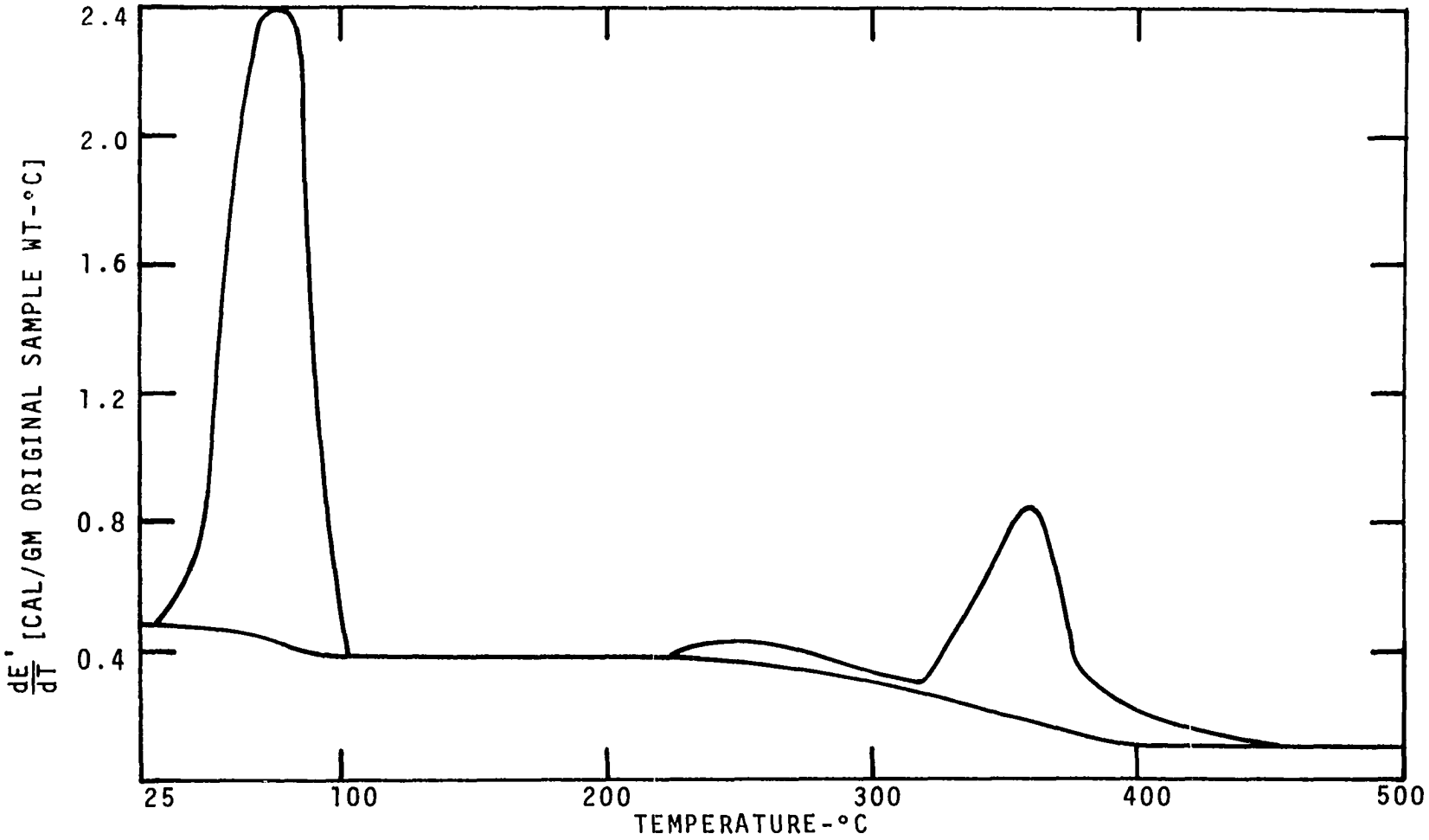

Figure H-9. Differential Energy versus Temperature Curve for Fourwing Saltbush Leaves. Heating Rate - 40°C/MIN.

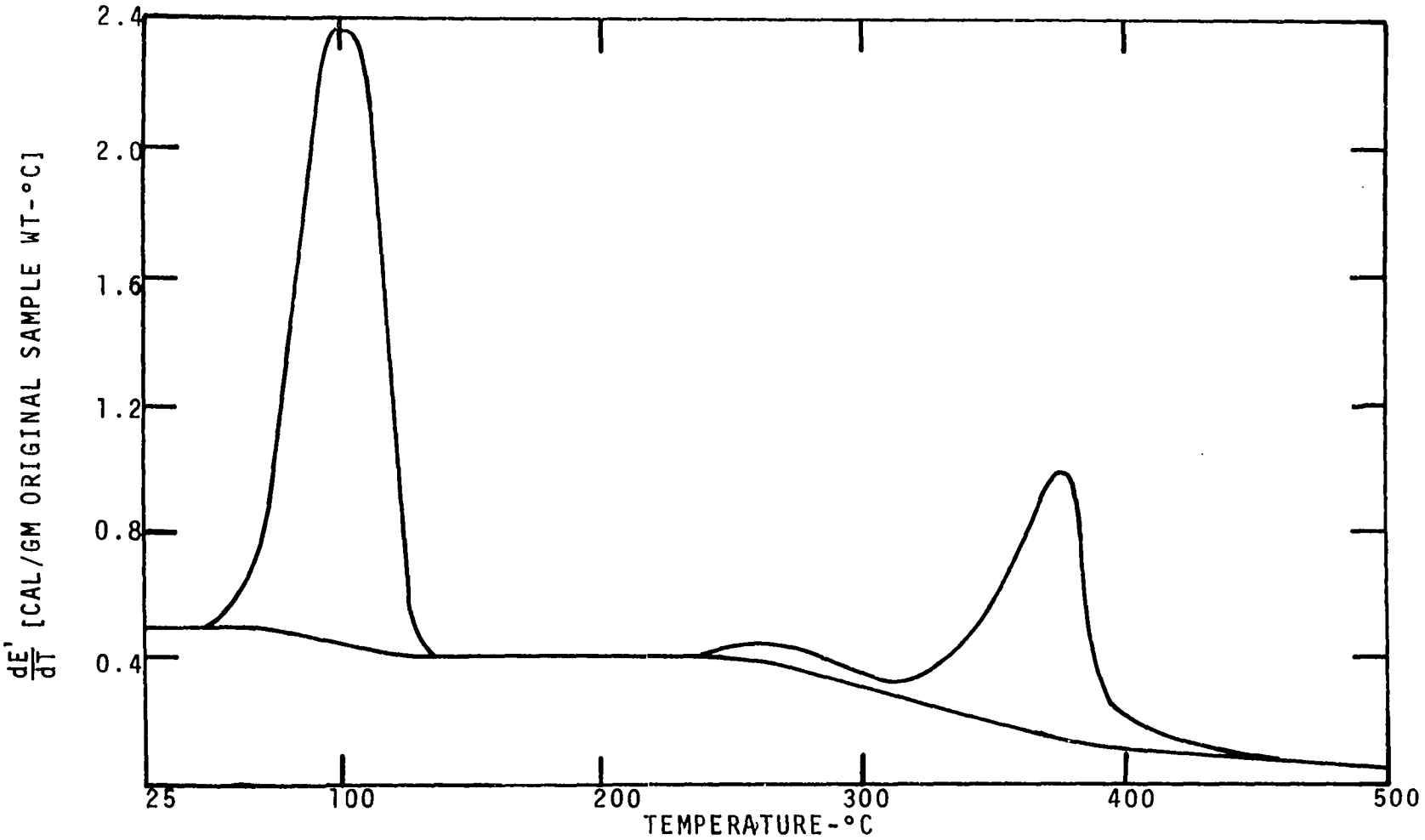

Figure H-10. Differential Energy versus Temperature Curve for Fourwing Saltbush Leaves. Heating Rate - 160°C/MIN.

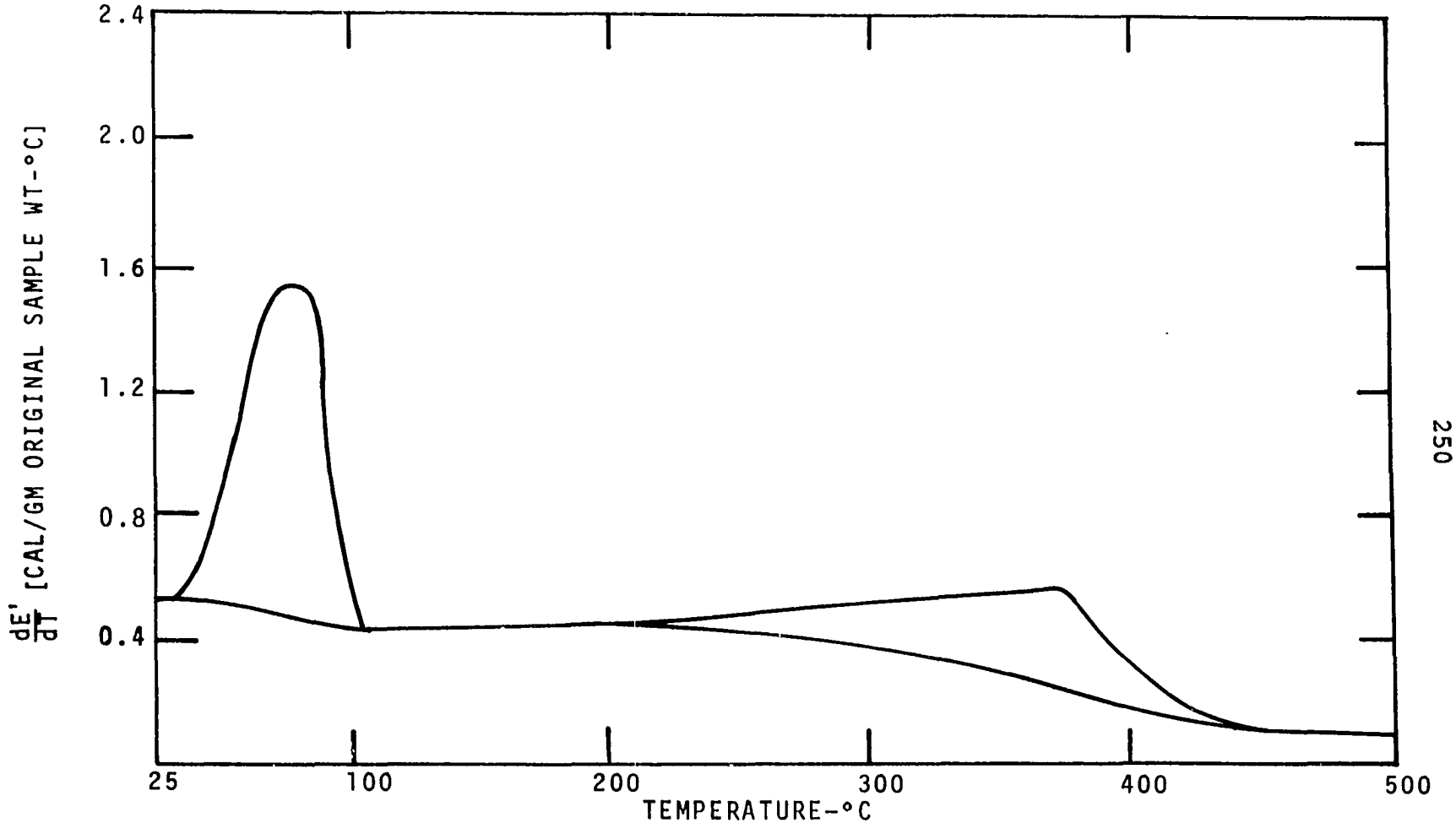

Figure H-11. Differential Energy versus Temperature Curve for Punky Wood. Heating Rate - 40°C/MIN.

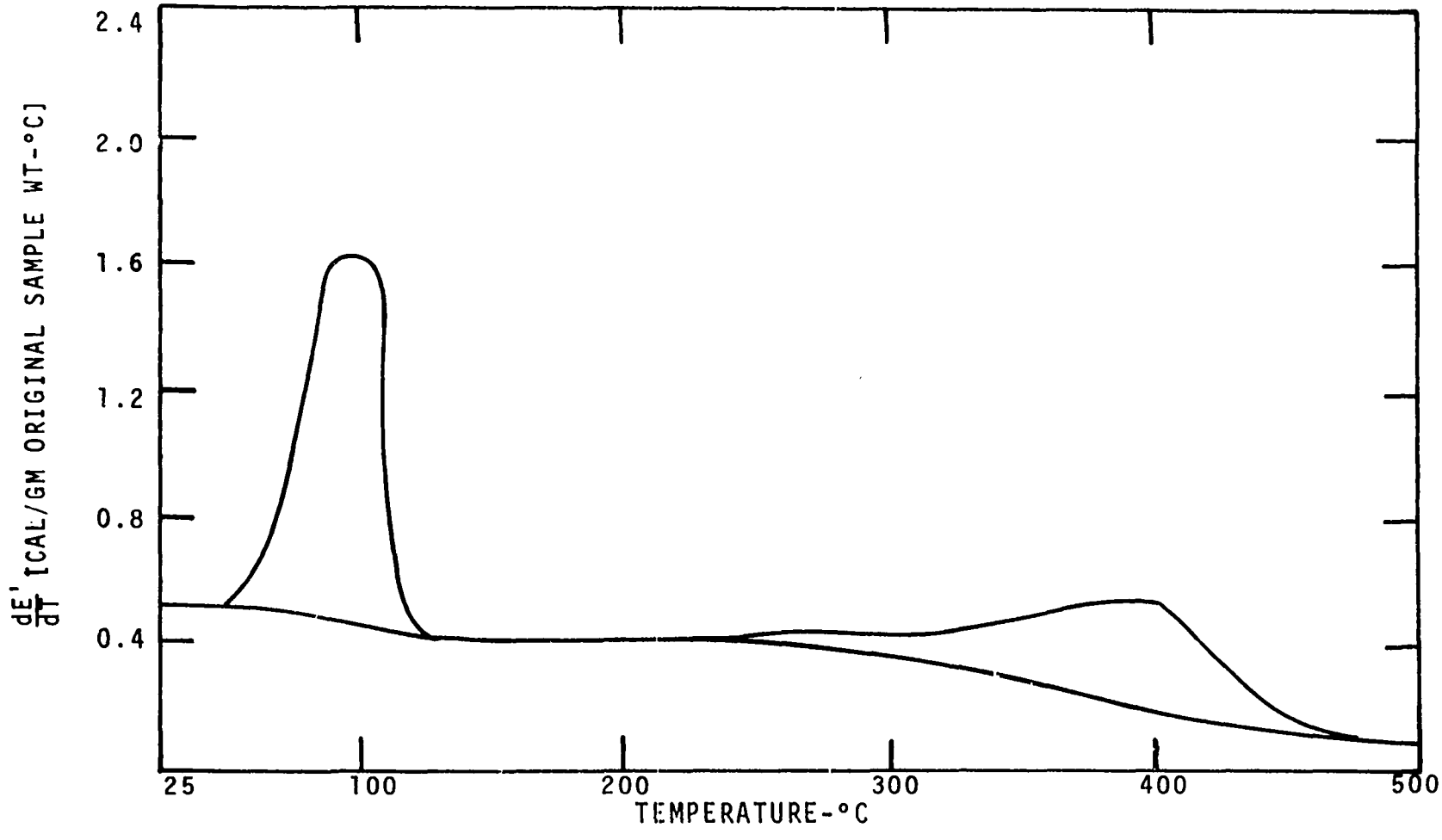

Figure H-12. Differential Energy versus Temperature Curve for Punky Wood. Heating Rate - 160°C/MIN.

APPENDIX I

WET SAMPLE TOTAL ENERGY CURVES

Wet sample total energy curves (E'vs T) for dead Ponderosa pine needles (extracted and unextracted), excelsior (extracted and unextracted), fourwing saltbush leaves, and punky wood at the heating rates of 40° and 160°C/MIN.

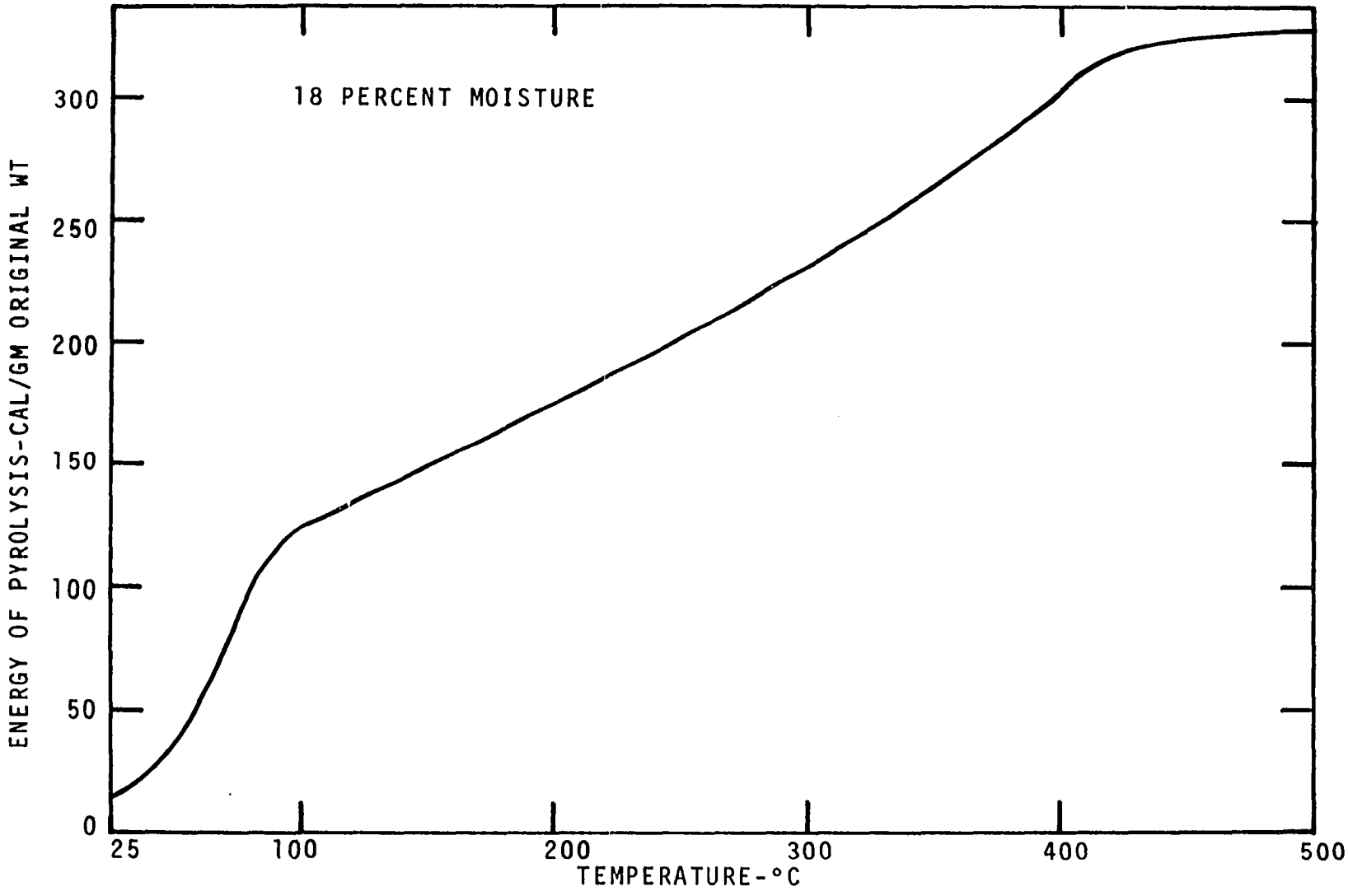

Figure I-1. Total Energy of Pyrolysis versus Temperature Curve for Dead Ponderosa Pine Needles. Heating Rate - 40°C/MIN.

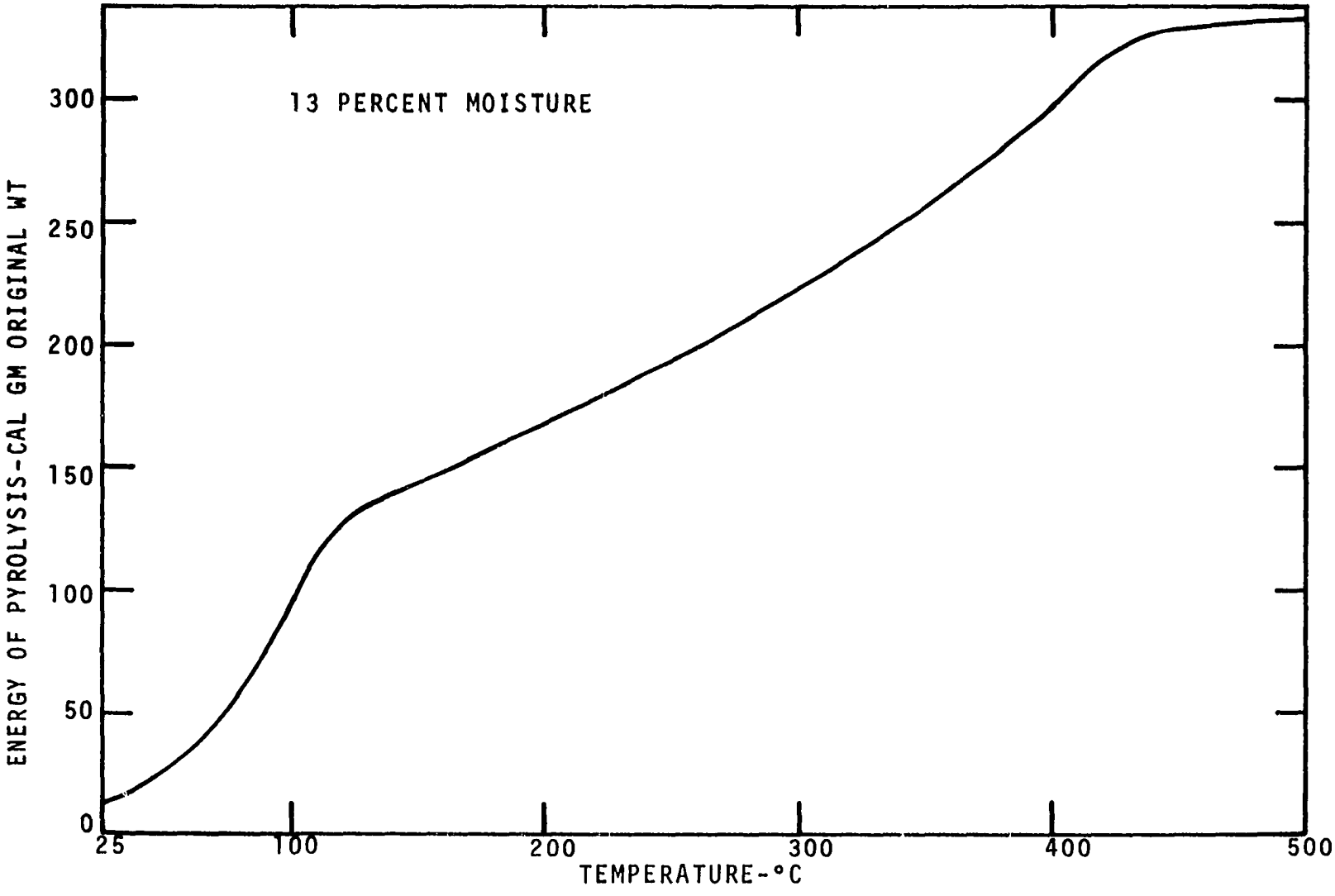

Figure I-2. Total Energy of Pyrolysis versus Temperature Curve for Dead Ponderosa Pine Needles. Heating Rate - 160°C/MIN.

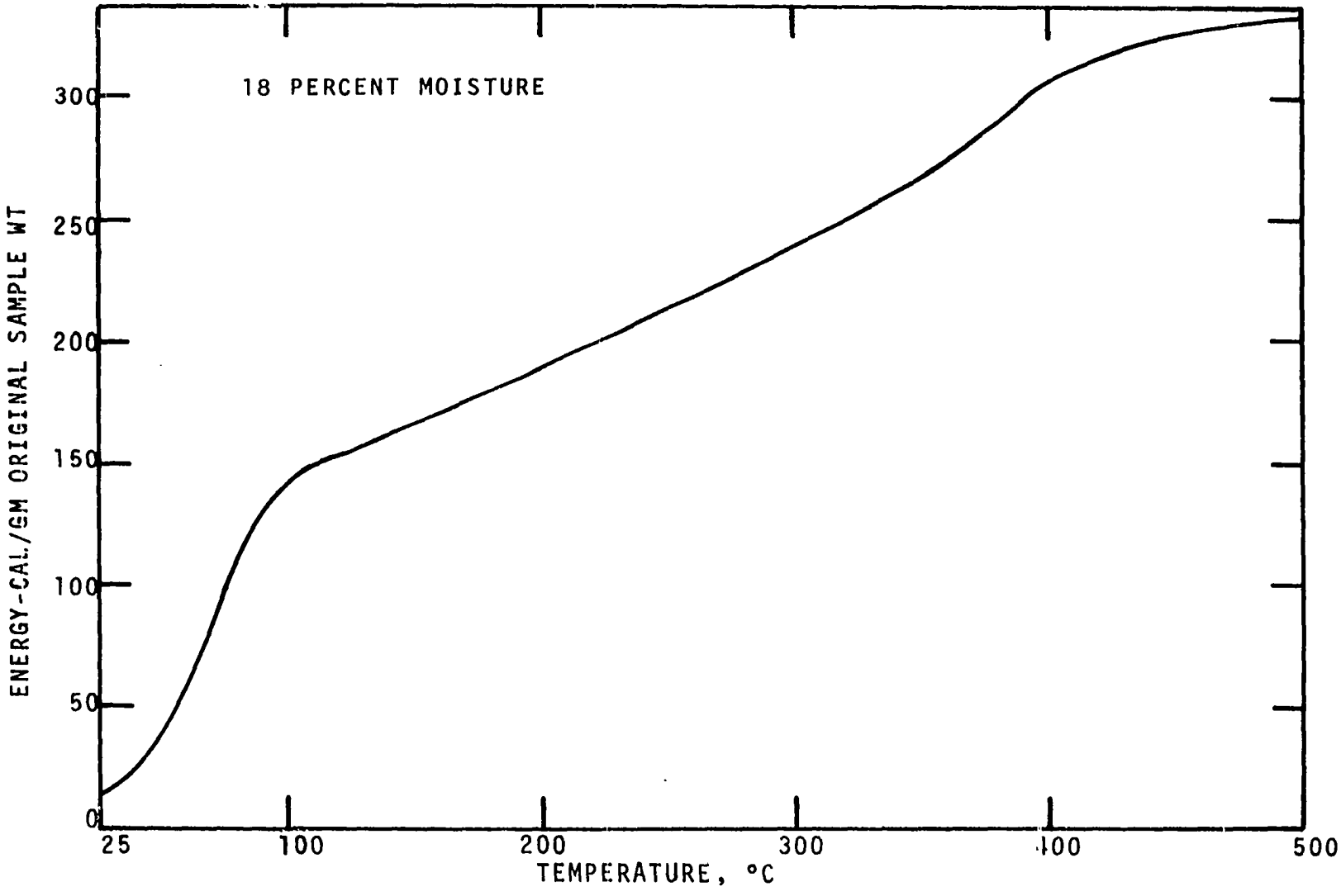

Figure I-3. Total Energy of Pyrolysis versus Temperature Curve for Extracted Ponderosa Pine Needles. Heating Rate - 40°C/MIN.

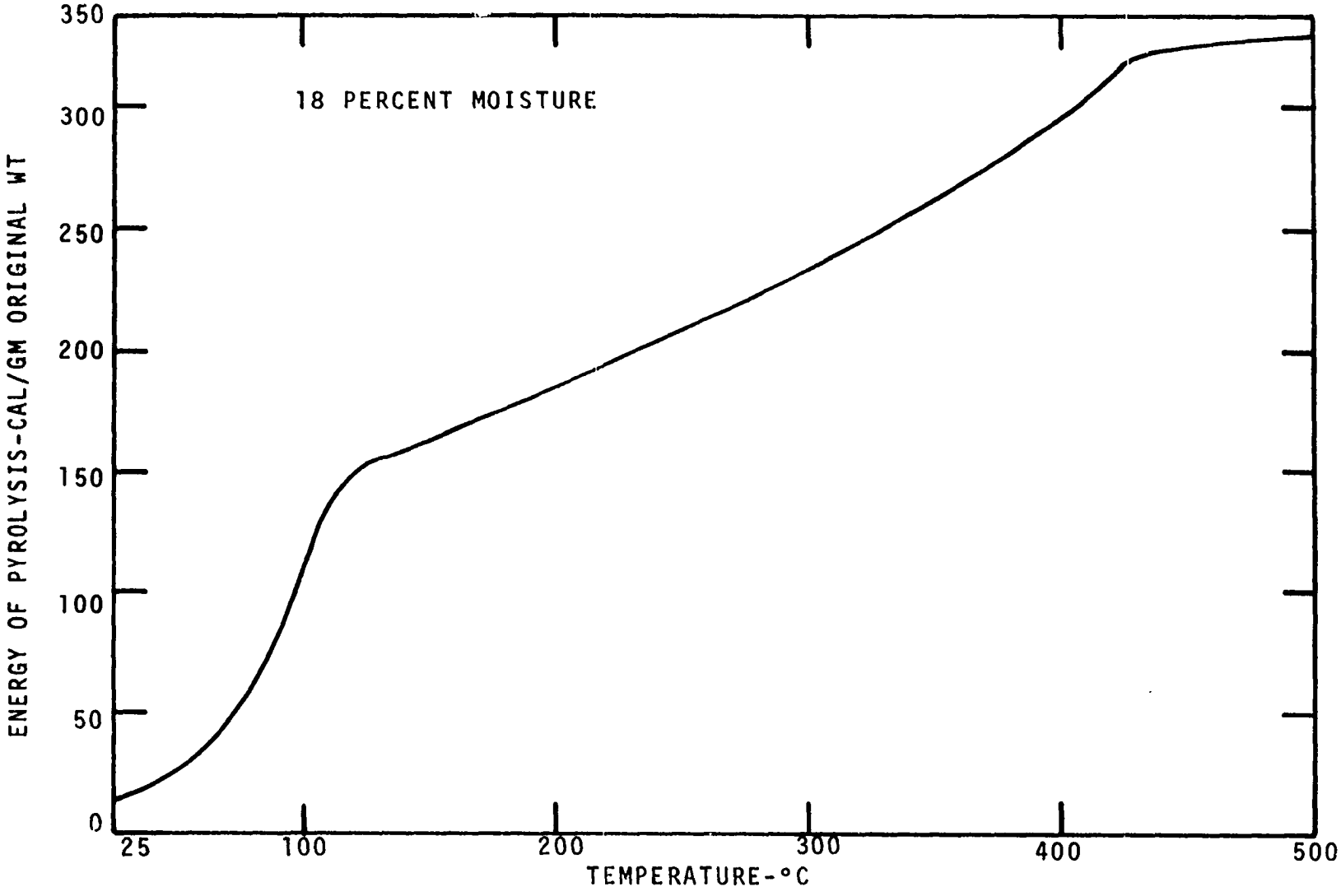

Figure I-4. Total Energy of Pyrolysis versus Temperature Curve for Extracted Ponderosa Pine Needles. Heating Rate - 160°C/MIN.

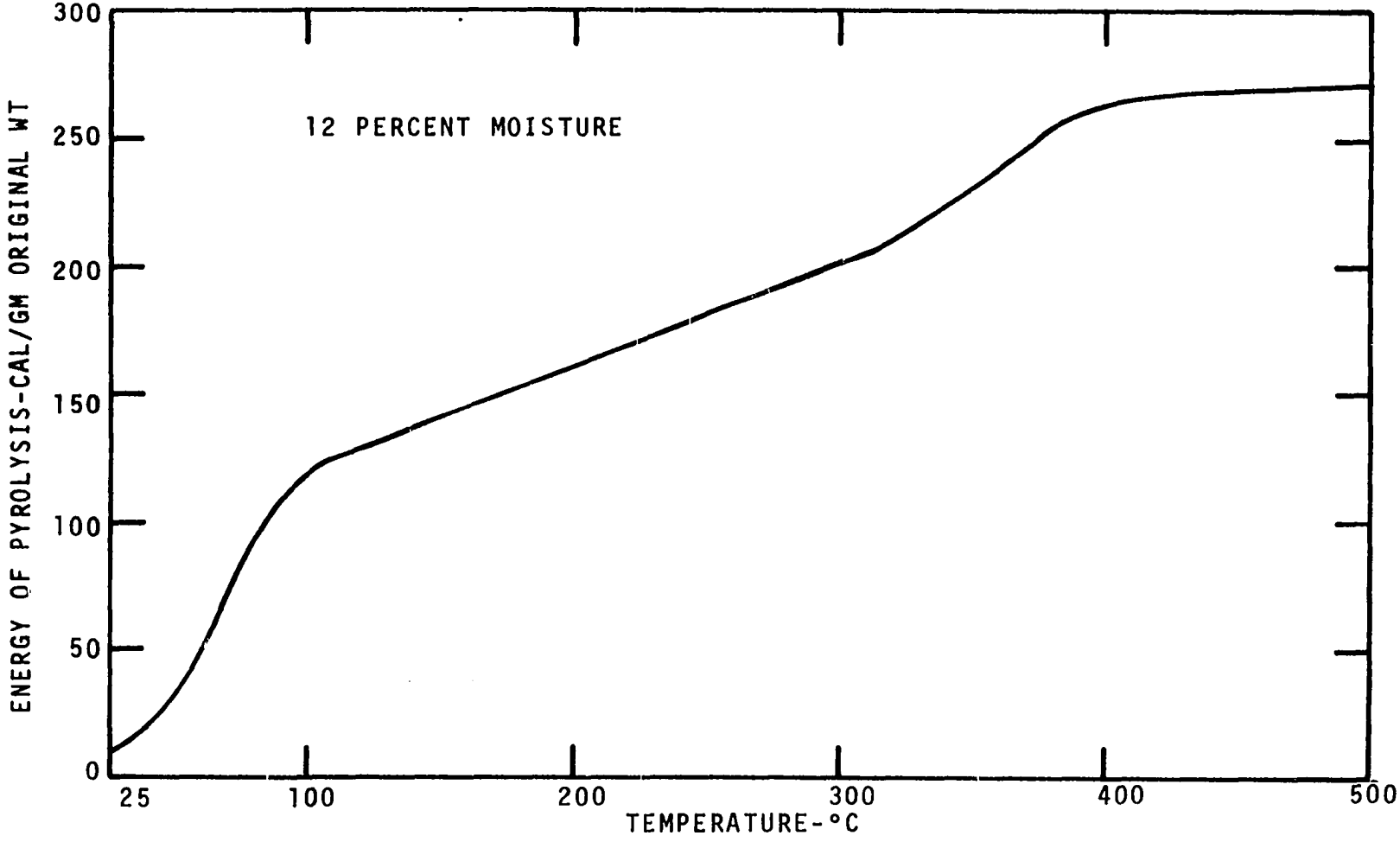

Figure I-5. Total Energy of Pyrolysis versus Temperature Curve for Excelsior. Heating Rate - 40°C/MIN.

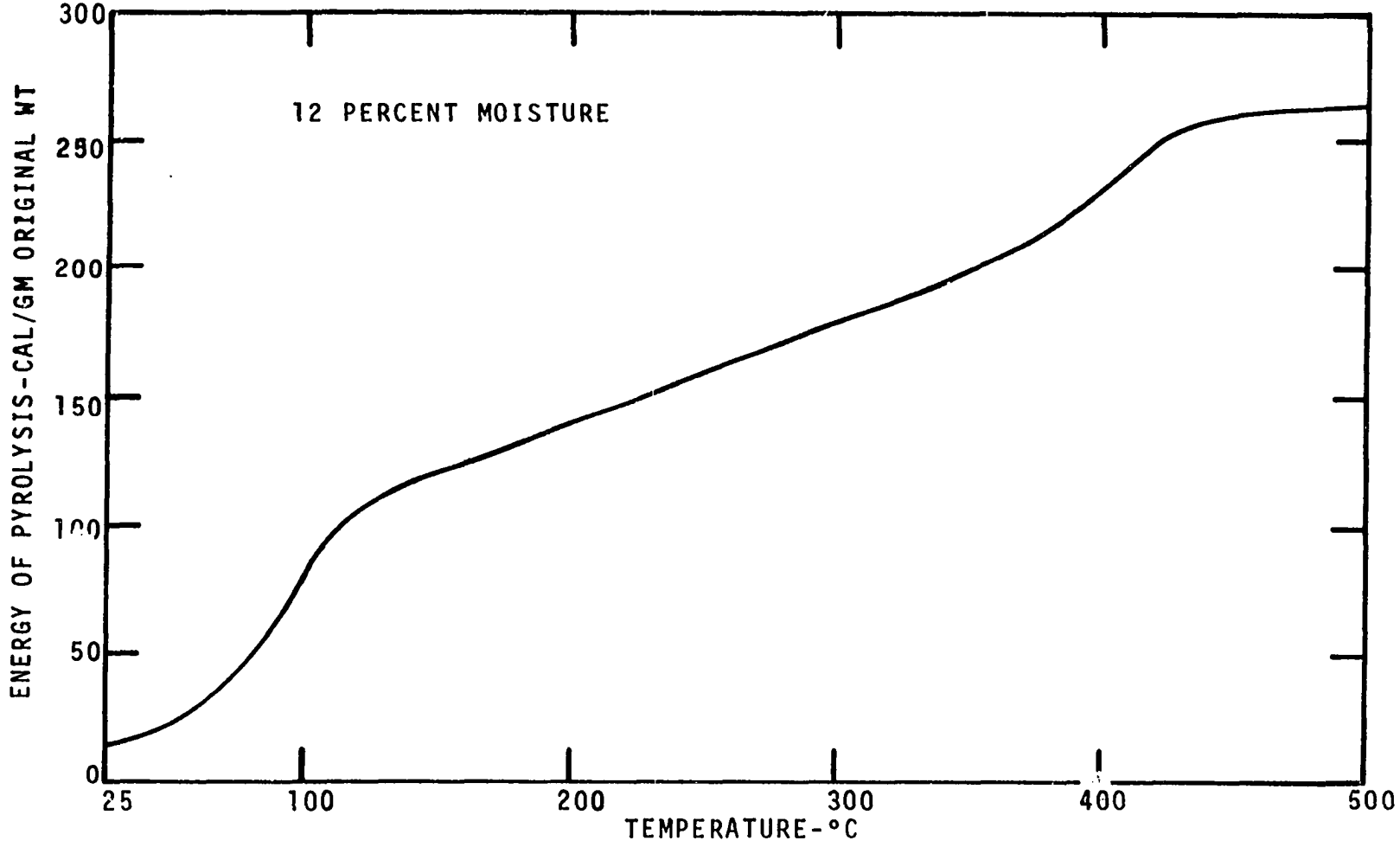

Figure I-6. Total Energy of Pyrolysis versus Temperature Curve for Excelsior. Heating Rate - 160°C/MIN.

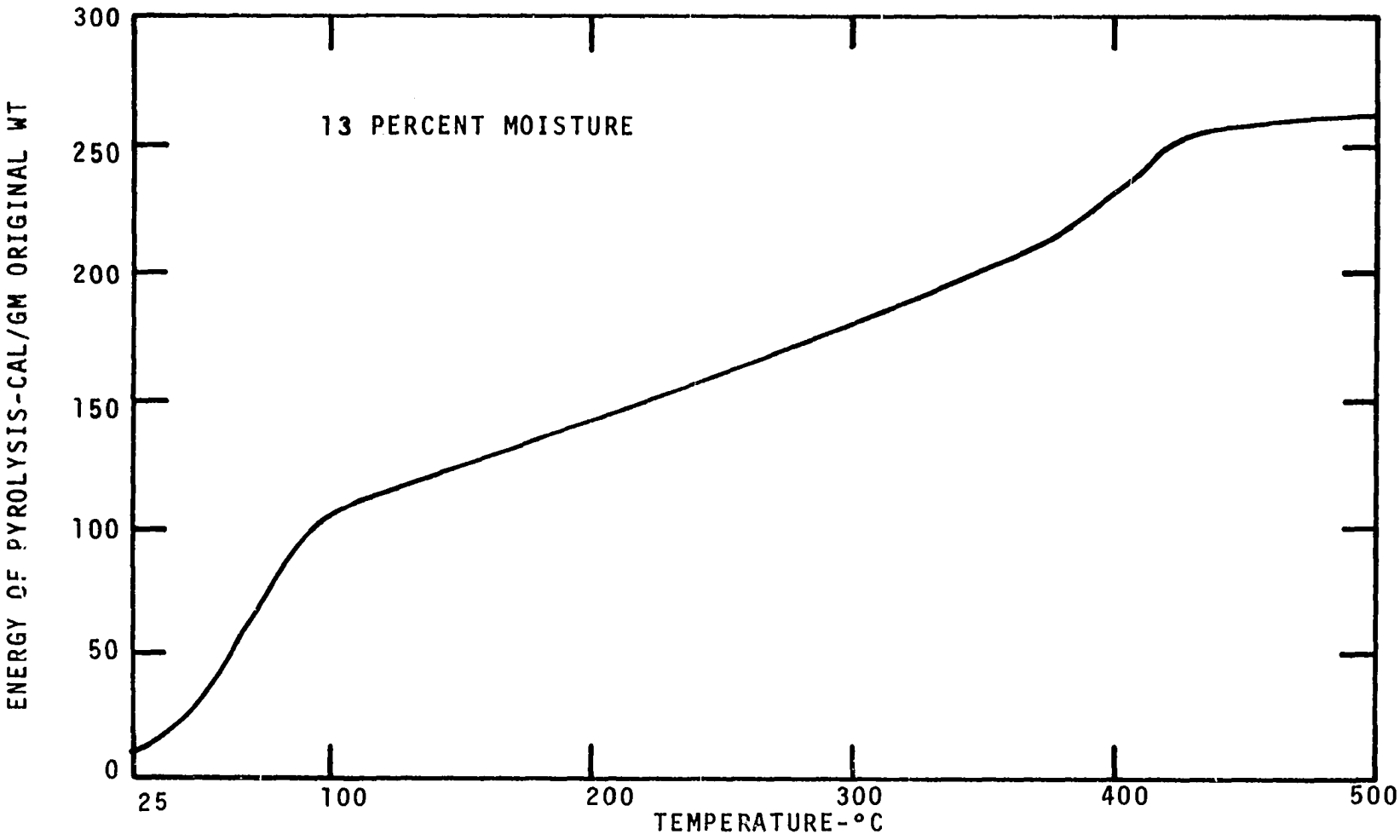

Figure I-7. Total Energy of Pyrolysis versus Temperature Curve for Extracted Excelsior. Heating Rate - 40°C/MIN.

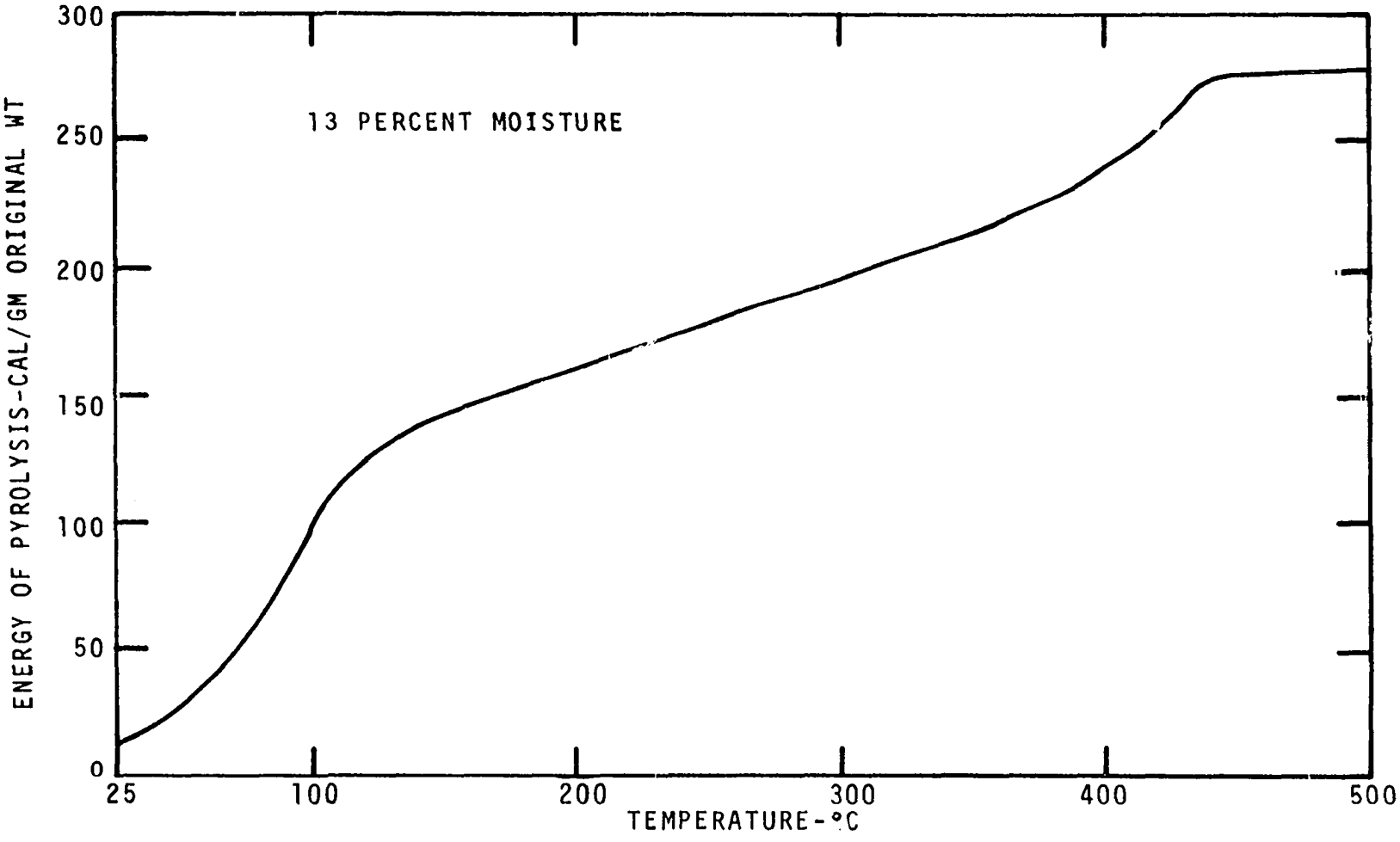

Figure I-8. Total Energy of Pyrolysis versus Temperature Curve for Extracted Excelsior. Heating Rate - 160°C/MIN.

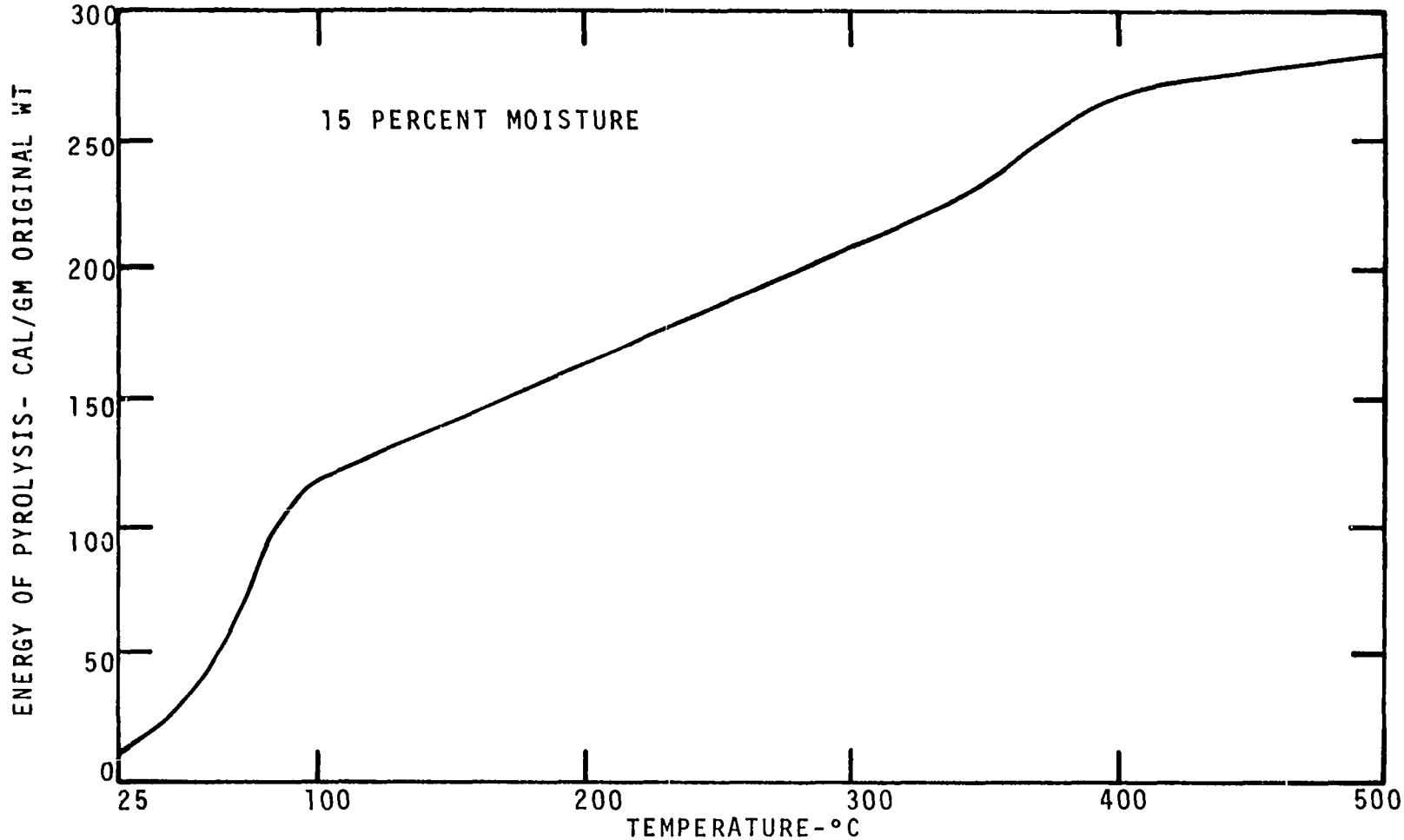

Figure I-9. Total Energy of Pyrolysis versus Temperature Curve for Fourwing Saltbush Leaves. Heating Rate - 40°C/MIN.

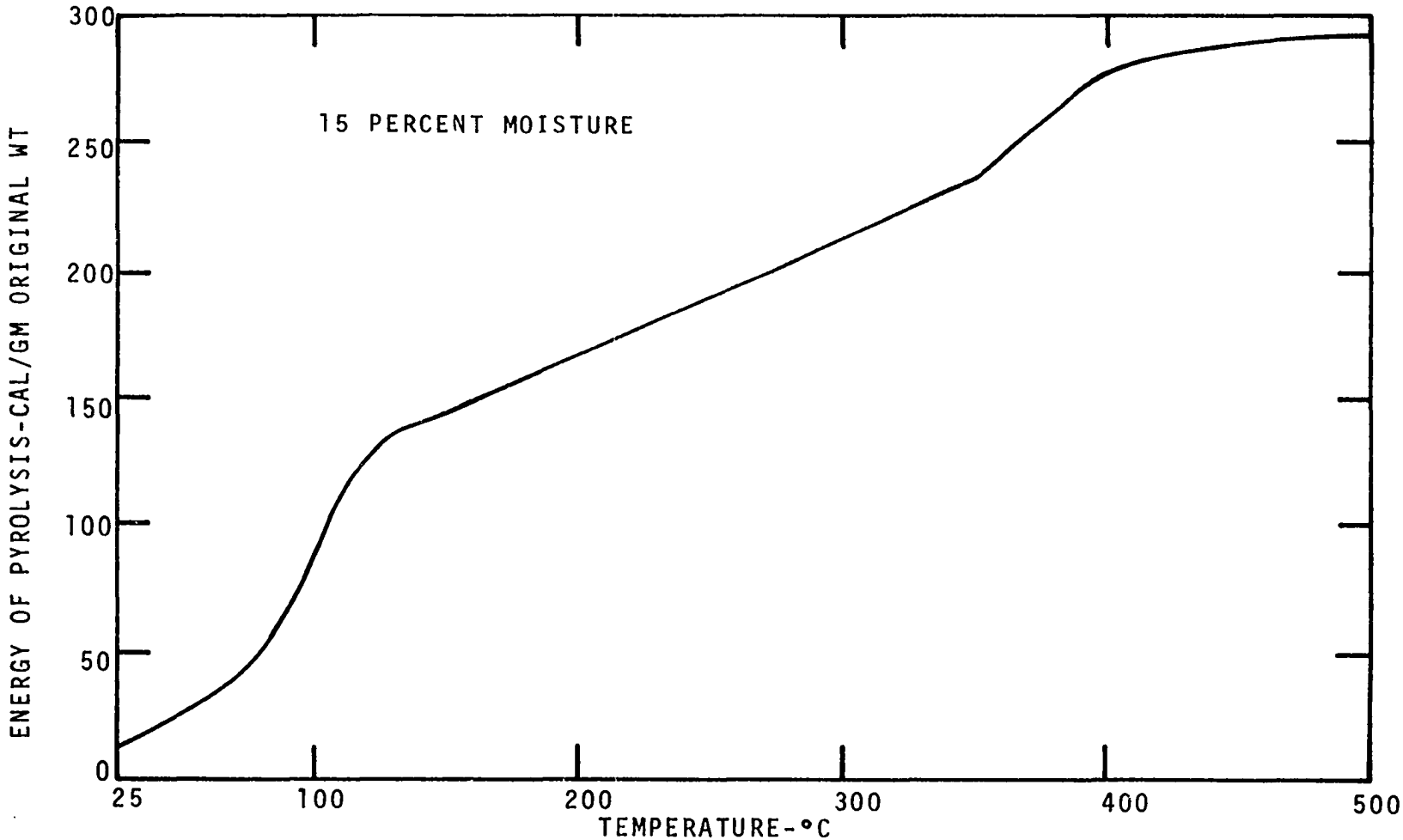

Figure I-10. Total Energy of Pyrolysis versus Temperature Curve for Fourwing Saltbush Leaves. Heating Rate - 160°C/MIN.

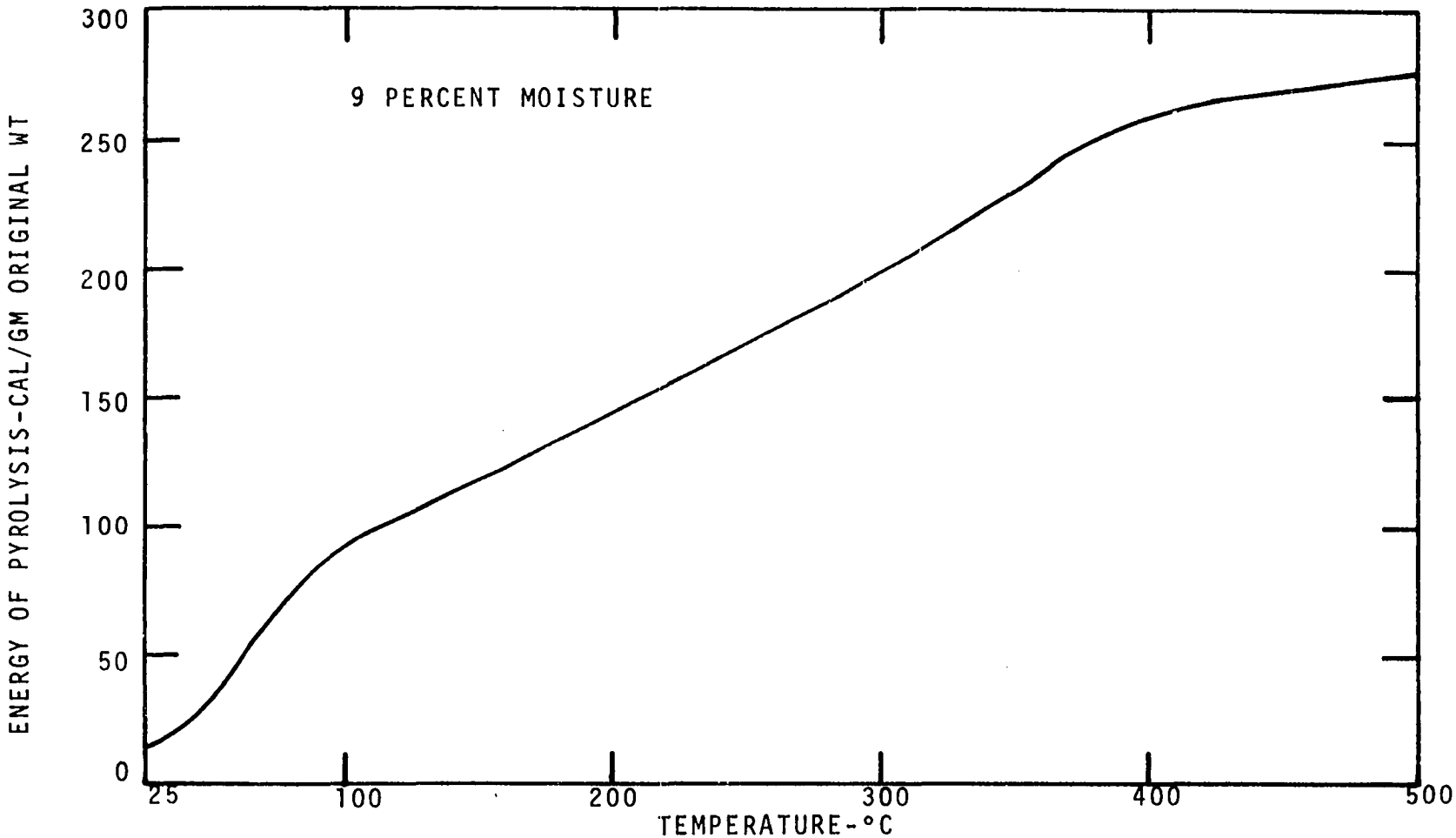

Figure I-11. Total Energy of Pyrolysis versus Temperature Curve for Punky Wood. Heating Rate - 40°C/MIN.

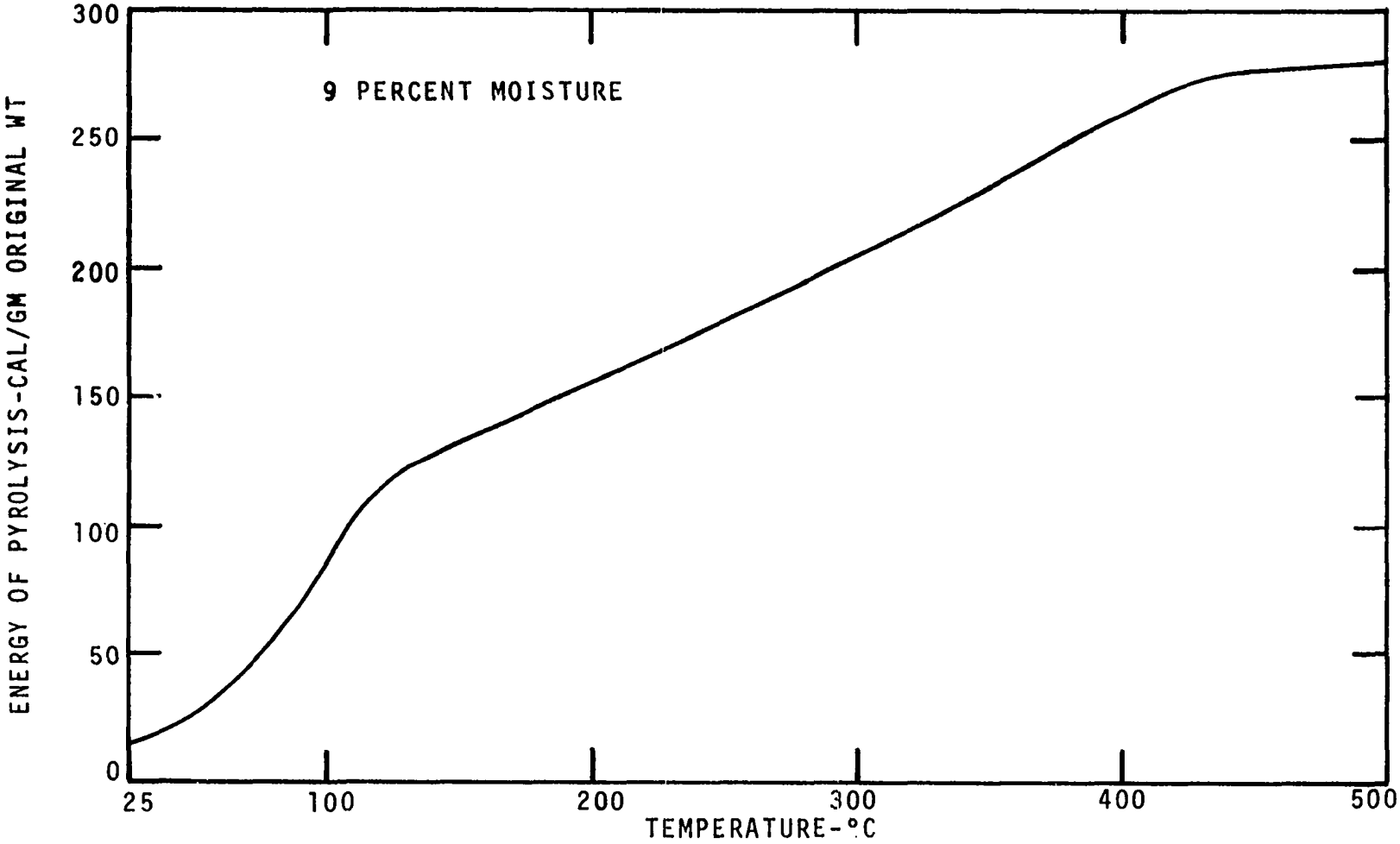

Figure I-12. Total Energy of Pyrolysis versus Temperature Curve for Punky Wood. Heating Rate - 160°C/MIN.